Fall 2011 | Winter 2012 | Spring 2012 | Summer 2012 | Volume XI, Number 3

JNMM Journal of Nuclear Materials Management

Non-Profit Organization
U.S. POSTAGE
PAID
Permit No. 2066
Eau Claire, WI

INMM
INSTITUTE OF NUCLEAR MATERIALS MANAGEMENT

Published by the Institute of Nuclear Materials Management

www.inmm.org www.inmm.org www.inmm.org www.inmm.org

Join INMM for the 53rd INMM Annual Meeting

FIFTY-THIRD ANNUAL MEETING

INMM

INSTITUTE OF NUCLEAR MATERIALS MANAGEMENT

July 15–19, 2012

Renaissance Orlando Resort
at SeaWorld
Orlando, Florida USA

Register Today www.inmm.org/meetings

INMM
INSTITUTE OF NUCLEAR MATERIALS MANAGEMENT

JNMM Journal of Nuclear Materials Management

JNMM (ISSN 0893-6188) is published four times a year by the Institute of Nuclear Materials Management Inc., a not-for-profit membership organization with the purpose of advancing and promoting responsible management of nuclear materials.

SUBSCRIPTION RATES: Annual (United States, Canada, and Mexico) $200; annual (other countries) $270 (shipped via air mail printed matter); single copy regular issues (United States and other countries) $55; single copy of the proceedings of the Annual Meeting (United States and other countries) $175. Mail subscription requests to *JNMM*, 111 Deer Lake Road, Suite 100, Deerfield, IL 60015 U.S.A. Make checks payable to INMM.

DISTRIBUTION and delivery inquiries should be directed to *JNMM*, 111 Deer Lake Road, Suite 100, Deerfield, IL 60015 U.S.A., or contact Anne Czeropski at +1-847-480-9573; fax, +1-847-480-9282; or E-mail, inmm@inmm.org. Allow eight weeks for a change of address to be implemented.

JNMM Journal of Nuclear Materials Management

Topical Papers

Charles Pietri's Influence on INMM Continues

By Scott Vance
INMM President

How can I describe my sadness at the passing of Charles Pietri, or Charlie as we all knew him? He was an accomplished professional and an exceptional human being. His work as chair of the Technical Program Committee will be missed– he performed his duties flawlessly for as long as I can remember, and his humble spirit made it easy to take all of his work for granted.

While we will be able to find someone else to perform those duties, no one will ever be able to replace Charlie's incredible sense of humor and ability to raise the mood of everyone with whom he came in contact. Even as his disease progressed, he never seemed to have a bad day and was always willing to brighten yours. I will miss him more than I can express, and will strive to replace a small portion of the happiness that has left this world with his passing.

Many of us had the privilege of spending some time with Charlie during the fall Executive Committee meeting. Even though he seemed weak, his overall demeanor was "typical Charlie." Therefore, news of his rapid deterioration in January seemed somewhat surreal—after all, we had just seen him and it seemed much too soon to say goodbye. But life is not predictable. Charlie's passing is a reminder to all of us that we need to live every day as if it is our last and leave this world with no regrets. What you do in your professional life is important. What you do for INMM is significant. But the way you treat your family and fellow humans is infinitely more important and significant. Charles' untimely death has reminded me of that.

Special Session on Fukushima

I am amazed that just over a year has passed since the earthquake and tsunami hit Japan, causing a series of significant impacts to a few of that country's nuclear units. There was significant pressure placed on Charles last year as the Technical Program chair to include a discussion of this event in last year's Annual Meeting. Charles resisted that pressure, believing that a few months was not sufficient time to accurately assess the impact of this event on the nuclear materials management community and recognizing that many facts regarding the event were still being gathered. However, Charles set in motion the steps to honor his commitment to provide an intelligent discussion of Fukushima at the 2012 Annual Meeting. As the Technical Program Committee met this past March, the wisdom of Charles' decision became apparent. This year's Annual Meeting will feature a special session on the nuclear material management aspects of the Fukushima event. Because this session will have the benefit of over one year of analysis supporting the presentations, and because the session has been organized by INMM's very active Japan Chapter, I am confident that you will find this Special Session to be one of the most technically sound discussions regarding Fukushima that has been organized to date. This session alone is worth your making plans now to attend the Annual Meeting this July in Orlando.

Time to Vote

At about the same time as you receive this issue of the *Journal*, you should also be receiving an e-mail from INMM Headquarters. Unfortunately, if this year is like most, you are likely to ignore the e-mail—I'd like to encourage you to do otherwise. The email will announce that it is once again time for our membership to vote for open positions on the Executive Committee. Participation in this annual exercise is extremely limited, and that is unfortunate. The Executive Committee often hears that the voting process is a pointless exercise because there is no real decision to be made; only a single individual is nominated to the highest offices. I want to respond to this sentiment.

First of all, election of Members-at-Large has been a competitive election for several years; generally there are twice as many nominees as open positions. These individuals become full voting members of the Executive Committee and their input and participation is crucial to the operation of INMM. So, the input of our membership into the question of who will serve as a Member-at-Large is very important.

Regarding the election of the Executive Committee officers, the winner may be a foregone conclusion since we do not typically conduct a completive campaign for these positions. However, a "vote of confidence" from the membership regarding these officers is very important. The Nominating Committee conducts an extensive review each year of individuals who have demonstrated the characteristics necessary to assume one of the officer positions. Confirmation of this selection by the general membership lets both the nominating committee and the nominee know that the membership concurs with this assessment. I encourage you to respond to the ballot when you receive it this year.

XXXXXXX

By Dennis Mangan
INMM Technical Editor

In Memoriam Charles E. Pietri | 1930–2012

It is with great sadness that we report the death of Charles E. Pietri on February 10, 2012, after a battle with acute leukemia.

Charlie was an essential part of the Institute of Nuclear Materials Management. He served as the Technical Program Committee chair for more than twenty-five years. His friendly smile, his kindness and humor, and of course his famous "Black List" for errant annual meeting speakers were all fixtures of the INMM Annual Meeting. Charlie spent countless hours year round making sure the INMM Annual Meeting was a vital, interesting, and valuable experience for all attendees. In addition to chairing the Technical Program Committee Meeting each spring, Charlie worked with speakers, session chairs, committee members, INMM headquarters staff, and attended all INMM Executive Committee Meetings. His grace and presence will be missed.

The *Journal of Nuclear Materials Management* asked Charlie's long-time friend, Yvonne Ferris, to write about him.

Charles E. Pietri
1930–2012

By Yvonne Ferris
INMM Past President, Former Chair of the INMM Awards Committee

Though the news of Charles Pietri's death was not unexpected, the news was nevertheless devastating. Paraphrasing words from the *Sound of Music*,

How do you solve the heartache of losing Charles?
Many a thing you know you'd have liked to tell him.
Many a thing you know you'd have liked to ask him.
How do you hold a memory in your heart?

Born in New York in 1930, Charles Edward Pietri graduated from The Bronx High School of Science and earned a bachelor's degree in chemistry from New York University. He accepted the position of chemist for DuPont Co. in Wilmington, Del., prior to becoming a research chemist at the New Brunswick Laboratory, which was then in New Jersey.

In the mid-1970s, Charles moved to the Chicago area after the lab relocated to Argonne. He worked as a science administrator, senior scientist, and assistant director for operations. He retired in the late 1990s, but continued for several years as a consultant at the lab, as well as with the International Atomic Energy Agency.

That Charles was dedicated to each endeavor he undertook is an understatement. His brilliant mind, his ability to cut through to the heart of a situation, his wit, his infectious laughter, his calm demeanor, his love of family, his respect for community and country, his devotion to the Boy Scouts… the list goes on.

I remember working with Charles on the Plutonium Sample Exchange program as far back as the 1960s. He was working at the New Brunswick Chemistry Laboratory (it was in New Brunswick, New Jersey, at that time). I was the statistician in charge of randomizing the samples and analyzing the measurement values that Rocky Flats received from the participating laboratories. From the very beginning, Charles was eager to participate, learn from the other laboratory personnel, and share his laboratory's analytical techniques. As others have said, Charles was always the consummate professional. Never a harsh word, never accusatory, never secretive.

I also recall that after an annual meeting Charles wanted to discuss the Technical Program with me. This was around 1983/84 when i was Vice Chairman of INMM. He had some suggestions for improving the program that I thought were excellent. I, of course, asked him to be Technical Program Committee chair and begin implementing his ideas. He was somewhat taken aback as I am sure he expected me to take his suggestions and begin implementing them. After thinking about my request for a short while, Charles accepted the challenge, and the rest is history, as they say. Thereafter, Charles would warn INMM members (in a joking way) about making too many suggestions to me or they would find themselves suddenly in charge of implementing those suggestions.

Charles's demeanor at the annual meeting was one of calm control. As Jim Tape, past president, observed "During the annual meetings, Charles always reminded me of the duck floating on the pond—serene on the surface, but probably paddling like crazy below the surface. I do not recall ever seeing him panic or lose his temper over the numerous, inevitable SNAFUs at a large meeting. And I do not know when he slept—he was often in the bar 'working' until late in the evening and then bright-eyed and bushy-tailed

at the speakers' breakfast first thing in the morning. In many ways the speakers' breakfast exemplified Charles's quiet leadership style, using humor and examples to encourage annual meeting speakers to improve their presentations and to ensure that session chairs were trained and could keep the increasingly complex meeting running smoothly. All of us who had the privilege of serving as officers, in particular when we were in the role of vice president in charge of the annual meeting oversight, knew how dependent we were on Charles and Sherwood, working closely together, for the success of the meeting."

Charles was a quiet but powerful leader who always had a way of finding the light at the end of the tunnel. When at the start of the 2004 INMM Annual Meeting several speakers and leaders were called back to their facility, Charles and his team didn't miss a beat. The show went on and probably only a handful of participants realized what shuffling of papers and personnel took place almost literally hours before the start of the meeting. Also, when a plenary speaker was prevented from presenting his or her paper at the very last minute, Charles was always prepared to ensure that the paper would be presented. He never failed to have a back-up plan.

Charles's work on the Analytical Laboratory N15.51 ANSI Standard will be remembered throughout the world. His national and international contacts were vital to the success of this standard, ensuring that it reflected worldwide best practices.

"What was special about Charlie is that he did what he did so seamlessly, year after year, with humility, a smile, and an incredible sense of humor that just drew people to him," said Scott Vance, president of the Institute. "He was at the center of all of our gatherings." You could always find Charles in the front row of the plenary sessions, or at one of the paper or poster sessions.

Charles's work was noted and rewarded by the Institute in 1996 by naming him a Fellow.

But Charles was not all business all the time. He was also fond of sushi and at INMM meetings or Sample Exchange meetings, we could always count on him knowing the best sushi restaurant in town and organizing a group for dinner. Also, through the years Charles and I—and whoever else wanted to join in, would meet in the bar after the Awards Banquet and have a glass of brandy. It was a great time for all of us to relive the wonderful banquet and joy of the award recipients – and just wind down before the next day's demands. It became a lovely tradition. Charles also loved New Orleans and January would usually find he and Bettina enjoying Dixie Land jazz and the general ambiance of the city. We would all love hearing about the food, the music and the culture that they enjoyed each year. The devastation wreaked by Katrina was devastating to Charles, too, but ever the optimist, he looked forward to its total recovery.

He was a valued colleague, an ardent supporter of the INMM, and a role model for us all. He leaves a very large footprint.

Charles loved to attend karaoke night during the Annual Meetings. Pictured (Left to Right) John Feng, "Professor" Paul Ebel, Charles Pietri, and INMM Immediate Past President Steve Ortiz.

Charles enjoying cake during a reception at an INMM Annual Meeting with INMM Executive Director Jodi Metzgar

Charles Pietri with Vince DeVito, who served as Secretary of the INMM until his death in 2010.

Charles Pietri addressing a Speakers' Breakfast at the INMM Annual Meeting.

(Left to Right) Former INMM Executive Director Leah McCrackin, Charles Pietri, INMM Meeting Director Lyn Maddox, and INMM Executive Director Jodi Metzgar

The Next Generation Safeguards Initiative's Spent Fuel Nondestructive Assay Project

Marc A. Humphrey and Kevin D. Veal
Office of Nonproliferation and International Security, National Nuclear Security Administration, U.S. Department of Energy, Washington, DC USA

Stephen J. Tobin
Los Alamos National Laboratory, Los Alamos, New Mexico USA

Abstract

In 2009, the Next Generation Safeguards Initiative (NGSI) of the U.S. Department of Energy's National Nuclear Security Administration (DOE/NNSA) began a five-year effort to develop one or more integrated instruments capable of determining plutonium mass in, and detecting diversion of pins from, spent commercial fuel assemblies using nondestructive assay (NDA). The project began with a rigorous, simulation-based evaluation of fourteen individual measurement techniques against a virtual library of sixty-four spent fuel assemblies. Efforts have now turned to the construction of three or more integrated systems comprised of the most promising and complementary techniques that are ready for near- to medium-term implementation. Field demonstrations with international partners are in process for the coming years and deployment paths are being explored. This paper provides context on the need and utility of direct and independent plutonium assay in spent fuel, provides an overview of the NGSI project's status, and introduces a few of the fundamental technical challenges that must be overcome to enable the practical deployment of improved methods of nondestructive spent fuel assay.

Introduction

When discharged from a commercial power reactor, a spent nuclear fuel assembly contains about 1 percent plutonium. For a typical pressurized water reactor (PWR) assembly, this corresponds to approximately 5 kg of total elemental plutonium, or approximately one-half of a significant quantity (SQ) of irradiated, direct use material.[1] The special nuclear material content of *fresh* fuel assemblies can be quantified by direct measurement using standard gamma and neutron detection techniques. However, due to the intense background radiation fields associated with irradiated assemblies, plutonium quantification in spent fuel relies on indirect measurement, computer models, and operator-supplied information.

Typically, measurement of total neutrons originating from ^{244}Cm, gross gamma rays from fission products, and gamma peak ratios from selected fission products (e.g., ^{137}Cs, ^{134}Cs, ^{60}Co, and ^{154}Eu) provide consistency checks for operator-supplied information on assembly burnup and cooling time. Based on declared operating parameters, burnup codes are applied to determine the elemental plutonium content in the assembly, with uncertainties of approximately 5 percent. Between and after such assembly-level determinations, use of the Cerenkov viewing device and containment and surveillance (C/S) measures help to maintain continuity of knowledge and deter diversion of nuclear material.

While these measures are effective for routine safeguards for spent nuclear fuel assemblies, they would be incapable of addressing irregular situations, such as loss of continuity of knowledge or exceptional suspicion about operator-reported reactor histories. New measures could also provide improved assembly-level accountancy at the input stages of geologic repositories or reprocessing facilities. In these and other potential cases, the capability of direct and independent quantification of plutonium in spent fuel assemblies would be desirable.

To address long-standing deficiencies in spent fuel assay capability, the Next Generation Safeguards Initiative (NGSI) of the U.S. Department of Energy's National Nuclear Security Administration (DOE/NNSA) began in 2009 a five-year project to develop one or more nondestructive assay (NDA) instruments capable of determining Pu mass in, and detecting diversion of pins from, spent commercial fuel assemblies.[2] While it is thought that no existing NDA technique is capable of determining Pu content singlehandedly to acceptable accuracy, the guiding premise of this effort is that Pu quantification can be achieved through integration of several NDA techniques with complementary capabilities. The objective is to produce one or more NDA instruments capable in the near-term of direct and independent quantification of Pu with an uncertainty of better than 5 percent, recognizing that with additional efforts in calibration, improved accuracies should be achievable. Deployment of NDA technologies to quantify Pu in spent fuel by 2013 was identified as a selected initiative in NNSA's 2011 Strategic Plan.[3]

This project brings together measurement and modeling

experts from six DOE national laboratories: Idaho National Laboratory, Lawrence Berkeley National Laboratory, Lawrence Livermore National Laboratory, Los Alamos National Laboratory, Oak Ridge National Laboratory, and Pacific Northwest National Laboratory. More than thirty student and postdoctoral researchers have contributed to this effort. Participation has also included several universities and international partners.

NGSI is a robust, multi-year program to develop the policies, concepts, technologies, expertise, and international safeguards infrastructure necessary to strengthen and sustain the international safeguards system as it evolves to meet new challenges over the next twenty-five years. The initiative consists of five strategic sub-programs: Policy Development and Outreach, Concepts and Approaches, Technology Development, Human Capital Development, and International Engagement. This project has successfully integrated efforts across multiple NGSI sub-programs.

Applications of Spent Fuel NDA

By 2020, the International Atomic Energy Agency (IAEA) has estimated that a total of 445,000 tons of heavy metal (tHM) will have been discharged from the world's commercial nuclear power plants in the form of spent fuel, one quarter of which is expected to be reprocessed while the remainder would be held in storage.[4,5] Given that this corresponds to hundreds of thousands of individual spent fuel assemblies, it would be impractical to measure every assembly as part of routine safeguards. However, there exist a number of scenarios where instruments with improved capability could be applied to improve the safeguards regime:

- ***Loss of continuity of knowledge.*** Containment and surveillance (C/S) measures are applied to assemblies throughout their lifetime, but in the event that continuity of knowledge is lost (e.g., due to a loss in surveillance from improperly functioning cameras or an extended power outage), the integrity of all the assemblies formerly under surveillance would be in question. It is anticipated that the integrated NDA instruments being developed by NGSI will give improved capability to assure that the assemblies in question have not been tampered with. Whereas standard safeguards instruments measure the total gamma, total neutron, or photon (Cerenkov) emission from the water around pins, the new techniques would give greater confidence in the integrity of the assemblies.
- ***Termination of safeguards at geologic repositories.*** The next decade should see the construction of the world's first geologic repositories for spent fuel. Due to the extreme cost and difficulty associated with retrieving assemblies after sealing the repository, buried assemblies are likely to be classified as "practicably irrecoverable" and therefore subject to termination of safeguards.[6] Regulators[7] are in the process of determining the acceptable requirements for terminating safeguards. It is possible that direct mass accountancy or greater assurance of non-diversion will be required. Understanding the capability of new technologies will be needed to inform these decisions.
- ***Input accountability at reprocessing facilities.*** For those assemblies that will be reprocessed, a shipper-receiver difference (SRD) is determined, sometime years after the shipment. This SRD is not determined using measurements made at both the shipping and receiving sites; rather, the SRD is determined by comparing unverified burnup code calculations done by the reactor facility to input accountability tank measurements made at the reprocessing facility. Moreover, novel processes such as electrochemical refining may not be suitable for input tank accountancy. Technologies that would allow nondestructive assay at the assembly level could improve SRD measurements. They could also improve the timeliness and independence of plutonium accountancy at reprocessing facilities, of potential benefit to both regulators and operators.
- ***Enhanced "containment" during transshipment.*** Containment and surveillance is the safeguards approach maintained from the time assemblies are removed from a reactor through shipment to a subsequent storage or processing facility. Even if NDA technologies prove incapable of highly accurate plutonium determination, these capabilities could be used to measure other assembly attributes (such as fissile content) at the shipper side and receiver side. Provided that the measured signature has not changed beyond some to-be-determined amount, regulators could then conclude that the contents have not been changed during shipment.
- ***Deterrence of diversion.*** "The objective of safeguards is the timely detection of diversion of significant quantities of nuclear material from peaceful nuclear activities … *and deterrence of such diversion by the risk of early detection.*"[8] Even if advanced nondestructive assay technologies for spent fuel are not integrated into routine safeguards activities, the mere existence and limited implementation of these will help deter diversion and therefore strengthen international safeguards. In particular, NDA instruments that measure multiplication provide a signal that is more penetrating and harder to spoof than the status quo.
- ***Non-safeguards applications.*** In addition to the aforementioned safeguards applications, nondestructive assay of spent fuel could also be used for the determination of burnup credit (so that fuel can be stored and shipped more efficiently), for more efficient facility operations (such as optimized reactor core reloading or optimized selection of assemblies for a reprocessing campaign), and for heat-load determination in a repository.

The success of this project will not be determined solely by the measurement capabilities of the technologies developed, but by their applicability to real-world challenges. Therefore, in parallel with the technology development effort, NGSI is also working to identify potential end-users and conducting a systems-

Table 1: The fourteen NDA techniques evaluated during phase 1 of the NGSI spent fuel NDA project

Passive Neutron Albedo Reactivity (PNAR)	^{252}Cf Interrogation with Prompt Neutrons (CIPN)
X-ray Fluorescence (XRF)	Assembly Interrogation with Prompt Neutrons (AIPN)
Passive Gamma (PG)	Self-Interrogation Neutron Resonance Densitometry (SINRD)
Neutron Multiplicity (NM)	Differential Die-Away Self-Interrogation (DDSI)
Differential Die-Away (DDA)	Lead Slowing Down Spectrometer (LSDS)
Delayed Neutrons (DN)	Neutron Resonance Transmission Analysis (NTRA)
Delayed Gamma (DG)	Nuclear Resonance Fluorescence (NRF)

level analysis to more rigorously explore potential applications for the integrated instruments under development.

Project Overview

Phase 1: Modeling and Peer-Review

The first phase of this effort began in 2009 with a two-year, simulation-based evaluation of fourteen individual NDA techniques that were identified as having potential in the area of spent fuel NDA (Table 1). While the majority of these techniques have previously been studied in other contexts, the DDSI technique was developed specifically for this NGSI spent fuel NDA project.

In order to enable a direct, side-by-side comparison of these techniques, research during this phase focused on simulated detector responses against a common library of sixty-four virtual spent fuel assemblies.[9] These 17x17 pressurized water assemblies spanned a broad range of values for initial enrichment (2, 3, 4, and 5 wt percent), burnup (15, 30, 45, and 60 GWd/tU), and cooling time (one, five, twenty, and eighty years). Detector responses were simulated in air, water, and borated water. The majority of the simulations were made using the MCNPX (Monte Carlo N-Particle eXtended) radiation modeling computer code, though some work was done using the GEANT4 code. In addition, the investigations of X-ray fluorescence (XRF), passive gamma (PG), and delayed gamma (DG) were supplemented by benchmark measurements using commercial spent fuel pins and small uranium and plutonium samples.

As part of this effort, a number of new capabilities were added to MCNPX. The following have all been migrated to the DOE release version of MCNP/MCNPX ensuring perpetual availability and maintenance: first fission tallies to identify the first nuclide to fission in a chain; energy-deposition capture tallies to enhance modeling of ^{3}He alternative detectors; and time-dependent mesh tallies to enable visualization of neutron population propagation.

In addition to a systematic exploration of detector response, Phase-1 investigations also included an estimate of the effect of assembly movement relative to the detector hardware, one likely source of systematic error. A study was also made into each technique's potential to detect diversion of pins from within a 17x17 PWR assembly. An additional library of partially diverted assemblies was created, whereby 8, 24, and 49 pins were removed from three different geometric regions across the assembly (inner, outer, and middle); the diverted pins were replaced by depleted uranium pins. From these nine different scenarios, detector responses were simulated to provide a rough measure of the sensitivity of each technique to pin diversion.

Table 2: Composition, key attributes, and potential safeguards applications of the four integrated instruments subject to further study under the NGSI spent fuel NDA project. TN refers to total neutron.

	Techniques	Key Attributes	Potential applications
1	PNAR SINRD PG TN	Passive Lightweight Relatively low cost Short measurement time Robust	Enhanced containment during shipment
2	CIPN SINRD PG TN	Active (source requires shielding) Lightweight Relatively low cost Short measurement time Robust	Input accountability for repository or reprocessing facility Recovery from loss of continuity of knowledge
3	DDSI SINRD PG TN	Passive Relatively heavy Intermediate cost Longer measurement time Robust	Input accountability for repository or reprocessing facility Recovery from loss of continuity of knowledge
4	DN DDA DG PG TN	Active Relatively heavy Relatively high cost Longer measurement time Less robust Potential for high accuracy	Input accountability for new reprocessing facility

Given the importance of an impartial and objective evaluation of each of the initial fourteen techniques, NGSI commissioned an external committee of international experts (thirteen individuals from ten different institutions) to conduct an in-depth review prior to the down-selection process.[10] The composition of the committee was chosen to provide a diversity of viewpoints, and it included academics, technology development experts, and safeguards practitioners. Following a pair of week-long meetings, at which researchers presented their findings from Phase 1, the review committee provided NGSI with a detailed report of its findings.

Phase 2: Down-selection, Integration, and Prototype Development

This systematic investigation of each of the fourteen techniques, along with the review committee's recommendations, allowed NGSI to determine the important strengths, weaknesses, and complementary features of each. From this determination, we are pursuing four integrated instruments consisting of different combinations of those techniques that appeared most promising for near-term deployment.[11-17] Table 2 lists some key attributes of and potential applications of each.

In addition to each technique's detector response and potential for diversion detection, the down-selection process took careful consideration of maturity, simplicity, and robustness. In addition, significant attention was paid to complementary features that could be exploited through integration. It must be emphasized that the elimination of any given technique does not represent a judgment on its standalone merit. Rather, it reflects the review committee's and NGSI's view of its ability to address spent nuclear fuel measurements in an operational environment in the near to medium term.

The NGSI spent fuel project has now begun prototype development for the first three of these integrated instruments. This involves development of a design to integrate the techniques, occasional modeling to optimize these designs, and actual hardware construction. Since the fourth, neutron-generator-based instrument, would be significantly larger, more expensive, and less robust than the other three, it will be pursued only if it can be demonstrated that it has the potential to quantify plutonium with significantly better accuracy. Therefore, NGSI is conducting additional research designed to determine whether further development of this system is merited.

Phase 3: Field Tests and Deployment

This project will culminate in a serious of in-field demonstrations of the integrated systems developed during Phase 2. The primary objective of these tests will be to compare the measured and simulated response of each instrument to real commercial spent fuel assemblies. These tests will also allow for a determination of whether the integration of techniques provides sufficient information to yield an accurate quantification of plutonium.

These tests will likely be conducted in cooperation with international partners through the NGSI International Nuclear Safeguards and Engagement Program (INSEP). We expect to complete prototype development of instruments 1 and 2 in 2012 and field trials with two international partners are in process for early 2013. Prototype development for instrument 3 is expected for 2013, and a field trial with an international partner is anticipated for 2014. Finally, a decision on prototype development for instrument 4 will be made in 2013, and potential field trials would take place in 2015.

If successful, the deployment path for a spent fuel NDA instrument or system developed by NGSI would likely be through a national or regional regulatory body or through a facility operator, and, as appropriate, in collaboration with the IAEA to ensure that these techniques are appropriate for use in safeguards approaches to meet international safeguards objectives. It is possible that the near-term requirements of the first geological repositories will drive the greatest early interest in the refinement and full-scale deployment of spent fuel NDA. In addition, the prospect of assembly-level input accountability at reprocessing facilities and more optimized facility operation might provide an incentive to facility operators to adopt the technologies developed by NGSI. A proven track record, established through these deployments, would increase the attractiveness of these technologies to international safeguards practitioners.

Cross-Cutting Technical Challenges

Besides the technique- and instrument-specific research, development, and deployment path outlined in the preceding sections, two cross-cutting technical challenges are likely to impact the ultimate viability of the technologies under development through this project: calibration and uncertainty; a brief discussion of each problem is included in this section. Additional cross-cutting issues are addressed in the accompanying technical overview by Tobin et al.[18]

In order for an integrated spent fuel NDA instrument to produce accurate and reliable measurements, calibration will be necessary. Ideally, one would be able to compare the Pu mass measured by NDA to the known mass of the well-characterized assembly. Unfortunately, few if any such well-characterized assemblies exist today. In pursuit of (1) quantifying the performance of the NDA instruments, (2) improving the state-of-the-art in spent fuel assembly characterization, and (3) ultimately producing a set of calibration standards, NGSI is seeking to create a few well-characterized assemblies, or "working standards." Work in this area is still in the preliminary stages, but it will likely involve iteration between NDA and burnup codes and possibly include additional information from destructive analysis.

The effective deployment of any of the systems under development will require a rigorous determination of measurement uncertainty. Relative to most NDA measurements conducted in the course of routine safeguards, uncertainty determination of Pu mass in spent fuel is particularly challenging. This is due to the presence of so many variables, including five significant isotopes of plutonium, two isotopes of uranium, several significant neutron absorbers, fission fragment gamma emitters, and ^{244}Cm neutron production. Furthermore, error propagation will require a combination of measured and simulated signatures and their associated uncertainties. NGSI has begun a careful and rigorous examination of the quantification of uncertainty for the various instruments under development.

Conclusion

The standard measures for safeguarding spent nuclear fuel have changed little over several decades (total neutron, total and spectral gamma, and the relative photon intensity from the water in an assembly). The status quo for quantifying plutonium in spent fuel relies on indirect measurements (radiation from ^{244}Cm and fission products), computer simulation (burnup codes), and operator-supplied information (assembly operating history, including burnup and cooling time). While these measures have proven sufficient for routine application of safeguards, there exist a number of situations for which new technologies would strengthen spent fuel safeguards: recovery from loss of continuity of knowledge, assembly-level input accountancy at repository or reprocessing sites, or enhanced containment of spent fuel during transshipment. Even limited application of spent fuel nondestructive assay would provide greater deterrence to diversion.

Direct quantification of plutonium in spent fuel using NDA is a significant technical challenge due to the isotopic complexity of the fuel and the immense background fields of irradiated assemblies. It is therefore expected that no current NDA technique will be capable of Pu quantification singlehandedly. We believe, however, that the integration of several techniques with complementary attributes may allow this to be achieved. Guided by this premise, NGSI undertook in 2009 a five-year effort to develop one or more integrated NDA instruments capable of quantifying plutonium in spent fuel. Two years into this effort, the project has down-selected from fourteen standalone techniques, is currently developing four different integrated instruments, and will perform a series of field tests of these with international partners over the coming years.

While it is premature to predict whether these instruments will be capable of direct Pu quantification to better than 5 percent uncertainty, it is clear that the research performed will add new capabilities to the international safeguards toolkit. Moreover, the project has already achieved several tangible accomplishments, including the development of a virtual spent fuel library, improvements to MCNPX code, and the training of dozens of new students and postdoctoral researchers at U.S. national laboratories. Regardless of the final outcome, this project will advance our understanding of the capabilities and limitations in the area of spent fuel NDA and strengthen international nuclear safeguards in the decades to come.

Acknowledgement

The authors would like to acknowledge the efforts of Steve Lamontagne to initiate this project in 2009. We'd also like to recognize the work of the many researchers, including many students and post-doctoral fellows, who have contributed. Finally, we thank the members of the external review committee, whose feedback helped to shape the future path of this effort.

Note: Technical reports for all fourteen NDA techniques are available through correspondence with the author.

Dr. Marc A. Humphrey is the acting team leader for the Safeguards Technology Development subprogram of the Next Generation Safeguards Initiative (NGSI) in the Office of Nuclear Safeguards and Security at the U.S. Department of Energy's National Nuclear Security Administration (DOE/NNSA). He has B.S. degrees in physics and applied math from Western Michigan University and a Ph.D. in physics from Harvard University. Prior to joining DOE/NNSA, Humphrey worked at the United States Department of State in the Office of Nuclear Energy, Safety, and Security.

Dr. Stephen J. Tobin is currently the principle investigator for a multi-laboratory/university collaboration sponsored by the Next Generation Safeguards Initiative to determine the plutonium mass in spent fuel assemblies. He has a B.S. degree in physics from Xavier University and M.S. and Ph.D. degrees in nuclear engineering from the University of Michigan. Tobin currently works at the Los Alamos National Laboratory in Nuclear Nonproliferation Division.

Dr. Kevin D. Veal is the acting director of the Office Nuclear Safeguards and Security and manages the Next Generation Safeguards Initiative for the U.S. Department of Energy's National Nuclear Security Administration (DOE/NNSA). He has a B.S. degree in physics from Mississippi State University and a Ph.D. in nuclear physics from the University of North Carolina at Chapel Hill. Prior to joining DOE/NNSA, Veal spent eleven years working at Los Alamos National Laboratory in the Safeguards Science and Technology group.

References

1. A standard UO_2 spent PWR fuel assembly (900 MWe PWR fuel with a burnup of 33 GWd/tHM) has an initial heavy metal content of about 500 kg and contains about 1 percent (5 kg) plutonium when discharged. Source: International Atomic Energy Agency, *Spent Fuel Reprocessing Options, IAEA-TECDOC-1587* (Vienna, IAEA, 2008), 76.
2. Veal, K. D., S. A. LaMontagne, S. J. Tobin, and L. E. Smith. 2010. NGSI Program to Investigate Techniques for the Direct Measurement of Plutonium in Spent LWR Fuels by Nondestructive Assay, *Proceedings of the Institute of Nuclear Materials Management 51st Annual Meeting.*
3. National Nuclear Security Administration Strategic Plan (May 2011), 6.
4. International Atomic Energy Agency, *Spent Fuel Reprocessing Options, IAEA-TECDOC-1587* (Vienna, IAEA, 2008), 2.
5. International Atomic Energy Agency. 2009. Costing of Spent Nuclear Fuel Storage, IAEA Nuclear Energy Series No. NF-T-3.5 (Vienna, IAEA), 1.
6. International Atomic Energy Agency. 1972. *The Structure and Content of Agreements Between the Agency and States Required in Connection with the Treaty on the Non-Proliferation of Nuclear Weapons, INFCIRC/153 (corrected)* (Vienna, IAEA), paragraph 11.

7. This includes regulators at various levels: national (e.g., State Systems of Accounting and Control), regional (e.g., EURATOM), or international (IAEA).
8. IAEA INFCIRC/153, paragraph 28 (emphasis added).
9. Galloway, J. D., H. R. Trellue, M. L. Fensin, and B. L. Broadhead. 2012. Design and Description of the NGSI Spent Fuel Library with an Emphasis on Passive Gamma Signal, *Journal of Nuclear Materials Management,* Vol. 40, No. 3.
10. Charlton, W. S., and M. A. Humphrey. 2012. The Next Generation Safeguards Initiative's Spent Fuel Nondestructive Assay Project: External Review Committee Process and Findings, *Journal of Nuclear Materials Management,* Vol. 40, No. 3.
11. Hu, J., H. R. Trellue, S. J. Tobin, T. J. Ulrich, A. M. LaFleur, C. R. Freeman, H. O. Menlove, and M. T. Swinhoe. 2012. The Performance of Self-Interrogation Neutron Resonance Densitometry in Measuring Spent Fuel, *Journal of Nuclear Materials Management,* Vol. 40, No. 3.
12. Gerhart, J. J., C. R. Freeman, J. L. Conlin, H. O. Menlove, and S. J. Tobin. 2012. Passive Neutron Albedo Reactivity with Fission Chambers (PNAR-FC), *Journal of Nuclear Materials Management,* Vol. 40, No. 3.
13. Hu, J., S. J. Tobin, H. O. Menlove, D. Henzlova, J. Gerhart, M. T. Swinhoe, and S. Croft. 2012. Developing The Californium Interrogation Prompt Neutron Technique to Measure Fissile Content and to Detect Diversion in Spent Nuclear Fuel Assemblies, *Journal of Nuclear Materials Management,* Vol. 40, No. 3.
14. Belian, A., H. O. Menlove, M. T. Swinhoe, and S. J. Tobin. 2012. New Design of the Differential Die-Away Self-Interrogation Instrument, *Journal of Nuclear Materials Management,* Vol. 40, No. 3.
15. Henzl, V., M. T. Swinhoe, S. J. Tobin, and H. O. Menlove. 2012. Measurement of the Multiplication of a Spent Fuel Assembly with the Differential Die-Away Method within the Scope of the Next Generation Safeguards Initiative Spent Fuel Project, *Journal of Nuclear Materials Management,* Vol. 40, No. 3.
16. Blanc, P., H. O. Menlove, S. J. Tobin, S. Croft, and A. Favalli. 2012. An Integrated Delayed-Neutron, Differential-Die-Away Instrument to Quantify Plutonium in Spent Nuclear Fuel, *Journal of Nuclear Materials Management,* Vol. 40, No. 3.
17. Mozin, V. V., B. Ludewigt, S. J. Tobin, A. Hunt, L. Campbell. 2012. Delayed Gamma-Ray Assay for Spent Nuclear Fuel Safeguards, *Journal of Nuclear Materials Management,* Vol. 40, No. 3.
18. Tobin, S. J. et al. 2012. Technical Cross-Cutting Issues for the Next Generation Safeguards Initiative's Spent Fuel Nondestructive Assay Project, *Journal of Nuclear Materials Management,* Vol. 40, No. 3.

External Review of the Next Generation Safeguards Initiative's Spent Fuel Nondestructive Assay Project

William S. Charlton
Nuclear Security Science & Policy Institute, Texas A&M University, College Station, Texas USA

Marc A. Humphrey
Office of Nonproliferation and International Security, National Nuclear Security Administration, U.S. Department of Energy, Washington, DC USA

Abstract
The Next Generation Safeguards Initiative spent fuel nondestructive assay project is developing new safeguards technologies for use in verification of bulk plutonium content in spent nuclear fuel assemblies. In this paper, we discuss the spent fuel safeguards project in general and an external review process that was used to inform down selection among the fourteen different techniques studied. The review committee process was an excellent way of collecting expert analysis of the techniques and to provide unbiased input to project management decisions. The committee's overall impression was that the work performed by the researchers on this effort was impressive in both depth and breadth and will have a significant impact on safeguards technology development.

Introduction
In 2009, the Next Generation Safeguards Initiative (NGSI) of the U.S. Department of Energy's National Nuclear Security Administration (NNSA) began a five-year effort to develop one or more instruments capable of determining plutonium (Pu) mass in and detecting diversion of pins from spent commercial fuel assemblies.[1] This is a very challenging safeguards problem and one whose fundamental difficulty has driven many of the characteristics that exist in modern safeguards. A practical means for meeting this goal could have a significant long-term impact on safeguards systems.

The first phase of this effort was a two-year, simulation-based evaluation of the fourteen individual NDA techniques shown in Table 1. While it is believed that no technique will be capable of determining Pu content singlehandedly, the guiding premise of this effort is that Pu quantification can be achieved through the integration of several techniques with complementary capabilities. The majority of these techniques have previously been studied in other contexts. The Differential Die-Away Self-Interrogation (DDSI) technique, however, was developed specifically for this project.

The second phase of this effort was a side-by-side comparison of the simulated responses of the various techniques against a common library of sixty-four virtual spent fuel assemblies, which spanned a broad range of initial enrichment, burnup, and cooling time values.[2] Once the important strengths, weaknesses, and complementary features of each technique had been identified, a down-selection was performed (as described later in this paper) to focus efforts and resources on the combinations of techniques most likely to address the expected safeguards applications in the near to medium term.

Table 1. The fourteen NDA techniques evaluated during phase 1 of the NGSI Spent Fuel NDA project

Passive Neutron Albedo Reactivity (PNAR)[3]	^{252}Cf Interrogation with Prompt Neutrons (CIPN)[4]
X-ray Fluorescence (XRF)[5,6,7]	Assembly Interrogation with Prompt Neutrons (AIPN)[8]
Passive Gamma (PG)[9,10]	Self-Interrogation Neutron Resonance Densitometry (SINRD)[11,12]
Neutron Multiplicity (NM)[13]	Differential Die-Away Self-Interrogation (DDSI)[14]
Differential Die-Away (DDA)[15]	Lead Slowing Down Spectrometer (LSDS)[16]
Delayed Neutrons (DN)[17]	Neutron Resonance Transmission Analysis (NTRA)[18]
Delayed Gamma (DG)[19]	Nuclear Resonance Fluorescence (NRF)[20]

Review Committee Process
Given the importance of an impartial and objective evaluation to inform the down-selection process, NGSI commissioned an external committee to conduct an in-depth peer review. This review committee was charged with assessing the maturity of each of the techniques at the time of the review and providing recommendations for future efforts. The complexion of the committee was chosen to provide a diversity of viewpoints, and the final committee included academics, technology development experts, and safeguards practitioners. The review committee members included:

- William S. Charlton, Texas A&M University, Chair
- Mark Abhold, Los Alamos National Laboratory
- Anthony Belian, International Atomic Energy Agency
- Alessandro Borella, Belgian Nuclear Research Centre
- Bryan Broadhead, Oak Ridge National Laboratory
- Daniel Decman, Lawrence Livermore National Laboratory
- William Geist, Los Alamos National Laboratory
- Sophie Grape, Uppsala University
- Young Ham, Lawrence Livermore National Laboratory
- Richard Kouzes, Pacific Northwest National Laboratory
- Roland Schenkel, Director General of Joint Research Centers of the European Union (retired)
- Jasmina Vujic, University of California at Berkeley

The committee was divided into two groups, one of which looked at the smaller, lighter, and less-expensive techniques (referred to as the *light* techniques): PNAR, SINRD, CIPN, AIPN, DDSI, NM, PG, and XRF. The other half focused on the larger, more expensive, but potentially more accurate techniques (referred to as the *accuracy* techniques): DG, DN, DDA, XRF, CIPN, NRTA, LSDS, and NRF. Note that CIPN and XRF were covered by both groups. The reviewers were provided with extensive written reports detailing the researchers' results from their modeling studies of each technique. In addition, a week-long review meeting was held for each grouping, at which researchers presented findings from the technique-by-technique evaluations and from which committee members provided recommendations to NGSI about the promise for each as part of an integrated NDA instrument.

Review Committee Findings

The review committee was impressed by both the depth and breadth of the research performed on these fourteen techniques. The committee was also impressed with the level of human capital that was produced by this program. There were a total of forty-nine researchers involved in the effort and twenty-six of those (more than half) were postdocs or students. This work will have a significant impact on safeguards technology development as well as safeguards human resource development. In reviewing these fourteen techniques, several important characteristics were observed, each of which had an important influence on the down-selection process.

The committee observed that many of the techniques are heavily driven by assembly sub-critical multiplication. The techniques most dependent on this are CIPN, DDSI, PNAR, DDA, and DN. In terms of technique integration, this could be either a hindrance or a benefit. If two techniques have a common physics component (e.g., multiplication), it may be possible to remove that component through the integration of these techniques; this would lead to more information being available about other physics components. This also could be a hindrance if there is too much similarity between two techniques because little might be gained through integration.

Also, the techniques have a tendency to either be quite similar (e.g., reliant on multiplication) or quite orthogonal (e.g., passive X-ray vs. active neutron). As a result, the committee noted that there exist two separate and possibly both fruitful options for integration. For techniques that are similar, data analysis might be used to cancel out the similar term and produce a more isolated data stream that could more directly correlate with the characteristics of interest. For the orthogonal techniques, integration will likely cover the deficiencies of each.

In addition, the committee noted that many of the techniques cannot measure Pu directly and instead measure total fissile content of the assembly. This total fissile content was for most techniques characterized by the researchers using a weighted average quantity called $^{239}Pu_{eff}$. This weighted average included a weighted sum of the main fissile isotopes in the assembly (namely, ^{235}U, ^{239}Pu, and ^{241}Pu). The concept of $^{239}Pu_{eff}$ is analogous to the $^{240}Pu_{eff}$ quantity regularly used by the IAEA in coincidence counting. However, $^{239}Pu_{eff}$ is more difficult to evaluate than $^{240}Pu_{eff}$ and would benefit from additional study.

Many of the techniques require some means to estimate relative concentrations of Pu isotopes in the spent fuel (in some cases just the ratio of $^{239}Pu/Pu$ but in other cases more detailed knowledge of isotopic distribution is required). The researchers expect to use reactor physics simulations to estimate these quantities, a reliance that could conceivably lead to verification issues. Thus, the committee recommended integration of techniques that would minimize reliance on reactor physics codes for the plutonium isotopic ratios.

The committee compiled a summary assessment of all of the techniques, the results of which are shown in Tables 3 and 4. The information in the tables is broken into five main areas: general characteristics of the detector system, the capability of that detector system to quantify desirable attributes of a PWR spent fuel assembly, the sensitivity of the detector system to pin diversions from a PWR spent fuel assembly, the independence of the technique's fissile mass quantification to other assembly parameters (burnup, cooling time, and initial enrichment), and an overall prioritization of the techniques for future work. The references in the table to "number of rows" is with respect to a PWR 17x17 fuel assembly counting from the outside of the assembly (row 1) to the center of the assembly (row 9). By assessing the orthogonal characteristics of different techniques out of these tables, it is straightforward to determine possible viable integration combinations.

For the light techniques, we find that all of these made use of mature hardware and thus the development time for all of them was short. Thus, maturity and development time were not significant differentiators. One can also see that only XRF had the ability to quantify elemental Pu; however, XRF had such low penetrability that its usefulness is predicated upon the accuracy of

reactor physics simulations to extrapolate the XRF signal across the assembly. Because of this weakness, it was ranked lower than some of the other techniques. Only SINRD had the ability to quantify individual Pu isotopes (as opposed to $^{239}Pu_{eff}$) and only the larger of the light techniques could penetrate deep within an assembly. Based on these characteristics, an obvious coupling that could prove fruitful in an integrated light technique system would be SINRD coupled to either PNAR, CIPN, or DDSI. PG might also prove useful since it can help to identify fission product absorbers, burnup, and cooling time rather easily.

For the accuracy techniques, there is strong differentiation between the techniques due to development time and hardware maturity. Some of these techniques will require more basic science and engineering development prior to system testing and analysis. DDA and DN have good penetrability and very practical implementation. DG had potentially lower penetrability but is generally independent of burnup, cooling time, and initial enrichment. For these reasons, DN, DDA, and DG could prove useful techniques for integration as well. In general, the information presented in these tables had a very strong influence on NGSI's deliberations in the down-selection process, which is described in more detail in the following section.

Table 2. Summary of reviewer assessments for *light* techniques

	PG	XRF	SINRD	DDSI	NM	PNAR-FC[a]	PNAR-^{3}He[b]	CIPN	AIPN
General Characteristics									
Time Required for Development	Short	Short	Short	Short	Short	Short	Short	Short	Short
Portable	Maybe	Maybe	Y	N	N	Y	N	N	N
Cost (High, Med, Low)[c]	L	M	M	M	M	L	M	H	L
Practical Implementation for Short Notice Inspection	Y	N	Y	N	N	Y	N	N[d]	N
Hardware Maturity	High	High	High	High	High	High	High	High	High
Quantification Ability in Assemblies for:									
Elemental Pu	N	Y	N	N	N	N	N	N	N
^{239}Pu	N	N	Y	N	N	N	N	N	N
^{235}U	N	N	Y	N	N	N	N	N	N
^{241}Pu	N	N	Maybe	N	N	N	N	N	N
^{240}Pu	N	N	Maybe	N	N	N	N	N	N
$^{239}Pu_{eff}$	N	N	Y	Y	Y	Y	Y	Y	Y
Fission product absorbers	Maybe	Maybe	N	N	N	N	N	N	N
Other actinide absorbers	Maybe	Maybe	N	N	N	N	N	N	N
$^{239}Pu_{eff}$ Quantification Penetrability (# rows)	3-5	<1	3-4	9	~9	3-6	3-6	9	9
Burnup	Y	Maybe	Y	Y	Y	Y	Y	Y	Y
Initial Enrichment	N	N	Maybe	N	N	N	N	N	N
Cooling Time	Y	N	N	N	N	N	N	N	N
Pin Diversion Sensitivity[e] (High, Med, Low) in:									
Outer Region (rows 1-2)	None	None	H	M	NR[f]	M	M	M	L
Middle Region (rows 3-5)	None	None	M	M	NR	M	M	M	L
Center Region (rows 6-9)	None	None	None	H	NR	L	L	M	L
For Fissile Mass Quantification is it Independent of:									
Burnup	N	Y	Y	N	N	N	N	N	N
Initial Enrichment	N	Y	Maybe	N	N	N	N	N	N
Cooling Time	N	Y	Maybe	N	N	N	N	N	N
Priority for More Work	4	5	1	2	8	3	7	6	9

a. This refers to a PNAR system constructed from fission chambers; this is the version of PNAR that was selected for further study by NGSI.
b. This refers to a PNAR system constructed from ^{3}He detectors; this version of PNAR was not selected for further study by NGSI.
c. Low is less than $300k, Medium is less than $1,000k, High is greater than $1,000k.
d. The ^{252}Cf source considered here is impractical for anything but a fixed installation, but this may be more practical with a DT or DD generator.
e. With substitution by U-bearing pins at 30 GWd/tU and five-year cooled.
f. No results for pin diversion sensitivity for NM were reported.

Down-Selection

Based on the aforementioned findings of the review committee, NGSI has down-selected among the original fourteen NDA techniques. In addition to the simplicity and dynamic range of each technique's response to spent fuel, the down-selection process also considered maturity, simplicity, and robustness as key factors. Consideration was also given to complementary features that could be exploited through integration, as recommended by the review committee. It must be emphasized that the elimination of any given technique does not represent a judgment on its standalone merit. Rather, it reflects the review committee's and NGSI's view of its ability to address spent nuclear fuel measurements in an operational environment in the near to medium term. This is a crucial point because some of the instruments had been studied in much greater detail than others as part of this effort.

The NGSI spent fuel project is now focused on the further development of four integrated systems with varying cost, size, robustness, and accuracy (Table 4). For each of these four systems, prototype construction will soon begin, and NGSI is pursuing field test opportunities with domestic and international partners.

Table 3. Summary of reviewer assessments for *accuracy* techniques

	DDA	DN	DG	LSDS	NRF	NRTA	XRF	CIPN
General Characteristics								
Time Required for Development	Short	Short	Medium	Medium	Long	Long	Short	Short
Portable	N	N	N	N	N	N	Maybe	N
Cost (High, Med, Low)[g]	H	H	H	H	H	H	M	H
Practical Implementation when Fixed in a Facility	Y	Y	Y	N	N	N	Y	Y[h]
Hardware Maturity	High	High	High	High	Low	High	High	High
Quantification Ability for Assemblies for:								
Elemental Pu	N	N	N	N	N	N	Y	N
^{239}Pu	N	N	Maybe	Maybe	Y	Y	N	N
^{235}U	N	N	Maybe	Maybe	Y	Y	N	N
^{241}Pu	N	N	Maybe	Maybe	Y	Y	N	N
^{240}Pu	N	N	N	Maybe	Y	Maybe	N	N
^{239}Pueff	Y	Y	Y	Maybe	Y	Maybe	N	Y
Fission product absorbers	N	N	Maybe	N	Maybe	Maybe	Maybe	N
Other actinide absorbers	N	N	Maybe	N	Maybe	Maybe	Maybe	N
^{239}Pueff Quantification Penetrability (# rows)	9	9	5	9	9	5-7	<1	9
Burnup	N	N	N	N	N	N	N	Y
Initial Enrichment	N	N	N	N	N	N	N	N
Cooling Time	N	N	N	N	N	N	N	N
Pin Diversion Sensitivity[i] (High, Med, Low) in:								
Outer Region (rows 1-2)	M	M	H	M	M	H	None	M
Middle Region (rows 3-5)	M	M	M	M	M	M	None	M
Center Region (rows 6-9)	M	M	L	M	M	L	None	M
Independence of (for Fissile Mass Quantification):								
Burnup	N	N	Y	Y	Y	NR[j]	Y	N
Initial Enrichment	N	N	Y	Y	Y	NR	Y	N
Cooling Time	N	N	Y	Y	Y	NR	Y	N
Priority for More Work	2	2	1	5	6	4	3	3

g. Low is less than $300k, Medium is less than $1,000k, High is greater than $1,000k.
h. Yes, with a DD generator, less practical with ^{252}Cf source.
i. With substitution by U-bearing pins at 30 GWd/tU, 5-year cooled.
j. Independence quantities were not reported for NRTA.

Table 4. Summary of integrated instrumentation packages selected for continued study as part of the NGSI spent fuel project. Note that TN refers to total neutron counting.

	Techniques	Key Attributes	Potential applications
1	PNAR SINRD PG TN	Passive Lightweight Relatively low cost Short measurement time Robust	Enhanced containment during shipment
2	CIPN SINRD PG TN	Active (source requires shielding) Lightweight Relatively low cost Short measurement time Robust	Input accountability for repository or reprocessing facility Recovery from loss of continuity of knowledge
3	DDSI SINRD PG TN	Passive Relatively heavy Intermediate cost Longer measurement time Robust	Input accountability for repository or reprocessing facility Recovery from loss of continuity of knowledge
4	DN DDA DG PG TN	Active Relatively heavy Relatively high cost Longer measurement time Less robust Potential for high accuracy	Input accountability for new reprocessing facility

Conclusions

The NGSI spent fuel nondestructive assay project is paving new ground in the development of safeguards technology. It is developing solutions to one of the most challenging safeguards problems: verification of bulk Pu content in spent fuel. This effort originally studied fourteen separate techniques that showed promise for meeting this challenge. A review committee was used to provide fair and informed input to the NGSI down-selection process, which has resulted in a selection of four integrated instruments for further study.

The review committee process was an excellent way of collecting expert analysis of the techniques, and it provided unbiased input to project management decisions. The committee reviewed research on each of the fourteen techniques in order to (1) quantify the expected capability of each technique as an independent instrument for producing safeguards-relevant information, and (2) provide recommendations on how to integrate several techniques together in order to determine elemental Pu mass and detect pin diversion. When reviewing work of this volume, a large review committee is invaluable (in this case, the committee consisted of twelve reviewers), and division of the committee into major focus areas made the process manageable.

The committee's overall impression was that the work performed by the researchers on this effort was impressive in both depth and breadth and will have a significant impact on safeguards technology development. The committee was also very impressed with the level of human capital that was developed by this program. The committee expects this project to continue to flourish as it moves into its next phases.

Dr. William S. Charlton serves as the director of the Nuclear Security Science & Policy Institute (NSSPI) at Texas A&M University (TAMU) and as an associate professor in the nuclear engineering department at TAMU. He previously served as an assistant professor at the University of Texas at Austin from 2000-2003 and as a technical staff member in the Nonproliferation and International Security Division at Los Alamos National Laboratory from 1998-2000. Dr. Charlton earned a Ph.D. in nuclear engineering from Texas A&M University. Dr. Charlton was named the George Armistead Jr. '23 Faculty Fellow at TAMU in 2005 and was awarded the Special Service Award from the Institute of Nuclear Materials Management in 2010.

Dr. Marc A. Humphrey is the acting team leader for the safeguards technology development subprogram of the Next Generation Safeguards Initiative (NGSI) in the Office of Nuclear Safeguards and Security at the U.S. Department of Energy's National Nuclear Security Administration (DOE/NNSA). He has B.S. degrees in physics and applied math from Western Michigan University and a Ph.D. in physics from Harvard University. Prior to joining DOE/NNSA, Dr. Humphrey worked at the United States Department of State in the Office of Nuclear Energy, Safety, and Security.

References

1. Humphrey, M. A., S. J. Tobin, and K. D. Veal. 2012. The Next Generation Safeguards Initiative's Spent Fuel Nondestructive Assay Project, *Journal of Nuclear Materials Management,* Vol. 40, No. 3.
2. Galloway, J. D., H. R. Trellue, M. L. Fensin, and B. L. Broadhead. 2012. Design and Description of the NGSI Spent Fuel Library with an Emphasis on Passive Gamma Signal, *Journal of Nuclear Materials Management,*Vol. 40, No. 3.
3. Gerhart, J. J., C. R. Freeman, J. L. Conlin, H. O. Menlove, and S. J. Tobin. 2012. Passive Neutron Albedo Reactivity with Fission Chambers (PNAR-FC), *Journal of Nuclear Materials Management* [remaining citation info to be completed at publication].
4. Hu, J., S. J. Tobin, H. O. Menlove, M. T. Swinhoe, and S. Croft. 2012. Developing The Californium Interrogation Prompt Neutron Technique to Measure Fissile Content and to Detect Diversion in Spent Nuclear Fuel Assemblies, *Journal of Nuclear Materials Management,* Vol. 40, No. 3.
5. Charlton, W. S., D. Strohmeyer, A. Stafford, S. Saavedra, A. S. Hoover, and C. Rudy. 2009. The Use of Self-Induced XRF to Quantify the Pu Content in PWR Spent Nuclear

Fuel, *Proceedings of 31st Annual Meeting of ESARDA.*
6. Freeman, C., V. Mozin, S. Tobin, M. Fensin, W. Charlton, H. Trellue, J. Galloway, and A. Rajasingam. 2010. Using X-Ray Fluorescence for Quantifying Plutonium Mass in Spent Fuel Assemblies, Report LA-UR-11-00513, Los Alamos National Laboratory, Los Alamos, New Mexico.
7. Romano, C., A. Stafford, A. Solodov, and M. Ehinger. 2010. Direct Measurement of Plutonium in Spent Fuel with X-Ray Fluorescence, Report ORNL/LTR-2010/344, Oak Ridge National Laboratory, Oak Ridge, Tennessee.
8. Richard, J., S. J. Tobin, J. Hu, and H. O. Menlove. 2010. Determining the Pu Mass in Low Enriched Uranium Spent-Fuel Assemblies Using Assembly Interrogation Prompt Neutron (AIPN) Detection, Report LA-UR-10-05383, Los Alamos National Laboratory, Los Alamos, New Mexico.
9. Fensin, M. L., S. J. Tobin, M. T. Swinhoe, H. O. Menlove, W. Koehler, N. P. Sandoval, S. Lee, V. Mozin, J. Richard, M. Schear, J. Hu, and J. Conlin. 2011. Determining the Pu Mass in LEU Spent Fuel Assemblies – Focus on Passive Gamma Detection, Report LA-UR-11-00511, Los Alamos National Laboratory, Los Alamos, New Mexico.
10. Romano, C., A. Solodov, and M. Ehinger. 2010. Passive Gamma Measurements for Verification of Operation Declarations for Spent Nuclear Fuel, Report ORNL/LTR-2010/343, Oak Ridge National Laboratory, Oak Ridge, Tennessee.
11. LaFleur, A. M., W. S. Charlton, H. O. Menlove, and M. Swinhoe. 2009. Development of Self-Interrogation Neutron Resonance Densitometry (SINRD) to Measure the ^{235}U and ^{239}Pu Content in a PWR 17x17 Spent Fuel Assembly, *Proceedings of 31st Annual Meeting of ESARDA.*
12. Hu, J., C. R. Freeman, A. L. LaFleur, H. O. Menlove, S. J. Tobin, H. R. Trellue, and T. J. Ulrich. 2012. Self-Interrogation Neutron Resonance Densitometry Performance in Measuring Fissile Content in Spent Fuel, *Journal of Nuclear Materials Management,* Vol. 40, No. 3.
13. Croft, S., L. G. Evans, M. A. Schear, and M. T. Swinhoe. 2010. Feasibility of Classic Multiplicity Analysis Applied to Spent Nuclear Fuel Assemblies, Report LA-UR-11-00512, Los Alamos National Laboratory, Los Alamos, New Mexico.
14. Menlove, H. O., S. H. Menlove, and S. J. Tobin. 2009. Fissile and fertile nuclear material measurements using a new differential die-away self-interrogation technique, *Nuclear Instruments and Methods in Physics Research Section A: Accelerators, Spectrometers, Detectors and Associated Equipment*, Volume 602, Issue 2, 21 April 2009, Pages 588-593
15. Henzl, V., M. T. Swinhoe, S. J. Tobin, and H. O. Menlove. 2012. Measurement of the Multiplication of a Spent Fuel Assembly with the Differential Die-Away Method within the Scope of the Next Generation Safeguards Initiative Spent Fuel Project, *Journal of Nuclear Materials Management,* Vol. 40, No. 3.
16. Smith, L. E., C. J. Gesh, K .K. Anderson, A. M. Casella, and M. W. Shaver. 2011. Lead Slowing-Down Spectroscopy for Direct Measurement of Plutonium in Spent Fuel, Report PNNL-20158, Pacific Northwest National Laboratory, Richland, Washington.
17. Blanc, P., H. O. Menlove, S. J. Tobin, S. Croft, and A. Favalli. 2012. An Integrated Delayed-Neutron, Differential-Die-Away Instrument to Quantify Plutonium in Spent Nuclear Fuel, *Journal of Nuclear Materials Management,* Vol. 40, No. 3.
18. Sterbentz, J. W., and D. L. Chichester. 2011. Further Evaluation of the Neutron Resonance Transmission Analysis (NRTA) Technique for Assaying Plutonium in Spent Fuel, Report INL/EXT-11-23391, Idaho National Laboratory, Idaho Falls, Idaho.
19. Mozin, V. V., B. Ludewigt, S. J. Tobin, A. Hunt, and L. Campbell. 2012. Delayed Gamma-Ray Assay for Spent Nuclear Fuel Safeguards, *Journal of Nuclear Materials Management,* Vol. 40, No. 3.
20. Ludewigt, B. A., B. J. Quiter, and S. D. Ambers. 2011. Nuclear Resonance Fluorescence to Measure Plutonium Mass in Spent Nuclear Fuel, Report LBNL- 4425E, Lawrence Berkeley National Laboratory, Berkeley, California.

Technical Cross-cutting Issues for the Next Generation Safeguards Initiative's Spent Fuel Nondestructive Assay Project

S. J. Tobin, H. O. Menlove, M. T. Swinhoe, P. Blanc, T. Burr, L. G. Evans, A. Favalli, M. L. Fensin, C. R. Freeman, J. Galloway, J. Gerhart, A. Rajasingam, E. Rauch, N. P. Sandoval, H. Trellue, T. J. Ulrich, J. L. Conlin, S. Croft, J. Hendricks, V. Henzl, D. Henzlova, J. M. Eigenbrodt, W. E. Koehler, M. A. Schear, D. W. Lee, T. H. Lee and M. A. Schear
Los Alamos National Laboratory, Los Alamos, New Mexico USA

M. A. Humphrey, Office of Nonproliferation and International Security, NNSA-DOE
U.S. Department of Energy, Washington, DC USA

L. E. Smith, K. K. Anderson, L. W. Campbell, A. Casella, C. Gesh, M. W. Shaver, and A. Misner
Pacific Northwest National Laboratory, Richland, Washington USA

S. D. Amber, B. A. Ludewigt, and B. Quiter
Lawrence Berkeley National Laboratory, Berkeley, California USA

A. Solodov, W. Charlton, J. M. Eigenbrodt, A. Stafford, and A. M. LaFleur
Texas A&M University, College Station, Texas USA

C. Romano, J. Cheatham, and M. Ehinger
Oak Ridge National Laboratory

S. J. Thompson, D. L. Chichester and J. L. Sterbent
Idaho National Laboratory, Idaho Falls, Idaho USA

M. A. Schear and J. Hu
University of Illinois, Champaign, Illinois USA

A. Hunt
Idaho State University, Pocatello, Idaho USA

W. E. Koehler
University of Michigan, Ann Arbor, Michigan USA

T. H. Lee
Korea Atomic Energy Research Institute, Daejon, South Korea

V. Mozin
Lawrence Livermore National Laboratory, Livermore, California USA

J. G. Richard
Massachusetts Institute of Technology, Cambridge, Massachusetts USA

L. E. Smith
International Atomic Energy Agency, Vienna, Austria

Abstract

Ever since there has been spent fuel (SF), researchers have made nondestructive assay (NDA) measurements of that fuel to learn about its content. In general these measurements have focused on the simplest signatures (passive photon and total neutron emission) and the analysis has often focused on diversion detection and on determining properties such as burnup (BU) and cooling time (CT). Because of shortcomings in current analysis methods, inspectorates and policy makers are interested in improving the state-of-the-art in SF NDA. For this reason the U.S. Department of Energy, through the Next Generation Safeguards Initiative (NGSI), targeted the determination of elemental Pu mass in SF as a technical goal. As part of this research effort, fourteen nondestructive assay techniques were studied. This wide range of techniques was selected to allow flexibility for the various needs of the safeguards inspectorates and to prepare for the likely integration of one or more techniques having complementary features. In the course of researching this broad range of NDA techniques, several cross-cutting issues were identified. This paper will describe some common issues and insights. In particular we will describe the following: (1) induced and non-induced fission-based techniques, (2) the role of neutron absorbers with emphasis on how these absorbers vary in SF as a function of initial enrichment, BU, and CT, as well as how some NDA techniques are more or less sensitive to neutron absorbers; (3) the need to partition the measured signal among different isotopic sources and why this partitioning indicates which NDA techniques best integrate; (4) the importance of the "first generation" concept in the context of both diversion detection and in the context of determining Pu mass because the first generation indicates both the spatial and isotopic origins of the detected signal; (5) the unique role played by ^{238}U and why in most cases it primarily acts as an amplifier of the signal generated by ^{235}U, ^{239}Pu, and ^{241}Pu.

Introduction

In the first two papers of this *JNMM* special issue, Humphrey et al. and Charlton et al. provide overviews of the Next Generation Safeguards Initiative's (NGSI) Spent Fuel (SF) Nondestructive Assay (NDA) Project and the Review Committee's process and conclusions, respectively. This paper complements these articles by providing technical detail on issues that are common to most of the NDA techniques such as the unique origin of each NDA signal, the partitioning of their respective signals, the role of neutron absorbers, and issues concerning integration among techniques.

The current suite of NDA techniques being researched as part of the NGSI SF NDA Project are the following: ^{252}Cf Interrogation with Prompt Neutron Detection (CIPN)[3], Delayed Gamma Rays (DG)[4], Delayed Neutrons (DN),[5] Differential Die-Away (DDA)[6] Differential Die-Away Self-Interrogation (DDSI),[7] Passive Gamma Rays (PG), Passive Neutron Albedo Reactivity (PNAR),[8] Self-Interrogation Neutron Resonance Densitometry (SINRD),[9] and Total Neutron (TN). Aside from the two techniques traditionally applied to SF (PG and TN), each of these has a separate report in the *JNMM* special issue.

Partitioning of the Measured Signal

It is possible to organize the NDA techniques under current investigation into two groups: **Group 1** includes all the techniques that derive their signal predominantly from the induced fission of ^{235}U, ^{239}Pu and ^{241}Pu (**CIPN**, **DG**, **DN**, **DDA**, **DDSI**, and **PNAR**). Due to the fact that the signal includes the combined contribution of three primary isotopes, we need to discern what fraction of the signal originates from each of these three fissile isotopes in order to quantify Pu mass. Note that most of these techniques could also include the contribution of ^{238}U in their signal if this was desirable, yet since the ^{238}U cross-section is extremely low below ~1 MeV, one can minimize fission in ^{238}U. For measurements made in water, and through the use of neutron spectrum tailoring, the ^{238}U contribution to the gross signal is less than 10 percent in all cases and can be subtracted from the gross signal as background.

Group 2 includes the remaining three NDA techniques (**SINRD**, **PG**, and **TN**). SINRD is unique among all the techniques. Through appropriately packaged fission chambers SINRD is able to measure the relative neutron flux in different regions of the neutron energy spectrum and, in some cases, leverage the unique resonance structure of the material in the fission chamber to quantify ^{235}U and ^{239}Pu. Unlike Group 1, the signal does not involve induced fission directly; rather, SINRD is sensitive to the absence of neutrons at a given energy relative to other parts of the energy spectrum. As such SINRD may be sensitive to neutron absorption in unique ways that are still under investigation. The signals from PG and TN are not generally used to quantify the fissile isotopes in isolation, but both provide information that is expected to improve the analysis of all the other techniques such as burnup (BU), cooling time (CT), and initial enrichment (IE). As such we anticipate that both PG and TN will be part of any integrated system. The PG signal measures the intensity of the gamma emission from a few fission products produced in the reactor; these gamma rays are the clearest indicator of reactor operation and as such provide useful information to help quantify properties of the fuel that are dependent on reactor operation (e.g., neutron absorbers). The TN signal is primarily proportional to the mass of ^{244}Cm times the net multiplication for these ^{244}Cm source neutrons.

Because our primary goal is to determine the elemental Pu mass, and because the net signal from all the techniques in Group 1 is a combination of at least three sub-signals from ^{235}U, ^{239}Pu, and ^{241}Pu, it is necessary to determine the relative contribution

*Technical reports for all 14 NDA techniques are available through correspondence with the author.

from each of these isotopes. For CIPN, DN, DDSI, and PNAR the response is a function of a linear sum of the signal from each of the isotopes given by the following:

$$^{239}Pu_{effective} = C_1 * ^{235}U + ^{239}Pu + C_2 * ^{241}Pu \quad (1)$$

where $^{239}Pu_{effective}$ is equivalent to the fissile content, C_1 and C_2 are weighting constants, and ^{235}U, ^{239}Pu, and ^{241}Pu represent the masses of the respective isotopes. The C_1 and C_2 constants weight the relative neutron production of the three fissile isotopes; therefore, they depend on fission cross section and neutron yield per fission. They are also impacted by the energy-dependent competition for neutrons among themselves and neutron absorbers in the fuel.

For DG, a different $^{239}Pu_{effective}$ equation could be determined for each DG peak, or the spectra could be analyzed using combinations of basis spectra for each of the fissile isotopes to best match the measured spectra. It may also be possible to determine weightings among the fissile isotopes by integrating the counts over broad regions of the DG spectra. For DDA, it appears that more than one $^{239}Pu_{effective}$ equation can be determined depending on the time interval of integration. It is also worth noting that simulations done at the fuel pin level indicate that DDSI has the capability to separate the mass of ^{235}U relative to ^{239}Pu; this is a topic of ongoing research to determine whether this capability is useful at the assembly level.

The Role of Neutron Absorbers

Especially for water-based interrogation, all the Group 1 techniques that generate their signal from induced fission are influenced by the presence of neutron absorbers in the fuel for two fundamental reasons: (1) most fissions occur at thermal energies due to the large fission cross sections at that energy, and (2) neutron absorption in non-fissile isotopes, relative to fissile isotopes, is significant at thermal energies. To illustrate this point, Figure 1 depicts two cases of simulated DDA signal[10] (i.e., count rate for all the assemblies of the NGSI SF library #1,[11] 0.2 to 1.0 ms gate). The black data points simulate the signal from each assembly with full isotopic detail; in particular the strongest 20 or more neutron absorbers are included. The gray data points simulate the signal from a virtual assembly containing only ^{16}O, ^{17}O, ^{235}U, ^{238}U, ^{239}Pu, and ^{241}Pu; in other words, the fission products and other actinides (between ~2 percent and ~8 percent of the mass) were removed while the density of the fuel was adjusted to account for this removal of mass.

Two conclusions can be drawn from Figure 1, and these can be generalized to all the techniques in Group 1 to varying degrees: (1) the presence of neutron absorbers significantly suppresses the count rate simply because the fission rate is suppressed; in the case of DDA this suppression is between a factor of 2 and 4 depending on the isotopic mixture of the assembly, and (2) the

Figure 1: DDA signal as a function of the ^{239}Pueffective mass (or fissile content) when sixty-four assemblies were simulated in water for two different cases. In case 1 (black points) the assemblies contained a wide range of isotopes. In case 2 (gray points) the assemblies contained only ^{16}O, ^{17}O, ^{235}U, ^{238}U, ^{239}Pu, and ^{241}Pu. The guidelines are for IE values of 2, 3, 4, and 5 percent, (from left to right).

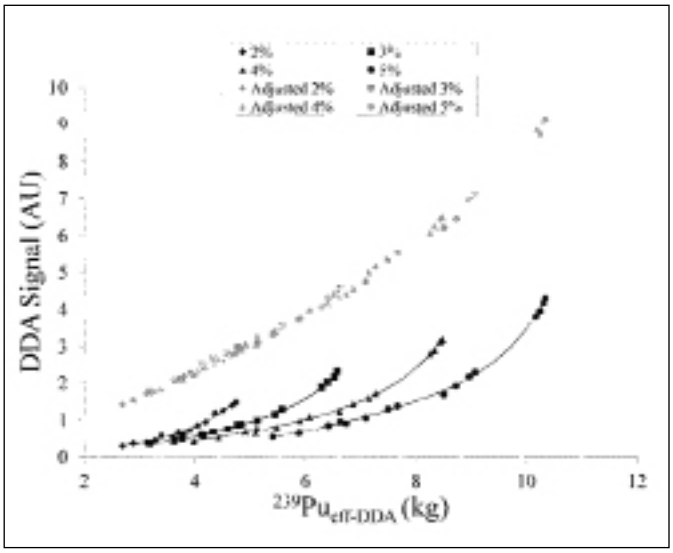

suppression of the count rate is a function of the assemblies' IE, BU, and CT, because the buildup of the significant absorbing isotopes is also a function of IE, BU, and CT. Focusing on the 5 percent IE case (rightmost guideline), four groups of four data points are observable. Each group of four represents a different BU. Within each BU are four CTs. The impact of the absorbers is expected to be roughly the same magnitude for CIPN, DN, DDA, and PNAR because all these techniques generate their signal by external neutron interrogation and because these neutrons undergo multiplication and absorption both on the way into the assembly and on the way out; it is worth mentioning that the "in and out" characteristic applies to PNAR even though the driving neutrons for PNAR originate in the fuel; this is due to the fact that PNAR involves a ratio of two measurement for which the only difference is thermal neutrons interrogating from the exterior.

It is expected that DG and DDSI will be less sensitive to neutron absorbers. In the case of DG, the measurement involves neutron transport from the interrogating source into the assembly but photon transport on the way out of the assembly – the latter having no sensitivity to neutron absorbers. In the case of DDSI, the interrogating source, ^{244}Cm, is embedded in the assembly so the transport only involved neutron transport out of the assembly. The magnitude of the reduction remains to be quantified for both techniques.

The role of neutron absorbers could be significantly reduced by making measurements in air and keeping the neutron energy spectrum elevated. However, for air measurements, fission in ^{238}U will likely dominate all fissions since it comprises approximately

95 percent of the heavy metal in a high-BU assembly (compared to ~1 percent ^{235}U, ~0.5 percent ^{239}Pu, and ~0.2 percent ^{241}Pu) and since, for ~2 MeV neutrons, the fission cross section of ^{238}U is within a factor of 2 to 4 of the fissile isotopes (compared to 7 orders of magnitude lower for thermal neutrons). Furthermore, due to the elevated cross sections of ^{235}U, ^{239}Pu, and ^{241}Pu at thermal energies, thermal fission is expected to be significant and as such neutron absorbers will still play a role in air measurements.

Integration Among Techniques

Following an initial side-by-side comparison among the original fourteen NDA techniques, the NGSI effort is now focusing on four different instruments that integrate techniques with complementary features: (a) PNAR/SINRD, (b) CIPN/SINRD, (c) DDSI/SINRD, and (d) DDA/DN/DG. In addition, PG and TN will be deployed with each integrated instrument.

To demonstrate the considerations that guided our integration of techniques into these four different instruments, it is instructive to compare the use of Equation 1 for both DN and DDA. For a fully burned assembly, the C_1 and C_2 values for DN were 1.54 and 2.90, respectively. For DDA (200 to 500 ms integration), the C_1 and C_2 values were 0.526 and 1.60, respectively. Interpreting these constants, one would expect 1 gram of ^{239}Pu to contribute as much to the DN count rate as 0.65 grams of ^{235}U. In contrast, for DDA one would expect 1 gram of ^{239}Pu to contribute as much to the DN count rate as 1.90 grams of ^{235}U. These mass differences indicate how the different physics of DN and DDA emphasize ^{239}Pu relative to ^{235}U and how these techniques therefore complement one another. In contrast, there is little benefit to integrating CIPN, DDA, DDSI, and PNAR since they weight a unit mass of ^{239}Pu and ^{235}U about the same. In other words, they have similar C_1 and C_2 constants: the values of C_1 in water for CIPN, PNAR, and DDA are 0.512, 0.551, and 0.526, respectively.

Integration with DN would have benefited CIPN, DDA, DDSI, and PNAR; however, since the same hardware for DDA can be used for DN, this is the natural option. Research to date on DG indicates that an analogous separation can be obtained between ^{239}Pu and ^{235}U among the most favorable of the strong, high-energy, DG lines. For this reason it makes sense to *integrate* DG with itself since systematic uncertainties are likely to be minimized by taking ratios of lines (assuming analysis of individual lines proves to be the preferred analysis approach). Obtaining better ^{235}U and ^{239}Pu separation is a point of active research for DG. Integration of CIPN and DN was also researched and proved to be technically viable; but the cost of the required size of the ^{252}Cf source rendered this approach impractical.

The decision to integrate CIPN, DDSI, and PNAR with SINRD was made to service the safeguards need for robust and relatively low-cost systems. It is worth noting that one could make a system with any one of these techniques combined with PG and TN and a BU simulation. The SINRD signature provides a unique signature while CIPN, DDSI, and PNAR provide diversion detection throughout the assembly since they are multiplication based techniques.

Since the net signal for each of the four integrated NGSI instruments will be a mixture of contributions from ^{235}U, ^{239}Pu, and ^{241}Pu (as indicated in Equation 1), there is the need to quantify three relationships among these isotopes. The research to date on integration is preliminary but some logical paths are clear. As noted, some of the NDA techniques respond noticeably differently to the three different isotopes. Other techniques, such as DG and DDA, may possibly provide enough information to minimize the need for integration with other techniques. Also, the ratio of ^{239}Pu to ^{241}Pu, which evolves as the fuel is burned in the reactor, can be inferred from estimates of IE, BU, and CT that will likely come from PG and TN.

Consider water-based measurements for the techniques in Group 1. All the techniques have a net signal that is roughly proportional to the fissile mass (Equation 1), particularly after a correction has been performed to account for the impact of neutron absorbers. Note that the net signal is obtained by subtracting out the contribution of small but non-negligible contributors to the signal, such as the direct fission of ^{238}U by the interrogating source.

The Group 1 techniques divide into sub-groups in terms of how each weights a given unit mass of ^{235}U, ^{239}Pu, and ^{241}Pu. CIPN, DDA, DDSI, and PNAR all involve prompt fission, which primarily weights isotopes according to their fission cross section and neutron emissions per fission. There is some energy-spectrum and spatial sensitivity, but these are relatively small effects. DG also depends on the fission cross section since the detected lines are emitted from fission products. Yet, due to fission product yield variation among ^{235}U, ^{239}Pu, and ^{241}Pu, the percentage of the signal that can be accredited to fission of these isotopes varies with each DG line. DN also depends on the fission cross section since the detected neutrons are also emitted from fission products. And like DG, the fission product yield varies among ^{235}U, ^{239}Pu, and ^{241}Pu. The big difference between DN and DG in this context is that DN has only one signal—the total delayed neutron count rate—and hence only one relationship like Equation 1. Conversely, analysis for the DG technique could use a relationship like Equation 1 for each DG line. It is for this reason that one should be able to use the DG signal, in isolation, to de-convolve the contribution from ^{235}U, ^{239}Pu, or ^{241}Pu using various DG lines. Alternatively, the de-convolution could be done by other analysis schemes.

In contrast, the signal from SINRD is unique. Its base signal involves detecting the relative absence of neutrons at a given part of the energy spectrum. In particular, the goal is to focus on energies where ^{235}U and ^{239}Pu are particularly strong absorbers. This unique physics brings with it its own unique interferences which are a subject of ongoing research.

Origin Of The Detected Signal

In order to quantify the Pu mass in an assembly from NDA signals, it is necessary to know both the isotopic mix that contributes to the net signal as well as the location from which the signal originated. The former point was covered in Section 2; the latter point is addressed in this section. It is necessary to understand the location from which the net signal originates because assemblies are not homogeneous due to the way they are irradiated in a reactor. It is also necessary to understand the spatial sensitivity of each NDA technique to understand its sensitivity to diversion. The lack of homogeneity is important because the various physics of the different techniques lead to net signals that weight certain pins in the assembly more than others. In Table 1 both the physics origin and the spatial origin of the detected signal for the six NDA techniques in Group 1 are listed. These techniques are of particular interest in that they all utilize neutron multiplication to some degree. As discussed below, this makes them particularly suited for detecting diversion. Note that CIPN, DN, and DDA were designed so that the pin-by-pin detection efficiency variation counteract, or balance, the fission gradient caused by the interrogating source. A similar approach could be applied to DG.

An important factor in understanding the detected signal from all of the Group 1 techniques is the role of neutron multiplication. This will be illustrated using two examples for a CIPN measurement: (A) The interrogating neutrons from the external ^{252}Cf source penetrate one side of the assembly, inducing fission primarily in the first ~3 rows; we call the neutrons resulting from fission induced by ^{252}Cf neutrons "first-generation" neutrons. (B) Not many of the neutrons produced in first-generation fissions are directly detected because the location where the fissions occurred is far from the detectors (recall the ^{252}Cf and the neutron detectors are on opposite sides of the assembly). Instead, because these first generation neutrons have an average energy of ~2 MeV (Watt fission spectrum), they penetrate in all directions, inducing fissions in all directions. Through this stepwise, multiplication-based process, the first generation neutrons will contribute to the signal.

The parts of the assembly where the processes A and B take place are different although they do overlap some. If a proliferator were to divert material from the region where process A dominates, he would have to match the neutron-production rate of relatively low-energy neutrons entering along one side of the assembly to match the response of the $^{239}Pu_{effective}$ in that region of the assembly. In the region where process B takes place, one would need to match the multiplication of Watt fission spectrum neutrons across the assembly. The latter case could take the form of replacing the center ~25 percent of the assembly with fresh LEU fuel that has identical prompt-neutron multiplication to the SF removed. The CIPN signal would not be altered by such a diversion. Yet, such a diversion would be detected in the total neutron count rate unless an appropriate amount of a neutron source such as ^{252}Cf or ^{244}Cm were also included. Neither passive gamma nor SINRD would be able to detect this diversion scenario directly, but Cherenkov glow would detect the diversion unless the proliferator inserted a sufficient gamma source in the top of the rod to produce the desired optical glow. Because this is a very complicated diversion scenario (matching multiplication, matching spontaneous fission source, creating sufficient Cherenkov glow), it has taken several NDA instruments working in concert to catch the diversion. It is desirable to minimize the number of instruments.

Table 1. Physics origin and physical location of the detected signal for the six NDA techniques in Group 1; the signals from all of these techniques are based on multiplication

Techniques	Physics Origin of Detected Signal	Location from which Signal Originated
CIPN	Prompt neutrons emitted from first-generation induced fission, where the neutron inducing the fission is from the external source (^{252}Cf).	Given the location of the ^{252}Cf source ~5 cm from the assembly, the vast majority of the detected signal originates in the ~3 rows nearest to the ^{252}Cf source.
DG	Delayed gamma rays emitted from a fission product produced during an active interrogation interval. No distinction is necessary among fission generation.	Multiplication of the neutrons originating from the neutron generator (NG) during the interrogation time produce fission products with a gradient that decreases with distance from the NG.
DN	Same as DG, except for neutrons rather than gamma rays.	Same as DG provided they have the same neutron generator setup.
DDA	Prompt neutrons emitted from first-generation induced fission, where the neutron inducing the fission was from the external neutron generator.	Given the location of the NG and spectrum tailoring, the vast majority of the detected signal originates in the rows nearest to the NG. The spatial distribution has a steeper gradient than DG or DN.
DDSI	Prompt neutrons emitted from first-generation induced fission, where the neutron inducing the fission was from the internal source (primarily ^{244}Cm).	Since the ^{244}Cm is relatively uniform in distribution about the assembly, and since multiplication effectively propagates neutrons out to the detectors, the DDSI signal is obtained from all the pins in the assembly in a nearly uniform distribution.
PNAR	Prompt neutrons emitted from first-generation induced fission, where the neutron inducing the fission was reflected back into the assembly; this external source has an energy below ~0.5 eV.	Given that the interrogating source is low in energy and is reflected from all sides of the assembly, the vast majority of the detected signal originates in the ~3 rows nearest to the exterior edges.

With a DN or DG instrument, the first generation starts with the neutrons or photons being emitted from fission fragments during the delayed radiation counting interval. Therefore, the distinction between processes A and B is no longer relevant. What is relevant is the location where fission occurs in the assembly. It does not matter what generation of fissions was created during the interrogation time. For this reason the first generation for DN and DG is more penetrating although it is still a gradient falling off away from the NG. This is an important feature in being able to detect the diversion scenario of fresh LEU being added to the center of the assembly. DN and DG would both emit a significantly different signal from the LEU region of the assembly. This "diverted signal" would compete with the non-diverted signal. For DG the photons would be attenuated as they propagate outward. For DN the signal would multiply as it propagated outward.

The PNAR signal would be very similar to the CIPN signal except that the signal comes from all sides. In the context of the fresh LEU diversion case, the response of DDA would be very similar to CIPN (assuming DDA only operated with one temporal window); it is anticipated that, by using different time intervals, DDA may be able to detect an LEU substitution. DDSI has one advantage over other techniques in that its signal is nearly uniform among all pins. It may also be possible to leverage the fact that, while the multiplication of LEU may match that of the spent fuel, the neutron multiplicity would not. Furthermore, the capability of DDSI to discern ^{235}U from ^{239}Pu according to the temporal distribution of detected neutrons has only been demonstrated for individual pins. The viability of such capability is a topic of current research.

A final topic that is of general interest to all multiplying techniques is fission in ^{238}U. This has been treated as a background term to be minimized so that the net signal will be proportional to the weighted sum of ^{235}U, ^{239}Pu and ^{241}Pu. It is important to note that the neutrons resulting from the fission of ^{238}U will be treated differently in the analysis depending on the technique and when ^{238}U experienced fission. The CIPN example in this section is useful to make this point. If ^{238}U fissioned during process A (i.e., ^{238}U fission is induced by a neutron originating from ^{252}Cf, and subsequent fissions result in detected neutrons), the ^{238}U neutrons need to be subtracted as background; one can think of these as *bad* ^{238}U fissions. However, for ^{238}U fissions that arise during process B (i.e., during subsequent fissions that start with a first-generation fission of ^{235}U, ^{239}Pu, and ^{241}Pu), the ^{238}U neutrons do not need to be subtracted because it is part of the multiplication process connecting the first generation to the detector; one can call these *good* ^{238}U fissions. Without the first-generation fission of ^{235}U, ^{239}Pu, or ^{241}Pu, fission in ^{238}U never would have been induced. The signals from DDA, PNAR, and DDSI are like that of CIPN since all these techniques involve prompt multiplication. However for DN and DG all ^{238}U fissions during the interrogation time interval are *bad* because any fissions at that time produce fission products that will emit radiation during the delayed counting interval. To summarize, fissions of ^{238}U during the delayed radiation counting interval are *good*, and fissions of ^{238}U during the interrogation time interval by neutrons from the NG are *bad*.

Conclusion

The goal of the NGSI SF Project is to improve the state-of-the-art in the NDA of SF. Quantifying the Pu mass in SF assemblies, while being able to detect diversion of material, is the unifying research focus. Techniques (Group 1) that involve the multiplication of neutrons are particularly well suited for probing the entire assembly; such techniques, particularly when implemented in water, also have signals that are a mixture of the three main fissile isotopes and have signals that are impacted by neutron absorption. In order to determine Pu mass we need to quantify both the contribution of the three main fissile isotopes as well as correct for neutron absorption. We expect the most accurate system will integrate a few complementary NDA techniques.

Acknowledgement

The authors would like to acknowledge the support of the Next Generation Safeguards Initiative (NGSI), Office of Nonproliferation and International Security (NIS), National Nuclear Security Administration (NNSA).

References

1. Humphrey, M. A., S. J. Tobin, and K. D. Veal. 2012. The Next Generation Safeguards Initiative's Spent Fuel Nondestructive Assay Project, *Journal of Nuclear Materials Management* ,Vol. 40, No. 3.
2. Charlton, W.S. and M.A. Humphrey. 2012. The Next Generation Safeguards Initiative's Spent Fuel Nondestructive Assay Project: External Review Committee Process and Findings, *Journal of Nuclear Materials Management* , Vol. 40, No. 3.

3. Hu, J., S.J. Tobin, H.O. Menlove, M.T. Swinhoe, and S. Croft. 2012. Developing The Californium Interrogation Prompt Neutron Technique to Measure Fissile Content and to Detect Diversion in Spent Nuclear Fuel Assemblies, *Journal of Nuclear Materials Management* , Vol. 40, No. 3.
4. Mozin, V.V., B. Ludewigt, S.J. Tobin, A. Hunt, L. Campbell. 2012. Delayed Gamma Ray Assay for Spent Nuclear Fuel Safeguards, *Journal of Nuclear Materials Management* [remaining citation info to be completed at publication].
5. Blanc, P., H.O. Menlove, S.J. Tobin, S. Croft, and A. Favalli. 2012. An Integrated Delayed-Neutron, Differential Die-Away Instrument to Quantify Plutonium in Spent Nuclear Fuel, *Journal of Nuclear Materials Management,* Vol. 40, No. 3.
6. Henzl, V., M. T. Swinhoe, S. J. Tobin, and H. O. Menlove. 2012. Measurement of the Multiplication of a Spent Fuel Assembly with the Differential Die-Away Method within the Scope of the Next Generation Safeguards Initiative Spent Fuel Project, *Journal of Nuclear Materials Management,* Vol. 40, No. 3.
7. Belian, A., H. O. Menlove, M. T. Swinhoe, and S. J. Tobin. 2012. New Design of the Differential Die-Away Self-Interrogation Instrument, *Journal of Nuclear Materials Management,* Vol. 40, No. 3.
8. Gerhart, J.J., C.R. Freeman, J.L. Conlin, H.O. Menlove, and S.J. Tobin. 2012. Passive Neutron Albedo Reactivity with Fission Chambers (PNAR-FC), *Journal of Nuclear Materials Management,* Vol. 40, No. 3.
9 Hu, J., C.R. Freeman, A.L. LaFleur, H.O. Menlove, S.J. Tobin, H.R. Trellue, and T.J. Ulrich. 2012. Self-Interrogation Neutron Resonance Densitometry Performance in Measuring Spent Fuel, *Journal of Nuclear Materials Management,* Vol. 40, No. 3.
10 Lee, T. H., H. O. Menlove, M. T. Swinhoe, and S. J. Tobin. 2011. "Monte Carlo Simulations of Differential Die-Away Instrument for Determination of Fissile Content in Spent Fuel Assemblies," *Nuclear Instruments and Methods in Physics Research* A 652, pp.103-107, 2011.
11 Galloway, J. D., H. R. Trellue, M. L. Fensin, and B. L. Broadhead. 2012. Design and Description of the NGSI Spent Fuel Library with an Emphasis on Passive Gamma Signal, *Journal of Nuclear Materials Management*, Vol. 40, No. 3.

Design and Description of the NGSI Spent Fuel Library with Emphasis on the Passive Gamma Signal

Jack D. Galloway, Holly R. Trellue, and Michael L. Fensin
Los Alamos National Laboratory, Los Alamos, New Mexico USA

Bryan L. Broadhead
Oak Ridge National Laboratory, Oak Ridge, Tennessee USA

Abstract

One goal of the Next Generation Safeguards Initiative Spent Fuel Project is to estimate the amount of plutonium in an assembly using nondestructive assay (NDA). For the purpose of quantifying how a wide range of NDA techniques are expected to perform as a function of various reactor conditions (initial enrichment, burnup, and cooling time), two sets of virtual spent fuel assemblies in the form of MCNP (Monte Carlo N particle transport code) input files were developed to represent pressurized water reactor (PWR) assemblies under those conditions. The first library was created using infinitely reflected boundary conditions for four different values of initial enrichment, burnup, and cooling time (sixty-four total combinations). The second library consisted of more realistic irradiation conditions with a 1/8 core geometry model of a PWR with shuffling of fuel assemblies and more realistic combinations of input parameters. Several different assembly-shuffling sequences were examined, and impacts of shuffling assemblies (moving the assemblies to different locations within the core) on the resulting passive gamma count rate are explored in this paper. The main goal of these spent fuel libraries is to predict isotopic concentrations within each pin of a fuel assembly under expected operational conditions. These concentrations are then used to assist in the design and assessment of the various candidate NDA instrument techniques, primarily evaluated through further MCNP simulations. The passive gamma geometry used to simulate the detector response involved a two-step process using MCNP. In the first step, we computed the energy-dependent photon spectrum crossing a collimator face in the direction toward the detector. This spectrum was then used as the source for a detector response calculation. This same process was performed for each of the three sides of the assembly in the second library, thus generating three passive gamma signals for each assembly using various values of initial enrichment, burnup, and cooling time, since each side of the assembly will emit unique signals dependent on the shuffling sequence employed. This approach for passive gamma signal estimation was performed for each side of each assembly in the second library so that a large database for cross-checking passive gamma signals could be created.

Introduction

According to the model comprehensive safeguards agreement with the International Atomic Energy Agency,[1] the key technical objective of international nuclear safeguards is "… the timely detection of diversion of significant quantities of nuclear material from peaceful nuclear activities … and deterrence of such diversion by risk of early detection." In support of this objective, a five-year research effort was begun in March 2009 by the Next Generation Safeguards Initiative (NGSI) of the U.S. Department of Energy.[2] Initial efforts have been invested in Monte Carlo N-particle (MCNP or MCNPX) simulations of various detector designs. One item of great importance to the accurate assessment of the effectiveness of a particular nondestructive assay (NDA) technique is the isotopic composition in the spent fuel assemblies being analyzed. To allow for a direct and systematic comparison of different techniques, we have developed a set of virtual spent fuel libraries that include isotopic distributions spanning a broad range of parameters.[15] A large number of isotopes important to all of the techniques are available; only a select few are missing because of a lack of cross-section data.

The first phase of spent nuclear fuel modeling in support of the NGSI effort included significant effort by Fensin et al. in the creation of Spent Fuel Library number 1 (SFL1)[3] using the MCNPX in-line burnup (BU) capabilities.[4] The simulation was performed using a generic 17x17 PWR fuel bundle with reflective boundary conditions on all sides and 1/8 assembly symmetry. In an effort to more accurately capture the asymmetric spectral effects resulting from a fuel shuffling sequence (defined below), a second spent fuel library (SFL 2a)[5] was developed, which utilizes increased computational capabilities coupled with new updates in MCNPX 2.7.d2 that reduce memory requirements,[6] to allow more realistic core shuffling sequences to be modeled. Using SFL2a and two alternate shuffling sequences (2 and 3), additional virtual assemblies were generated for the assessment of the effects of spatial BU variation on signal for numerous NDA techniques, including passive gamma, which we describe later in this paper. These effects were induced by the simulation of fuel rotation (core loading patterns) in which one side of the assembly sees a higher neutron flux (i.e., gradient) than other sides, as opposed

Table 1. Combinations of IE and BU included in the NGSI Spent Fuel Libraries. For SFL1, CT values of one, five, twenty, and eighty years were used. For the remaining libraries, CT values included fourteen days, one, five, twenty, forty, and eighty years

IE/BU	2wt%	3wt%	4wt%	5wt%	MOX
Fresh	*	*	*	*	*
15 GWd/MTU	XO	XO	XO^	XO	
30 GWd/MTU	XO	XO	XO^	XO	
45 GWd/MTU	X	X	XO^	XO	
60 GWd/MTU	X	X	X	XO	

X = Library #1 * = Library #2b
O = Library #2 ^ = Library #2c, 3

to the initial approach of reflective boundary conditions, which is symmetric on all sides yet less realistic.

The asymmetric BU distribution computed in SFL2 presented a more realistic starting point for performing passive gamma simulations in support of bundle average BU estimation in comparison to that available in SFL1. Numerous studies have been performed investigating the accuracy of passive gamma measurements for BU determination including work by Hsue et al.,[7] Tsao and Pan, [8] · Fensin et al.,[9,12,13] and Phillips and Bosler.[11] In this study, we characterize he variability in passive gamma signal intensity as a function of fuel shuffling. In addition the difference in passive gamma signal as a result of two different detector geometries is investigated.

Description of Spent Fuel Libraries

The first spent fuel library created in support of the NGSI effort simulated irradiation of an infinitely reflected assembly with four radial fuel regions per pin. SFL1 included a fully populated matrix consisting of four initial enrichments (IE) at 2, 3, 4, and 5 wt percent, four BU values of 15, 30, 45, and 60 GWd/MTU, and four cooling times (CT) of one, five, twenty, and eighty years (see Table 1). In the creation of the second spent fuel library, some virtual assemblies were removed since they represented an unrealistic reactor operation. We removed assemblies that had simultaneously high BU (45, 60 GWd/MTU) and low IE (2, 3 wt percent), as well as the virtual assemblies with 4 wt percent IE and 60 GWd/MTU. For those assemblies that remained, the number of CT values was increased to include fourteen days as well one, five, twenty, forty, and eighty years. SFL2a, which comprises this matrix of values, was generated by following one assembly through three cycles of irradiation in a 1/8 core PWR model with only one radial region per fuel pin.[5]

To better understand sensitivities to different shuffling sequences, two additional simulations were performed to create SFL2c (SFL2b will be described shortly). Instead of running these assemblies over the full suite of conditions described above, these sensitivity studies utilized only an IE value of 4 wt percent, BU values of 15, 30, and 45 GWd/MTU, and CTs of one, five, twenty, and eighty years. The second shuffling sequence was chosen to closely mimic traditional core shuffling practices (the highest burned fuel on the periphery being the most important), creating a second set of assemblies to compare to the results from SFL2a. In contrast, the third shuffling sequence utilized an older rotation pattern, which started with one bundle of fresh fuel on the core periphery. This choice, while undesirable from the standpoint of fuel cycle economics, served to create a very strong BU gradient across the bundle allowing for studies of the sensitivity to one of the most extreme conditions conceivable in modern day light water reactor operation. This bundle was rotated back to an internal location in the core after the first cycle, which was terminated at15 GWd/MTU.

Two other libraries were also generated as part of the NGSI spent fuel effort: SFL2b and SFL3, which analyze (1) real-life assemblies that may be measured as part of the NGSI program, and (2) assemblies with variations such as burnable poisons and changes in temperature, respectively.

SFL2b contains MCNP input files that represent: (1) fresh fuel in a PWR lattice for UO_2 with enrichments of 2 wt percent, 3 wt percent, 4 wt percent, 5 wt percent and two sample mixed oxide (MOX) fuel compositions, and (2) realistic assemblies that may be measured as part of the NGSI effort. Note that SFL2b is still under development and will not be further described here.

SFL3 returns to the infinitely reflected geometry used in SFL1 but only contains one radial fuel region. Variations examined relative to the base case are: boron concentration in the moderator, presence of burnable absorber rods and/or boron coating on fuel rods, moderator density and temperature, and fuel temperature.

Different codes were used to produce the various libraries: SFL1 used the MCNPX depletion capability at LANL,4 SFL2 (parts a, b, and c) employed *Monteburns*, a linkage code between MCNP and CINDER90 at LANL,5 and SFL3 used the SCALE/TRITON capability at Oak Ridge National Laboratory (ORNL). MCNP performs high-fidelity calculations for any type of reactor but requires relatively long run times. *Monteburns* was chosen because it still uses MCNP but offers the flexibility of fuel rotation schemes, while the ORNL code has the capability of performing a high number of sensitivity studies in a relatively short amount of time. Passive gamma calculations were currently only performed for SFL1 and SFL2a/2c. Thus, the other two libraries are only mentioned briefly in this paper.

SFL 2a & 2c Shuffling Sequences

Figure 1 illustrates the shuffling sequence used for SFL2a. Bundle type 2 is the bundle of interest for simulation purposes. This bundle was modeled as individual pins (with axial reflection) for both BU and transport purposes. For each of the other nine bundles (1, 3-10) each assembly was burned as a homogeneous region with each pin treated separately for transport purposes. Computational limitations were the reason for this simplification, as

Figure 1. SFL2a shuffling sequence 1 (default)

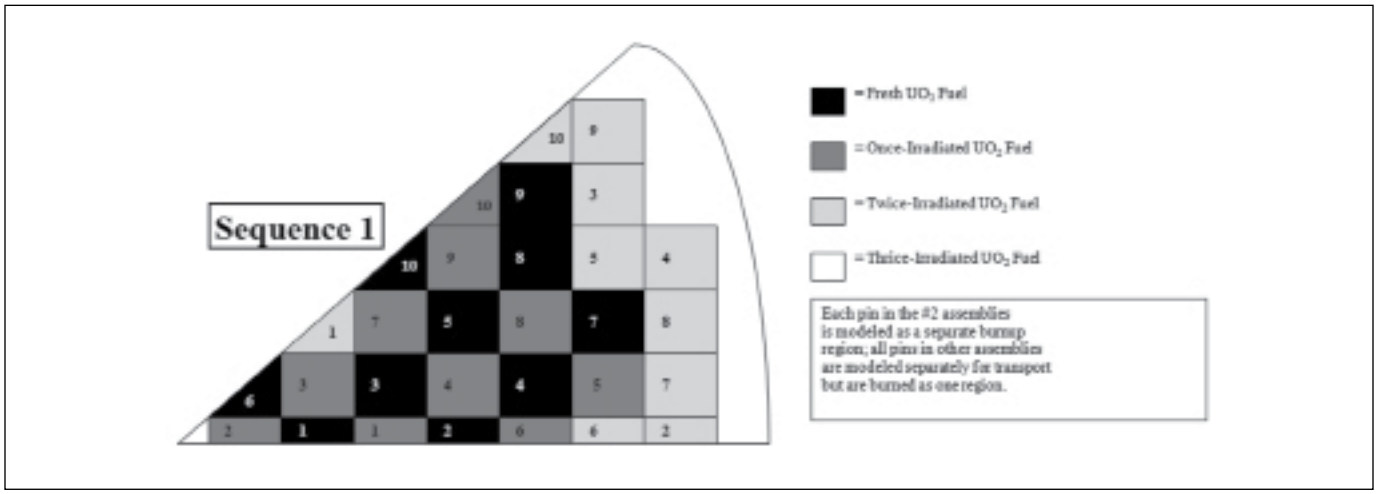

Figure 2. SFL 2c shuffling sequences 2 and 3

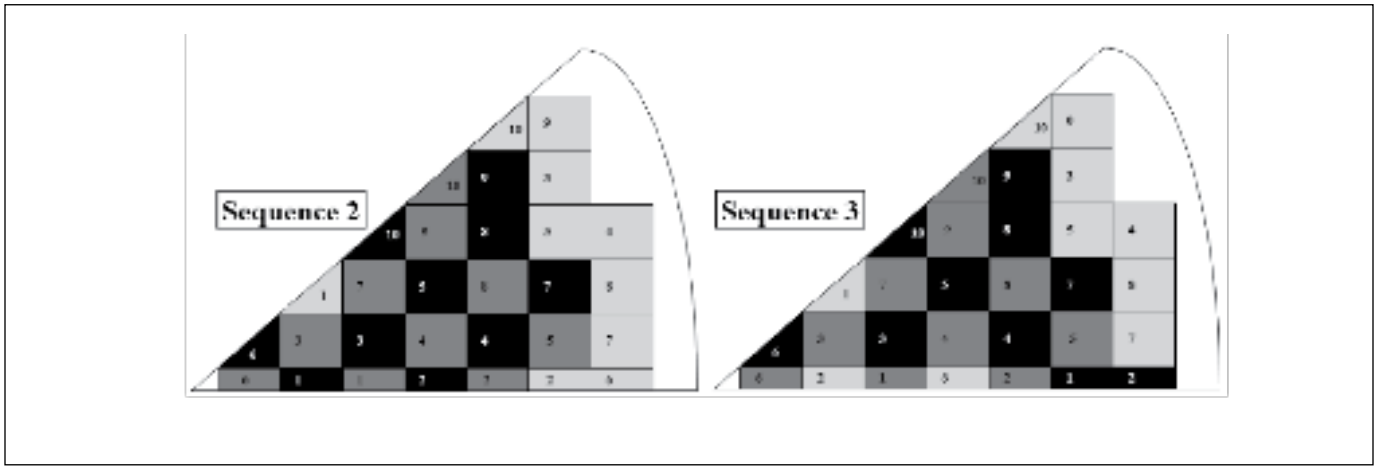

opposed to modeling each pin as independent burn regions. In this shuffling sequence it is observed that the fresh bundle starts in the core interior, rotates to another internal fuel location for the second cycle before being moved to the core periphery for the final cycle, following traditional core loading practices.

Figure 2 illustrates the alternate shuffling sequences 2 and 3 in SFL2c. In sequence 2 a similar rotation pattern was used as in SFL2a. In this case, the bundle starts on the core interior as a fresh bundle, moves to an alternate interior location after one cycle, and then is shuffled to the core exterior for the final cycle. In contrast, shuffling sequence 3 follows a more dated pattern that diverts from current practice. In this case the fresh bundle starts on the core edge and is adjacent to a fresh assembly, inducing a strong BU gradient across the bundle. While this would not be traditionally adopted from the perspective of fuel cycle economics, this case represents an extreme example of strong BU spatial gradients, whereas most assemblies will have much smaller gradients than those seen in shuffling sequence 3.

SFL2a Burnup Profile

Figure 3 shows the BU map at 15 and 30 GWd/MTU for the 2 wt percent IE as well as 30 and 45 GWd/MTU for the 4 wt percent IE case. For the 2 wt percent case and 3 wt percent IE case (not shown because its behavior is similar to 2 wt percent IE), the bundle gradient was stronger at 15 than at 30 GWd/MTU, having a maximum to minimum radial percentage change in BU across the assembly of nearly 30 percent at 15 GWd/MTU and 13-15 percent at 30 GWd/MTU. Visually apparent is also the change in the gradient from the left side being more highly burned than the right side, primarily driven by the second cycle during which a fresh bundle was adjacent on the right edge while a thrice-burned bundle was adjacent on the left side. This caused a relative flattening of the bundle spatial BU profile in the second cycle.

While the bundle appears to have an absence of water rods/guide tubes, this is not the case. A total of twenty-five guide tubes were present in the simulation, however in order to better view the BU trends, the BU for the cells pertaining to water rods was

Figure 3. SFL2a BU distributions for IE values of 2 wt percent and 4 wt percent

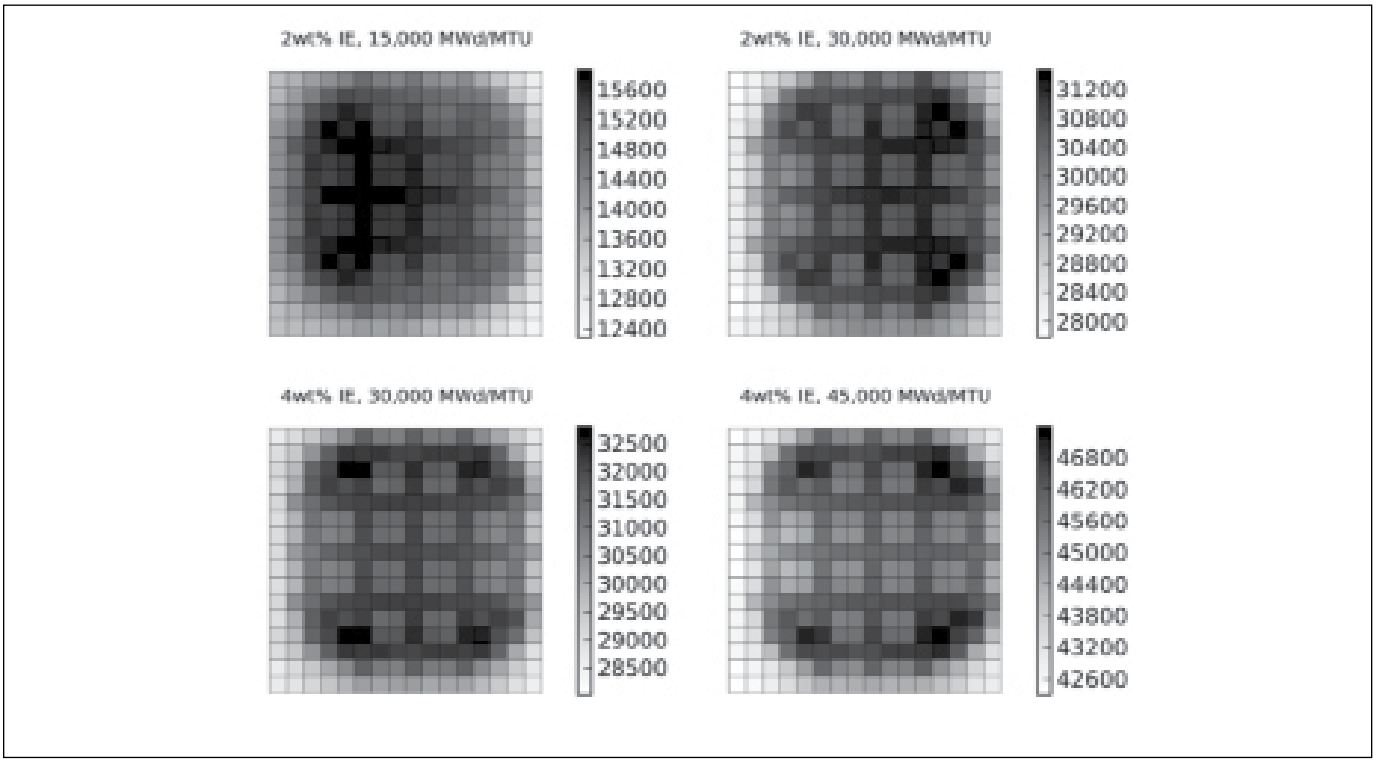

Figure 4. SFL2a BU distributions for an IE value of 5 wt percent

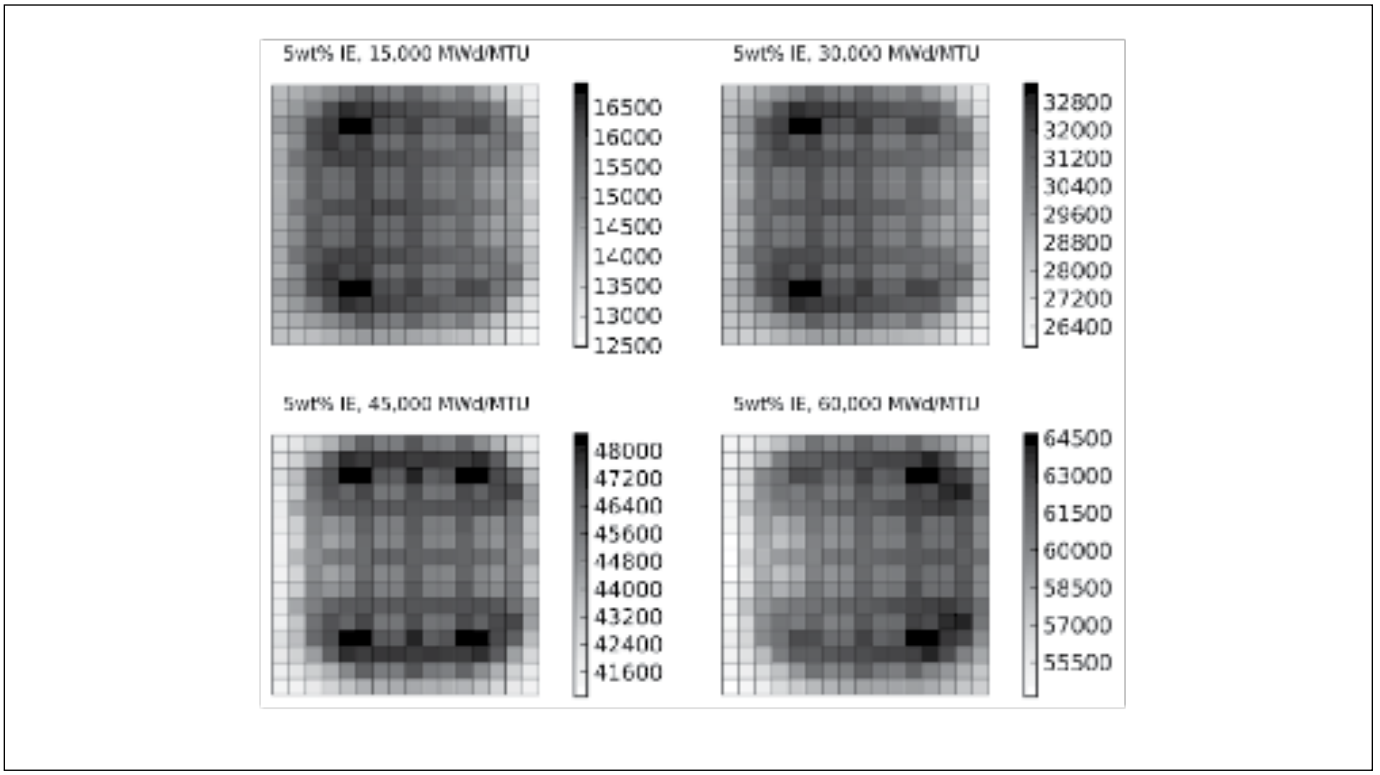

Figure 5. SFL 2c BU distributions for shuffling sequence 2 (top row) and 3 (bottom row) for an IE value of 4 wt percent

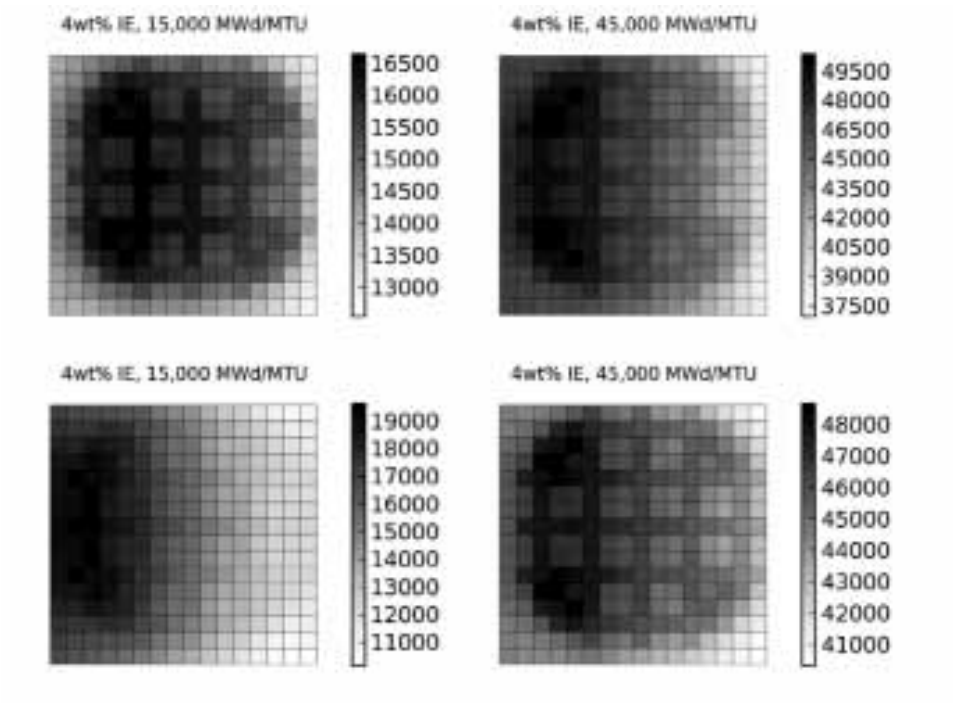

set to be the average of the four face adjacent fuel pins. The strong effect of these guide tubes upon BU distribution is observed by the BU distribution being stronger in the bundle interior. The strong moderating effect of the water in the guide tubes causes the fuel pins in the vicinity to take advantage of higher cross sections and thus achieve higher level of BU than fuel pins located further away, such as at the edge of the bundle, thus in a bundle with reflective boundary conditions a spatial variation will be present due to guide tube contributions, but no bundle BU gradient will exist since each side of the bundle will experience the same neutron flux.

Regarding the 4 wt percent IE results, the percentage change across the bundle decreased from ~30 percent (for a BU of 15 GWd/MTU) to 17 percent (for 30 GWd/MTU) to 12 percent (for 45 GWd/MTU). A similar trend is observed as previous with the gradient being left to right at 15 GWd/MTU before flattening out in later cycles. At 30 GWd/MTU, it should be noted that there is almost no gradient across the bundle; the percentage changes within the bundle primarily occur in fuel rods next to guide tubes that contain water, which slow neutrons down in energy, increasing the probability of neutron fission and thus overall burnup. At 45 GWd/MTU, even greater flattening across the assembly occurs as any residual fissile material is consumed to produce the required power and the bundle is rotated to the outside, a particularly inactive region of the core. The slight radial variation that occurs during this cycle is because one side of the assembly is next to a fuel assembly and the other side next to the periphery of the core (i.e., water).

Figure 4 illustrates the distribution at higher BU values for SFL2a at 5 wt percent IE. In this case, the percentage change across the bundle decreases from ~35 percent (for 15 GWd/MTU,) to 29 percent (for 30 GWd/MTU) and to 19 percent (for both 45 and 60 GWd/MTU). The deviation from the previous observed trends are because BU values of 30 GWd/MTU are achieved during the first cycle, and once shuffled, more even irradiation of the assembly occurs. The nearly identical bundle gradient for both 45 and 60 GWd/MTU is due to a similar scenario. Once the bundle was shuffled to the once-burned fuel location the BU was again put on quite rapidly with 60 GWd/MTU being reached at the same time the rotation to the core periphery was occurring.

SFL2c and Sequence 2 and 3 Burnup Profiles

The primary difference between the first and second shuffling sequence is that in the second sequence the fuel bundle is shuffled in a manner to induce the same gradient throughout the in-core lifecycle of the bundle. From the fresh fuel position, to once-burned, to twice-burned, the bundle face on the left side is exposed to a more reactive environment. This effect is observed in Figure 5: at all BU values there is a noticeable gradient across the bundle, which is most pronounced at 45 GWd/MTU. The relative difference across the bundle decreases from 33 percent (for 15 GWd/MTU) to 30 percent (for 30 GWd/MTU), but then

Figure 6. Sequence 2 plutonium concentration (in g) for a BU value of 15 GWd/MTU

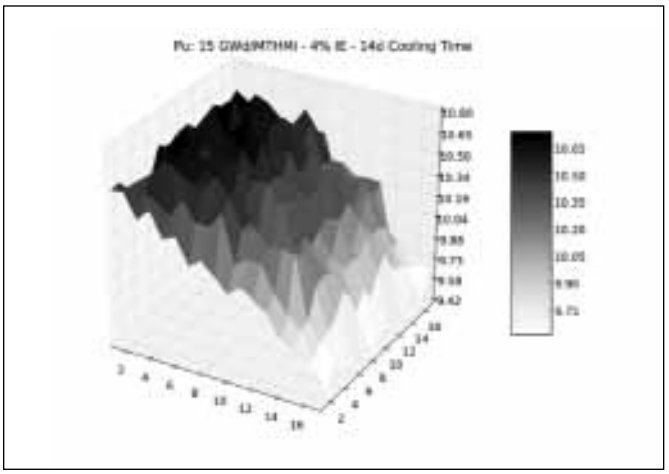

Figure 7. Sequence 2 plutonium concentration (in g) for a BU values of 45 GWd/MTU

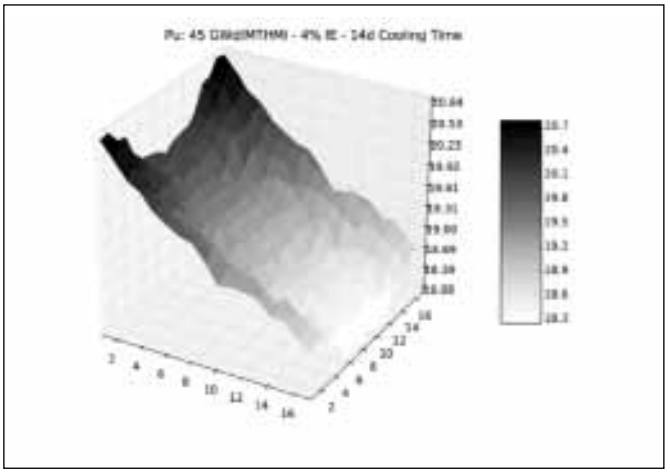

Figure 8. Sequence 2 ^{239}Pu concentration (in g) for a BU values of 15 GWd/MTU

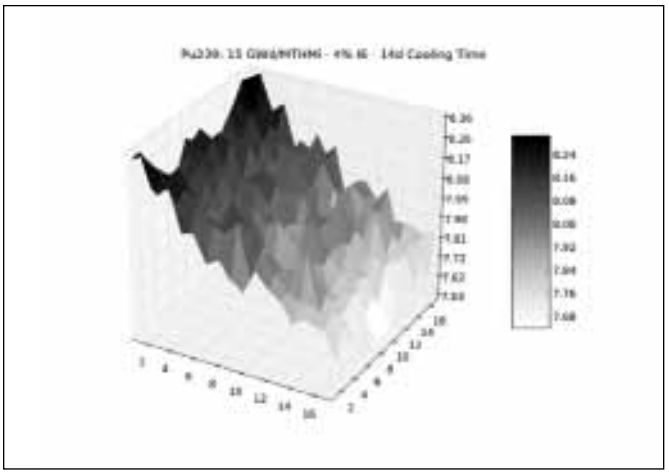

Figure 9. Sequence 2 ^{239}Pu concentration (in g) for a BU value of 45 GWd/MTU

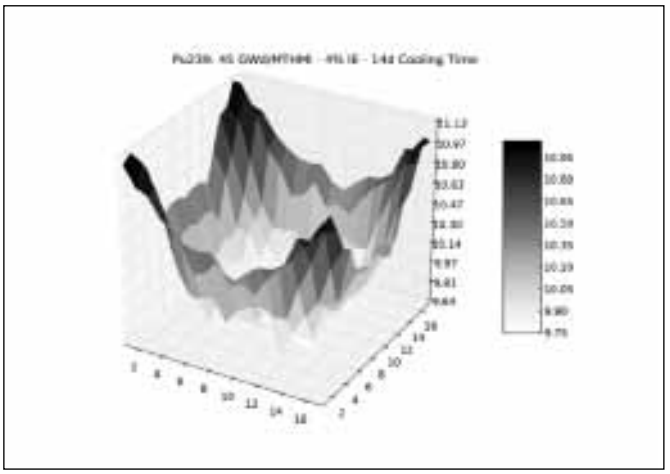

increases to 36 percent with the most pronounced gradient for 45 GWd/MTU. This persistent BU gradient provides an alternative to the previous fixed-bundle average BU cases for the evaluation of the sensitivity of NDA techniques. In the example of 45 GWd/MTU, for sequence 1 the maximum and minimum pin BU values were 47,000 and 42,000 MWd/MTU. In comparison, for sequence 2 the maximum and minimum pin BU values were 50,000 and 37,000 MWd/MTU. The different neutron energy distributions to which these bundles were exposed will cause spatial variation in isotopic distributions.

As mentioned previously the last shuffling sequence contained the strongest gradients to better gauge the sensitivity of NDA techniques to strongly asymmetric assemblies. Seen in Figure 2, the shuffling sequence placed the assembly on the core periphery adjacent to a fresh bundle. This caused severe gradients across the bundle, primarily at 15 GWd/MTU, observed in the second row of plots in Figure 5. With a minimum BU of 10,000 MWd/MTU and a maximum of 19,500 MWd/MTU, the relative difference across the bundle was 93.5 percent, which is nearly a two-fold difference between the maximum and minimum values. After being placed on the core periphery the bundle was then shuffled to internal locations which allowed for a flattening of the BU distribution, although a left-to-right gradient is observable at all BU values. At 30 GWd/MTU the relative difference dropped to 37 percent before reducing further to 20 percent at 45 GWd/MTU.

Shuffling Impact on Plutonium Distribution

The proliferation concern associated with plutonium is well known, and one item of interest is the difference in Pu accumulation as a result of shuffling procedures. The Pu distribution, as a function of shuffling sequence for a given BU, can inform NDA instrument performance requirements because this characterizes the range of expected variability in Pu concentration. For a BU

Figure 11. Passive gamma measurement geometry

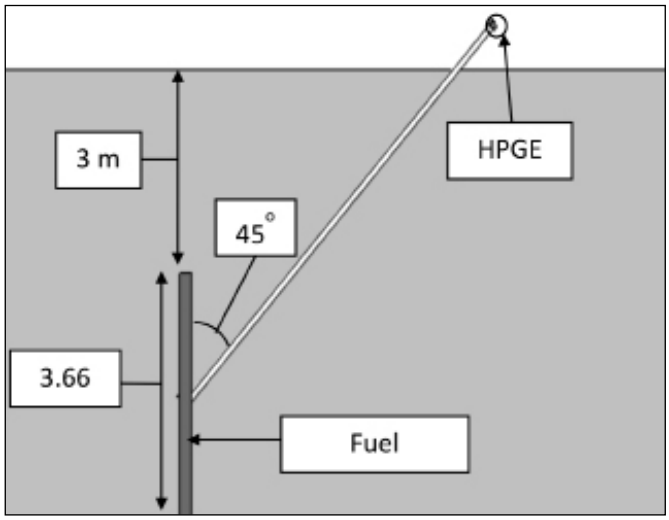

Figure 12. Bundle geometry

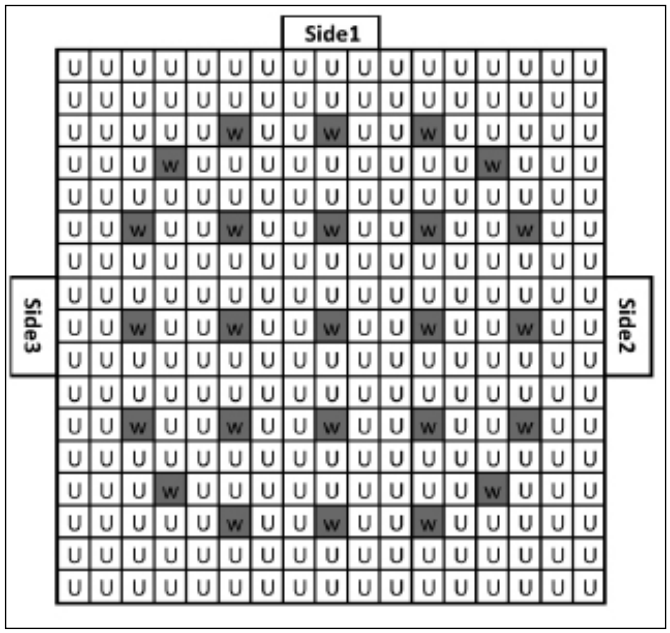

of 15 GWd/MTU, the value with the largest variability due to the shuffling practices employed, the total Pu accumulation for shuffling sequence 2 is 6.8 percent higher than that for shuffling sequence 3. At this BU the majority of this elemental Pu concentration is driven by ^{239}Pu accumulation, which accounts for 77 percent of elemental Pu. However, at higher BU values, for which ^{235}U is further depleted within the assembly, the isotopic contribution of ^{239}Pu drops to 63 percent at 30 GWd/MTU and 53 percent at 45 GWd/MTU. Yet, ^{239}Pu is still the most abundant Pu isotope. The nearly 7 percent difference in elemental Pu accumulation, observed at 15 GWd/MTU BU, between shuffling sequences 2 and 3 is decreased to 1.5 percent for 45 GWd/MTU.

One further observation noted about the Pu distribution is the shift in spatial concentration from low to high BU values, as seen in Figure 6 and Figure 7 for elemental Pu. At lower BU, power production comes primarily from ^{235}U and Pu tends to build up near the guide tubes which are internally located. As the reactor operates, ^{235}U is consumed and Pu (primarily ^{239}Pu) contributes increasingly to fission energy. The spatial concentration of Pu is higher towards the bundle edge, where higher energy neutrons cause increased ^{238}U neutron capture and fewer thermal neutrons are present to induce ^{239}Pu fission.

This shift in Pu concentration towards the bundle edge is most clearly seen in Figure 8 and Figure 9, illustrating the shift in ^{239}Pu from a fairly uniform distribution at 15 GWd/MTU to a heavily edge-weighted distribution that is highest at the corners.

Passive Gamma (PG) Simulations

Passive gamma techniques in NDA for spent nuclear fuel have been investigated and used for BU determination for several decades.[7-13] Given this pedigree, passive gamma will likely be integrated into all instruments studies as part of the NGSI effort. In support of this effort, accurate measurements of assembly-averaged BU, IE, and CT are desired. The intent is to couple this passive gamma information with simulated data obtained from other NDA techniques to provide a more accurate estimate of plutonium mass. Due to the asymmetric effects introduced during fuel shuffling sequences, passive gamma will need to be applied to multiple sides of an assembly, either on all four sides or four corners of the assembly, or potentially even more locations depending on how accurate a result is needed. Because of computational limitations, for SFL2a/2c one-half assembly reflection symmetry was employed and PG simulations were required on only three sides of the assembly. In simulations performed with reflective boundary conditions on all sides, the PG signal would be identical on each side of the assembly, however since a fuel shuffling sequence was employed with reflection on only one side, the result is that three sides of the assembly were each exposed to different neutron fluxes.

Figure 10 shows the geometry for a potential PG field measurement, where a high purity germanium detector (HPGe) is located at the end of a long evacuated collimator. Due to the difficulty of solving this radiation transport problem, we made certain simplifications, which primarily included tallying the photon spectrum 100 cm out from the bundle edge as an estimation of the expected spectrum 6.5 m up the tube, when simulating this geometry. In addition, we simulated a second geometry that included a HPGe detector placed close to the edge of the fuel. Figure 11 shows which pins contain fuel and which are guide tubes ("w") in the assemblies under study.

Pin Contributions to PG Signal

Using the radiation transport code MCNPX and the newly developed tally tag feature (an ability to track information about

Figure 13, PG signal importance map at side 2 edge; values are shown relative to the 662 keV peak of ^{137}Cs

0.00%	0.00%	0.00%	0.00%	0.00%	0.00%	0.00%	0.00%	0.00%	0.01%	0.01%	0.01%	0.01%	0.01%	0.02%	0.03%	0.08%
0.00%	0.00%	0.00%	0.00%	0.00%	0.00%	0.00%	0.00%	0.00%	0.01%	0.03%	0.03%	0.02%	0.03%	0.04%	0.06%	0.14%
0.00%	0.00%	0.00%	0.00%	0.00%	0.00%	0.00%	0.00%	0.00%	0.01%	0.02%	0.00%	0.09%	0.06%	0.09%	0.13%	0.25%
0.00%	0.00%	0.00%	0.00%	0.00%	0.00%	0.00%	0.00%	0.01%	0.01%	0.03%	0.06%	0.10%	0.00%	0.18%	0.30%	0.51%
0.00%	0.00%	0.00%	0.00%	0.00%	0.00%	0.00%	0.01%	0.01%	0.03%	0.04%	0.08%	0.21%	0.41%	0.38%	0.62%	1.15%
0.00%	0.00%	0.00%	0.00%	0.00%	0.00%	0.00%	0.01%	0.00%	0.02%	0.06%	0.00%	0.18%	0.42%	0.00%	1.46%	2.80%
0.00%	0.00%	0.00%	0.00%	0.00%	0.00%	0.01%	0.01%	0.02%	0.04%	0.08%	0.14%	0.27%	0.58%	1.25%	2.77%	6.50%
0.00%	0.00%	0.00%	0.00%	0.00%	0.01%	0.01%	0.02%	0.03%	0.06%	0.11%	0.22%	0.40%	0.70%	1.59%	3.82%	11.07%
0.00%	0.00%	0.00%	0.01%	0.01%	0.00%	0.02%	0.04%	0.00%	0.08%	0.19%	0.00%	0.47%	1.36%	0.00%	4.68%	13.04%
0.00%	0.00%	0.00%	0.00%	0.00%	0.01%	0.01%	0.02%	0.03%	0.06%	0.11%	0.22%	0.40%	0.70%	1.59%	3.82%	11.07%
0.00%	0.00%	0.00%	0.00%	0.00%	0.00%	0.01%	0.01%	0.02%	0.04%	0.08%	0.14%	0.27%	0.58%	1.25%	2.77%	6.50%
0.00%	0.00%	0.00%	0.00%	0.00%	0.00%	0.00%	0.01%	0.00%	0.02%	0.06%	0.00%	0.18%	0.42%	0.00%	1.46%	2.80%
0.00%	0.00%	0.00%	0.00%	0.00%	0.00%	0.00%	0.01%	0.01%	0.03%	0.04%	0.08%	0.21%	0.41%	0.38%	0.62%	1.15%
0.00%	0.00%	0.00%	0.00%	0.00%	0.00%	0.00%	0.00%	0.01%	0.01%	0.03%	0.06%	0.10%	0.00%	0.18%	0.30%	0.51%
0.00%	0.00%	0.00%	0.00%	0.00%	0.00%	0.00%	0.00%	0.00%	0.01%	0.02%	0.00%	0.09%	0.06%	0.09%	0.13%	0.25%
0.00%	0.00%	0.00%	0.00%	0.00%	0.00%	0.00%	0.00%	0.00%	0.01%	0.03%	0.03%	0.02%	0.03%	0.04%	0.06%	0.14%
0.00%	0.00%	0.00%	0.00%	0.00%	0.00%	0.00%	0.00%	0.00%	0.01%	0.01%	0.01%	0.01%	0.01%	0.02%	0.03%	0.08%

Figure 14. PG signal importance map 100cm from side 2 edge; values are shown relative to the 662 keV peak of ^{137}Cs

0.00%	0.00%	0.00%	0.00%	0.00%	0.00%	0.00%	0.00%	0.00%	0.00%	0.00%	0.00%	0.00%	0.00%	0.00%	0.00%	0.00%
0.00%	0.00%	0.00%	0.00%	0.00%	0.00%	0.00%	0.00%	0.00%	0.00%	0.00%	0.00%	0.00%	0.00%	0.00%	0.00%	0.00%
0.00%	0.00%	0.00%	0.00%	0.00%	0.00%	0.00%	0.00%	0.00%	0.00%	0.00%	0.00%	0.00%	0.00%	0.09%	0.00%	0.00%
0.00%	0.00%	0.00%	0.00%	0.00%	0.00%	0.00%	0.00%	0.00%	0.00%	0.00%	0.00%	0.00%	0.00%	0.05%	0.05%	0.00%
0.00%	0.00%	0.00%	0.00%	0.00%	0.00%	0.00%	0.00%	0.00%	0.00%	0.00%	0.00%	0.00%	0.00%	0.00%	0.00%	0.00%
0.00%	0.00%	0.00%	0.00%	0.00%	0.00%	0.00%	0.00%	0.00%	0.00%	0.00%	0.00%	0.00%	0.05%	0.00%	0.00%	0.05%
0.00%	0.00%	0.00%	0.05%	0.05%	0.05%	0.09%	0.18%	0.18%	0.23%	0.14%	0.09%	0.18%	0.42%	0.65%	1.94%	4.80%
0.00%	0.00%	0.00%	0.00%	0.09%	0.00%	0.09%	0.14%	0.23%	0.14%	0.14%	0.23%	0.14%	0.65%	1.34%	4.66%	16.56%
0.00%	0.00%	0.00%	0.00%	0.00%	0.00%	0.09%	0.00%	0.00%	0.18%	0.28%	0.00%	0.65%	1.57%	0.00%	6.37%	23.43%
0.00%	0.00%	0.00%	0.00%	0.09%	0.00%	0.09%	0.14%	0.23%	0.14%	0.14%	0.23%	0.14%	0.65%	1.34%	4.66%	16.56%
0.00%	0.00%	0.00%	0.05%	0.05%	0.05%	0.09%	0.18%	0.18%	0.23%	0.14%	0.09%	0.18%	0.42%	0.65%	1.94%	4.80%
0.00%	0.00%	0.00%	0.00%	0.00%	0.00%	0.00%	0.00%	0.00%	0.00%	0.00%	0.00%	0.00%	0.05%	0.00%	0.00%	0.05%
0.00%	0.00%	0.00%	0.00%	0.00%	0.00%	0.00%	0.00%	0.00%	0.00%	0.00%	0.00%	0.00%	0.00%	0.00%	0.00%	0.00%
0.00%	0.00%	0.00%	0.00%	0.00%	0.00%	0.00%	0.00%	0.00%	0.00%	0.00%	0.00%	0.00%	0.00%	0.05%	0.05%	0.00%
0.00%	0.00%	0.00%	0.00%	0.00%	0.00%	0.00%	0.00%	0.00%	0.00%	0.00%	0.00%	0.00%	0.00%	0.09%	0.00%	0.00%
0.00%	0.00%	0.00%	0.00%	0.00%	0.00%	0.00%	0.00%	0.00%	0.00%	0.00%	0.00%	0.00%	0.00%	0.00%	0.00%	0.00%
0.00%	0.00%	0.00%	0.00%	0.00%	0.00%	0.00%	0.00%	0.00%	0.00%	0.00%	0.00%	0.00%	0.00%	0.00%	0.00%	0.00%

the last reaction a particle underwent), an importance map for PG simulations was developed to indicate which pins were significantly contributing to the PG signal. First shown in Figure 13 is the result for the geometry of HPGe measurements close to the assembly edge. Highlighted in the map are any contributions greater than or equal to 1 percent of the total signal; these results were determined for a SFL2a assembly with 4 wt percent IE, 45 GWd/MTU BU and five-year CT.

This importance map looks distinctly different for measurements simulated using the long collimated geometry. Because there were insufficient computational resources to simulate the significant attenuation of this case, photon tallies were performed at two different locations in the collimator tube: one at the circular, 2.5 cm radius, collimator face, and one at a location of 100 cm from the assembly inside the collimator tube. In each of these instances the importance maps show either the decrease or increase in relative importance of the pins within the assembly. The results for the 100 cm tally are shown in Figure 14. All importance maps are shown relative to the 662 keV peak of ^{137}Cs.

Figure 15. SFL2a gamma spectra

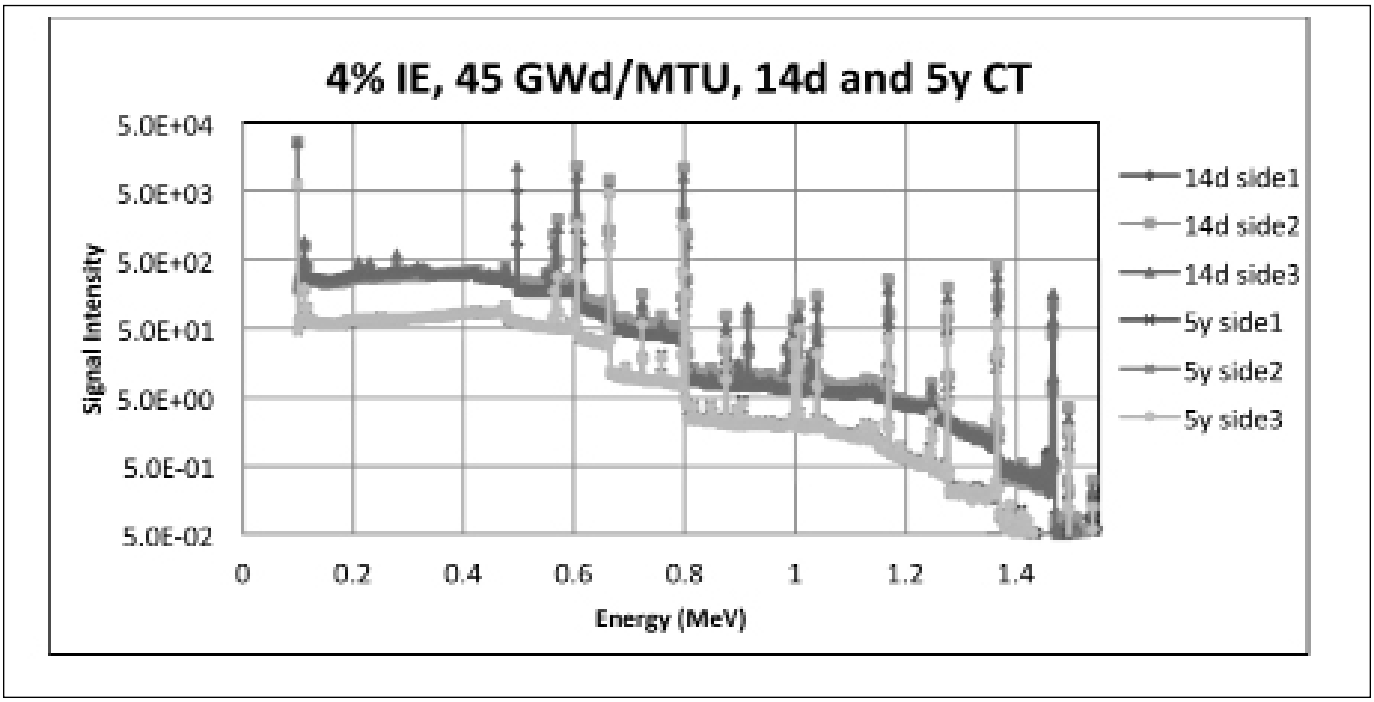

The effect of moving from bundle edge to 100 cm causes the significant contribution to only come from those pins that are directly in line with the collimator face, thus those pins possessing a solid angle aligned with the collimator outlet become the primary contributors. Although the count rate is likely to be prohibitively large, scanning near the bundle edge the detector will get a better estimate of the contribution of the outer third of the bundle which accounts for nearly 90 percent of the total signal, whereas in the long collimated case the detector sees almost solely the ten fuel pins near the collimator face which account for 85 percent of the total signal with the closest five fuel pins accounting for 66 percent.

PG Asymmetric Results

Figure 15 shows the PG spectra for SFL2a assemblies with 4 wt percent IE, 45 GWd/MTU BU and fourteen-day and five-year CT. After only 14 days of CT, the fuel had strong asymmetries when comparing signal strength from the three sides. In comparing the continuum around 660 keV, it was observed that the signal from the three sides of the assembly varied by 20 percent and 40 percent when compared to the least reactive side. However, after five years of CT, the short-lived fission products decayed away and this difference was greatly reduced to 1.7 percent and 2.8 percent, respectively.

Figure 16 contrasts the irradiation history of the previous bundle where a relatively flat BU distribution was observed with the history for the 15 GWd/MTU assembly for shuffling sequence 3. In this case the steep BU gradient was intentionally introduced and the effects were quite noticeable. There was a relative difference of 48 percent in signal intensity (with respect to the 662 keV ^{137}Cs peak) from side three to side two as well as a 12.8 percent difference in intensity from side one to side two, illustrating the strong dependence the passive gamma signal has on the BU distribution. While not shown here, it was noted that by 45 GWd/MTU for shuffling sequence 3, a more even BU distribution had developed across the assembly. This was evident in reduced signal variation for the ^{137}Cs peak, having a 5.5 percent difference from side three to side two and a 0.75 percent difference from side one to side two.

Conclusion

Three different libraries have been created for the NGSI effort to characterize the response of various NDA instruments to spent fuel assemblies. The majority of previous calculations were performed using spent fuel library one (SFL1), which inherently has no gradient due to the use of reflective boundary conditions on all sides but represented an approximation of BU, IE, and CT effects. To better support advanced NDA instrument design, spent fuel library two (SFL2) was developed based on more realistic assembly parameters and fuel shuffling schemes. Three different shuffling schemes were simulated for assemblies with 4 wt percent IE and up to 45 GWd/MTU to allow for determination of instrument sensitivity to various core shuffling patterns. In particular, shuffling sequence three employed atypical shuffling practices to deliberately create a strong BU gradient to help bound the domain space of potential shuffling

Figure 16. SFL2c, shuffling sequence 3 gamma spectra

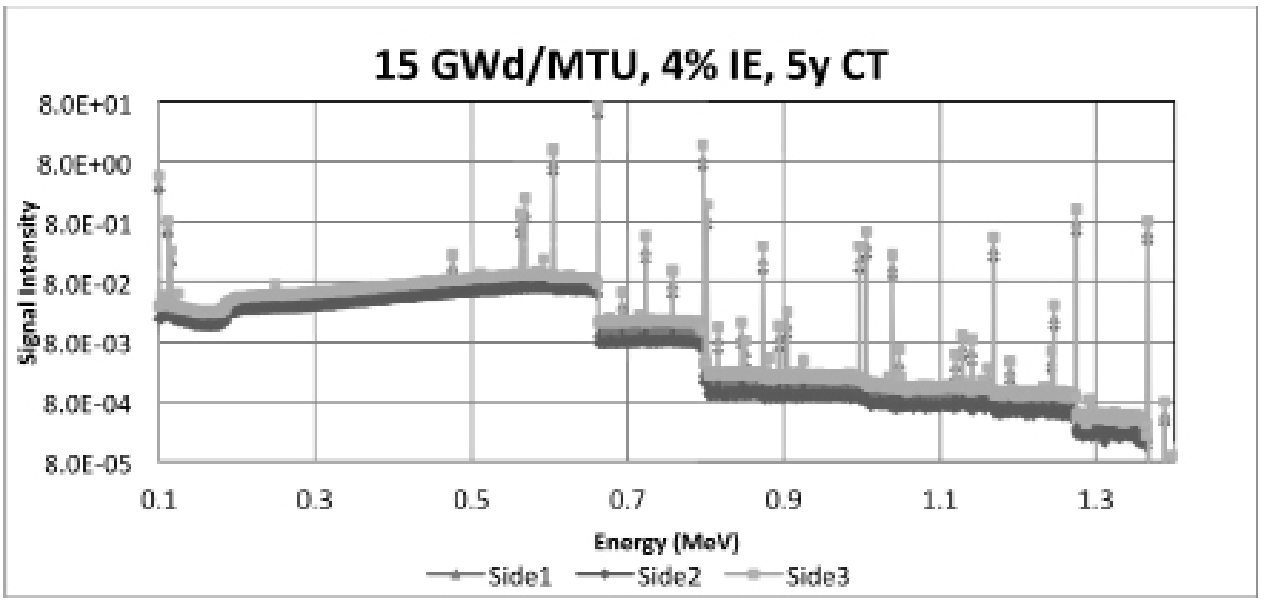

anomalies that instruments need to be qualified for. Isotopic information was well characterized across the assemblies such that any isotopic trends important to either instrument design or proliferation concerns could be assessed. The final spent fuel library (three) provided data to analyze variations in fuel assembly behavior that may result from reactor operation.

We have also simulated passive gamma measurements at the bundle edge and at the end of a collimator tube. We assessed the sensitivity to fuel-shuffling practices and observed the sensitivity to short-lived fission products. Passive gamma signals were calculated for every combination of IE, CT, and BU values in SFL 2a and 2c on all three sides of the assembly, in order to generate a comprehensive library of passive gamma signals. Additionally the characterization of which pins contribute significantly to the passive gamma signal was performed for both detector geometries. For a detector located near the bundle face, the first three rows of fuel pins dominated the signal, accounting for nearly 90 percent of the total signal with the three closest fuel pins accounting for 35 percent. For a detector at the end of a collimator tube, the closest ten fuel pins account for 85 percent of the total signal and 66 percent accounted for in the closest five pins, reducing the overall bundle contribution but also allowing for better fidelity for characterizing local regions of a fuel bundle.

Acknowledgements

The authors would like to acknowledge the support of the Next Generation Safeguards Initiative (NGSI), Office of Nonproliferation and International Security (NIS), National Nuclear Security Administration (NNSA).

References

1. International Atomic Energy Agency. 1972. *The Structure and Content of Agreements Between the Agency and States Required in Connection with the Treaty on the Non-Proliferation of Nuclear Weapons, INFCIRC/153 (corrected)* (Vienna, IAEA), paragraph 28.
2. Humphrey, M. A., S. J. Tobin, and K. D. Veal. 2012. The Next Generation Safeguards Initiative's Spent Fuel Nondestructive Assay Project, *Journal of Nuclear Materials Management,* Vol. 40, No. 3.
3. Fensin, M. L., S. J. Tobin, N. P. Sandoval, S. J. Thompson, and M. T. Swinhoe. 2009. A Monte Carlo Linked Depletion Spent Fuel Library for Assessing Varied Nondestructive Assay Techniques for Nuclear Safeguards, *Los Alamos National Laboratory Report: Full Paper: LA-UR 09-01188,* Proceedings of the American Nuclear Society's Advances in Nuclear Fuel Management IV.
4. Fensin, M. L., J. S. Hendricks, and S. Anghaie. 2010. The Enhancements and Testing for the MCNPX 2.6.0 Depletion Capability, *Journal of Nuclear Technology,* 170, pp. 68-79.
5. Trellue, H. R. 2011. Description of Irradiated UO_2 Fuel Compositions Generated for NGSI Spent Fuel Libraries, *Los Alamos National Laboratory Report: LA-UR 11-0030* (January 2011).
6. Fensin, M. L. 2009. MCNPX Memory Reduction Patch—FY 2009, *Los Alamos National Laboratory Report: LA-UR-09-06308* (October 2009).

7. Hsue, S. T., T. W. Crane, W. L. Talbert, and J. C. Lee. 1978. Nondestructive Assay Methods for Irradiated Nuclear Fuels, *Los Alamos National Laboratory Report: LA-6923*, Los Alamos, NM (1978).
8. Tsao C. S., and L. K. Pan. 1993. Reevaluation of the Burnup of Spent Fuel Pins by the Activity Ratio of $^{134}Cs/^{137}Cs$, *Application of Radiation and Isotopes*, 44, pg. 1041-1046.
9. Fensin, M. L., S. J. Tobin, M. T. Swinhoe, and H. O. Menlove. 2009. Quantifying the Passive Gamma Signal from Spent Nuclear Fuel in Support of Determining the Plutonium Content in Spent Fuel with Nondestructive Assay, *Proceedings of the Institute of Nuclear Materials Management 50th Annual Meeting.*
10. Reilly, D., N. Ensslin H. Smith, and S. Kreiner. 1991. *Passive Nondestructive Assay of Nuclear Materials,* NUREG/CR-5550, Washington, DC (1991)
11. Phillips, J. R., and G. E. Bosler. 1994. Calculated Response Contributions of Gamma Rays Emitted from Fuel Pins in an Irradiated PWR Fuel Assembly, *Los Alamos National Laboratory Report: LA-9837-MS,* Los Alamos, New Mexico.
12. Fensin, M. L., W. E. Koehler, and S. J. Tobin. 2010. MCNPX Simulation of a Passive Prompt Gamma System to be Used in a Spent Fuel Plutonium Assay Strategy, *Los Alamos National Laboratory Report: LA-UR-10-00074,* Proceedings of the American Nuclear Society's Annual Meeting.
13. Fensin, M. L., S. J. Tobin, M. T. Swinhoe, H. O. Menlove, W. Koehler, N. P. Sandoval, S. Lee, V. Mozin, J. Richard, M. Schear, J. Hu, and J. Conlin. 2011. Determining the Pu Mass in LEU Spent Fuel Assemblies – Focus on Passive Gamma Detection, *Los Alamos National Laboratory Report: LA-UR-11-00511* (January 2011).
14. Sandoval, N. P., and M. L. Fensin. 2008. Burnup Automation MCNPX File Data Retrieval Tool (BAMF-DRT): Data Extraction and Input File Creation Tool Users Manual, *Los Alamos National Laboratory Report: LA-UR-09-01259,* Los Alamos, New Mexico.
15. Trellue, H. R. 2012. Release of NGSI Spent Fuel Libraries, Los Alamos National Laboratory document LA-UR 12-00051 (2012).

The Performance of Self-interrogation Neutron Resonance Densitometry in Measuring Spent Fuel

Jianwei Hu, Holly R. Trellue, Stephen J. Tobin, T. J. Ulrich, Adrienne M. LaFleur, Corey R. Freeman, Howard O. Menlove, and Martyn T. Swinhoe
Los Alamos National Laboratory, Los Alamos, New Mexico USA

Abstract

The Self-Interrogation Neutron Resonance Densitometry Technique (SINRD) technique is one of the fourteen nondestructive assay (NDA) techniques investigated under the Next Generation Safeguards Initiative (NGSI) effort. SINRD shows promising capability in determining the ^{239}Pu and ^{235}U content in spent nuclear fuel. SINRD is a relatively low-cost and light-weight instrument, and it is easy to implement in the field. SINRD makes use of the passive neutron source existing in a spent fuel assembly, and it uses ratios between the count rates collected in fission chambers that are covered with different absorbing materials. These ratios were correlated to certain attributes of the spent fuel assembly such as the total mass of ^{239}Pu. Using count rate ratios instead of absolute count rates makes SINRD less vulnerable to systematic uncertainties. Building upon the previous research performed by Lafleur et al., this work focuses on the underlying physics of the SINRD technique: understanding the neutron energy spectrum at various locations inside and at the edge of the fuel assembly; understanding which isotopes have major impacts on the SINRD signal, by weighting the resonance absorption caused by each of a few isotopes deemed important in certain energy windows (dictated by the absorbing material covering the fission chambers); and understanding the spatial dependence of the count rate on each row of the fuel rods. The results of these studies show that water gap of 0.5 cm or more smears out the structure of the spectrum in the energy ranges important to SINRD; ^{239}Pu is the most important nuclide that affects the count rate in the "Gd-Cd" window, and ^{235}U has a significant impact as well, especially in the low burnup case; only the first three rows next to the detector has a significant impact on the signal. In short, this work provides insights into the factors that affect the performance of SINRD most and it will help to improve the hardware design and the algorithm used to interpret the signal for the SINRD technique.

Introduction

The Self-Interrogation Neutron Resonance Densitometry Technique (SINRD) technique is one of the fourteen nondestructive assay (NDA) techniques investigated under the Next Generation Safeguards Initiative (NGSI) effort.[1] SINRD has been studied significantly at LANL by Lafleur et al.[2,3] SINRD is a relatively low-cost and lightweight instrument that does not require an active source since it makes use of the neutrons emitted by spontaneous fissions from ^{244}Cm and other isotopes. These passive neutrons travel through the spent fuel assembly and create more neutrons when they induce fissions with fissile isotopes such as ^{239}Pu and ^{235}U. The SINRD analysis relates the ratio of neutron count rates measured in certain energy ranges to the ^{239}Pu and ^{235}U content in the assembly. Figure 1(a) shows a sketch of this instrument.[2] As shown, SINRD sits right next to one side of the fuel assembly. There are four fission chambers (FCs) used in this detector, three of which are covered with filtering materials: the Gd+Hf FC (covered with 0.01-mm Gd and 2.6-mm Hf), also referred to as Gd FC if there is no Hf coverage; the Bare FC (no filtering material coverage); the Cd FC (covered with 3-mm Cd); and the Fast Flux Monitor (FFM) FC (embedded in polyethylene that is lined with 1.0-mm Cd). These filtering materials absorb neutrons within certain energy ranges, and the remaining neutrons may be detected in the FCs. Subtracting count rates between two different FCs (covered with different filters) will capture a specific *window* in the neutron energy spectrum. Count rates in the window are impacted by the amount of certain isotopes present in the spent fuel assembly. For example, the large resonance absorption around 0.3 eV by ^{239}Pu has a major impact on the neutron energy spectrum in the window around 0.3 eV, i.e., the more ^{239}Pu in the assembly, the more depressed the count rate is in the window. Figure 1 (b) and (c) shows the cutoff energies of the filters (Gd, Cd, Boron, and Hf) covering on the fission chambers in the SINRD detector relative to cross-sections of ^{235}U, ^{239}Pu and ^{240}Pu.[2] As shown, the 0.01-mm thick Gd filter will largely block neutrons with less than ~0.1 eV energy from entering the FC, while the 3.0-mm thick Cd filter will largely block neutrons with less than ~1.3 eV energy. Subtracting the count rate of the Cd covered FC from the Gd covered FC will quantify the neutron energy spectrum within the range of [~0.1eV, ~1.3 eV], referred to as "Gd-Cd" window (or "Gd+Hf-Cd" if there is Hf covering the Gd FC). If there were only ^{239}Pu and ^{235}U in the assembly with comparable amount, ^{239}Pu would have a dominant impact on the count rate in this window because of its prominent resonance absorption cross-section around 0.3 eV.

Lafleur et al.[2,3] published interesting results generally showing the correlations between the quantities of certain isotopes (mainly ^{239}Pu and ^{235}U) and ratios of count rates. This was most often done by taking the ratio of the count rate in the "Gd-Cd" window

Figure 1. (a) Configuration of the SINRD detector (note that two ^{239}Pu FCs, as shown in this figure, are used in the calculations for this work, while due to the shortage of ^{239}Pu FCs, all FCs will probably be ^{235}U FCs in the actual device);[2] (b) Cutoff energies of Gd, Cd, and B_4C relative to the fission cross-sections of ^{235}U and ^{239}Pu;[2] (c) Cutoff energies of Hf relative to the fission cross-section of ^{239}Pu and capture cross-sections of ^{240}Pu.[2]

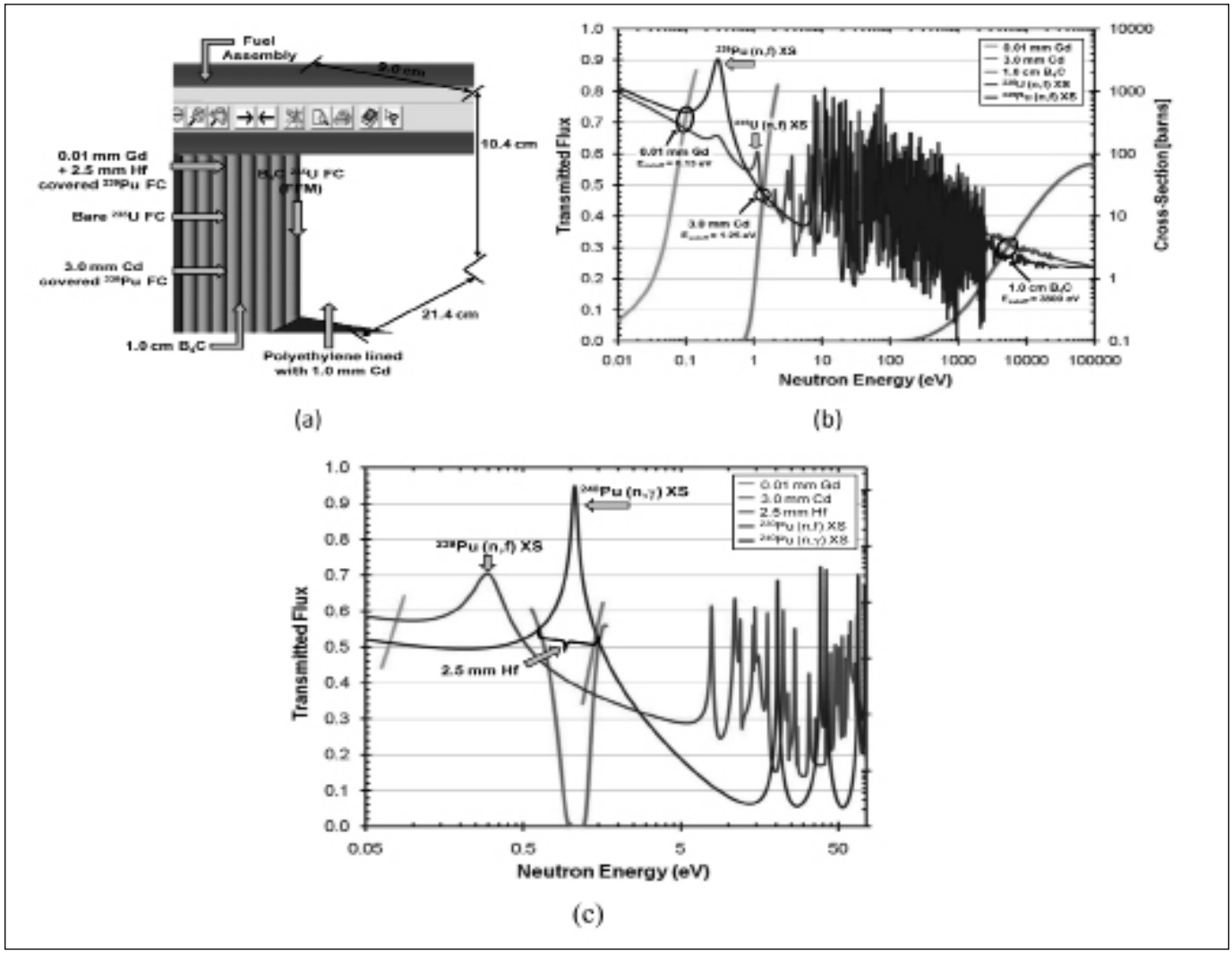

(or "Gd+Hf-Cd") to either a) the Bare FC (primarily the thermal part of the spectrum) or b) the FFM (primarily the high energy part of the spectrum). The results were promising, and motivated further research into the physics of SINRD. For example, how much of the observed correlations were due to absorptions by ^{235}U and ^{239}Pu is very much of interest. This work focuses on the underlying physics aspects of the SINRD technique using MCNPX simulations.[4] The current focus is to understand the following: a) neutron energy spectrum at various locations, b) what isotopes affect SINRD signal, and c) the impact of each row of fuel rods in a spent fuel assembly. The impact of each isotope on SINRD signal was evaluated by weighting the resonance absorption caused by each of a few isotopes deemed important in certain energy windows (dictated by the filtering material over the FC surface)

The Neutron Energy Spectrum at Various Locations in Spent Fuel

Since the SINRD technique involves comparing the relative intensity of the neutrons at various parts of the neutron energy spectrum, understanding how the total neutron energy spectrum changes with variables such as locations and burnup (BU) is important. The neutron energy spectrum in the fuel rods is determined by what we call the "neutron life cycle." For a spent nuclear fuel assembly sitting in water or borated water, in the absence of an active neutron source, the life cycle of neutrons can be described as follows: neutrons are born with a fast energy spectrum because higher actinides (e.g., ^{244}Cm, ^{242}Cm, ^{241}Am, etc.), accumulated during fuel irradiation, experience spontaneous fissions and emit Watt fission spectrum neutrons (average energy ~2

Figure 2: Normalized neutron energy spectrum in the fuel rods for five different fuel assemblies. There are one fresh fuel assembly (4 percent UO_2) and four spent fuel assemblies, which all have 4 percent IE and five-year CT, but with four different BU (15, 30, 45, and 60 GWd/tU respectively).

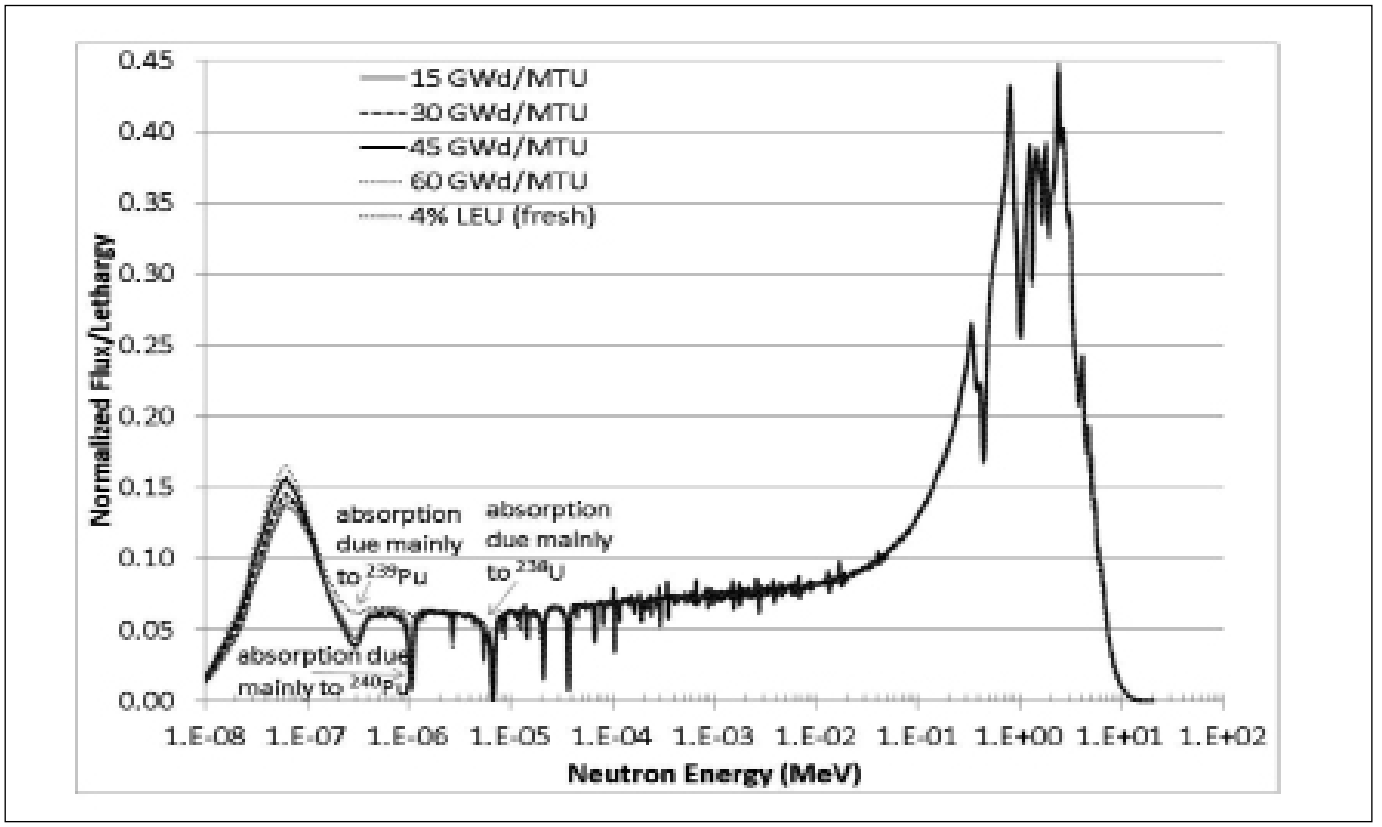

MeV). As these neutrons born in spontaneous fission lose energy through collisions with other nuclei in water or in fuel, they slow down; if they do not escape or are not absorbed, they become thermal. The physics that SINRD is targeting is visible in this spectrum because a few isotopes (e.g., ^{238}U, ^{240}Pu, ^{239}Pu, etc.) have significant resonance absorption cross-sections at specific energies, particularly in the epithermal or thermal region. Hence, reductions in the neutron flux at these energies are observed with increases in the mass of these respective isotopes.

Figure 2 shows the neutron life cycle in five different assemblies; one fresh fuel assembly and four spent fuel assemblies each with a different BU (15 to 60 GWd/tU). Note that in this figure and in Figures 3 and 4, the neutron flux is normalized by lethargy. All the four spent fuel assemblies have an enrichment (IE) of 4 percent and a cooling time (CT) of five years. There are two major humps: one in the fast energy region (because virtually all neutrons are born fast) and the other in the thermal energy region (because neutrons achieve equilibrium with the environment). There are also three major depressions in the epithermal regions, as labeled in the figure, caused by resonance absorption of ^{238}U ~7 eV, of ^{240}Pu ~1 eV, and of ^{239}Pu ~0.3 eV. However, for the fresh fuel assembly, there is no depression around 1 eV or 0.3 eV because there is no ^{240}Pu or ^{239}Pu present. Note that at thermal energy, the thermal flux is lower for lower BU because the absorption is greater given the increased amount of fissile content in lower BU fuel compared to higher BU fuel. Although there are less fission product absorbers in the lower BU fuel, the fissile isotopes have such a strong thermal absorption effect that they dominate the absorption at thermal energies.

The SINRD concept involves measuring the "absence of neutrons" due to resonance absorption of one particular isotope by reducing the measured signal into a small window. By using two different filters, and if possible by using a matching material in the fission chamber, an energy window with a certain width can be established, which then can be related to a particular resonance absorption. Note the *dips* in Figure 2, or "absence of neutrons," are the key pieces of information in the SINRD technique.

The neutron energy spectrum varies significantly as a function of location in the assembly. The impact of the absorption peaks will be strongest in the fuel region at the energy where the absorption takes place. The presence of the absorption peaks will become less evident external to the fuel region (especially in regions immersed in water) since neutron moderation will "fill in" the peaks as neutrons slow down from their fast *birth*

Figure 3: The normalized neutron flux per unit lethargy in the fuel, cladding, and water is illustrated for an assembly (immersed in water) with 4 percent IE, 45 GWd/tU BU, and five-year CT

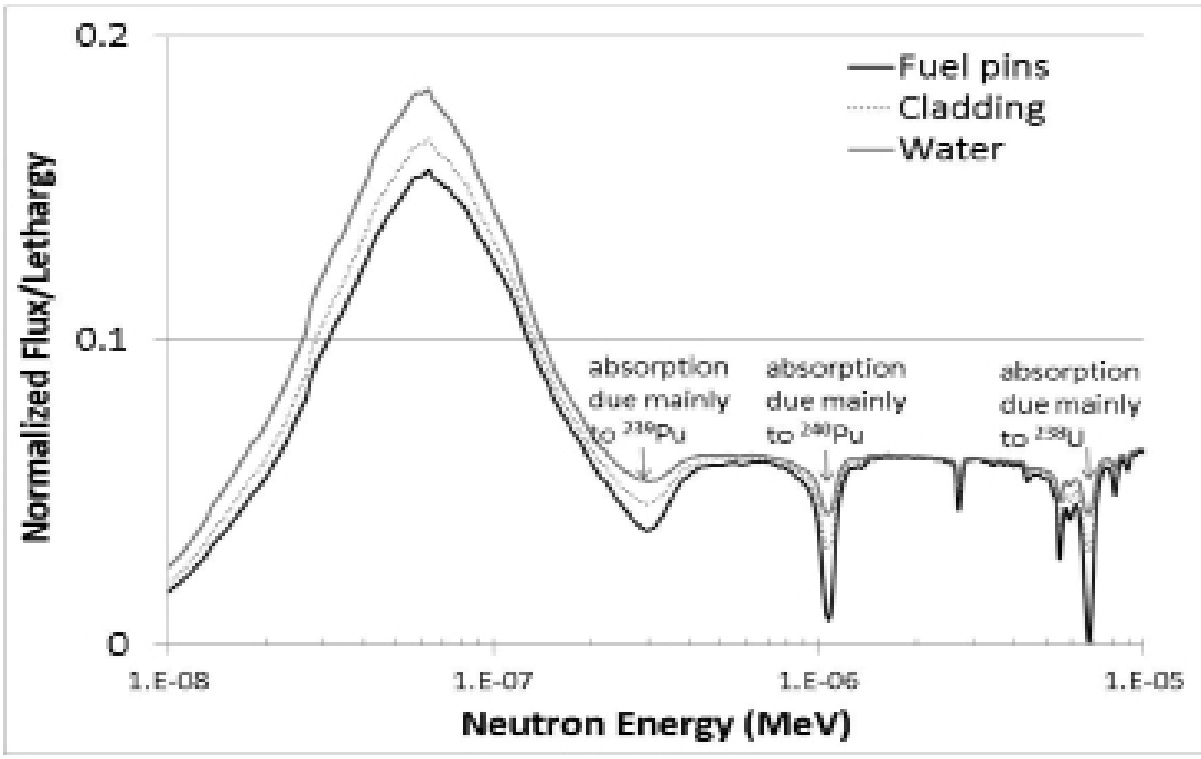

energy to thermal energies. To illustrate this point, in Figure 3 the normalized neutron flux per unit lethargy for a 4 percent IE, 45 GWd/tU BU and five-year cooling time assembly in isolation in water is depicted for three locations: (1) averaged over the entire fuel region in the assembly, (2) averaged over all the cladding in the assembly, and (3) averaged over all the water region "inside of the assembly." Note that water occupies ~55 percent of the volume inside of an imaginary container (the smallest flat-sided container that totally encompasses the full assembly) surrounding the assembly.

In Figure 3, the strong absorption resonance in ^{239}Pu at ~0.3 eV and an even stronger resonance in ^{240}Pu at ~1 eV can be easily identified. Recall that the Gd (0.01 mm) and Cd (3.0 mm) filters used in SINRD have cutoff energies ~0.1 eV and ~1.3 eV, respectively. As discussed below, a few other isotopes (particularly ^{235}U) can absorb a significant number of neutrons in the energy window formed by the Gd and Cd filters. The strong ^{238}U resonance at ~7 eV is also visible. The main point of Figure 3 is to illustrate how the impact of the absorption resonances decreases relative to the rest of the spectrum as a function of location within the assembly. The resonances are very strong in the fuel, saturating in some cases. In the cladding, at the interface between the water and the fuel, the resonances are significantly reduced (~40 percent) compared to the average in the fuel. In the water the resonances are reduced further but can still be identified in the spectrum.

A practical safeguards instrument needs to be located on the outside of the assembly. Hence, it is important to understand the variations in the neutron energy spectrum at the surface of the assembly and the variations that would be observed as the SINRD unit moves horizontally away from the assembly. Figure 4 depicts, for an actual experimental case, the normalized neutron flux per unit lethargy of an assembly in a large pool of water (for an assembly with 4 percent IE, 45 GWd/tU BU, and five-year CT). Three spectra on the front face of the SINRD unit are illustrated for three cases: (1) the SINRD detector is in contact with an assembly, (2) the detector is 0.5 cm away from the assembly and (3) the detector is 1.0 cm away from the assembly.

Figure 4 illustrates that the neutron energy spectrum varies significantly with location over the scale of a few millimeters. The spectrum identified as "Assembly surface" is particularly noteworthy because it is the simulation of the experimental case we expect for field applications if the SINRD detector were in direct contact with the side of an assembly in a pool. For this contact measurement, the resonant structure is still clearly present. Yet, if the SINRD unit is moved back 0.5 cm, essentially all clear energy dependent structures is lost. It is worth noting that general depressions in the energy spectrum may still be detectable with

Figure 4: For a 4 percent IE, 45 GWd/tU BU, and five-year cooling time assembly, the normalized flux spectrum per unit lethargy on the front face to the SINRD for three different locations of the SINRD unit: (1) detector is in contact with an assembly, (2) detector is 0.5 cm away from the assembly and (3) detector is 1.0 cm away from the assembly

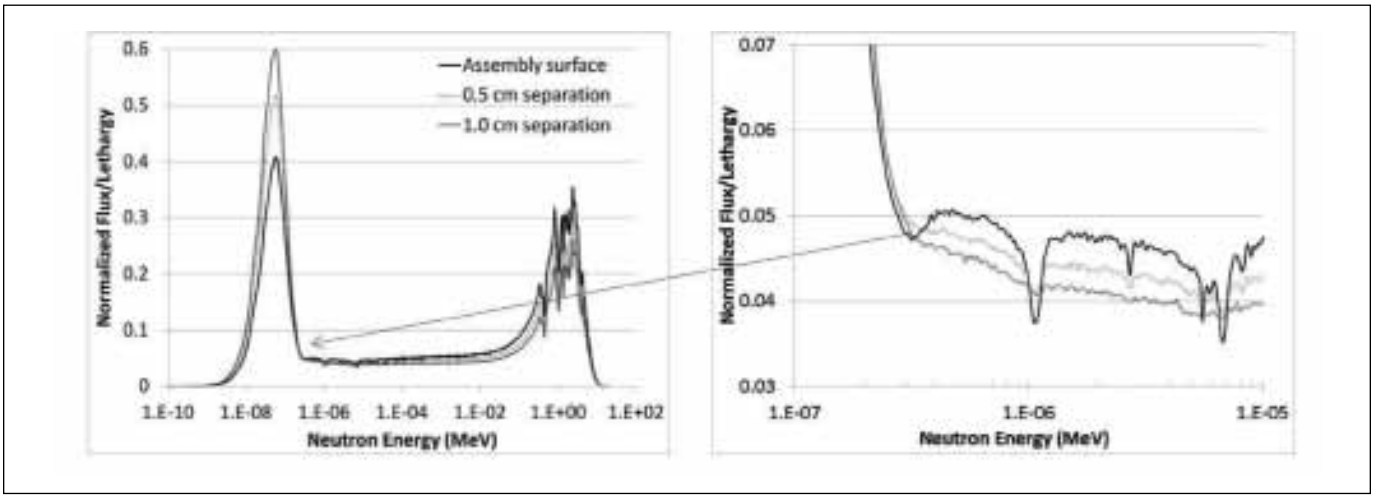

some water separation; in fact preliminary simulations indicate that the SINRD concept may still work with a water gap of ~1 cm. But it is worth emphasizing that the amount of water separation needs to be well known since a ~1 mm difference is significant. For this reason, contact measurements are desirable and care will have to be taken to reduce systematic error associated with displacement of the detector from the assembly.

The "Tally in the Fuel" Approach

As previously discussed, each FC of SINRD detects neutrons from different energy. Before we use the "tally in the fuel" approach to evaluate the impact of a few isotopes on count rate, we have to decide the count rate of which FC (or count rate difference between which FCs) are of interest. The count rate difference Gd+Hf-Cd, which is the difference between the Gd+Hf covered FC and the Cd covered FC, is of most interest because it was most frequently used in the correlations reported in previous publications. [2,3] For example the ratio FFM/(Gd+Hf-Cd) was used to correlate to the mass of ^{239}Pu in the fuel. The Gd+Hf detector is designed to detect neutrons with energy within ~0.13 and ~0.6 eV and above ~1.25 eV. The Cd detector is designed to detect neutrons above ~1.25 eV. Thus, the (Gd+Hf-Cd) signal mainly focuses on the range of [~0.13, ~0.6] eV. Similarly, the (Gd-Cd) signal, when Hf is not added onto the FC covered with Gd, focuses on the range of [~0.13, ~1.25] eV. Note all the energy cutoffs are not 100 percent because there is significant leak-through.

To quantify the contribution of a few important isotopes to the absorption within the range of [~0.13, ~0.6] eV, or the Gd+Hf-Cd signal, the so-called "tally in the fuel" approach was adopted. In this approach, a MCNPX flux tally with energy bins is applied to each fuel rod, and then a flux multiplier tally representing the absorption cross-section of a particular isotope is also applied.[4] The results are then adjusted with the actual atom density of a specific isotope in the fuel. This exercise was performed on three different fuel assemblies: 45 GWd/tU with 4 percent IE and one-year CT, 45 GWd/tU with 4 percent IE and eighty-year CT, and 15 GWd/tU with 4 percent IE and one-year CT.

Table 1 shows the relative percent absorption by a list of isotopes in the energy window of "Gd+Hf-Cd" (the "with Hf" cases) and "Gd-Cd" (the "w/o Hf" cases). As shown in Figure 1(c), the Hf filter largely absorbs neutrons within the range of [~0.6, ~1.25 eV], thus the "with Hf" cases focus on the range of [~0.13, ~0.6] eV while the "w/o Hf" cases focus on the range of [~0.13, ~1.25] eV. As shown in the table, ^{239}Pu contributes to the majority of the absorption in general but the role of ^{235}U becomes increasingly important in the low burnup case (15 GWd/tU). This seems contradictory to what is shown in Figure 2, but Figure 2 shows that the depression around 0.3 eV was mainly caused by ^{239}Pu, while the energy window of interest here covers a wider energy range. Also Hf reduces the contribution of ^{240}Pu significantly. Since ^{241}Pu decays into ^{241}Am with half life around fourteen years, and they both have similar absorption cross-section in the energy window of interest, the absorption by ^{241}Pu in the 45 GWd/tU BU, 4 percent IE, and one-year CT case ("45G_4p_1yr") is similar to the absorption by ^{241}Am in the "45G_4p_80yr" case. Note that all results shown in this table and Table 2 have an uncertainty of less than 0.3 percent, and it is the statistical uncertainly associated with MCNPX calculations and does not include the uncertainty on nuclear data. Figure 5 shows the cross-sections ("fn." for fission and "ab." for absorption) of the same list of isotopes around the energy window. The absorption cross-section of ^{149}Sm and ^{155}Gd are exceptionally high but the quantities of these two isotopes are low, so the impacts of these two isotopes are minor. (Although fission is just one form of absorption, since the fission cross-sections for the fissile isotopes

Figure 5: Fission cross-section of ^{235}U, ^{239}Pu, ^{241}Pu; absorption cross-section of ^{240}Pu, ^{155}Gd, ^{149}Sm and ^{241}Am around the energy region of interest. Note that "fn." stands for fission and "ab." stands for absorption.

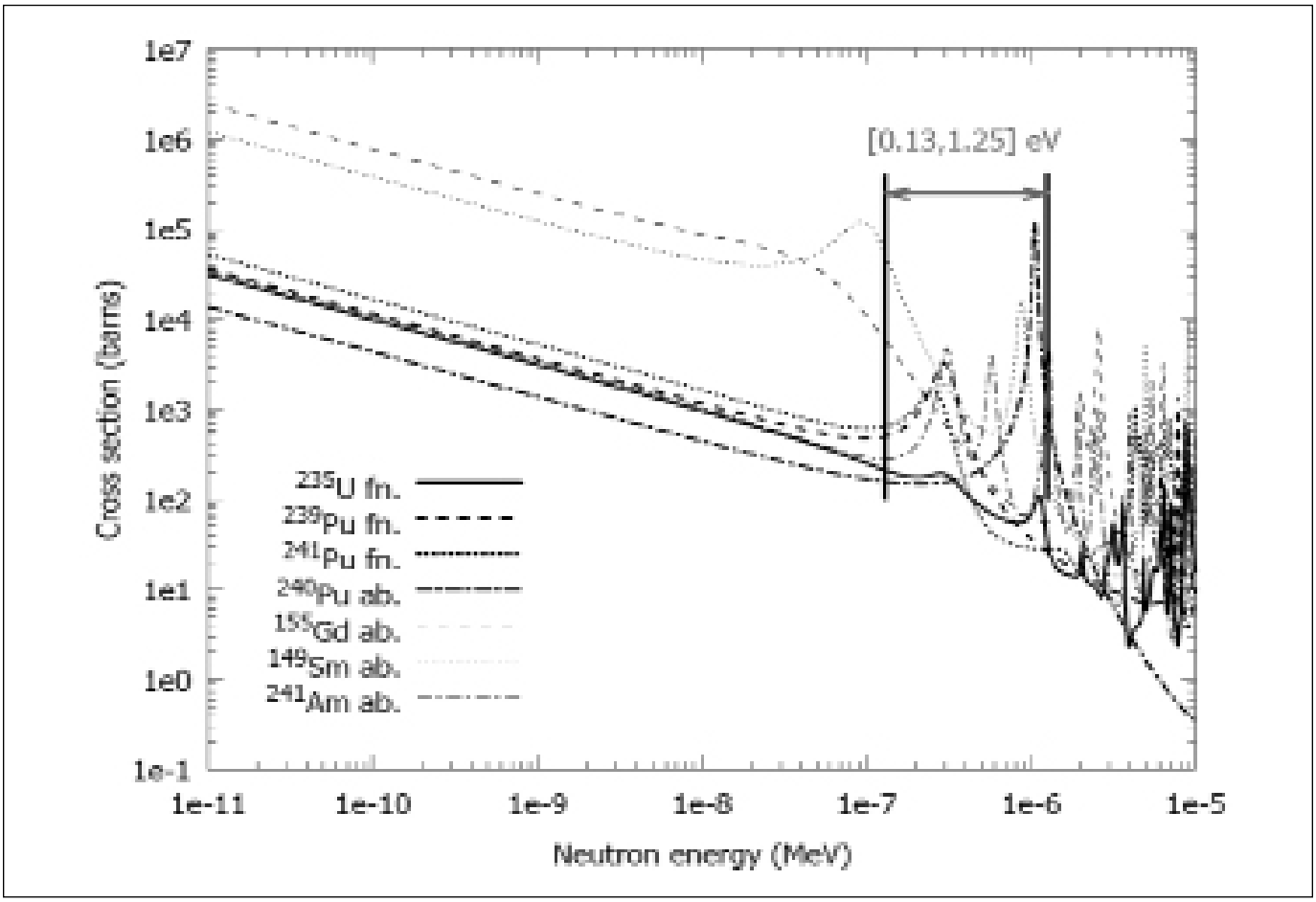

Table 1. Relative absorption (percent) of selected isotopes in the energy window defined by (Gd+Hf-Cd) (the "with Hf" cases) and (Gd-Cd) (the "w/o Hf" cases). The uncertainty for all values is less than 0.3 percent.

	Relative absorption (percent) by each isotope in energy window					
	45G_4p_1yr		45G_4p_80yr		15G_4p_1yr	
Isotope	with Hf	w/o Hf	with Hf	w/o Hf	with Hf	w/o Hf
^{239}Pu	70.4	50.0	70.0	48.8	54.3	42.2
^{235}U	13.9	11.5	14.0	11.3	41.2	37.7
^{240}Pu	3.5	29.7	3.6	30.0	1.1	17.4
^{241}Pu	10.8	7.6	0.2	0.2	2.7	2.1
^{241}Am	1.0	0.8	11.5	9.2	0.2	0.2
^{149}Sm	0.4	0.3	0.4	0.3	0.4	0.4
^{155}Gd	0.03	0.02	0.2	0.2	0.01	0.00

such as ^{235}U, ^{239}Pu, and ^{241}Pu are much larger than the sum of other absorptive processes, only the fission cross-section is shown in this figure for these three isotopes.) In summary, if Hf is not used on the Gd covered FC, ^{239}Pu, ^{240}Pu, and ^{235}U are the three major isotopes affecting the "Gd-Cd" count rate, and the contribution of ^{240}Pu goes up to 30 percent; if Hf is used on the Gd covered FC, ^{239}Pu and ^{235}U are the two major isotopes affecting the "Gd+Hf-Cd" count rate, and the contribution of ^{240}Pu is significantly reduced. In both case, the contribution of ^{235}U becomes increasingly important in low burnup assemblies, nearly comparable to ^{239}Pu in 15 GWd/tU fuel.

Impact of Each Row on Count Rate

Since the SINRD instrument sits on only one side of the fuel assembly, it is important to understand the spatial dependence of the count rate on each row of fuel. It is expected that the fuel rods in the outer rows will have a larger impact on the signal than those in inner rows. A study was performed to quantify the impact of each row of fuel rods on count rate in the "Gd-Cd"

Figure 6. The arrangement of the "row replacement" experiment. In this experiment, all fuel rods were filled with ^{238}U-only UO_2 in the base case. One chosen row (row 3 in this case) was replaced by spent fuel, and then the count rate was compared to the base case.

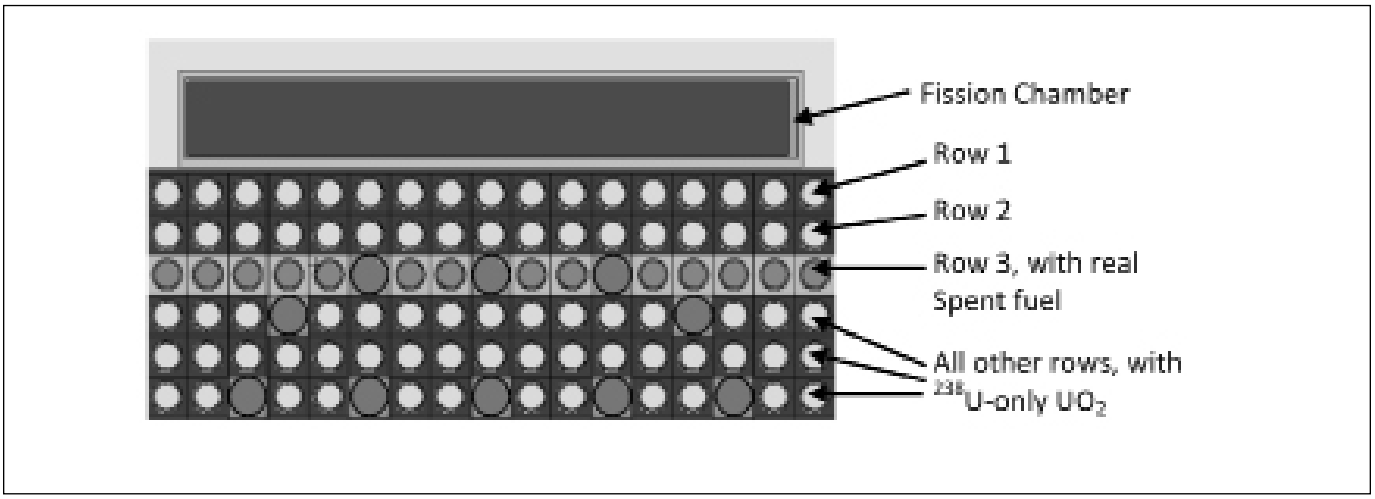

window (this study can serve a reference for the "Gd+Hf-Cd" window as well). Because SINRD involves detecting the "absence of neutrons," simulating a row-by-row sensitivity is challenging.

To quantify the row-by-row effect, a simplified fuel assembly was simulated with all fuel rods filled with the same UO_2 fuel that contains only ^{238}U (i.e., 0 percent ^{235}U enrichment), and the count rate difference between the Gd FC and the Cd FC, or as referred to as "Gd-Cd," was quantified and recorded as the base case. Then a chosen row is completely replaced with "real" spent fuel (45 GWd/tU BU, 4 percent IE, and five-year CT in this exercise) and the count rate in the "Gd-Cd" window was simulated again and compared to the base case. Since the only change between these two cases is the replacement of the ^{238}U-only UO_2 fuel by *real* spent fuel, the change of "Gd-Cd" count can be attributed to the presence of spent fuel, and it indicates the impact of this particular row of fuel rods on the count rate in the context of "real" spent fuel assembly. Nine rows, one row at a time, have been analyzed for this virtual experiment.

Figure 6 shows the arrangement of this *experiment* and Table 2 summarizes the results. The figure shows the fuel assembly is filled with ^{238}U-only UO_2 fuel except that row 3 is filled with "real" spent fuel (the larger circles are water holes). As shown in the table, the first three rows have significant impact on "Gd-Cd" count rate, and the replacement with *real* spent fuel in the first three rows brought changes of -29.1 percent, -26.2 percent and -13.2 percent (compared with the base case) respectively, indicating the count rate is mainly determined by the first three rows. This finding is consistent with the conclusion of Lafleur et al. that SINRD would be much less sensitive to diversion in the inner part of the assembly.[2] The isotopes with both large absorption cross-sections in the "Gd-Cd" window and those present in large quantity in spent fuel (e.g., ^{239}Pu, ^{240}Pu and ^{235}U) are responsible for causing these changes. For rows farther away from the detector, the neutrons have to go through a greater amount of material (fuel and moderator) before being detected, and in this process, the *signal* produced by the ^{239}Pu resonance in those rows (i.e., the depression of neutron energy spectrum around 0.3 eV) moves to lower energies and possibly out of the "Gd-Cd" window. In the meantime, the *signal* produced by the ^{238}U resonance around 7 eV moves to lower energies and possibly into the "Gd-Cd" window. The combined effects of these two factors also play a role in determining the impact of each row on the signal, which partly explains why some rows introduced positive changes.

Table 2. Relative change (percent) in the count rate in the "Gd-Cd" window caused by the replacement of ^{238}U-only UO_2 by spent fuel in a particular row. The uncertainty for all values is less than 0.3 percent.

	Change from base case, Percent
Base case	0
Row 1	-29.1
Row 2	-26.2
Row 3	-13.2
Row 4	-6.5
Row 5	0.7
Row 6	-0.4
Row 7	2.8
Row 8	4.1
Row 16	-0.1

Figure 7. (a) Count rate ratio of FFM/(Gd+Hf-Cd) vs. ^{239}Pu mass [2]; (b) Mass ratio of ^{235}U/^{239}Pu vs. ^{235}U mass

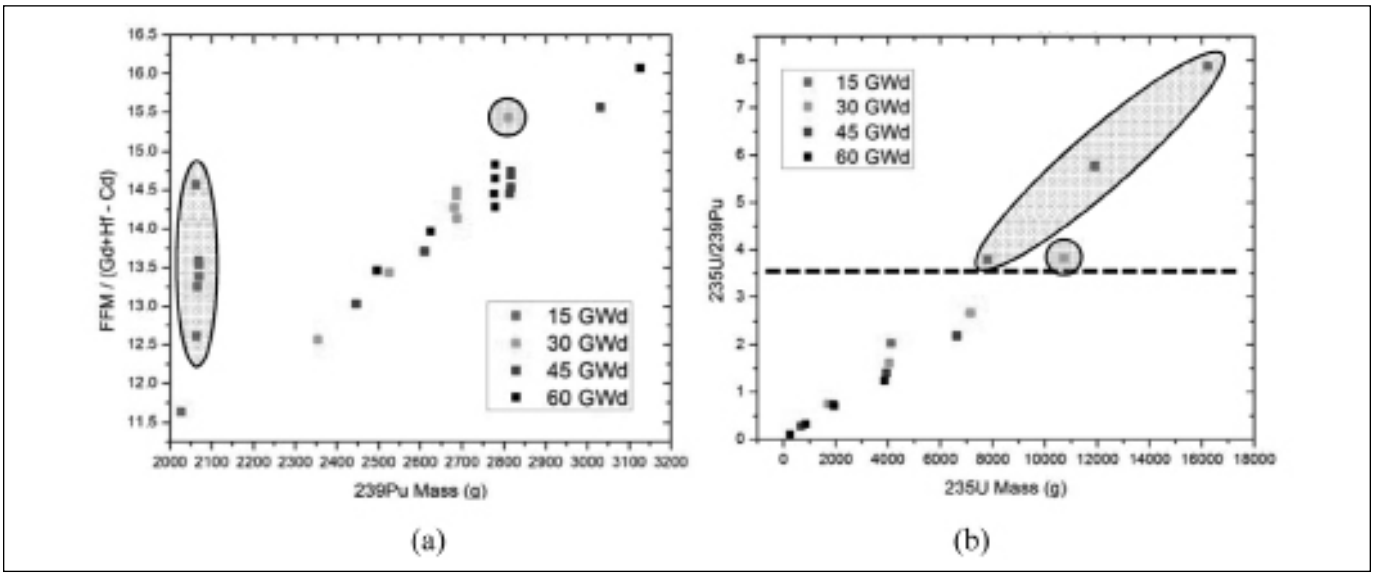

The Impact of Mass Ratio of ^{235}U/^{239}Pu

During the initial phase of the NGSI spent fuel project [1], the detector responses from fourteen NDA techniques were determined over a wide range of spent fuel assemblies [5]. Figure 7(a) shows the correlation between one of the SINRD count rate ratios, FFM/(Gd+Hf-Cd), and the mass of ^{239}Pu.[2] The low-burnup assemblies (15 GWd/tU) deviate from the general trend. Consistent with the results depicted in Table 1, we expected the deviation is due to the fact that the low-burnup assemblies have more ^{235}U and less ^{239}Pu than higher burnup assemblies. As shown, there are six assemblies, as circled, that deviate from the general trend, and five of them have a burnup of 15 GWd/tU and one has a burnup of 30 GWd/tU. By examining the mass ratio of ^{235}U/^{239}Pu, all (and only) these six outlier assemblies have a ^{235}U/^{239}Pu ratio above 3.5 and a ^{235}U mass greater than 7 kg, as illustrated in Figure 7(b). Note that same assemblies with different cooling times would have the same amount of ^{235}U and ^{239}Pu, therefore there are fewer data points in Figure 7(b). This study shows that the correlation between FFM/(Gd+Hf-Cd) and ^{239}Pu mass works better for assemblies with lower ^{235}U/^{239}Pu ratio. This study also concludes that SINRD, if only this FFM/(Gd+Hf-Cd) vs. ^{239}Pu correlation is used, would only be applicable for assemblies with BU values equal or greater than 30 GWd/tU, however, this includes the vast majority of commercial spent fuel. This result agrees with the findings described above that ^{235}U plays a larger role in "Gd-Cd" count rate in low burnup assemblies.

Summary

This paper summarizes recent work to further understand the underlying physics of the SINRD technique. The results of the neutron energy spectrum at various locations inside and at the edge of the assembly illustrate how the spectrum changes according to the local condition of moderation and fissile content. Since SINRD is designed to detect a specific window of the spectrum, it is insightful to see the spectrum results. These results also show that water gap of 0.5 cm or more smears out the structure of the spectrum in the energy ranges important to SINRD. The results of total neutron absorption caused by a few important isotopes such as ^{239}Pu, ^{235}U, ^{240}Pu, and ^{241}Pu etc. show that ^{239}Pu is the most important nuclide that affects the count rate in the "Gd-Cd" window; ^{235}U has a significant impact as well, especially in the low burnup case; ^{240}Pu can contribute up to 30 percent if the Hf filter is not in place; and the role of ^{241}Pu and ^{241}Am is interchangeable at different cooling times. The results of the impact of each row of pins within an assembly show that only the first three rows next to the detector cause a significant impact on the count rate in the window, which also confirms that SINRD is less sensitive to diversion in the middle of the assembly.[2] The spectrum structure caused by resonance absorption of certain isotopes is "smoothed out" when the spectrum has to travel though multiple rows of fuel rods and/or several centimeters of water before being detected. The ^{235}U/^{239}Pu mass ratio affects the relationship between FFM/(Gd-Cd) and ^{239}Pu mass and reconfirms that in the low burnup case, ^{235}U has a significant impact on the count rate in the "Gd-Cd" window. In short, SINRD detects absence of neutrons in certain energy range (caused by resonance absorption) and thus the underlying physics is somewhat more complex that other NDA techniques. This work provides insights into the factors that would most affect the performance of SINRD, and it will help to improve the design of the hardware and the algorithm to relate the count rate to important attributes of spent fuel assemblies, especially when the SINRD instrument is taken into field tests at some international spent fuel facilities as plan in 2012.

Acknowledgments

The authors would like to acknowledge the support of the Next Generation Safeguards Initiative (NGSI), Office of Nonproliferation and International Security (NIS), National Nuclear Security Administration (NNSA).

References

1. Humphrey, M. A., S. J. Tobin, and K. D. Veal. 2012. The Next Generation Safeguards Initiative's Spent Fuel Nondestructive Assay Project, *Journal of Nuclear Materials Management,* Vol. 40, No. 3.
2. Lafleur, A. M., H. O. Menlove, S. J. Tobin, and M. T. Swinhoe. 2011. Development of Self-Interrogation Neutron Resonance Densitometry to Measure the Fissile Content in PWR 17×17 Spent LEU Fuel, Los Alamos National Laboratory report (LA-UR 11-00516), 2011.
3. Lafleur, A. M. 2011. *Development of Self-Interrogation Neutron Resonance Densitometry (SINRD) to Measure Fissile Content in Nuclear Fuel*, PhD dissertation, Texas A&M University, 2011.
4. Pelowitz, J. F. (Editor). 2008. MCNPX User's Manual Version 2.6.0. Los Alamos National Laboratory report, LACP-07-1473.
5. Galloway, J. D., H. R. Trellue, M. L. Fensin, and B. L. Broadhead. 2012. Design and Description of the NGSI Spent Fuel Library with an Emphasis on Passive Gamma Signal, *Journal of Nuclear Materials Management,* Vol. 40, No. 3.

Passive Neutron Albedo Reactivity with Fission Chambers

Jeremy J. Gerhart, Corey Freeman, Jeremy L. Conlin, Howard O. Menlove, and Stephen J. Tobin
Los Alamos National Laboratory, Los Alamos, New Mexico USA

Abstract

Passive Neutron Albedo Reactivity with Fission Chambers is one of the instruments being researched by the Next Generation Safeguard Initiative Spent Fuel Nondestructive Assay Project. The instrument uses neutrons generated from within the spent fuel assembly, mainly from Cm, to interrogate the assembly by reflecting the neutrons back into the assembly. Two measurements are taken of the assembly, one of which has a Cd sleeve between the instrument and the assembly and the other does not; the ratio of these two measurements is correlated to the fissile content in the assembly. This current publication updates results published by Conlin et al. In particular the optimization of the cadmium liner length, improvements to the weighting constants used in determining the $^{239}Pu_{eff}$ mass are described. The improvements to the weighting constants involved removing an absorption term and utilization of a new capability added to the MCNPX code called "First Fission."

Introduction

In March 2009 the Next Generation Safeguards Initiative (NGSI) sponsored by the U.S. Department of Energy's National Nuclear Security Administration began an effort to develop nondestructive assay (NDA) technologies capable of quantifying the Pu mass in spent fuel assemblies.[1] This report provides a brief update of the Passive Neutron Albedo Reactivity using Fission Chamber (PNAR-FC) technique developed by the NGSI research effort.[2]

Passive Neutron Albedo Reactivity

Technique Overview

The Passive Neutron Albedo Reactivity (PNAR) concept measures the reactivity of radioactive materials that contain fissile mass; in the case of this report, spent nuclear fuel is the material of interest. The technique utilizes neutron self-interrogation of the fuel. PNAR is implemented by surrounding the fuel with a polyethylene block that reflects the neutrons back into the assembly. Two measurements of the fuel are taken, in one case the full neutron energy spectrum is reflected back into the assembly and in the other case the spectrum is modified through the use of a cadmium sleeve that is inserted between the fuel assembly and the polyethylene. A ratio of counts from the case without cadmium to the case with cadmium is then calculated. This ratio is correlated to the fissile content in the spent fuel[3] and is known as the cadmium ratio (CR).

Figure 1. PNAR-FC cross-sections. A horizontal slice is shown on the left and a vertical slice is shown on the right. The two diagrams are not on the same scale.

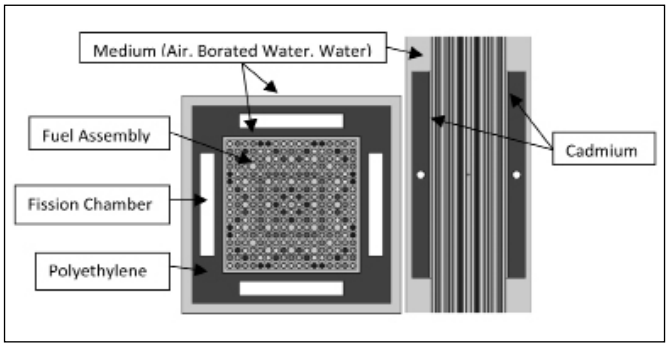

Detector Configuration

Two versions of the PNAR technique were investigated as part of the NGSI effort, one using ^{3}He tubes and one using fission chambers.[3] The focus of this report is the fission chamber technique, known as PNAR-FC. Figure 1 shows two cross-sections of the detector, one horizontal and the other vertical. In the diagrams the fuel assembly lies in the center, and the dark region surrounding the fuel is the polyethylene. Inside of the polyethylene lie four fission chambers orthogonal to the vertical axis of the assembly. The fuel to detector gap and the region outside of the detector represent the medium within which the assembly is located; this medium can be water, borated water, or air. Each of the media were investigated in the development of PNAR-FC, however, only the borated water results will be presented here as borated water is considered the most likely medium the PNAR-FC detector will encounter. See Conlin et al.[2] for details on detector dimensions, and results for other media.

^{239}Pu Effective Mass

Basic Concept

The $^{239}Pu_{effective}$ mass concept was introduced as a way to quantify the fissile content in a spent fuel assembly. This approach is similar to the $^{240}Pu_{eff}$ mass concept used in neutron coincidence counting.[4] Using the Monte Carlo N-Particle eXtended (MCNPX)[5] the contribution of the three major contributors to fission (^{235}U, ^{239}Pu, and ^{241}Pu) was quantified. In order to combine these individual masses into a single $^{239}Pu_{eff}$ term the neutron production from the ^{235}U and ^{241}Pu fissions must be weighted relative to

^{239}Pu. This is achieved by using a weighting coefficient for ^{235}U and ^{241}Pu so that their neutron production can be equated to ^{239}Pu on a per unit mass basis, as seen in the following equation:

$$^{239}Pu_{eff} = C_1 M_{^{235}U} + M_{^{239}Pu} + C_2 M_{^{241}Pu} \quad (1)$$

Here, Mx is the mass of the isotope x and C_1 and C_2 represent the weighting coefficients for ^{235}U and ^{241}Pu, respectively. The weighting coefficients are determined using the following:

$$C_1 = \frac{\int_V \int_E \nu_{^{235}U}(E)\sigma_{f_{^{235}U}}(E)\,\Phi(E,V)dEdV \; Per\ gram\ ^{235}U}{\int_V \int_E \nu_{^{239}Pu}(E)\sigma_{f_{^{239}Pu}}(E)\,\Phi(E,V)dEdV \; Per\ gram\ ^{239}Pu}$$

$$C_2 = \frac{\int_V \int_E \nu_{^{241}Pu}(E)\sigma_{f_{^{241}Pu}}(E)\,\Phi(E,V)dEdV \; Per\ gram\ ^{241}U}{\int_V \int_E \nu_{^{239}Pu}(E)\sigma_{f_{^{239}Pu}}(E)\,\Phi(E,V)dEdV \; Per\ gram\ ^{239}Pu}$$

Here, ν is the number of neutrons produced per fission, σ_f is the fission cross section, and Φ is the neutron flux. All of these parameters are provided by MCNPX through the use of a tally multiplier. Note that the current determination of the C_1 and C_2 constants is different from previous publications that included an absorption term. The absorption term was removed in this case for three reasons: (1) to base the weighting constants on a neutron production basis only, which is consistent with the detected signal, (2) to reflect that fact that a given fissile isotopes absorbs neutrons from all neutron production sources, and as such, does not weight one fissile isotope preferentially, and (3) to be consistent with the definition of $^{240}Pu_{eff}$ used in coincidence counting.

Research and Developments

Detector Height Characterization

For fission chambers located at one vertical location, the length of the cadmium liner impacts the measured Cd ratio until the point that the Cd liner is of such a length that the Cd ratio reaches its maximum value. Figure 2 shows the fission chamber response for "with Cd" and "without Cd" cases as a function of Cd and polyethylene height when the distance was measured vertically upward from the center of the fission chamber. As expected, the count rate for the "without Cd" case increases as the polyethylene height increases since borated water is being displaced; however, for the "with Cd" case as the Cd and polyethylene height increases, the signal decreases since the Cd liner located very close to the fuel reduces the multiplication in the fuel more than the borated water that it is replacing does. The data shows that to optimize the Cd ratio response, it is ideal to have a polyethylene slab at least 60 cm tall (30 cm on both ends of the fission chamber). This is the length utilized by Conlin et al.[2]

Figure 2. Detector response with Cd and without Cd as a function of polyethylene, and/or Cd height from the center of the fission chamber. The MCNPX uncertainty on the data points is smaller than the markers used for the points.

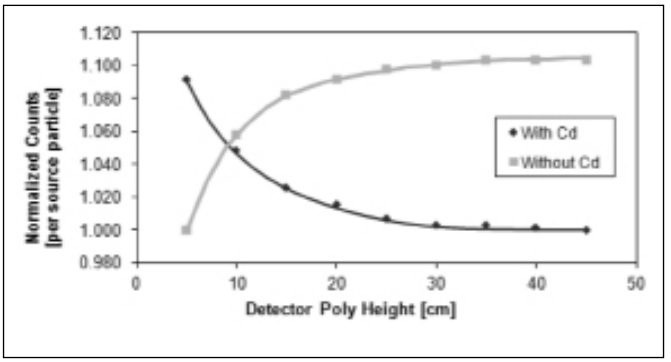

First Fission Tally Results

A new tally capability was added to MCNPX specifically for the NGSI spent fuel effort, known as the "First Fission" capability. This capability was added to give both spatial and isotopic information about the detected signal. For many of the techniques investigated as a part of the NGSI Spent Fuel NDA project, there is an interrogating source that induces fissions; in the case of PNAR the "interrogating source" is the neutrons below the Cd cutoff energy that reflect back into the fuel. The neutrons produced by the first induced fission reaction are often not directly detected, rather these neutron undergo multiplication on the way to the detector. This multiplication is prompt multiplication, which treats all neutrons essentially equally in the spent fuel context. As such, prompt multiplication after the first induced fission can be thought of as a "means of communication" between the induced signal and the detected signal. Because we are interested in interpreting the detected signal and because the detected signal was produced by induced fission in the first generation, we want to know what percentage of the detected signal came from which fissile isotopes.

By tagging the first induced fission, the First Fission capability gives us the capability to quantify what percentage of the detected signal came from which fissile isotopes. This new capability gives us a more accurate means of determining the C_1 and C_2 constants than previous approaches. In Conlin et al.[2] the C_1 and C_2 constants were determined by tallying all neutron production in the fuel. It was then assumed that the neutron production rate in the fuel was proportional to the detection rate for each isotope. This would be essentially true if the assembly was homogeneous in isotopic distribution, however homogeneity is not the case for real-world spent fuel assemblies. The new First Fission capability indicates what percentage of the detected signal comes from each isotopes based on tagging the first fission and transporting all neutrons to the detectors. In summary, the new C_1 and C_2 constants are more accurate than those used previously since an absorption term is not included and because we no longer make the spatial assumption of isotopic homogeneity.

Table 1. Comparison of C_1 coefficients from First Fission capability with the previous method.[2] Medium is borated water.

Fuel Assembly	First Fission	Previous Method	Difference [%]
15GWd 2%	0.3897 ± 0.0026	0.3649 ± 0.0003	6.36 ± 0.66
15GWd 4%	0.3659 ± 0.0019	0.3509 ± 0.0002	4.12 ± 0.53
30GWd 3%	0.3945 ± 0.0027	0.3667 ± 0.0003	7.05 ± 0.68
30GWd 4%	0.3815 ± 0.0022	0.3622 ± 0.0003	5.06 ± 0.58
45GWd 4%	0.3948 ± 0.0028	0.3678 ± 0.0003	6.83 ± 0.71

Table 2. Comparison of C_2 coefficients from First Fission capability with the previous method.[2] Medium is borated water.

Fuel Assembly	First Fission	Previous Method	Difference [%]
15GWd 2%	0.3897 ± 0.0026	0.3649 ± 0.0003	6.36 ± 0.66
15GWd 4%	0.3659 ± 0.0019	0.3509 ± 0.0002	4.12 ± 0.53
30GWd 3%	0.3945 ± 0.0027	0.3667 ± 0.0003	7.05 ± 0.68
30GWd 4%	0.3815 ± 0.0022	0.3622 ± 0.0003	5.06 ± 0.58
45GWd 4%	0.3948 ± 0.0028	0.3678 ± 0.0003	6.83 ± 0.71

The First Fission capability was used to determine the C_1 and C_2 for the following assemblies taken from the NGSI virtual spent fuel library,[6] and the results are summarized in Table 1 and Table 2:

15 GWd/tU BU, 2 percent IE, 5 yr CT
15 GWd/tU BU, 4 percent IE, 5 yr CT
30 GWd/tU BU, 3 percent IE, 5 yr CT
30 GWd/tU BU, 4 percent IE, 5 yr CT
45 GWd/tU BU, 4 percent IE, 5 yr CT

The 15 GWd/tU BU 2 percent IE, 30 GWd/tU BU 3 percent IE and 45 GWd/tU BU 4 percent IE were chosen because they represent fully burned assemblies, while the three assemblies with initial enrichment of 4 percent ^{235}U provide various ^{235}U to ^{239}Pu ratios to examine if the C_1 and C_2 constants vary with this ratio.

The results in Table 1 indicate that there is a 4 percent to 7 percent shift in the C_1 constants depending on the method (first fission or tally in the fuel) used to quantifying this constant. It is also noteworthy that the C_1 constants vary less than 2 percent among the fully burned assemblies using the First Fission method. In Table 2 there was only a ~1 percent change in the value of C_2 between the First Fission and tally in the fuel methods. Recalling C_2 is essentially a comparison between ^{239}Pu and ^{241} Pu weights; since both of these isotopes have similar spatial distributions and similar absorption to fission cross section ratios it is not surprising that the method of calculation of this weight does not vary. In contrast, the C_1 constant relates ^{235}U to ^{239}Pu, which do not have as similar a spatial distribution nor as similar absorption to fission cross section ratios.

Conclusion

The information presented in this report has demonstrated some of the advancement made on the Passive Neutron Albedo Reactivity with Fission Chambers technique. The variation in the cadmium ratio with cadmium liner height was quantified. The new First Fission capability in the MCNPX code was used in order to more accurately determine the weighting coefficient for the fissile isotopes and to compare to the previous, more approximate, method used. By using a set of select assemblies it was possible to quantify the agreement between the two approaches. Overall, the Passive Neutron Albedo Reactivity with Fission Chambers technique provides an inexpensive system with rapid measurement capability for nondestructive assay of spent nuclear fuel assemblies.

References

1. Humphrey, M. A., S. J. Tobin, and K. D. Veal. 2012. The Next Generation Safeguards Initiative's Spent Fuel Nondestructive Assay Project, *Journal of Nuclear Materials Management*, Vol. 40, No. 3.
2. Conlin, J. L., S. J. Tobin, J. Hu, T. Lee, H. O. Menlove, and S. Croft. 2011. Passive Neutron Albedo Reactivity with Fission Chambers, Report LA-UR-11-00521, Los Alamos National Laboratory, Los Alamos, New Mexico.
3. Menlove, H. O., and D. H. Beddingfield. 1997. Passive Neutron Reactivity Measurement Technique, Report LA-UR-97-2651, Los Alamos National Laboratory, Los Alamos, New Mexico.
4. Reilly, D. T. 1990. Passive Nondestructive Assay of Nuclear

Materials, Report LA-UR-90-732, Office of Nuclear Regulatory Research, NUREG/CR-5550.
5. Pelowitz, J. F., (Editor). 2005. MCNPX™ USER'S MANUAL Version 2.5.0, Report LA-CP-05-0369, Los Alamos National Laboratory, Los Alamos, New Mexico.
6. Galloway, J. D., H. R. Trellue, M. L. Fensin, and B. L. Broadhead. 2012. Design and Description of the NGSI Spent Fuel Library with an Emphasis on Passive Gamma Signal, *Journal of Nuclear Materials Management*, Vol. 40, No. 3.

Developing the Californium Interrogation Prompt Neutron Technique to Measure Fissile Content and to Detect Diversion in Spent Nuclear Fuel Assemblies

Jianwei Hu, Stephen J. Tobin, Howard O. Menlove, Daniela Henzlova, Jeremy Gerhart, Martyn T. Swinhoe, and Stephen Croft
Nuclear Nonproliferation Division, Los Alamos National Laboratory, Los Alamos, New Mexico USA

Abstract

^{252}Cf Interrogation with Prompt Neutron (CIPN) detection is one of the fourteen nondestructive assay (NDA) techniques researched under the Next Generation Safeguards Initiative effort. CIPN is a relatively low-cost and lightweight instrument, and it looks like a Fork detector combined with an active interrogation source. The study of CIPN evaluates its capability of measuring fissile content and detecting diversion of fuel pins in commercial spent nuclear fuel assemblies. The design and the underlying physics of the CIPN detector are described. The response of CIPN to a series of virtual spent fuel assemblies were quantified using MCNPX simulations. The net signal of CIPN is mainly due to multiplication of the Cf source neutrons; this multiplication is dependent on both the fissile content and the neutron absorbers present in spent fuel. Two novel corrections have been introduced to account for the absorption caused by neutron absorbers. With the help of empirical fitting developed in this work, the fissile content in a target spent fuel assembly can be determined from the CIPN signal. CIPN is also tested in a series of hypothesized diversion cases. Preliminary results show that CIPN can detect the replacement of at least eight fuel pins (3 percent of total mass) with depleted uranium provided the count rate of baseline case was previously measured. In short, CIPN shows promising capability for measuring fissile content.

Introduction

^{252}Cf Interrogation with Prompt Neutron (CIPN) detection is one of the fourteen nondestructive assay (NDA) techniques researched under the Next Generation Safeguards Initiative (NGSI) effort.[1] CIPN shows promising capability of quantifying fissile content in a spent fuel assembly (referred to as *assembly* or *assemblies* except noted otherwise). CIPN is also a lightweight and inexpensive (<$350k) detector. CIPN is similar to a Fork detector, which has been used in the field for decades to measure total neutron and gamma emission, in both size and shape.[2] Due to the limitations of the Fork detector, an active interrogation source (^{252}Cf) is introduced next to the assembly on the opposite side to the detector, which forms the basic concept of CIPN.

Figure 1. Diagram of conceptual CIPN signal composition (background and active assay).

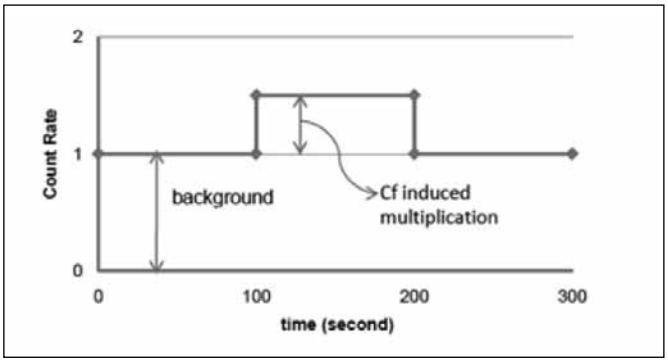

^{252}Cf source has been widely used in NDA instruments because of its high specific neutron intensity and portability. It has the intensity of a small accelerator without the electronics and irregular variations in yield. One particular example is a shuffler, which measures delayed neutrons using a 550-µg ^{252}Cf source.[3] Since the use of a Cf source would limit the portability of this technique, its application to safeguards would involve facility-level installation.

Fission chambers (FCs) were chosen as neutron detectors because of their insensitivity to gamma radiation. The geometry and physics of CIPN were modeled by using MCNPX 2.6.0.[4] The CIPN detector has been simulated with the NGSI spent fuel library[5] to quantify its capabilities of determining fissile content and detecting diversion of fuel pins in an assembly. The library covers a wide range of values for burnup (BU), initial enrichment (IE), and cooling time (CT), for PWR assemblies. From the library, sixty-four assemblies were selected, and each of them represents a unique combination of BU (15, 30, 45, and 60 GWd/tU), IE (2, 3, 4, and 5 percent) and CT (one, five, twenty, and eighty years).

The Concept of CIPN Assay

A conceptual diagram of CIPN signal composition is shown in Figure 1. The CIPN assay is comprised of two measurements, a background count and an active count. During an active count, the ^{252}Cf source is moved next to the assembly where it remains

Figure 2. (a) Horizontal cross section of CIPN; (b) Vertical cross section of CIPN.

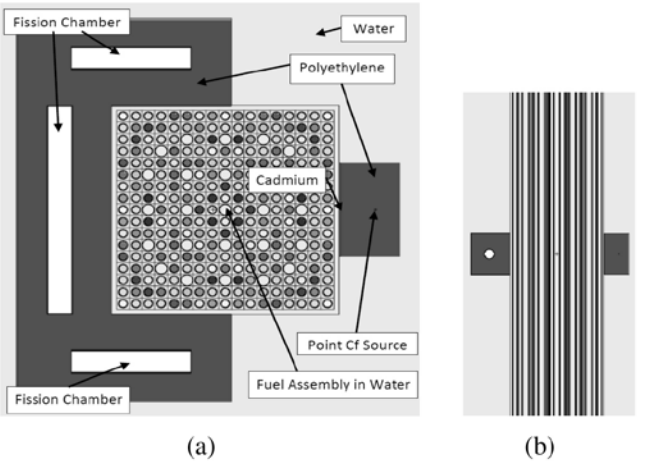

stationary for ~100 seconds. The neutrons detected during the background count are mainly from two sources: 1) direct contribution of passive source neutrons, namely spontaneous fission neutrons (mainly from ^{244}Cm and ^{242}Cm) and (a, n) reactions with ^{18}O etc.;[6] and 2) the multiplication of passive source neutrons due to fissile content in an assembly. In addition to background sources, two more sources contribute to the active count: 1) direct contribution of the ^{252}Cf source neutrons; and 2) the multiplication of ^{252}Cf source neutrons due to fissile content in an assembly. With design optimization, the contribution of direct Cf neutrons counts only a small fraction of the signal in water (or borated water). Hence, the increase in the active count rate above background count is almost entirely from the multiplication of neutrons in the fuel.

To relate multiplication to fissile content, corrections are needed to account for absorptions caused by neutron absorbers. Moreover, the ^{252}Cf source has to be of sufficient strength to override the background signal to reduce statistical uncertainty.

Design of CIPN Detector

The design of CIPN is briefly discussed here (more detailed discussion can be found in a LANL report[7]). The CIPN detector was optimized to achieve uniform sensitivity across the whole fuel assembly. Figure 2(a) shows the horizontal cross-section of CIPN, with a 17x17 PWR assembly located at the center (the vertical view is shown in Figure 2(b)). Surrounding the assembly on all sides is a 0.5-cm gap filled with water. The blue rectangle to the right is a block of polyethylene that contains a single point ^{252}Cf source. The distance from the source to the edge of the assembly is ~4 cm. There is a thin cadmium sheet (1-mm thick, not visible in the figure) inserted between the assembly and the polyethylene block to even out the fission rate in the assembly along the vertical direction. The vertical U-shaped block is filled with high-density polyethylene embedded with three fission chambers.

Figure 3. Count rate changes against the base case when 11 or 12 fuel rods removed at 6 different zones in the assembly.

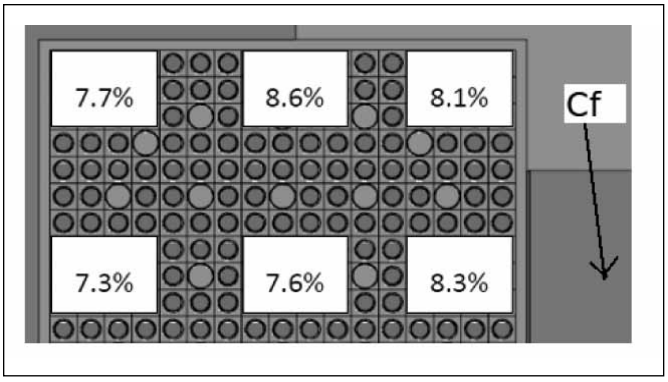

Figure 4. Mass of ^{252}Cf (μg) required to achieve certain Signal-to-Background (S/B) ratios as a function of burnup.

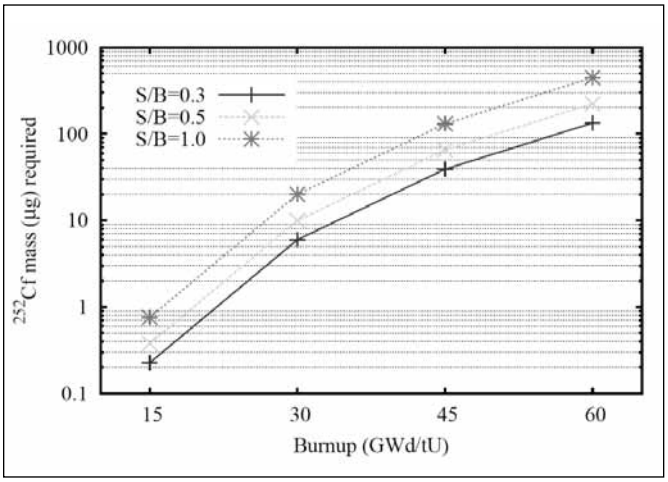

The thickness of the polyethylene wrapping around the FCs is ~3 cm. The polyethylene block has a cadmium liner all around except the walls directly facing the assembly or the source, in order to minimize signal from background neutrons. To estimate the response uniformity across the assembly, Figure 3 shows the count rate changes in percentage against the base case (no rods removed) when eleven or twelve fuel rods are removed from six different zones in an assembly each time (for this particular exercise, all the fuel rods are filled with fresh UO_2 with 2 percent ^{235}U enrichment). In each of the six cases, either twelve fuel rods or eleven fuel rods plus one water tube in some cases, which account for ~4.5 percent of total fuel, in one of the six zones were replaced by fuel two rods filled with depleted uranium (with 0.2 percent ^{235}U). Then the count rate was compared to the base case. This result shows that the current design of CIPN has nearly uniform response to the removal in different zones and that the CIPN detector is sensitive to diversion.

Table 1. The count rate change (%) in diverted cases from the corresponding un-diverted cases in three different zones for three different assemblies.

Case ID	location of diverted rods	# rods diverted	% mass diverted	Count rate change from the corresponding full case		
				15GWd/tU, (%)	30GWd/tU, (%)	45GWd/tU, (%)
1	inner zone	8	3.0	-4.6±0.30	-3.2±0.27	-2.4±0.32
2		24	9.1	-15.4±0.28	-10.1±0.29	-8.0±0.32
3		40	15.2	-27.5±0.28	-19.4±0.28	-14.1±0.31
4	middle zone	8	3.0	-3.8±0.30	-2.8±0.31	-2.0±0.32
5		24	9.1	-11.6±0.29	-7.8±0.30	-6.1±0.32
6		40	15.2	-20.0±0.28	-14.1±0.26	-11.0±0.31
7	outer zone	8	3.0	-4.1±0.30	-2.7±0.31	-2.4±0.33
8		24	9.1	-9.8±0.29	-7.2±0.30	-5.9±0.32
9		40	15.2	-17.3±0.28	-12.8±0.26	-10.4±0.32

Figure 5. The three zones in a 1717 PWR fuel assembly designated for diversion studies.

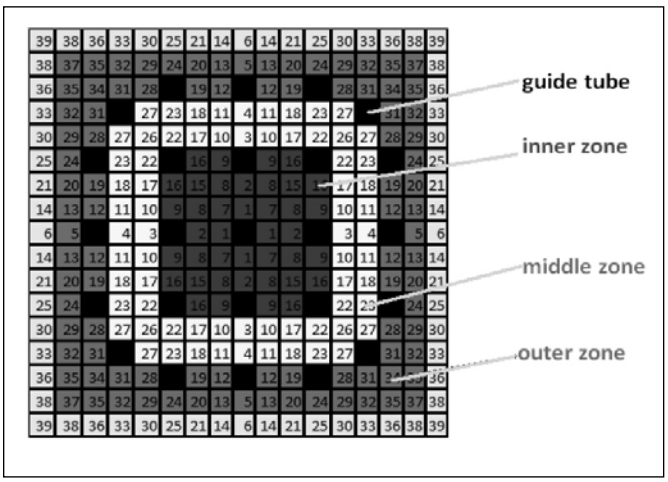

CIPN Source Strength Requirement

The Cf source has to be strong enough to override background signal. Spent fuel emits neutrons primarily from spontaneous fission of transuranic isotopes, such as ^{244}Cm and ^{242}Cm. These isotopes accumulate during the burnup of the fuel and thus the background count scales with BU. (The CIPN background is discussed in more detail in Reference 7.) Larger sources are required for higher BU. Figure 4 shows the required mass of ^{252}Cf (μg) as a function of burnup to achieve signal-to-background ratios of 0.3, 0.5 and 1.0. The BU of 45 GWd/tU was chosen as the reference case for source selection because it is close to the upper-limit of burnup in most commercial reactors today. As shown, a 40-μg ^{252}Cf source will produce a signal of 30 percent above the background, and a 60-μg ^{252}Cf source will produce a signal of 50 percent above the background for 45 GWd/tU. Given these two bounding cases, a 50-μg ^{252}Cf source was determined as needed at the end of life for the source. Since it is desirable for the source to last at least five years, given the ~2.65 year half-life of ^{252}Cf, a 200-μg Cf source was selected as the mass at the beginning of operation. Unless stated otherwise, the mid-life mass of a 100 μg (2.34_108 neutrons per second) was used for calculations in the remainder of this paper. A 200-μg ^{252}Cf source would cost ~$65,000.[8] As a point of reference, a 55-gallon-drum shuffler usually begins operation with a 550-μg source.[3] Furthermore, the largest ^{252}Cf source that is commercially available is 10,000-μg.[8] A DT neutron generator with medium strength can be an alternative to the Cf source for CIPN, although a yield monitor will need to be added.

The Capability of CIPN to Detect Diversion

To estimate the capability of CIPN to detect diversion, a few numerical experiments were performed using MCNPX. Three assemblies were selected to conduct these experiments: they all have 4 percent IE and five-year CT, but three different BUs (15, 30, and 45 GWd/tU). The fuel assembly is divided into three different zones as shown in Figure 5. The inner zone is indicated in purple, the middle zone in yellow, the outer zone in red, and the guide tubes in black. At each time, eight, twenty-four, or forty rods in each zone were replaced by depleted uranium (0.2 percent ^{235}U). The CIPN count rate in each diverted case was then compared to the corresponding undiverted case (or full case).

Table 1 shows the count rate change of each diverted case against the corresponding full case. One obvious observation is that the more fuel rods diverted the greater the change is in count rate. The 15 GWd/tU assembly has the most fissile material and the highest multiplication, while 45 GWd/tU has the least fissile material and the lowest multiplication. Correspondingly, as shown in this table, the 15 GWd/tU assembly has highest change in count rate in each diversion case and 45 GWd/tU has the lowest. The uncertainties listed in this table are the percent uncertainty for the diverted case determined from MCNPX tallies. The zones where the diversion takes place impact the count rate change as well. Generally speaking, with few exceptions, the diversion from the inner zone results in the highest count rate change whereas the lowest change comes from diversion in the outer zone; the middle zone lies in between. This implies that the same amount of fissile material carries more weight in terms of neutron creation if it resides in the inner zone of the fuel assembly due to the spatial dependence of multiplication. Overall, the lowest count rate change is 2.0 percent. Based on the statistical uncertainty of all CIPN measurements, which is less than 0.3 percent,[7] the diversion of at least eight fuel rods could be detected if the count rate of the full case is known or previously measured. For most measurement situation in safeguards, the base measurement is not available. In the absence of a base measurement, one cannot necessarily discern if a low count rate is due to pin diversion or due to less fissile mass in an un-diverted assembly. This more challenging case needs future research, as does the impact of systematic uncertainty. Also note that there could be numerous diversion scenarios and some of them might be even more challenging than the one studied here. Future work is suggested to investigate how CIPN responds to other forms of diversion scenarios.

Preliminary Analysis of CIPN Signal

Two simple cases were studied to initially illustrate how the net count rate (CR) changes with BU, IE and CT: Case 1 investigates CR vs. BU with CT held constant at five years. The net count rates of sixteen different assemblies (they are all five-year cooled but with different BU or IE) were quantified as a function of BU and CT; Case 2 investigates CR vs. CT with IE held constant at 4 percent. The count rates of sixteen different assemblies (they all have 4 percent IE but different BU or CT) were quantified as a function of BU and CT. As shown in Figure 6(a), the CIPN net count rate varies significantly with both BU and IE (Case 1). For a given curve of the same IE, the count rate decreases with BU because spent fuel with higher BU has lower fissile content and more neutron absorbers. For a given BU, spent fuel with higher IE has higher count rate because it has higher fissile content. In Figure 6(b), the variation in the CIPN net count rate with CT is illustrated (Case 2). The count rate decreases with longer CT but to a lesser degree than the variation with BU and IE. The observed change is due to two primary factors: (1) the fissile isotope 241Pu (T1/2 ≈14 yr) decays into a neutron absorbing isotope ^{241}Am (with a significant absorption cross-section); and (2) the stable isotope ^{155}Gd, which has a very large neutron absorption cross-section, grows with CT since it is a decay product of ^{155}Eu ($T_{1/2}$ ≈4:7 yr). The count rate drops at a slower pace at high CT because there is less ^{241}Pu and ^{155}Eu remaining to decay at higher CT. Hence, both ^{241}Am and ^{155}Gd accumulate over time, depressing the count rate at higher CT. The four curves in this figure are almost parallel to each other because the time dependence of the relevant factors is similar.

Figure 6. (a) Case 1: the CIPN net count rate as a function of BU for 16 different assemblies in water (with CT fixed at 5 years); (b) Case 2: the CIPN net count rate as a function of CT for 16 different assemblies in water (with IE fixed at 4%).

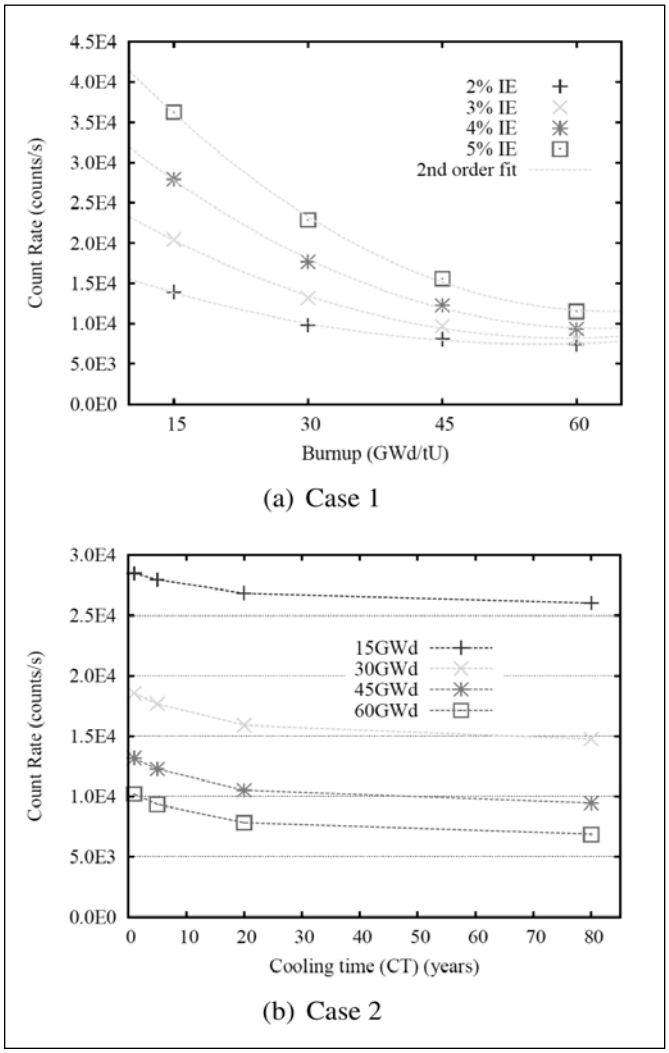

Figure 7. The fraction of neutron produced by 238U in all sixty-four assemblies (with the ID of each assemblygoes from 1 to 64). The ID of assemblyis ordered by CT→IE →BU.

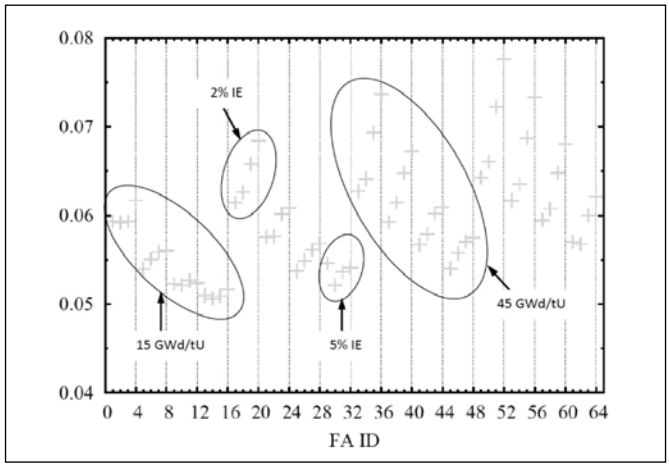

Further Analysis of CIPN Signal with $^{239}Pu_e$

The concept of $^{239}Pu_e$

The fissile content is the main factor that affects the count rate. In spent fuel, there are three major fissile isotopes: ^{235}U, ^{239}Pu and ^{241}Pu. Inspired by the convention in the safeguards profession of using the concept of $^{240}Pu_{effective}$ for passive Pu coincident neutron counting,[2] a similar term, $^{239}Pu_e$ CP was introduced to represent a weighted linear combination of the three fissile isotopes (the subscript "e" here stands for "effective"). $^{239}Pu_{e\_CP}$ is defined as:

$$^{239}\mathrm{Pu}_{\mathrm{e\_CP}} \equiv C_1{}^{235}\mathrm{U}_m + {}^{239}\mathrm{Pu}_m + C_2{}^{241}\mathrm{Pu}_m. \quad (1)$$

Specifically, Equation 1 weights the masses of ^{235}U and ^{241}Pu by constants C_1 and C_2, respectively, relative to ^{239}Pu in terms of their specific contributions to the count rate. $^{239}Pu_e$ can also be considered as the "fissile content equivalent" of a spent fuel assembly. The subscript "CP" stands for "CIPN technique" and is needed to distinguish the $^{239}Pu_e$ determined with a CIPN instrument from that determined by other instruments. The subscript "m" stands for mass of each isotope.

Besides the aforementioned three fissile isotopes, ^{238}U also produces neutrons, but its contribution is sufficiently depressed in water and its mass changes slowly with burnup. Besides, since ^{238}U has a ~1 MeV fission cross section threshold, the majority of the $^{23}8U$ fission is caused by the fission neutrons of the three aforementioned fissile isotopes, since only a small fraction of ^{238}U directly interacts with Cf source neutrons. So most of the ^{238}U fission (~90 percent) can be *tied* to the multiplication of the three main fissile isotopes. The neutron contribution from ^{238}U fission among all assemblies was also quantified. Figure 7 shows the fraction of neutrons produced by ^{238}U in all sixty-four assemblies. The assemblies are ordered by CT→IE →BU, e.g., the first four assemblies have a BU of 15 GWd/tU, IE of 2 percent, and CT of one, five, twenty, and eighty years, respectively. The neutron contribution of ^{238}U ranges from 5 percent to 7.5 percent with the average around 6 percent. Since the contribution from ^{238}U is relatively small and varies about a range of a few percent, and since most ^{238}U fission can be attributed to the multiplication of the three main fissile isotopes, ^{238}U can be treated as a small (less than 1 percent) background factor.

"Gross Neutron Production" Concept Used to Determine the Weighting Coefficient C_i

A useful concept for quantifying the relative impact of various isotopes on neutron count rate in spent fuel is the concept of "gross neutron production." In this concept, the weight of a specific isotope in terms of contribution to the count rate is assumed to be proportional to the number of neutrons created by this isotope during fission. Therefore the weighting coefficient C_1 and C_2 can be defined as follows:

$$C_i = \frac{\int_V \int_E \sigma_f(E)_i \nu_i(E) \Phi(E,V) dE dV}{\int_V \int_E \left[\sigma_f(E)\nu(E)\right]_{239_{\mathrm{Pu}}} \Phi(E,V) dE dV}, \quad (2)$$

where σf and n correspond to fission cross section and number of neutrons produced per fission, respectively. σis neutron flux. With Equation 2, C_1 (i = 1) can be obtained by plugging in relevant parameters of ^{235}U in the numerator, and C_2 (i = 2) can also be obtained for ^{241}Pu.

In order to obtain values of the C_1, C_2 coefficients, two approaches were used. The first one utilizes the "tally in the fuel" approach, where the neutron production caused by a specific fissile isotope in the spent fuel assembly is used to weight that particular isotope. In this approach, both the numerator and denominator in Equation 2 can be calculated using the product of the neutron flux tally (F4) and the fission neutron production tally (FM -6 -7). The neutron flux tally covers the entire fuel region in the assembly. Note that from this equation, C_1 and C_2 are obtained on a "per atom" basis; to convert to a "per gram" basis, the molar mass ratios of "239/235" and "239/241" are multiplied respectively to the value of C_1 and C_2 determined by this equation.

The second approach utilizes "first fission tally," a new capability added to MCNPX by Hendricks et al.[9] in order to track and quantify the contribution of first generation of fissions, caused by a specific isotope, to the detected neutron signal. With this new capability, the contribution of a particular isotope to the CIPN count rate in first generation of fissions can be quantified, which, after being normalized by total mass, is then used to calculate C_1 and C_2. More details can be found in Reference 9.

Figure 8. Value of weighting coefficient (Ci) for each of the sixty-four assemblies: (a) C_1; (b) C_2.

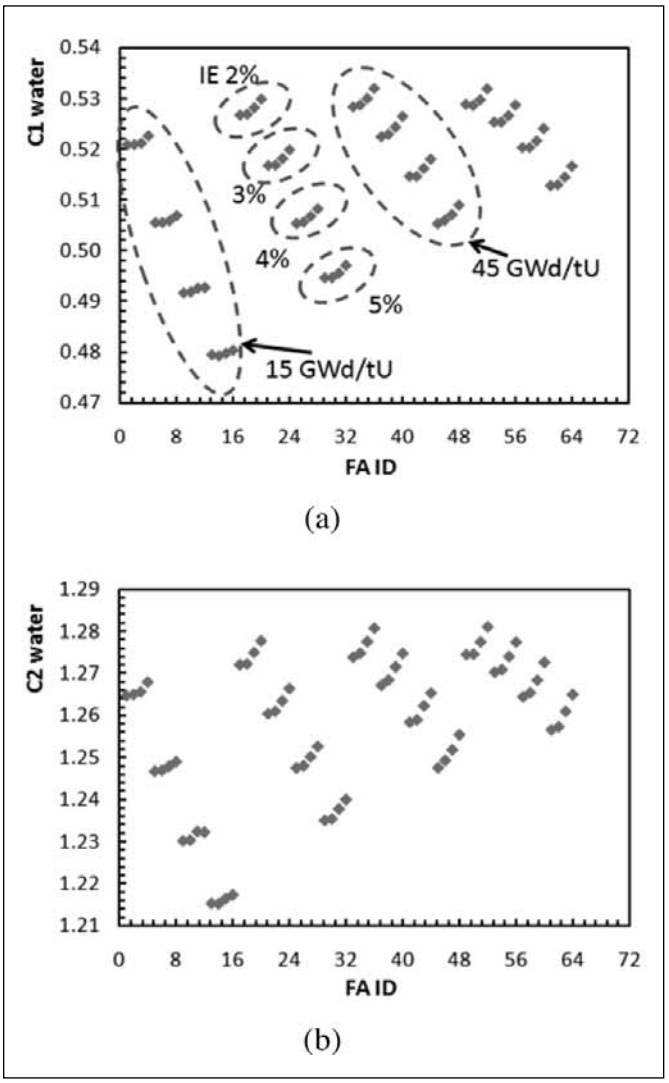

The values of C_1 and C_2 determined by these two approaches are close (differ less than 3 percent).[9] Using the "tally in the fuel" approach, the C_1 and C_2 coefficients were calculated for all sixty-four spent fuel assemblies. The results are depicted in Figure 8 (with FA ID goes from 1 to sixty-four in the same order as in Figure 7). (The results of C_1 and C_2 determined using "first fission tally" can be found in Reference 9.) It can be observed from these two figures that there is a clear trend of C_1 and C_2: higher IE, lower values for both C_1 and C_2. It also shows that C_1 and C_2 are dependent on BU and CT as well, but not as prominent as on IE. In general, for the same BU and CT, the neutron energy spectrum in assemblies with higher IE have lower thermal neutron peak. Also the neutron energy spectrum in the fuel is *shaped* by the presence of many isotopes, e.g., the unique resonant absorption of a particular isotope will depress the neutron flux in its resonant energy range. These two factors are suspected to contribute to the trend observed in C_1 and C_2. The variation in C_1 and C_2 depicted in Figure 8 is for IE, BU and CT that vary over a large range. Restricting IE, BU and CT to fully burnt fuel assemblies (e.g., 15 GWd/tU and 2 percent IE, 30 GWd/tU and 3 percent IE, 45 GWd/tU and 4 percent IE), which are usually encountered in the field, theC_1 and C_2 vary only by approx. 1 percent. The average values of C_1 and C_2 of these three fully burnt assemblies are 0.517 and 1.262, respectively. An alternative concept to determine C_1 and C_2 is the "net neutron contribution" concept, in which the "net neutron" production (neutrons generated by fission subtracted by neutrons absorbed by a specific fissile isotope) instead of "gross neutron" is used to wait a particular isotope. More details about the "net neutron" method can be found in References 7 and 10.

Figure 9: Count rate (counts/sec) vs. 239Pue CP (kg) for all 64 virtual assemblies. The count rate is normalized with a 100- µg 252Cf source, which releases 2:34108 neutrons/sec. Each assembly represents a unique combination of BU (15, 30, 45, and 60 GWd/tU), IE (2, 3, 4 and 5%) and CT (1, 5, 20, and 80 years). Each color represents one BU level. For the 16 assemblies with the same BU, four groups of data points are shown. And within each group, the four assemblies have the same IE but different CT.

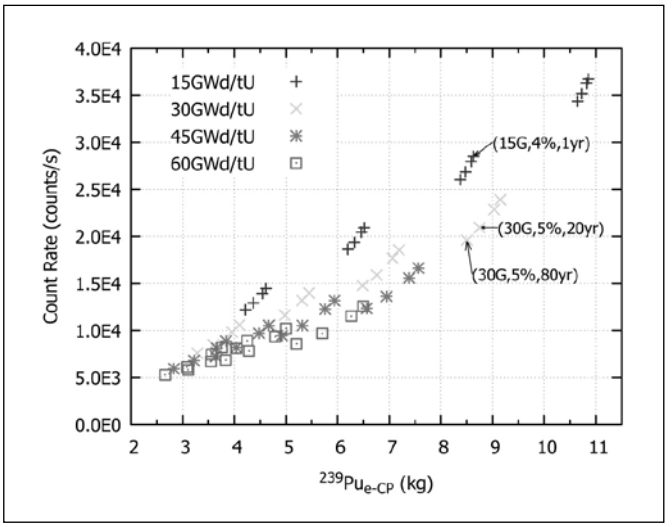

Count Rate vs. $^{239}Pu_{e\_CP}$

The count rate above background (net count rate) for each of the sixty-four assemblies was obtained using the MCNPX simulations. The mass of ^{235}U, ^{239}Pu, and ^{241}Pu of each assembly were obtained from the NGSI virtual library, which were generated using burnup calculations. $^{239}Pu_{e\_CP}$ was then calculated using Equation 1. The average values of C_1 and C_2 of fully burnt assemblies from the previous section were used in this calculation.

Figure 9 shows net count rate as a function of $^{239}Pu_{e\_CP}$ for all the sixty-four assemblies without any corrections. Each color

represents a specific BU level. For the sixteen assemblies with the same BU, four groups of data points are shown; one group represents each of the 4 IEs. Within each group of 4 assemblies with the same BU and IE, there are four assemblies with different CT. As shown, the data points are scattered, and there is no coherent functional relation between count rate and $^{239}Pu_{e\_CP}$ (i.e., given a count rate, a unique quantity of $^{239}Pu_{e\_CP}$ cannot be determined). An ideal outcome from Figure 9 would have the count rate of all sixty-four assemblies as a simple function of $^{239}Pu_{e\_CP}$ mass. This would indicate that Equation 1 using C_1 and C_2 properly weights the relative significance of the three fissile isotopes and that there are not any other significant factors impacting the count rate beside the three primary fissile isotopes. But that is not the reality. The main conclusions from Figure 9 are the following: 1) The count rate among the assemblies generally trend with the $^{239}Pu_{e\_CP}$, and 2) the structure in the data indicates that the count rate is a function of factors that scale with BU, IE and CT. The strongest dependence is a function of BU. In other words, $^{239}Pu_{e\_CP}$ is not the only influencing factor; other factors such as neutron absorbers must also be at play.

Count Rate vs. $^{239}Pu_{e\_CP}$ with Corrections

The two primary factors most likely to impede a smooth relationship between count rate and $^{239}Pu_{e\_CP}$ are 1) neutron absorption and 2) neutron production from isotopes other than the three main fissile isotopes. Both factors were investigated. Regarding the second factor, ^{238}U is a main neutron creator besides ^{235}U, ^{239}Pu, and ^{241}Pu. As discussed earlier, ^{238}U can be treated as a small background component in the medium of water. Two kinds of neutron absorbers play major role in terms of neutron absorption in spent fuel: (a) actinide neutron absorbers (e.g., ^{240}Pu) and (b) fission fragment absorbers (e.g., ^{149}Sm). Among these absorbers, most of them accumulate with burnup because the longer the fuel burns, the more actinides and fission fragments accumulate. Two notable exceptions are ^{155}Gd and ^{241}Am; they both grow dramatically with cooling time. ^{155}Gd, a decay daughter of ^{155}Eu with a half-life of 4.68 years, has an extremely large absorption cross section. ^{241}Am, a decay daughter of ^{241}Pu with a half-life of 14.4 years, has a large neutron absorption cross section as well (and only a small fission cross section). In order to include the impact of neutron absorbers, BU and CT corrections were introduced to $^{239}Pu_{e\_CP}$ based on their dependence on BU and CT. With these two corrections, changes to "$^{239}Pu_{e\_CP}$ with corrections" (also indicated by "X"). The BU and CT corrections are expressed as below:

$$X \equiv {}^{239}\mathrm{Pu}_{\mathrm{e\_CP}} \text{ with corrections} = C_{BU}\left[{}^{239}\mathrm{Pu}_{\mathrm{e\_CP}} + f(BU,CT)\right], \quad (3)$$

or,

$${}^{239}\mathrm{Pu}_{\mathrm{e\_CP}} = X/C_{BU} - f(BU,CT), \quad (4)$$

where C_{BU} (BU correction coefficient) is used to account for the absorption from the fission fragment absorbers, and actinide absorbers scale with BU. C_{BU} can be quantified by weighting the "absorbing power" of these absorbers at higher BU relative to 15 GWd/tU. The "absorbing power" can be calculated by using linear combination of all these stable absorbers with proper weighting of each isotope in each assembly with different BU. With the results of C_{BU} at different BU, an empirical relation of C_{BU} was established by using power-law fitting, as shown below:

$$C_{BU} = (BU/15)^{-0.302}, \text{ for } 15 \le BU \le 60 \text{ GWd/tU} \quad (5)$$

As discussed before, two major neutron absorbers are found to change dramatically with CT: ^{155}Gd and ^{241}Am. So the CT correction, f (BU;CT), can be written as:

$$f(BU,CT) = C_3{}^{155}\mathrm{Gd}_m + C_4{}^{241}\mathrm{Am}_m \quad (6)$$

As shown in Equation 6, the CT correction can be expressed as weighted sum of ^{155}Gd and ^{241}Am. The value of C_3 and C_4 can be obtained similarly as C_1 and C_2 by using Equation 2. Since both isotopes have negligible fission cross section, the value of C_3 and C_4 are both negative. The average value of C_3 and C_4 are -48.97 and -0.66 respectively. With these values, together with Equation 5 and Equation 6, Equation 3 now becomes:

$$X = \left(\frac{BU}{15}\right)^{-0.302}\left[{}^{239}\mathrm{Pu}_{\mathrm{e\_CP}} - 48.97{}^{155}\mathrm{Gd}_m - 0.66{}^{241}\mathrm{Am}_m\right] \quad (7)$$

With the equation above, the "X" value ("$^{239}Pu_{e\_CP}$ with corrections") can be easily calculated, with the masses of the five isotopes (i.e., ^{235}U, ^{239}Pu, ^{241}Pu, ^{155}Gd, and ^{241}Am) in a particular assembly obtained through burnup calculations. The value of "X" and count rate (CR) for each of the sixty-four assemblies is plotted in Figure 10. This figure illustrates the relation between count rate (CR) and "X", from which, a coherent universal relation between CR and "X" can be observed (i.e., given a certain count rate, the value of "X" can be uniquely determined, and vice versa). Note that CR does not reduce to zero when "X" goes to zero because of the Cf and ^{238}U background.

Figure 10: Count rate (counts/sec) vs."^{239}Pue CP with corrections" (X) (kg) for all the 64 assemblies. BU and CT corrections have been introduced to ^{239}Pue CP.

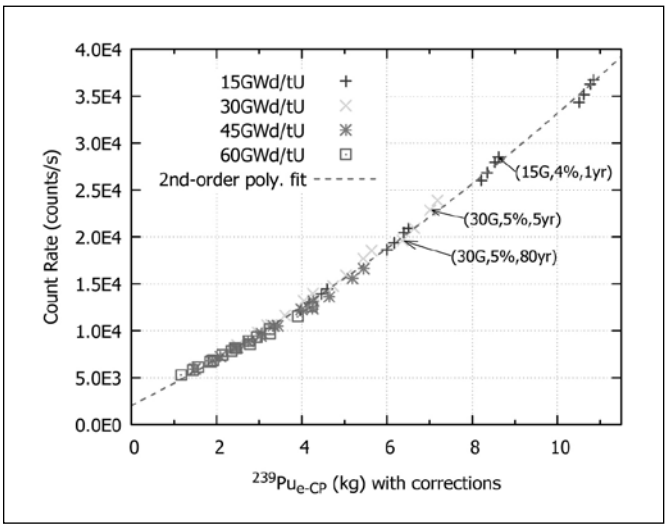

Also indicated by dashed line in this figure, the fitting curve agrees with the data points quite well. With the seconnd-order polynomial fitting, the empirical relation between CR and "X" is expressed as below:

$$CR = 80.65X^2 + 2307.4X + 2029.68 \qquad (8)$$

From a practical point of view, for an unknown assembly, once the CIPN count rate is measured, "X" can be uniquely determined through Figure 10 (using a calibrated version). The fissile content, $^{239}Pu_{e\_CP}$, can then be calculated using Equation 7, provided BU and the mass of ^{241}Am and ^{155}Gd can be quantified.

Usually, the BU of an assembly can be determined using the measured gross gamma emission obtained in a passive gamma technique,[11] and the CT can be verified based on the operator's declarations. However the mass of ^{241}Am and ^{155}Gd are usually unknown. Since the production path of both ^{241}Pu and ^{155}Gd are relatively simple, empirical relations can be established by using decay functions and by fitting existing data from burnup calculations, as discussed in the following subsection. An alternative is to measure the characteristic gamma lines of ^{241}Am and ^{155}Eu (or ^{154}Eu) obtained in a gamma spectrometry technique.[12, 13] Future research is needed for this option.

Empirical Relations for the Mass of ^{155}Gd and ^{241}Am in a Spent Assembly

^{155}Gd mainly results from the β-decay of ^{155}Eu, and the β-decay branching ratio is 100 percent. The buildup of ^{155}Gd can be decoupled into two separate processes: first its precursor (^{155}Eu) accumulates during reactor operation (which mainly scales wit BU) and it decays at the same time. Then, once the assembly is discharged, ^{155}Eu stops accumulating but decays to ^{155}Gd. ^{155}Gd can be assumed to be zero in a freshly discharged assembly (CT = 0) since it would be destroyed by neutrons during reactor operation due to its high absorption cross section. Therefore the mass of ^{155}Gd can be written as: $^{155}Gd_m = m_0 * f(BU) * f(CT)$, where m_0 is a normalization factor. By normalizing to one-year CT, m0 was found to be 0.16. According to decay law:

$$f(CT) = (1 - e^{-\lambda * CT})/(1 - e^{-\lambda * 1.0}) \text{ or,} \qquad (9)$$

$$f(CT) = (1 - e^{-0.1481CT})/0.1377, \text{ with } \lambda = ln2/T_{1/2} \qquad (10)$$

f (BU) could be obtained by solving the production and decay chain of ^{155}Eu. Rather than following this complex route, f (BU) can also be obtained empirically by fitting the ^{155}Gd mass in sixty-four assemblies, which results in:

$$f(BU) = 0.138 + 5.04E\text{-}3 * BU + 3.79E\text{-}3 * BU^2 - 3.47E\text{-}5 * BU^3 \qquad (11)$$

By combining Equation 10 and Equation 11, the mass of ^{155}Gd can be written as a function of BU and CT:

$$^{155}\text{Gd}_m = (0.022 + 8.07E\text{-}4 * BU + 6.07E\text{-}4 * BU^2 - 5.55E\text{-}6 * BU^3)(1 - e^{-0.1481CT})/0.1377. \qquad (12)$$

To test this function, the mass of ^{155}Gd in sixteen different assemblies predicted by this function were compared to the results from NGSI library. The results are shown in Figure 11. As shown, this function predicts the ^{155}Gd mass quite well in general. Similarly, the mass of ^{241}Am can be fitted as:

$$^{241}\text{Am}_m = (-223.6 + 32.3 * BU - 0.325 * BU^2 + 1.1E\text{-}3 * BU^3)(1 - e^{-0.0889CT}) \qquad (13)$$

Summary

In summary, a neutron detector, CIPN, was proposed to quantify fissile content in spent fuel assemblies. The capability of CIPN has been evaluated using a series of virtual assemblies and encouraging results have been obtained. Preliminary results show that CIPN is sensitive to the diversion cases simulated and it has almost uniform response to a unit of fissile mass at different locations across the assembly. With the schemes presented in this paper, together with given (either measured or declared) BU and CT, the fissile content

Figure 11: The mass of ^{155}Gd in sixteen different assemblies: comparison between the results predicted by function and NGSI library

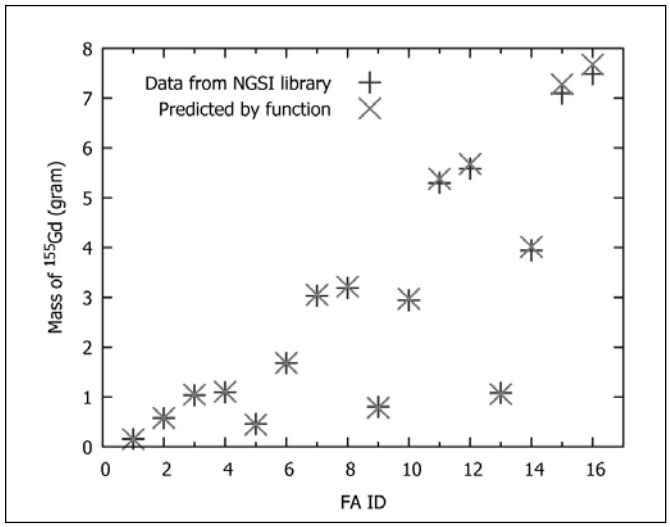

of a target assembly (or $^{239}Pu_{e\_CP}$) can be determined. The statistical uncertainty is less than 1 percent, obtained within 100 second. The accuracy will certainly be limited by the calibration and systematic errors. The neutron source needs to be ~ 2 x 10^8 n/s which corresponds to a ^{252}Cf source of 100 μg to create a viable S/N ratio given the strong passive background and short targeted assay time. It was demonstrated that burnup and cooling time corrections are needed to accurately predict the fissile content of a given assembly, and the mass of ^{155}Gd and ^{241}Am are needed to perform the cooling time correction. Empirical functions to predict the masses of these two isotopes are also proposed. While the standalone merits of this technique to quantify fissile content in spent fuel look promising, how it would be applied is subject to further research. Most likely, it would be combined with other instruments, and research on this is also underway. Meanwhile, fabrication of the CIPN instrument is planned for 2012 and measurement of spent fuel of CIPN, integration with other NDA techniques, is expected in 2013.

Acknowledgements

The authors would like to acknowledge the support of the Next Generation Safeguards Initiative (NGSI), Office of Nonproliferation and International Security (NIS), National Nuclear Security Administration (NNSA). The authors would also like to thank Dr. T. J. Ulrich, Dr. John Hendricks, Dr. Taehoon Lee, Dr. Jeremy Conlin, Ms. Melissa Schear and Dr. Michael Fensin for their valuable input to this project.

References

1. Humphrey, M. A., S. J. Tobin, and K. D. Veal. 2012. The Next Generation Safeguards Initiatives Spent Fuel Nondestructive Assay Project, *Journal of Nuclear Materials Management,* Vol. 40, No. 3.
2. Reilly, D., N. Ensslin, H. Smith Jr., and S. Kreiner. 1991. Passive Nondestructive Assay of Nuclear Materials, LA-UR-90-732.
3. Rinard, P. M. 2001. Application Guide to Shufflers. Los Alamos National Laboratory Report, LA-13819-MS.
4. Pelowitz, J. F. (Editor). 2008.MCNPX USER'S MANUAL Version 2.6.0. Los Alamos National Laboratory report, LACP-07-1473.
5. Galloway, J. D., H. R. Trellue, M. L. Fensin, and B. L. Broadhead. 2012. Design and Description of the NGSI Spent Fuel Library with an Emphasis on Passive Gamma Signal, *Journal of Nuclear Materials Management,* Vol. 40, No. 3.
6. Richard, J., M. L. Fensin, and S. J. Tobin. 2010. Characterization and analysis of the neutron source term of spent PWR fuel, P*roceedings of the Institute of Nuclear Materials Management 51st Annual Meeting.*
7. Hu, J., S. J. Tobin, H. O. Menlove, and S. Croft. 2011. Determining the Pu Mass in LEU Spent Fuel Assemblies—Using Californium Interrogation Prompt Neutron (CIPN) Detection, Los Alamos National Laboratory report. Unpublished at the time of writing.
8. Frontier Technology Corporation. 2011. "Californium – 252 neutron sources," http://www.ne.doe.gov/genIV/neGenIV4.html.
9. Henzlova, D., and J. Gerhart. 2011. Assessment of the Californium Interrogation Prompt Neutron (CIPN) Technique for the Next Generation Safeguards Initiative Spent Fuel Research Effort, Los Alamos National Laboratory report. Unpublished at the time of writing.
10. Hu, J., S. J. Tobin, H. O. Menlove, and S. Croft. 2010. Determining Plutonium Mass in Spent Fuel Using Californium Interrogation with Prompt Neutron Detection, *Proceedings of the Institute of Nuclear Materials Management 50th Annual Meeting.*
11. Tiitta, A., J. Hautamaki, and A. Turunen. 2011. Spent BWR Fuel Characterisation Combining a FORK Detector with Gamma Spectrometry, Report on Task JNT A 1071 FIN of the Finnish Support Programme to IAEA Safeguards, STUK-YTO-TR 175.
12. Eigenbrodt, J., W. S. Charlton, and A. A. Solodov. 2011. Sensitivity of Spent Nuclear Fuel Gamma-Ray Measurements, P*roceedings of the Institute of Nuclear Materials Management 51st Annual Meeting.*
13. Gauld, I., and M. Francis. 2010. Investigation of passive gamma spectroscopy to verify spent nuclear fuel content, *Proceedings of the Institute of Nuclear Materials Management 51st Annual Meeting.*

New Design of the Differential Die-away Self-interrogation Instrument for Spent Fuel Assay

Anthony Belian, Howard O. Menlove, Martyn T. Swinhoe, and Stephen J. Tobin
Nuclear Nonproliferation Division, Los Alamos National Laboratory, Los Alamos, New Mexico USA

Abstract

The Differential Die-away Self-Interrogation (DDSI) technique is being studied by the Next Generation Safeguard Initiative (NGSI) for the purposes of determining fissile mass, and eventually Pu mass, in spent fuel assemblies. The technique utilizes ambient neutrons primarily from the spontaneous fission of ^{244}Cm to interrogate the fissile materials (primarily ^{235}U, ^{239}Pu, and ^{241}Pu) in the assembly. The time separation of neutron detection events from spontaneous fission (early gate) and induced fission (late gate) enables the independent measurement of fertile and fissile masses in spent fuel. In-field testing of the DDSI technique with prototype hardware and commercial spent fuel assemblies will occur in 2014. The original NGSI DDSI design was annular and surrounded the fuel assembly on all four sides and required the operator to insert the assembly from above. A new side-entry design is being implemented because it is expected to be more acceptable to facilities and regulators responsible for spent fuel management and it is not expected to deteriorate the performance of the instrument significantly. The DDSI in this context has three banks of ^{3}He detectors surrounding the fuel assembly on only three sides. The efficiency and die-away time of this updated design are similar to the characteristics of the annular design.

Introduction

The fissile content in *fresh* fuel assemblies can be determined by using nondestructive assay (NDA) techniques to measure direct neutron and gamma signatures from the major fissile isotopes. In the case of spent fuel, however, these direct signatures are masked by the high gamma-ray dose from fission products and the high neutron background from spontaneous fission (SF) and (α, n) reactions. There are two main types of NDA techniques, passive and active, that have been used traditionally to estimate fissile content in spent fuel.[1] The much more common passive technique measures indirect signatures from the spent fuel to estimate burnup and then relates burnup to the ^{235}U and plutonium content using calculated or empirical correlations. The active technique measures prompt or delayed signals from spent fuel, via a pulsed neutron generator or an isotopic source. The resulting net induced fission response is directly proportional to the fissile content in the assembly. The interrogating source strength must be on the order of 10^{8} to 10^{9} n/s at a minimum to produce an induced fission signal comparable to the passive background signal.[1]

Figure 1. Neutron capture time distributions from spontaneous and induced fission events

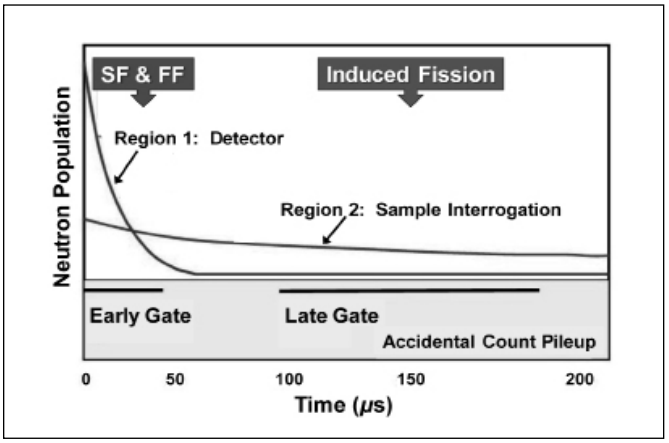

The development of NDA techniques to directly measure plutonium and/or fissile content in *spent* nuclear fuel is ongoing.[2] One of the methods being developed is the Differential Die-away Self Interrogation (DDSI)[3] technique that utilizes the inherent passive neutrons emitted from the fuel to interrogate the fissile isotopes: ^{235}U, ^{239}Pu, and ^{241}Pu. While similar in concept to traditional differential die-away analysis[4] the DDSI technique does not require an external pulsed neutron source to interrogate the sample. The DDSI technique resolves the detection time difference between correlated neutrons. The neutrons from induced fission are detected later, on average, since the neutrons produced by induced fission need to go through at least two thermalization intervals. The first is the thermalization of the interrogating neutrons that are born ~2 MeV but generally induce fission at energies near 1 eV. The second is the thermalization of the induced fission neutrons before their absorption in the ^{3}He detector. For a multiple induced fission chain, the detected neutron appears after several thermalization cycles. The initial interrogating neutrons are detected directly in ^{3}He, that is, after only one thermalization interval. Figure 1 illustrates this concept.

One subtle point worth clarification: the neutrons that initiate the fission chain reaction come from ^{244}Cm, yet the

Figure 2. Horizontal cross-section of the original DDSI detector. An enlarged schematic of Region 1 shows the structure of the Cd fins.

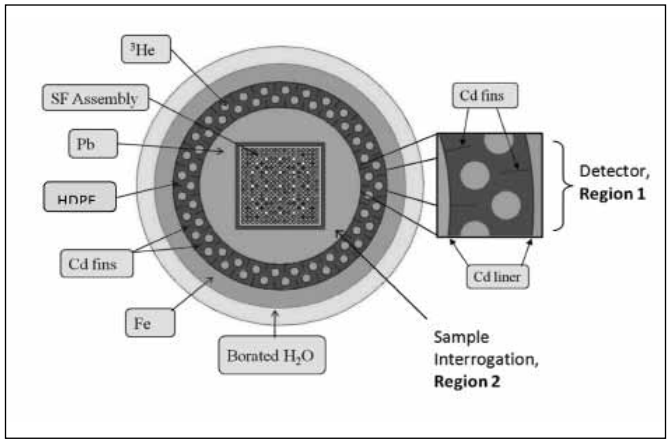

analysis that determines whether neutrons are coincident triggers on *every* detected neutron. The detection time analysis shows that there is a higher population of induced fission (IF) neutrons relative to spontaneous fission (SF) neutrons at later times compared to early times. The DDSI technique takes advantage of this difference. Note that there is a small component of fast fission (FF) events that also show up at early times that cannot be resolved from SF events.

DDSI Instrument Description

Original DDSI Instrument

The original DDSI design, described in detail in Reference 3, consisted of an annular detector body of high-density polyethylene (HDPE) with fifty-seven imbedded ^{3}He tubes at 6-atmospheres of pressure in two rows (see Figure 2). This configuration caused the outer row of tubes to have a larger pitch than the inner row and, thus, a longer die-away time. Cadmium (Cd) fins were added to minimize the die-away time in the detector region to allow for a shorter gate-width, which minimizes the accidentals count rate.

This design has a detector efficiency of 13 percent for a point ^{252}Cf source in the center of the sample cavity, and a 22 µs die-away time in the detector region. The lead between the fuel assembly and detector is to reduce the gamma ray dose below the pile-up threshold. In order for the redesigned DDSI detector to have similar performance with this original design, the efficiency and die-away characteristics must be similar.

The characteristics of the original detector were determined via MCNPX[5] simulations using the NGSI spent fuel libraries.[6] The die-away time of the detector was determined in water borated to 2,200 ppm, which is typical of spent fuel ponds, and the efficiency with a ^{252}Cf source in air. To benchmark the new design to the original, modeling was done assuming the same conditions. However, going forward, the new design will be evaluated in non-borated water in light of expected experimental plans.

Figure 3. Cross-sectional view of the new DDSI design

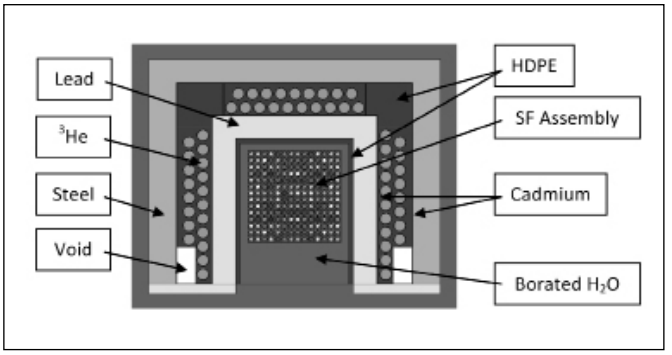

Re-designed DDSI Instrument

In order to enable side-entry fuel measurements, the configuration of the counter was modified as shown in Figure 3. The back–left and –right corners of the instrument (upper-left and upper-right in the figure) are neutronically isolated from the rest of the counter by 1 mm thick cadmium sheets to provide locations where alternatives to ^{3}He detectors can be tested. This design also uses fifty-seven imbedded ^{3}He tubes at 6-atmospheres of pressure. Lead surrounds the ^{3}He detector banks on all sides, top, and bottom to keep the dose < 10 R/hr and prevent gamma ray pile up events. The *void* shown in Figure 3 represent regions where the HPDE was removed to minimize the die-away time. (These can be filled with non-hydrogenous material if structural integrity requires.) The HDPE lining the inside of the sample cavity acts as a mechanical buffer for the assembly against the lead shielding.

MCNPX Simulations of DDSI Instrument

The Monte Carlo code, MCNPX, was used to model the DDSI detector represented in Figure 3. The total efficiency and die-away time are calculated to be 10% and 15.6 µs respectively. These compare favorably with the original design of 13 percent and 22 µs, thus lending confidence that the re-designed instrument will perform much like the original for which a great deal more simulation work has been completed.

One of the many enhancements to the MCNPX code made specifically for the NGSI Spent Fuel effort is a modification to the PTRAC capability. This modified PTRAC tool will, for every neutron detected, record the detection time and all the fission events that occurred in the chain prior to detection all the way back to the original SF event. This allows for a determination of the detection time relative to the initiating SF event. With this tool it is possible to see the timing of neutron detections as a function of the nature of the last fission event (spontaneous or induced). Figures 4 and 5 show the results of this PTRAC tool. It is clear that the SF neutrons are detected soon after the fission event itself; this is because only fast neutrons from the assembly enter the detector region since any neutrons that thermalize in the water between the assembly and the detectors are absorbed in the cadmium (Cd) surrounding the detector. Thus, only neutrons

Figure 4. Spontaneous fission time spectra for the original and re-designed DDSI instrument

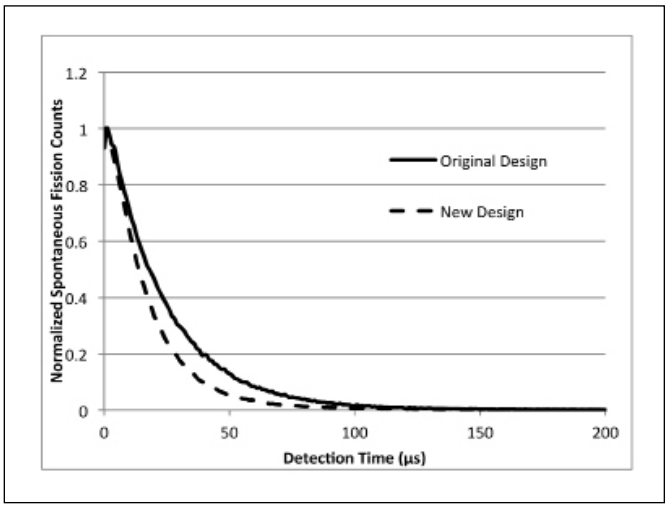

Figure 5. Induced fission time spectra for the original and re-designed DDSI instrument

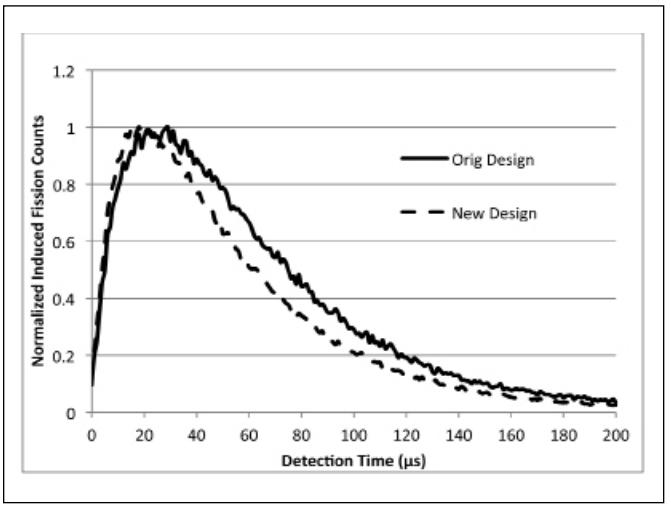

that thermalize in the detector region are detected. Neutrons from induced fission events generally have to go through at least two thermalization cycles, that is, the original SF neutron is thermalized in the water, then returns to the assembly and induces fission. The IF neutron then travels to the detector and thermalizes in the detector before being detected. In the case of a neutron detected from a long fission chain the detection time is many tens if not hundreds of micro-seconds after the initiating SF event. These effects are all seen in Figures 4 and 5, which show results for both the original and re-designed DDSI instruments in borated water. The shorter die-away time of the new design is clearly shown in the figures.

As a result of the reduced die-away time, the time separation of SF and IF neutrons is very good for the re-designed counter; for a 10 μs gate width and a 60 μs predelay the fraction of all coincidences that are due to IF is 76 percent (relative to 63 percent for the original design).

Conclusions

Previously, DDSI has been demonstrated as a promising technique for nondestructive assay of spent fuel.[3] To facilitate field-implementation of this technique, we have developed a re-designed instrument that allows for side-entry of an assembly. As demonstrated here, the re-designed DDSI instrument has similar characteristics to the original. The total efficiency and die-away time are calculated to be 10 percent and 15.6 μs respectively, which compare favorably with the values of 10 percent and 22 μs from the original design. In addition, the time separation of SF and IF neutrons is very good for the re-designed counter; for a 10 μs gate width and a 60 μs predelay the fraction of all coincidences that are due to IF is 76 percent. By contrast the original design gives 63 percent. The better separation for the new design is due to the shorter die-away time, however, since the overall efficiency of the new design is lower, a longer count time will be necessary to reach the same counting statistics.

References

1. Reilly, D. T. et al. 1990. Passive Nondestructive Assay of Nuclear Materials, Office of Nuclear Regulatory Research, NUREG/CR-5550, Los Alamos National Laboratory Document LA-UR-90-732 (1990), 529.
2. Humphrey, M. A., S. J. Tobin, and K. D. Veal. 2012. The Next Generation Safeguards Initiative's Spent Fuel Nondestructive Assay Project, *Journal of Nuclear Materials Management*, Vol. 40, No. 3.
3. Menlove, H. O., S. H. Menlove, and S. J. Tobin. 2009. Fissile and Fertile Nuclear Material Measurements Using a New Differential Die-Away Self-Interrogation Technique, *Nuclear Instruments and Methods in Physics Research Section A: Accelerators, Spectrometers, Detectors and Associated Equipment,* Volume 602, Issue 2, 21.
4. Jordan, K. A., and T. Gozani. 2007. Detection of 235U in Hydrogenous Cargo with Differential Die-Away Analysis and Optimized Neutron Detectors, *Nuclear Instruments and Methods in Physics Research Section A: Accelerators, Spectrometers, Detectors and Associated Equipment, Volume* 579, Issue 1, 21.
5. Pelowitz, D. 2008. MCNPX User's Manual version 2.6.0, LA-CP-07-1473.
6. Galloway, J. D., H. R. Trellue, M. L. Fensin, and B. L. Broadhead. 2012. Design and Description of the NGSI Spent Fuel Library with an Emphasis on Passive Gamma Signal, *Journal of Nuclear Materials Management,* Vol. 40, No. 3.

Measurement of the Multiplication of a Spent Fuel Assembly with the Differential Die-away Method Within the Scope of the Next Generation Safeguards Initiative Spent Fuel Project

Vladimir Henzl, Martyn T. Swinhoe, Stephen J. Tobin, and Howard O. Menlove
Los Alamos National Laboratory, Los Alamos, New Mexico USA

Abstract

As part of the Next Generation Safeguards Initiative (NGSI) spent fuel project, researchers evaluated the ability of fourteen different non-destructive assay techniques to determine elemental plutonium content in a spent fuel assembly (SFA); the Differential Die-away (DDA) technique is one of these techniques.[1] DDA uses short neutron pulses generated by an external neutron generator to actively interrogate the material within a SFA. The measured response is then predominantly prompt neutrons from induced fission of ^{235}U, ^{239}Pu, and ^{241}Pu detected by ^{3}He tubes positioned around the assayed SFA. Due to its rich and complex dynamic response, the neutron-generator-driven DDA technique is considered a potential candidate for high-accuracy applications (e.g., in nuclear fuel reprocessing plants or geologic repositories). In this paper, we use MCNPX simulations to investigate several methods to directly measure the multiplication (M) of the SFA, which is a crucial characteristic ultimately reflecting its initial enrichment (IE), burn-up (BU), and cooling time (CT). The results are based on the analysis of a simulated response of the DDA instrument to the active interrogation of sixty-four SFA's from NGSI Spent-Fuel Library 1 (SFL1).[2] Our findings indicate that the multiplication can be determined by three different approaches: (1) The ratio of count rates between the detectors nearest to and farthest from the neutron generator (i.e., back-to-front ratio) can be used to measure multiplication in the time domain soon after the interrogating pulse (0-200μs); (2) the die-away time constant is a suitable measure of multiplication only after approximately 500μs; and (3) the total number of prompt fission neutrons detected within the first millisecond after the neutron pulse scales with multiplication, although similar information may be obtained by detecting neutrons in a reduced time domain between 100 and 200 μs, which is generally less prone to electronics saturation directly following the interrogating neutron pulse.

Evaluation of DDA for the NGSI Spent Fuel project

In 2009, the Next Generation Safeguards Initiative (NGSI) of the U.S. Department of Energy's National Nuclear Security Administration (NNSA) began a five-year effort to develop one or more integrated instrument(s) capable of determining plutonium (Pu) mass in, and detecting diversion of pins from, spent commercial nuclear fuel assemblies.[1] Following a rigorous, simulation-based evaluation of fourteen individual nondestructive assay (NDA) techniques against a common library of sixty-four spent fuel assemblies,[2] efforts in 2012 will turn to the construction of two or more integrated systems comprised of the most promising techniques.

The differential Die-away (DDA) is among the NGSI techniques selected for the evaluation.[3] The technique uses a short neutron pulse generated by an external neutron source to actively interrogate the material within a spent fuel assembly (SFA). The main principle utilized by the DDA instrument is that the external neutrons will induce fission of the fissile isotopes, primarily after their thermalization, thus initiating a sudden increase of the neutron flux detectable by the ^{3}He tubes positioned along the SFA. The overall neutron yield and the dynamic properties of the induced neutron flux are closely related to the amount and isotopic composition of the fissile material in the SFA as well as the amount and quality of neutron absorbers, mostly products of burning in the nuclear reactor.

The Differential Die-away technique derives its name from a difference in die-away time of the population of epithermal and thermal neutrons in the assayed material with or without the presence of fissile material (FM). Typically, the external neutron source is a deuterium-tritium (DT) neutron generator (NG), which produces 14.1 MeV neutrons. The neutrons quickly thermalize and get absorbed with a characteristic time. Such decay time is called *die-away* time of the medium and depends on the material of the assayed sample and its density.

Absent FM, the population of fast and epithermal neutrons (i.e., those with energies above 0.4 eV) will decay on the order of a fraction of μs to a few μs, while the population of thermal neutrons on the order of hundreds of μs. Conversely, in the presence of FM, the thermal neutrons induce fission, thereby creating an additional source of fast and epithermal. The population of epithermal neutrons will then decay with die-away times much closer to those of the thermal neutron population. Neutron detectors (such as ^{3}He-filled proportional counters),

Figure 1. Schematic cross-sectional view of the DDA instrument used in the Monte Carlo simulations (left), and a typical temporal response of the DDA system in terms of the origin of the detected neutron (burst or fission) and the place of the detection (individual front or back detectors) (right)

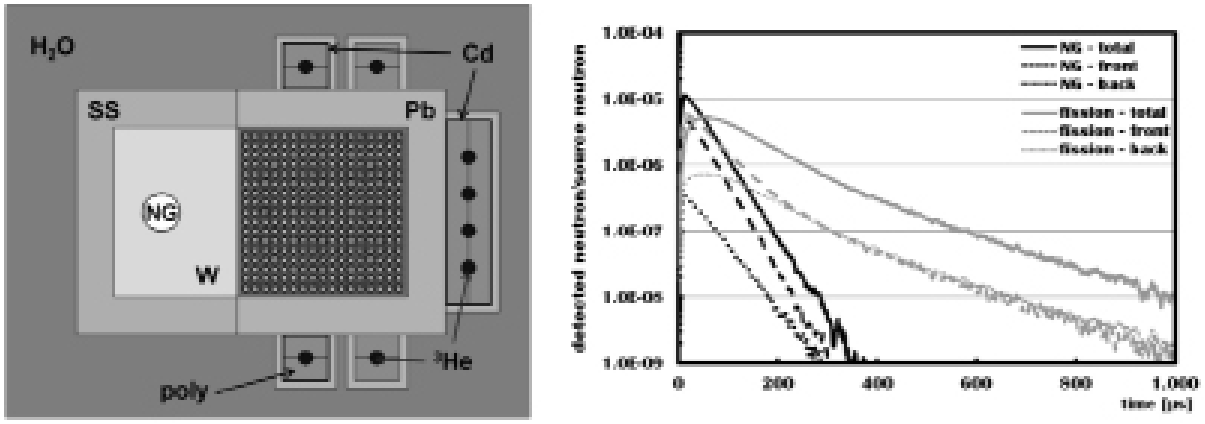

shielded from gamma rays (by lead) and thermal neutrons (by a cadmium liner) can be made sensitive exclusively to the fast and epithermal neutrons. These, if detected above the background level at times long after the interrogating neutron pulse, reveal the presence of FM such as ^{235}U, ^{239}Pu, and/or ^{241}Pu.

Instrument Design and MCNPX Simulations

Within the NGSI research effort we have used Monte Carlo N-Particle eXtended (MCNPX) simulations[4] to evaluate the ability of DDA technique to measure spent nuclear fuel. The instrument as simulated is depicted in the left panel of Figure 1. Its typical response as the function of time after the interrogating pulse and the position of detector is shown in the panel on the right. The NG is enclosed in a tungsten (W) block surrounded by a stainless-steel (SS) reflector. The 14.1 MeV energy of the neutrons from the DT generator is tailored by the multiple scattering and *(n,2n)* reactions in tungsten in such a way that the majority of neutrons entering the water-submerged SFA already have energies below the effective threshold for ^{238}U fission (1 MeV). This ensures that the fission neutrons detected by the instrument come predominantly from the fissile isotopes rather than the abundant fertile ^{238}U.

This modeling study simulated 17x17 Westinghouse light water reactor (LWR) assemblies, taken from the first NGSI spent fuel library (SFL1).[2] The lead collar (Pb) around each SFA serves to shield gamma radiation and prevents its interference with neutron detection in the ^{3}He. The ^{3}He detectors (4 atm; 5.08 cm long; 0.945 cm radius) are encapsulated in a high-density polyethylene (poly) serving to moderate the epithermal neutrons. The thermal neutrons are unable to penetrate the thin Cd liner isolating all but two ^{3}He tubes; the two detectors without Cd liners designated for a measurement of the delayed neutron (DN) signal[5] and are therefore not considered further in this particular study. Due to their nearly identical hardware requirements, the NGSI effort has anticipated integration of the DDA and DN techniques since its beginning. Analysis of the benefits and challenges associated with this integration is still in progress and exceeds the scope of the current paper.

The right panel of Figure 1 represents a typical temporal response of the DDA instrument, in this case for a SFA with 4 percent IE, 45 GWd/tU BU and 5y of CT using 10μs long neutron pulse. Unlike a real-world measurement, the simulation allows tracking of the detected neutrons back to their source. It also allows discrimination among neutrons that were involved in fission within the assembly ("fission neutrons") from those that reached the detector through multiple re-scattering only ("burst neutrons"); the latter carry no information on fissile content of the SFA.

The burst neutrons reach the ^{3}He detectors almost immediately after the interrogating pulse. However, their population dies out very quickly. The front (F) detectors observe the largest flux of the burst neutrons, since there is very little nuclear material in a direct line-of-sight between the NG and the F detectors. The contribution of burst neutrons to the signal on the back (B) detectors is significantly smaller due primarily to the amount of nuclear material between the NG and the ^{3}He detectors and the associated increased probability of induced fission.

The gray curves in the right panel of Figure 1 represent the time response, after the burst neutrons were excluded from the analysis, of the whole DDA instrument (full) and of the individual detectors at certain positions. It can be seen that the neutron flux peaks at the front detectors (dashed) before it peaks at the back detectors (dotted). Moreover, the neutron flux at the front detectors is significantly higher than at the back detectors until after 200μs when a dynamic equilibrium is established.

Figure 2. The yield of detected burst neutrons per NG source neutron in the front detectors (left) and the back detectors (right) for all sixty-four SFAs spanning a broad range of IE, BU, and CT values (see text for details). The error bars represent statistical uncertainty of the MCNPX calculation

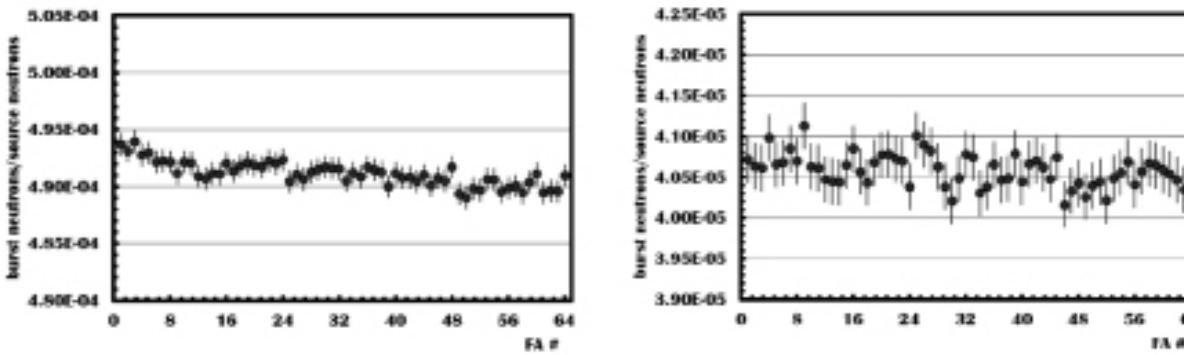

More importantly, the simulations demonstrated that the contribution of the burst neutrons relative to the DDA instrument response (shown as burst-source neutron ration in Figure 2) is almost independent of an assembly's operating history (i.e., values of IE, BU, and CT). For all practical purposes the burst neutron contribution can be considered as constant (although induced) background. The x-axis in Figure 2 represents the full range of sixty-four SFAs in SFL1, which span a broad range of IE (2, 3, 4, and 5 wt percent), CT (one, five, twenty, and eighty years), and BU (15, 30, 45, and 60 GWd/tU) values. The overall variation among all assemblies is less than 1 percent, while SFAs with the lowest IE (which are points 1 to 16 along the axis) seem to provide for the highest burst-to-source neutron ratio.

The dynamic evolution of the DDA signal and its dependence on the detector position led us to investigate the instrument response for each detector separately and in various time domains. In the early time domains (e.g., 50 μs to 100 μs from the beginning of the interrogating pulse), a measurement of the DDA signal immediately after the interrogation neutron pulse exceeds the traditional scope of the DDA method.[3] Additionally, due to too intense neutron flux possibly leading to saturation of data acquisition system and overall very high burst-to-fission neutron ratio (up to ~5) such measurement may be considered not practical or unfeasible. However, we think that the additional information gained would benefit the measurement scheme. Therefore, for the real-world applications we envision use of a low intensity setting of the NG to probe early time domains (to avoid saturation of the electronics) and use of a high intensity setting to probe those later, more traditional time domains. However the feasibility study of such bimodal active interrogation scheme is still in progress and exceeds the conceptual scope of the current paper.

Active vs. Passive Multiplication

Multiplication is an intrinsic property of a spent fuel assembly, depending on the fissile content and the neutron absorbers present. In order to achieve the NGSI goal of quantifying Pu mass, we need to research both the fissile content, of which Pu mass is a component, as well as neutron absorbers. Furthermore, because multiplication is central to several NDA techniques, the interpretation of multiplication is important.

Within the context of this study, we define the *net multiplication M* as the average number of neutrons produced in the system per one neutron delivered by the NG source. The M is then a quantity characterizing the amount and quality of the fissile material and neutron absorbers, their spatial and energy distribution, the geometry of the system, and properties of the neutron source.

From the point of view of an active interrogation and the subsequent detection of neutrons, the measured signal is determined by the *M* of the assembly. The multiplication is enhanced by the amount of the fissile material and suppressed by the amount of neutron absorbers present in the SFA. Since the quantities of fissile material and the neutron absorbers are dependent on an assembly's operating history—i.e., its initial enrichment (IE), burnup (BU), and cooling time (CT)—the multiplication is dependent on IE, BU, and CT. The ability to directly measure M of any SFA thus provides a key piece of information that can be used to verify the declared or independently measured values of IE, BU and CT. In certain cases, it can even lead to the determination of the Pu content.

It is currently beyond our capabilities to analytically determine *M* for every single SFA. Therefore we consider values of *M* calculated by MCNPX. We have chosen to define this in terms of "passive multiplication" (M_{pass}), derived from fissions induced from background ^{244}Cm spontaneous fission neutrons, and "active multiplication" (M_{act}), which reflects the number of neutrons produced per neutron of the NG. The main difference

Figure 3. Left - active (M_{act}) and passive (M_{pass}) multiplications of sixty-four SFA's from SFL1 are directly related. Right - Deviation of M_{act} from the fitted linear relationship between M_{act} and M_{pass} (quadruplets of points of the same shape and gray tone represent four different values of cooling time, with the lowest CT always corresponding to point with the lowest multiplication).

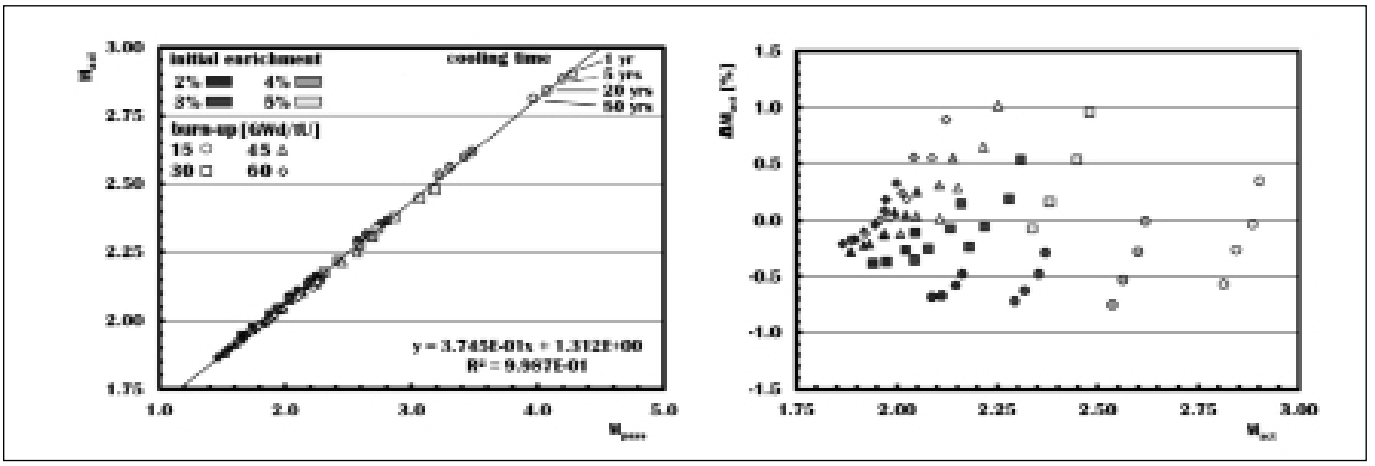

is that M_{pass} describes the multiplicative property of the SFA itself, while M_{act} characterizes the multiplicative property of the generator, assembly, and detector system as a whole. With these definitions, one could expect a direct relation between M_{pass} and M_{act}:

$$M_{act} = a_{inst} \cdot M_{pass} + b_{inst} \qquad (1)$$

where a_{inst} and b_{inst} are constants characterizing the specific instrument design.

The left panel of Figure 3 displays that the linear relationship described by Equation 1 holds in case of sixty-four SFAs from SFL1. In other words, knowing or measuring one kind of multiplication provides information about the other once the calibration parameters a_{inst} and b_{inst} are known. The right panel of Figure 3 displays the deviation from linear trend, from which it can be seen that the correlation between M_{act} and M_{pass} exhibits residual dependence on IE, BU, and CT. However, these perturbations typically do not exceed 1-2 percent, and for our intention to demonstrate how M can be measured by the DDA instrument can be neglected.

Back-to-Front (B/F) Detection Ratio

The right panel of Figure 1 demonstrates the dynamic evolution of the neutron flux across the SFA during the first millisecond after the interrogating neutron pulse. It shows that the neutron flux reaches its maximum in the front (F) detector before the back (B) detectors. Supposedly, this is because the neutrons on the way to the respective detectors sample parts of the SFA of different thickness and are thus subject to different multiplication. Only after the full equilibration of the neutron flux will F and B detectors measure the same. This implies that the number of neutrons detected by the back and front detectors (B/F ratio) should be a measure of the active multiplication M_{act}, especially in the early times after the NG pulse. Figure 4 displays the B/F ratio over six different time domains as a function of the M_{act} values determined by MCNPX for the first millisecond after the interrogating neutron pulse.

For earlier time domains (A, B, and C), Figure 4 indicates that the back detectors see more neutrons during assay of assemblies with higher M_{act}. We can also observe that in the time domain C, variation of M_{act} has the biggest relative effect on the B/F ratio (with a difference of ~52 percent between assemblies with the smallest and the largest M_{act}). In the later time domains (D and E) the average back-to-front ratio levels off at high M_{act} while the ratio at low M_{act} may deviate by as much as ~15 percent. At present, we are not sure about the exact origin of these deviations, but apparent dependency on CT suggests it is an effect of changing composition of the neutron absorbers due to their radioactive decay. Taken together, the individual panels of Figure 4 demonstrate how the interrogating neutron field evolves at a rate that depends on the operating histories of the assayed SFAs and provide an estimate of when dynamic equilibrium is reached.

The results in Figure 4 also indicate that M_{act} cannot be reliably measured in a narrow time window, since for SFAs with different operating parameters (*IE, BU,* and *CT*) the multiplication of the neutron flux progresses differently in time. In order to strip the B/F ratio of its inherent dependence on the assembly operating parameters, an integrated measurement over a long time domain is needed, such as that shown in panel F of Figure 4 (50-1000μs). However, since the time domain F also includes times when effects of neutron absorbers become dominant, the time window must be shortened to earlier times. Figure 5 *(left)* displays simulated results of B/F ratio in a time window from 0-200μs along with a third-degree polynomial fit. The right panel of Figure 5 displays the deviation of the actual M_{act} from the value determined by the

Figure 4. The ratio of the number of neutrons detected in back and front detectors (B/F ratio) for six different time domains A-F as the function of the value of M_{act} determined by MCNPX (four different values of CT represented as in Figure 3)

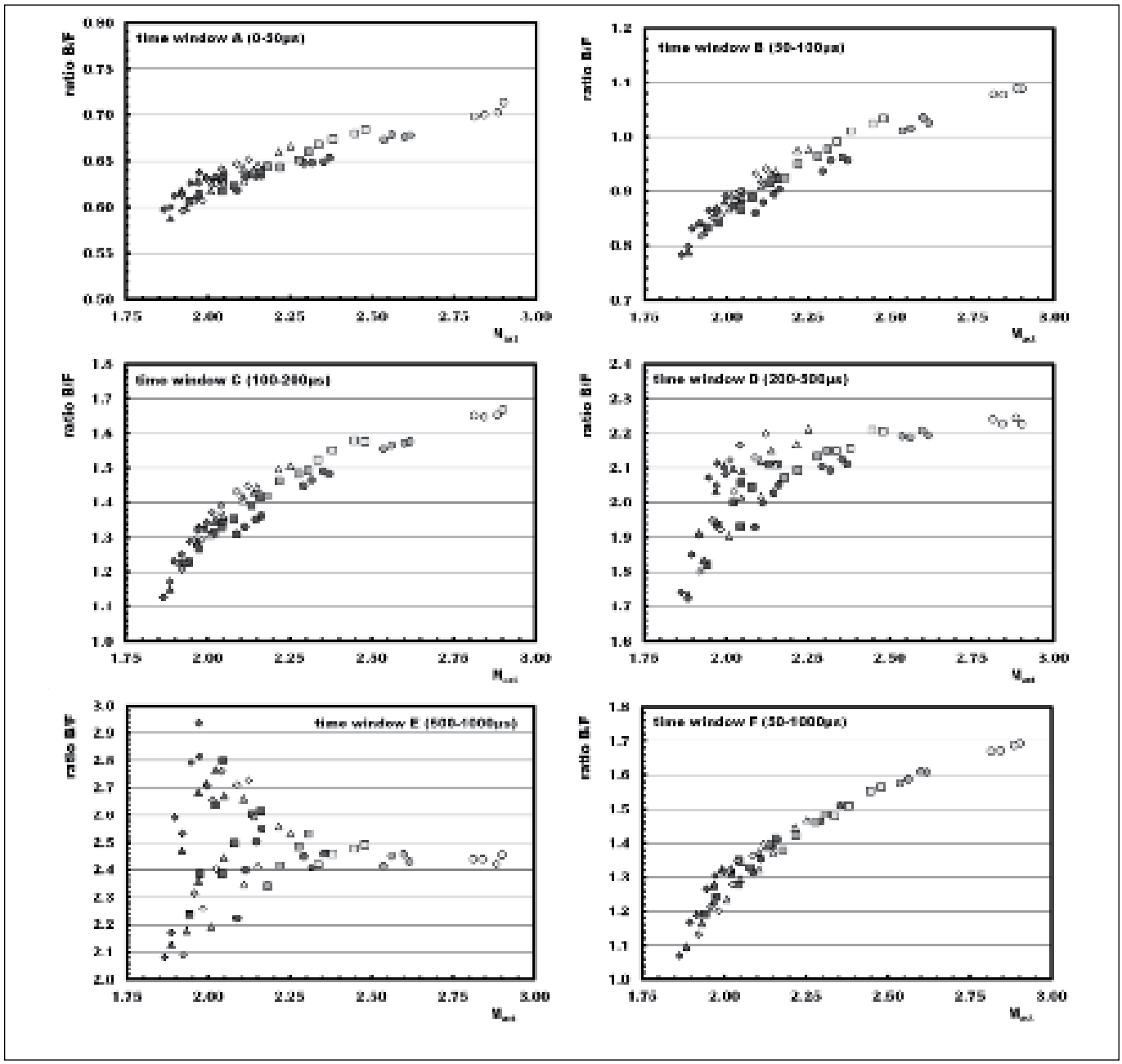

polynomial fit, from which it can be seen that the B/F can be used to infer the active multiplication to precision better than about 2 percent.

Die-away Time

Due to the subcritical nature of every SFA, the induced neutron population eventually dies out. The corresponding die-away time depends on the competition between the production of neutrons by induced fission and their absorption in, or escape from, the SFA. The apparent die-away time (τ_{DDA}) measured by the DDA instrument takes into the account the die-away time of the signal at the ^{3}He detectors and the length of the interrogating neutron pulse. Since both the induced fission and the absorption rates depend on the IE, BU, and CT values for each SFA, which also define its multiplication, we may expect τ_{DDA} and M_{act} to be func-

Figure 5. Left - The ratio of the number of neutrons detected in back and front detectors (B/F ratio) for a time domain 0-200 μs as the function of the value of M_{act} determined by the MCNPX. Right – relative deviation of actual M_{act} from values determined from a polynomial fit of B/F ratios.

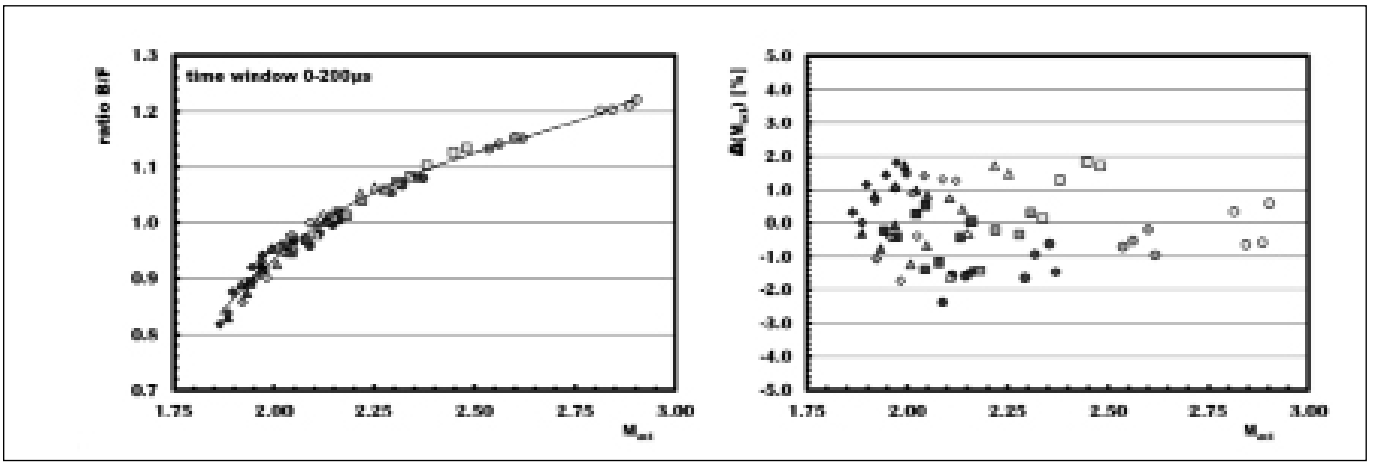

tionally related. In the case of a smooth dependence, one observable may be a measure of the other. In our analysis, we have investigated τ_{DDA} over several time domains and also its dependence on the position of the detector, since there is a different τ_{DDA} for F and B detectors in time domains before ~200 μs after the interrogation pulse (Figure 1). However, it turns out that the results for F and B detectors are qualitatively the same although they differ on absolute scale in the earlier time domains.

Figure 6 displays τ_{DDA} as the function of M_{act} for the sixty-four SFA's from SFL1 as determined for the back detectors in time domains C and D and for total DDA signal (front and back detectors combined) in time domain E. As with the back-to-front ratio, also τ_{DDA} undergoes a dramatic dynamic evolution during the first millisecond after the interrogating neutron pulse. In the earliest time domain for which τ_{DDA} can be properly defined (100-200 μs), τ_{DDA} is directly proportional to M_{act}. However, the constant of proportionality is strongly correlated with IE, making τ_{DDA} in this time domain potentially a measure of *IE*. The situation changes significantly in a later time domain (200-500 μs) where the IE dependency is much less apparent. In the latest time domain (500-1,000 μs) the τ_{DDA} values are virtually identical for the front and back detectors, which allows us to determine a single τ_{DDA} for the assembly.

In this latest time domain, characterized by the poorest statistics, the τ_{DDA} scales with the multiplication M_{act} without any apparent dependency on *IE, BU,* or *CT*. The lower right panel in Figure 6 displays the residuals of linear fit of τ_{DDA} vs. M_{act} the τ_{DDA} over this time domain. Neglecting any possible systematic errors, τ_{DDA} can be used to determine M_{act} within +/- 4 percent. This is about a factor of two worse than inferring M_{act}, from the B/T ratio. However, while the uncertainties of M_{act} determined from the B/F seem to be mostly systematic (i.e. depending on *IE, BU,* and *CT*), the uncertainty of M_{act} determined from τ_{DDA} is to a great extend statistical. If this holds true when real-world measurements are made, then τ_{DDA} would be an equally accurate if not superior method of determining M_{act}.

Total Neutron Signal

Probably the most natural approach to determine M_{act} stems from its very definition—the number of detected neutrons per neutron injected into the SFA from the NG. This should reflect the multiplicative property of the system. Since Figure 4 and Figure 6 predict vastly different neutron-flux evolution dynamics depending on the actual properties of an assayed SFA, the optimal choice of measurement window is not obvious. The first five panels of Figure 7 display how, in a given time interval, the total number of neutrons detected by all ^{3}He detectors (N_{DDA}) depends on M_{act} of an individual SFA.

In the earliest time domain (0-50 μs) we can observe structure of sixty-four data points that is dependent on *IE, BU,* and *CT*. In the early times after the interrogating neutron pulse (domains A and B), among the SFAs with similar M_{act}, the assemblies with higher *BU* and *IE* provide for higher N_{DDA} than the SFA's with lower *BU* and *IE*. However, the structure of the data almost completely disappears at intermediate time domain (100-200 μs) only to be restored at later time domain (200-500 μs), where the orientation of the data structure is inverted relative to the earlier time domains. At later times, low *BU* assemblies with low *IE* produce higher N_{DDA} signal. The most intriguing observation is that the cross-over of the trends seem to happen at the same time for all different SFA's, leading to the alignment of the data where N_{DDA} is almost directly proportional to M_{act}.

In addition, Figure 7 shows that over a very long, integrated time domain (G: 0-1,000 μs), we observe an almost perfect linear correlation between N_{DDA} and M_{act}. These results, however, are not really surprising. Considering that the values of τ_{DDA} in any time domain range from 70-240 μs, the intensity of the induced neutron

Figure 6. Die-away time (τ_{DDA}) as the function of M_{act} for sixty-four SFAs from SFL1 as determined for the back detectors in time domains C and D and for total DDA signal (front and back detectors combined) in time domain E. The lower right panel displays the relative deviation of M_{act} determined from the linear fit from the actual values of M_{act} (four different values of CT represented as in Figure 3).

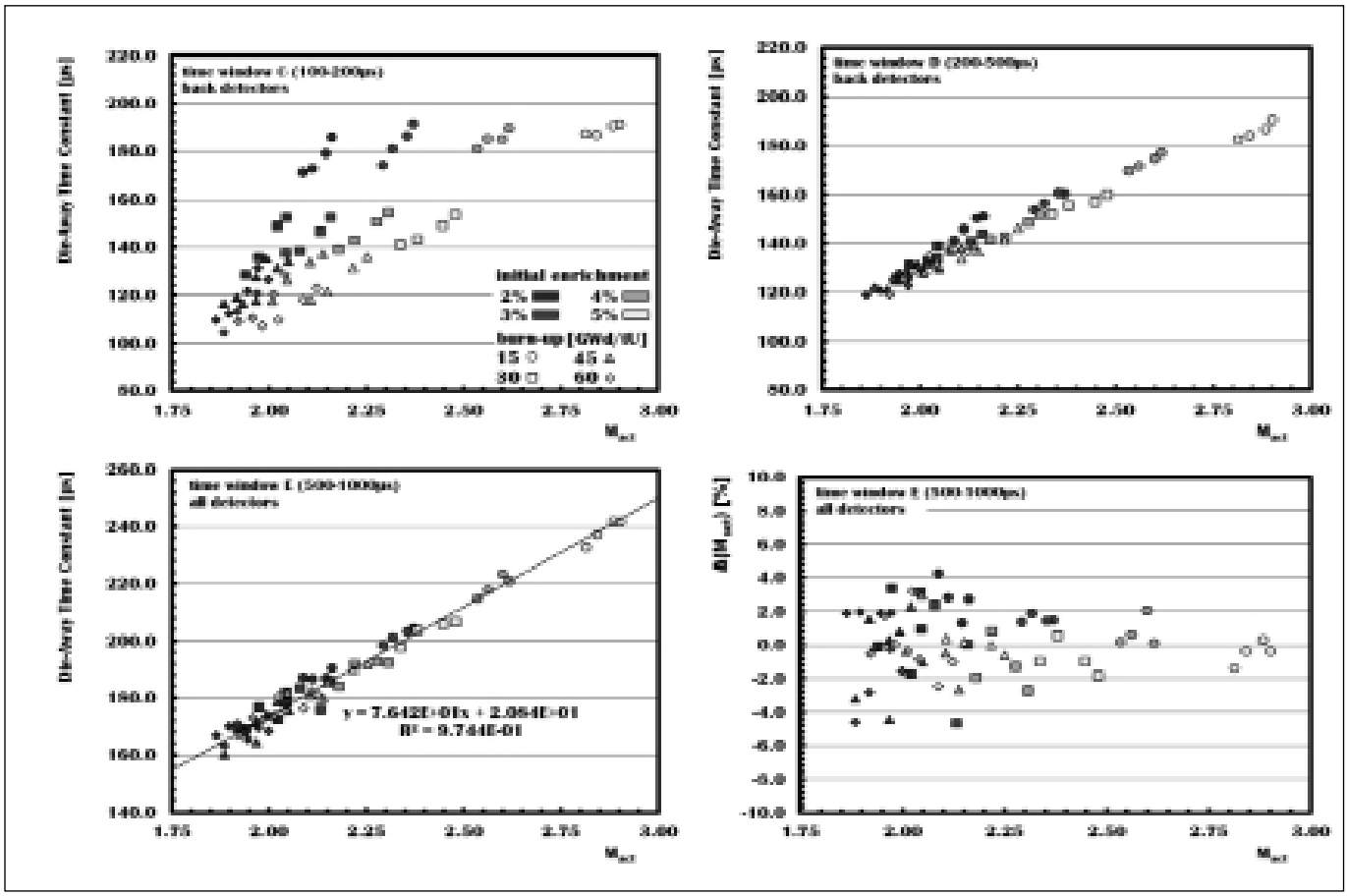

flux 1,000 μs after the interrogating pulse should be negligible. This means that the longest time domain from 0 to 1,000 μs covers the full evolution of the induced neutron population from the injected neutron pulse until its nearly complete extinction after about five to eight die-away times. N_{DDA} is then proportional to the number of neutrons created in the assembly per injected neutron, i.e. M_{act}. The lower right panel of Figure 7 displays the residuals of quadratic fit of N_{DDA} vs M_{act} for various SFAs measured from 0-1,000 μs after the interrogating pulse. The nonlinearity of the correlation between N_{DDA} vs M_{act} indicates that ^{3}He detector count rate increases less than the increase in the overall multiplication of the system M_{act}. This apparent "neutron detection deficiency" is likely a result of the delay between the time the neutron is created and immediately accounted for by MCNPX and the time the neutron is detected by the ^{3}He tube. In general, one could diminish the effect of this neutron detection deficiency by allowing for detection of neutrons during a longer time interval (e.g. 0-2,000μs); however, due to the possibility of insufficient signal-to-background ratio for certain SFAs, such a measurement scheme may be counterproductive. Despite the practical difficulties associated with the need to measure at both early times (possible electronics saturation) and very late times (potentially insufficient signal) we see N_{DDA} as a potentially high precision indicator of M_{act}.

On the other hand, the counterintuitive results displayed in the panel corresponding to the time window of 100-200 μs seem rather promising. Apparently, during this limited time interval various amounts of neutron absorbers (and the associated variation in *IE*, *BU*, and *CT*) do not seem to matter; the overall multiplication alone determines N_{DDA}. Thus, this time domain provides qualitatively similar information as the measurement of N_{DDA} in the full time range (0 to 1,000 μs) allowing avoidance of the most difficult-to-measure time domains. While the temporal shifting of the structure superimposed on the data can be clearly attributed to different evolution dynamics of the neutron flux within a given SFA, we do not yet have a simple explanation for the disappearance of this structure during this special time interval. The correlation of the DDA response measured during the 100-200 μs time domain is not as good as that for the time window F*. This could be attributed to the arbitrary choice of

Figure 7. Total neutron signal (N_{DDA}) over different time domains as a function of M_{act} for sixty-four SFAs from SFL1. The bottom right panel shows the relative deviation of the actual N_{DDA} from values predicted by a quadratic fit of the data in time domain G (four different values of CT represented as in Figure 3).

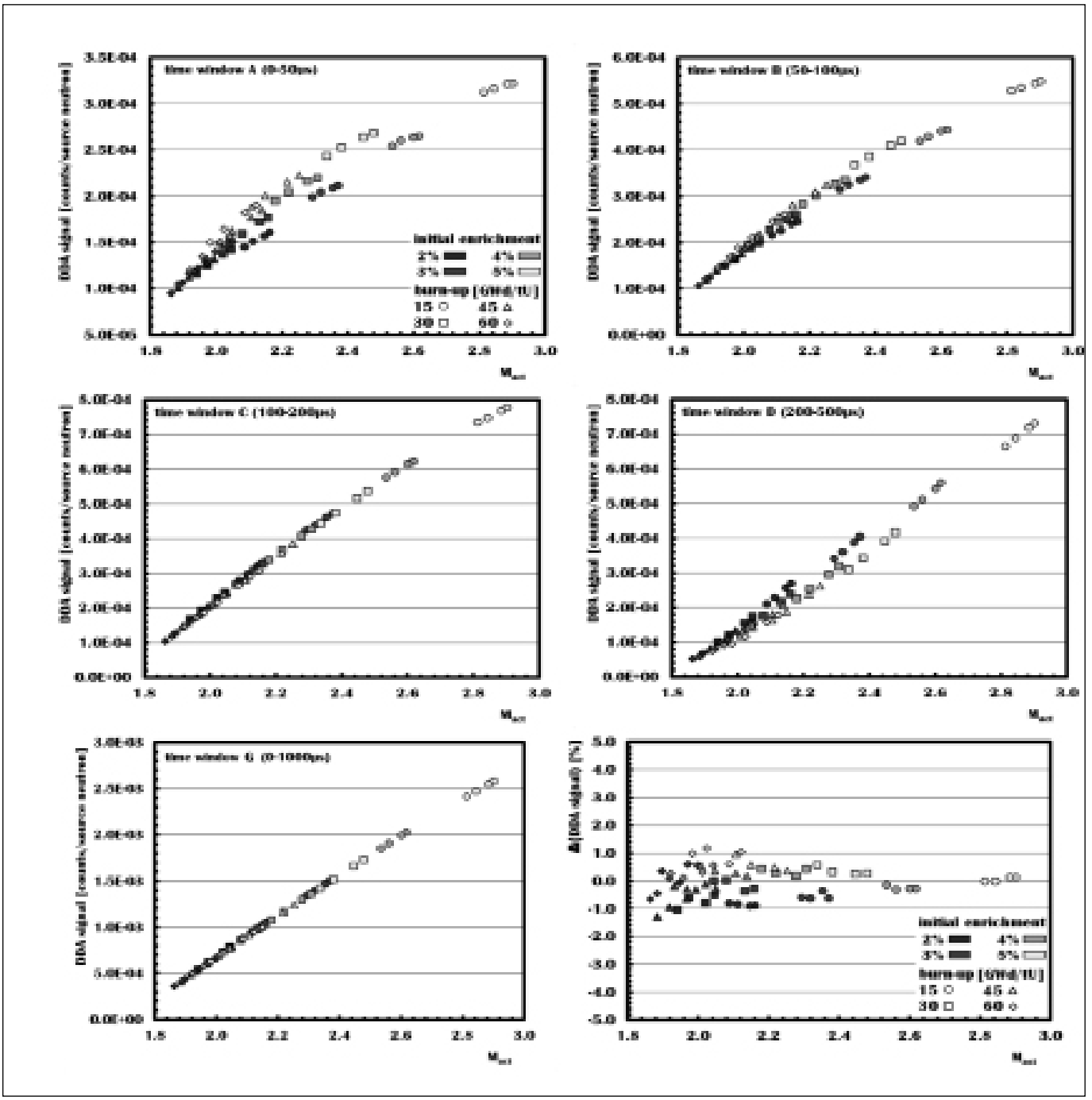

time domains. We suspect that a dedicated study with a better optimized time window could lead to a better alignment of the simulated data along a simple (probably quadratic) dependence as observed for data from time window G.

Conclusion

We have demonstrated that back-to-front detector ratio (B/F), die-away time τ_{DDA}, and total number of detected neutrons (N_{DDA}) can be used to measure the multiplication M of the SFA assayed by the proposed DDA instrument. But while B/F ratio

can measure M_{act} in rather early times after the interrogating neutron pulse, the τ_{DDA} gains its predictive power only in the later time domains. Additionally, two different time domains allow determining M_{act} by measuring N_{DDA}.

Acknowledgments

The authors would like to acknowledge the support of the Next Generation Safeguards Initiative (NGSI), Office of Nonproliferation and International Security (NIS), National Nuclear Security Administration (NNSA).

References

1. Humphrey, M. A., S. J. Tobin, and K. D. Veal. 2012. The Next Generation Safeguards Initiative's Spent Fuel Nondestructive Assay Project, *Journal of Nuclear Materials Management,* Vol. 40, No. 3.
2. Galloway, J. D., Trellue, H. R., Fensin, M. L., and Broadhead, B. L. 2012. Design and Description of the NGSI Spent Fuel Library with an Emphasis on Passive Gamma Signal, *Journal of Nuclear Materials Management,* Vol. 40, No. 3.
3. Jordan, K. A., and T. Gozani. 2007. Pulsed Neutron Differential Die Away Analysis for Detection of Nuclear Materials, *Nuclear Instruments and Methods* B (261), 365-368.
4. Pelowitz, J. F. (Ed.). 2005. MCNPX™ Users's Manual Version 2.5.0, *Los Alamos National Laboratory* report LA-CP-05-0369.
5. Blanc, P., H. O. Menlove, S. J. Tobin, S. Croft, and A. Favalli. 2012. An Integrated Delayed-Neutron, Differential-Die-Away Instrument to Quantify Plutonium in Spent Nuclear Fuel, *Journal of Nuclear Materials Management*, Vol. 40, No. 3.

An Integrated Delayed-neutron Differential-Die-away Instrument to Quantify Plutonium in Spent Nuclear Fuel

Pauline Blanc
Alternative Energies and Atomic Energy Commission (CEA, LIST) Saclay, France

Howard O. Menlove, Stephen J. Tobin, Stephen Croft, and Andrea Favalli
Los Alamos National Laboratory (LANL), Los Alamos, NM 87545, USA

Abstract

This paper evaluates the use of a neutron generator source to interrogate spent nuclear fuel to measure the plutonium content. The differential die-away (DDA) technique preferentially measures ^{239}Pu relative to ^{235}U while a delayed neutron (DN) measurement is complementary in that it provides a unique signature more sensitive to ^{235}U. The first section of this paper discusses the integration of a 14 MeV deuterium-tritium (DT) neutron generator with a system of neutron detectors to measure both delayed and prompt neutron (PN) signals in the same instrument. An evaluation of the design's ability to measure the DN for a wide range of virtual spent fuel assemblies (SFAs) is provided. Both DN and PN detections are active techniques that measure the signal emitted most prominently from the fissile isotopes of ^{235}U, ^{239}Pu and ^{241}Pu. The application of both the DN and PN signals will be evaluated for the potential discrimination of the ^{235}U and ^{239}Pu components in the fuel assemblies. This paper builds on previous conceptual design studies which have helped guide the present prototypical instrument design. The Monte Carlo N-Particles eXtended (MCNPX) radiation transport code (v27c) was used to calculate the interrogation and detector response. This paper quantifies the capability of a new design using an array of ^{3}He detectors to reasonably optimize both DN and PN detection. This new design was created to minimize the (DT) direct fission in ^{238}U. Attention was given to determining suitable time-interrogation patterns for both DN and PN, and the new design also achieved near homogeneous spatial responses in the fuel for both delayed and prompt neutron assays, essential for the detection of pin diversion in spent nuclear fuel. All was done within the constraints of a single practical instrument to reduce the instrument cost.

Introduction

The Next Generation Safeguards Initiative (NGSI) of the U.S. Department of Energy (DOE) has funded multiple laboratories and universities to develop a range of nondestructive assay (NDA) techniques to accurately quantify the plutonium (Pu) mass in spent nuclear fuel assemblies (SFA) and to detect potential diversion of fuel pins. In all, the NGSI effort has evaluated fourteen different NDA techniques. The goal of this instrument design is to integrate the delayed neutron (DN) and differential die-away (DDA) techniques in order to measure both delayed and prompt neutron (PN) signals in a same instrument design. This paper builds on previous conceptual design studies,[1,2] which have helped guide the present prototypical instrument design. The Monte Carlo N-Particles eXtended (MCNPX) radiation transport code[3] (v27c) was used to quantify the capability of a new design, using an array of ^{3}He detectors, to reasonably optimize both DN and PN detection.

A Design for DN and DDA

Both DN and DDA are active NDA techniques. The DN-DDA instrument has been designed to determine fissile content, and merging these techniques raises a diversity of challenges because they have somewhat conflicting needs. The DN technique consists of turning on and off an interrogating source, in this case the DT generator, and counting the delayed neutrons emitted after the source is turned off. The details of this technique together with preliminary results are given in publications by Blanc et al.[4,5] The time dependence of emitted DNs from the many delayed neutron precursors produced is described by six effective time groups in the Monte Carlo code MCNPX which have effective half-lives varying from ~0.2 sec to ~1 minute.[3] The delayed neutron signal comes from: (1) fast-neutron fissions in fissile isotopes induced by source neutrons; (2) first generation thermal-neutron fissions in the fissile isotopes; (3) second generation fissions in fissile isotopes that are induced by the fission-spectrum neutrons generated from fissile isotopes; and (4) fissions in the ^{238}U that are induced by the fission-spectrum neutrons generated from fissile isotopes. In the context of DN counting of low-enriched uranium spent fuel assemblies, the fission in ^{238}U has to be minimized; otherwise it could dominate the DN signal. Fission in ^{238}U can be a significant issue when the interrogating neutrons extend above the fission threshold energy since it represents ~ 95 percent of the actinide mass. To reduce the (D, T) fast-neutron fission back-

Figure 1. The solid line is the lethargy of the neutron flux at the entrance of the fuel assembly, steel and tungsten tailored D-T neutron spectrum as a function of the neutron energy and the dashed line is ^{238}U fission cross section as a function of the neutron incident energy from ENDF-VII-B

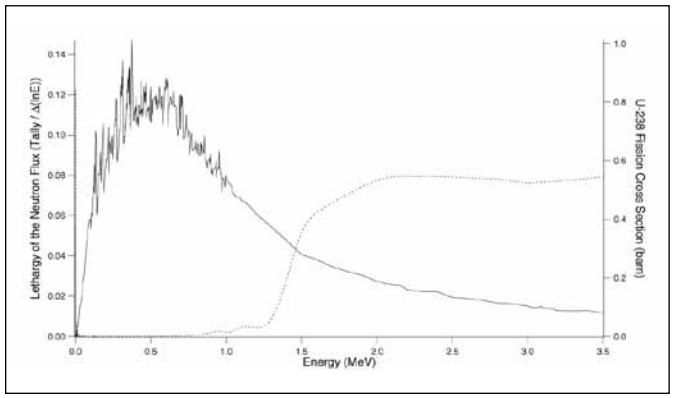

ground in the ^{238}U, we introduced a W and stainless steel neutron spectrum tailoring assembly around the DT neutron generator. The W has significant cross sections for inelastic scattering and (n, 2n) reactions that shift much of the 14 MeV source neutrons to lower energies. The water in and around the fuel assembly also plays the important role of increasing the thermal-neutron fission rates in the fissile isotopes. Neutron energy calculations were performed for several tailoring configurations and the peak neutron energy was shifted from 14 MeV to approximately ~0.5 MeV as shown in Figure 1, which corresponds to the tailoring assembly in air. Of course, the 14 MeV source term is still significant, but it is off scale in the plot. Figure 2 shows the tailoring assembly next to the fuel assembly in the water. In Figure 1 the steel and tungsten tailored D-T neutron spectrum is compared to ^{238}U fission cross section. We can easily observe that the neutron flux at the entry of the fuel assembly is well shifted to energy below ~1.5 MeV, fission low energy threshold in ^{238}U. This combination of spectrum tailoring and promotion of thermal-neutron fissions provides the reduction in the "active" ^{238}U background that is needed for the DN measurement. The ^{238}U fissions induced by source neutrons are gone after ~2 μs. However, the ^{3}He detectors for PN that are inside the Cd sleeves have a neutron slowing down time of ~ 40 μs, so the measured response extends into the longer time domain.

The ^{241}Pu has a delayed-neutron fraction very similar to ^{235}U, and so its presence will reduce the clarity of discrimination between ^{235}U and ^{239}Pu.[6] However, given that the mass of ^{241}Pu present is about an order of magnitude smaller than ^{235}U in spent fuel, signal degradation from ^{241}Pu is minor.

The "passive background" from spent fuel is mainly from spontaneous fission of ^{244}Cm amplified by induced fission neutrons owing to the fact that SFAs have multiplication factors of ~ 2 to 4 [depending on initial enrichment (IE), burnup (BU) and cooling time (CT)]. This passive background has to be

Figure 2. Diagram of the neutron spectrum tailoring assembly, 17x17 PWR fuel assembly, 3He detectors, and lead shielding for the integrated DDA-DN system

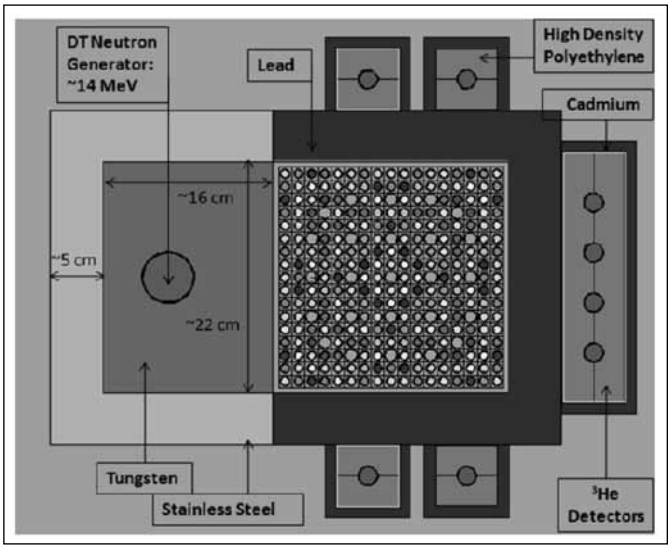

overridden by the interrogation source, and the challenge will be measuring delayed neutrons in the presence of prompt neutrons, because the DN yield is about two orders of magnitude smaller than for PN. Below, we will show how the DN instrument design is what determines the requirement for generator strength. The high-source strength required for the DN instrument is more than sufficient for the DDA instrument.

The water surrounding the tailoring assembly will generate a high thermal neutron flux; however, these thermal neutrons will not penetrate through the 5-cm-thick steel layer that covers the W spectrum tailoring block on five sides.

Also, the fuel assembly absorbs the thermal neutrons on the SFA side. Thus, the high-energy gammas that result from the neutron capture reaction in W are not expected to contribute to photo-fission in the ^{238}U.

In DDA, the PN population of induced fissions following a DT interrogation burst (~10 μs) dies away with a given decay time after the interrogation pulse.

The die-away time varies according to the fissile content and multiplication of the target material and the surrounding media. The induced fission reactions provide a unique signature to the fissile content of the interrogated fuel assembly. Thus, the signal of interest comes from prompt fission neutrons that were induced by the interrogation neutrons as well as multiplication. Further details and preliminary results are provided in publications by Lee et al.[2] and Blanc et al.[4,5]

Both the die-away time of the assembly and the PN signal increase with the amount of fissile material. The magnitude of the detected signal is impacted by neutron absorption in the fuel.

Important neutron absorbers include fission fragment absorbers, such as ^{99}Tc, ^{131}Xe, ^{133}Cs, ^{143}Nd, ^{145}Nd, ^{149}Sm, ^{150}Sm,

Figure 3. The solid line is the percentage of source neutrons to the net prompt neutron signal and the dashed line the relative standard deviation on the total prompt neutron signal as a function of time

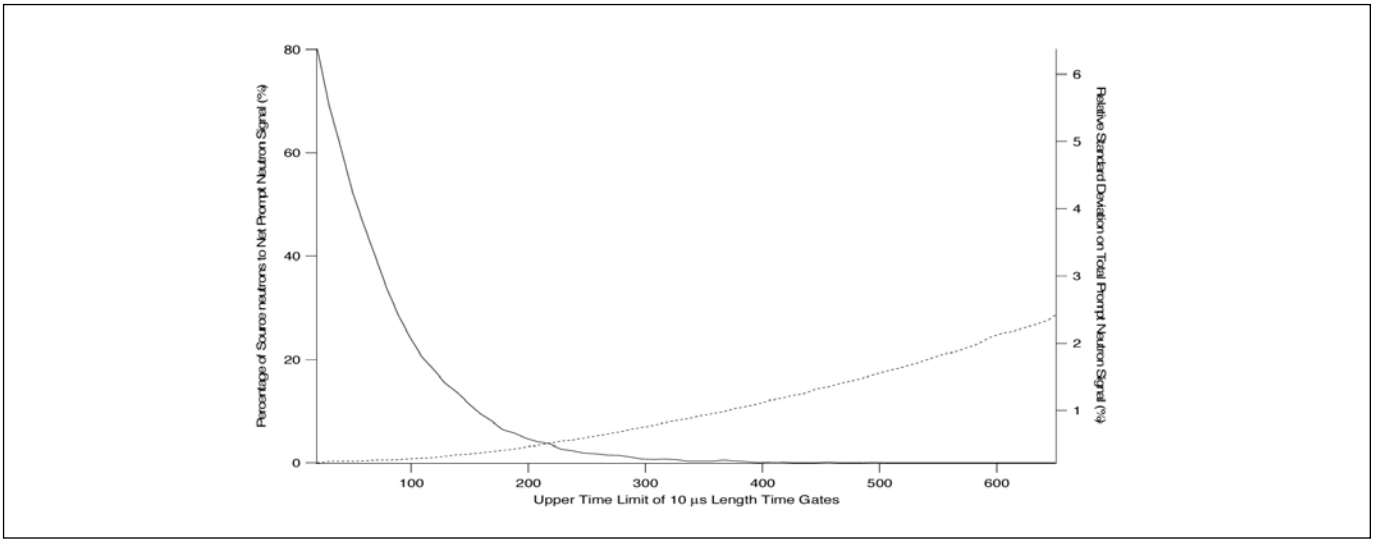

^{151}Sm, ^{151}Eu, ^{154}Eu, ^{155}Gd, ^{157}Gd, as well as fertile components such as ^{238}U and ^{240}Pu. The main challenge in designing a DDA instrument for spent nuclear fuel is to find a balance between neutron measurements early enough in time to obtain acceptable statistics and good penetration into the assembly, while also late enough to reduce the detection of source neutrons from the generator. Also, the gate must be long enough to provide adequate counting statistics to determine the fissile content. As the counting-time gate moves closer to the DT interrogation pulse, neutrons produced in the generator become an increasing fraction of the detected neutrons. Calculations were performed to determine the generator source neutron interference in the DDA time window. Ten μs wide windows were tallied from time zero to 280 μs and the interference fraction varied from more than 80 percent down to less than 1 percent. As a design goal, a threshold of 10 percent or less was set for the percentage of neutrons in the signal that originated either directly from the neutron generator or from fast fission of ^{238}U by calculating the relative standard deviation on the total prompt neutron signal together with the percentage of source neutrons to net prompt neutron signal as a function of time.

The RSD increases with time where the ratio decreases and finding a compromise to obtain the lowest value for both leads to a 8.7 percent interference fraction for a time gate of 140-200 μs as shown in Figure 3. Regarding delayed neutron counting, the source neutrons are negligible by the time the first DN gate is opened. For our simulations, the DN measurement cycle was a 2.0 s period with a 0.9 s neutron irradiation followed by a 0.1 s pause and a 1.0 s counting gate. This cycle was repeated until adequate statistics were accumulated.

Detector Design

The detector design shown in Figure 2 uses a DT generator and eight ^{3}He-filled proportional counters (4 atm) that are 1.9 cm in diameter and 5 cm long. The detectors were positioned behind 5 cm of Pb shielding to reduce the gamma dose from the SFA. The detectors are positioned on the sides and back of the SFA to balance the interrogation neutrons that induce more fission reactions in the front of the SFA. This detector configuration was selected to obtain a nearly uniform DN and PN response from all radial sections of the assembly. The SFA pin array (17x17) is ~366 cm long and 21.58 by 21.58 cm across. Each of the 264 fuel rods was divided into four separate radial cells to allow for radial variation of Pu peaking on the edge of the pellet. The medium surrounding the pins is water. On all sides of the SFA is a 0.5 cm water-filled gap which provides the mechanical tolerance for moving an assembly through the detector. The ^{3}He detectors are encased in high density polyethylene (HDPE) to increase the signal efficiency. Six of the detectors have been wrapped in Cd for PN detection, while the other two have no Cd and are used exclusively for DN detection. We estimate a factor of about 2 in the relative efficiency of the DN response from Cd to non-Cd wrapped detectors. The DT neutron generator is located in a 9.8 cm tall cylinder of 2.4 cm radius surrounded by a 16.25 by 22.4 by 20 cm W block surrounded by a 21.25 by 32.4 by 27 cm layer of stainless steel An important benefit when implementing spectrum tailoring is the substantial neutron boost (a factor of roughly 135 percent) obtained from (n, 2n) reactions in the tungsten. There is also a neutron energy reduction from the neutron inelastic scattering. To measure the DN signal above the ^{244}Cm background, we require a high-yield DT neutron source. To obtain a good signal/background ratio, we assume a neutron yield of ~109 n/s for the PN measurements and ~1,011 for the DN.

Figure 4. The uniformity of the DN response (left) and DDA response (right) as measured by the percent change in signal due to replacing spent fuel pins with depleted uranium (black pins) relative to a base case with no pin substitution

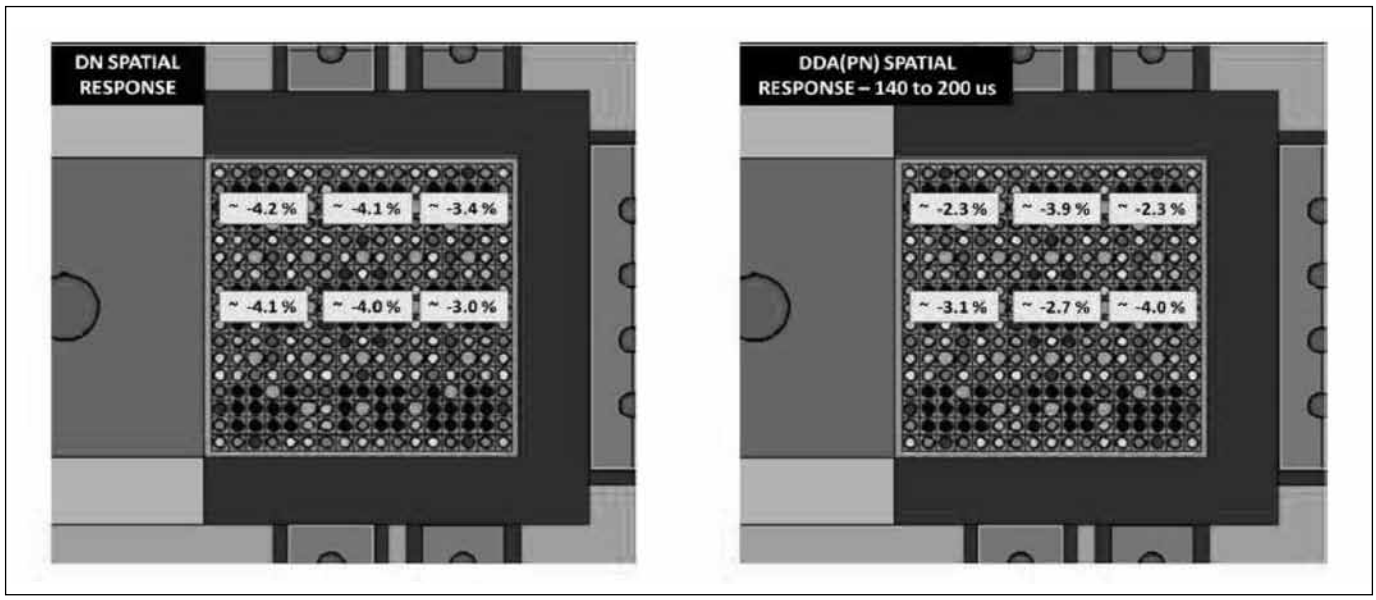

Counting Statistics

Within the context of the current delayed and prompt neutron research, it is important to propagate the uncertainty determined by MCNPX since this will impact the instrument's ability to detect diversion and make meaningful measurements.

The delayed neutron counting rates have been modeled to give the number of ^{3}He (n, p) reactions occurring for the sum of the detectors during a series of 1 s time bins. The following interrogation pattern was repeated 150 times: 0.9 s interrogation, 0.1 s pause, 1.0 s count time.

The detector counting rates and the DN interrogation cycle was used to estimate the statistical precision.

Achieving adequate precision is a prerequisite to the feasibility of the assay. Both DN and DDA must be clearly discernible above the passive neutron signal. The uncertainty details are developed in publications by Blanc et al.[4] Concerning DDA, the uncertainties have been taken directly from MCNPX outputs.

Time Gate Optimization for DDA

To determine the ideal time gates for prompt neutron measurements, time gates were needed that provide both good counting statistics and penetrability to the central region of the SFA. The early time gates in the DDA assay have higher energy neutrons than later gates, and thus have better penetrability into the center of the SFA. However, as the time gate approaches the end of the DT neutron pulse, the fraction of generator neutrons and fast fission from ^{238}U fission increases and competes with the desired signal from fissile material. We have selected a time gate to keep neutrons produced directly by the generator below 10 percent of the fissile signal. These source generator-induced neutrons are below the 10 percent target between 140 μs and 200 μs (and are less than 1 percent after ~280 μs). In the following section, an investigation will be made to ensure that this gate also provides good penetrability of the fuel, which is necessary for detection of pin diversion.

Detector Results for DN and DDA

To evaluate the uniformity of the measured DN and PN signals in the SFA, six spatial regions were selected across the assembly. Each region contained eleven or twelve fuel pins that were replaced by depleted uranium (DU, 0.2 weight percent ^{235}U), which are depicted as black pins in Figure 4. The "base case" is that in which no pins have been replaced. Six of the nine positions were simulated since the DN instrument is symmetric along the *y*-axis. Figure 4 displays the corresponding spatial response, representing the percent change relative to the base case for DN and DDA measurements, respectively. The base case assembly for our calculations was a SFA with a BU of 45 GWd/tU, CT of five years, and IE of 4 wt percent.

Relatively uniform responses are obtained when counting both DN and DDA. The DDA results were obtained using the 140 to 200 μs time gate. Prior DDA results by Lee et al.[2] showed that the typical DDA time gate (200-1000 μs) resulted in poor penetrability to the center of the SFA. We conclude that the early time gate (140-200 μs) gate, provided good penetrability.

Figure 5. Prompt neutron count rates (n/s) as a function of the time gate investigated (μs) where the dashed line is the source neutron signal and the solid line the net prompt neutron signal

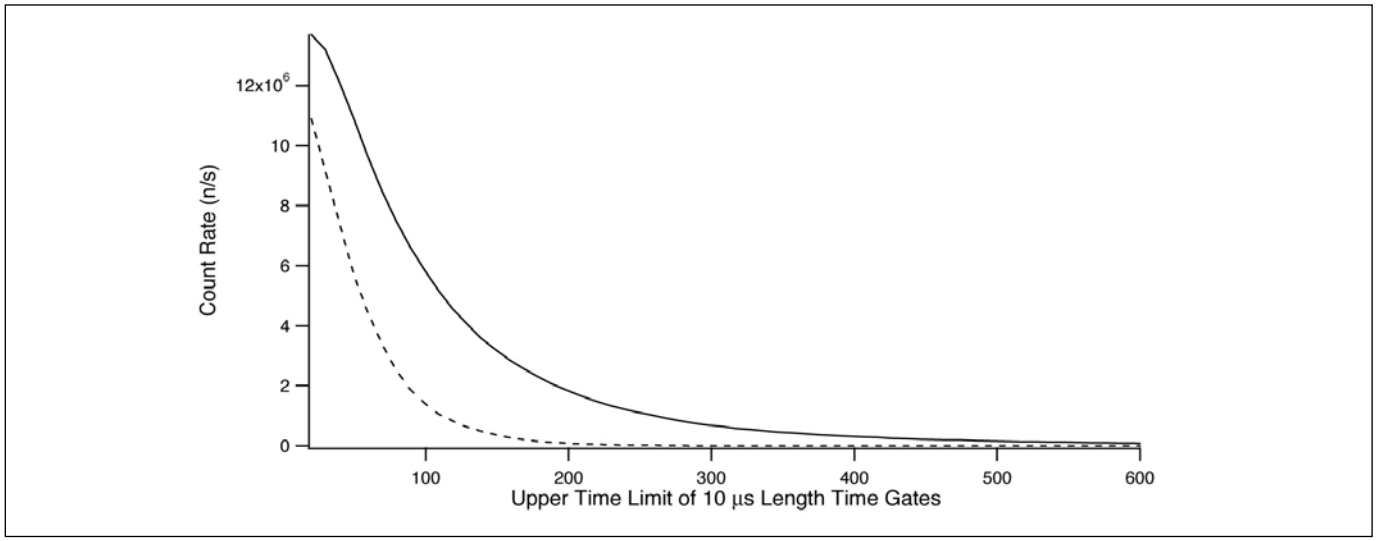

Signal to Background Ratio for DN

The spontaneous fission activity of SFAs results in a high neutron background. The passive neutron background for discharged fuel after a few years cooling comes primarily from spontaneous fission, mainly ^{244}Cm with an eighteen-year half-life. The neutron background rate is a strong function of BU. For the DN instrument, a neutron generator source strength of ~ $5x10^{10}$ n/s would provide a signal/background (S/B) ratio of ~30 percent for a SFA with 45 GWd/tU BU. For SFAs with higher BU values, source strengths of ~ 10^{11} n/s would be required to achieve an S/B ratio of better than 20 percent. Although a DT source strength of ~$5x10^{10}$ n/s would probably be sufficient, a ~10^{11} n/s has been used in this study to allow for assay of extremely high BU fuel (60 GWd/tU).

An additional DN background term can come from oxygen activation that can produce DN via (n,p) reactions in ^{17}O. The reaction will produce ^{17}N that will promptly decay with a half-life of ~4.2 s. This contribution could be significant, and thus has been quantified since both the fuel and the water around the fuel contain oxygen. However, this (n,p) reaction has a cross section threshold above ~7.9 MeV, and the neutron energy flux entering the fuel and water is predominantly below 1 MeV. The results of the simulations give a contribution of ~0.26 percent to the DN count rate from the 17O activation for fuel with 45 GWd/tU BU, 4 wt percent IE, and five year CT: 0.13 percent increase from 17O in the fuel and 0.13 percent from the water.[7]

Irradiation Cycles for DN and DDA

The DDA and DN irradiation cycles have different time requirements, so were therefore run separately. In MCNPX, the probability of a neutron being detected in a specific time interval per source neutron emitted was tallied from 1 to 300 seconds for delayed neutrons for a DT irradiation of 0.9 s. For a DDA instrument using prompt neutrons, it has been tallied from 10 μs to 1 ms after a DT irradiation of 10 μs. To integrate the divergent DDA and DN time signals, the irradiations would be performed in two stages. The first stage focused on the DDA time cycle and lasted about one minute because of the high counting rates. The second stage focused on the DN time cycle and lasted for several minutes until adequate statistics were accumulated.

DDA Assay

The goal of DDA is to exploit the differential timing between the source neutron and net prompt neutron populations as displayed in Fig.5. The net prompt neutron counts for a SFA (not including source neutrons) are substantially above the source neutrons counts themselves.

The same holds for short counting times. Note that in the usual application of DDA, the mass of total fissile mass is on the order of grams. In contrast, for spent fuel, the fissile content is several kilograms. The large fissile mass significantly pushes the net signal above the background and, through multiplication, enables penetration in the SFA which makes DDA an attractive tool to measure spent nuclear fuel.

Pin Diversion Detection for DN

Nine diversion cases were simulated over a wide range of scenarios. A set of three bases cases was selected (4 wt percent IE, and five year CT, and 15, 30, and 45 GWd/tU BU values). Simulated diversion scenarios involved the replacement of fuel pins with pins containing DU consisting of 0.2 weight percent ^{235}U. The

Table 1. Decrease in the counts from base case (no pins replaced) to each of the nine diversion cases, replacing,[8] twenty-four and forty pins in three separate regions across the assembly (middle, center and outer).

		Percent Difference from Base Case			
Diversion: # of pins	Region	% Mass Diverted	15 GWd/tU	30 GWd/tU	45 GWd/tU
			Calculated	Calculated	Calculated
Base	--	-	RSD x 3=1.70 percent	RSD x 3=1.85 percent	RSD x 3=1.90 percent
8 pins	Middle	3.0%	-5.03%	-2.81%	(-0.43%)
24 pins	Middle	9.1%	-21.01%	-12.69%	-7.08%
40 pins	Middle	15.2%	-40.19%	-26.81%	-17.68%
8 pins	Center	3.0%	-3.95%	-2.85%	(-0.24%)
24 pins	Center	9.1%	-14.94%	-8.79%	-4.84%
40 pins	Center	15.2%	-25.27%	-16.28%	-10.05%
8 pins	Outer	3.0%	-3.92%	-2.90%	(-1.67%)
24 pins	Outer	9.1%	-11.79%	-7.91%	-4.94%
40 pins	Outer	15.2%	-20.38%	-15.00%	-9.26%

pins were removed from one of three (middle, center, and outer) regions across the assembly.

Results from these diversion simulations are presented in Table 1. The negative percentages represent the decrease in the counts to the base case where no pins were replaced. Parentheses indicate that DN count rate decrease lies within three times the calculated (statistical) standard deviation for the base case; we thus consider the instrument to be incapable of detecting these three scenarios. Potential systematic errors, which have not been considered here, would further reduce the sensitivity to pin diversion.

The three most critical scenarios are when 8 pins are diverted from the three regions. As the BU increases, the ability to detect diversion decreases because of the reduced fissile content and the increased neutron background. For BU values of 15 and 30 GWd/tU, the eight-pin diversion is well outside the range of statistical uncertainty. For a BU value of 45 GWd/tU, diversion of twenty-four or forty pins from any region would be detectable above statistical error. Note that the potential of diversion detection for the DDA measurements, which has improved statistical precision and adequate penetration, would be better. All MCNPX runs from Table 1 include a relative standard deviation of ~0.6 percent.

Concept of Plutonium Effective Mass to Determine the Fissile Content in Spent Fuel

A DN-DDA instrument isn't capable of discerning what DN or PN came from which isotope. Instead, neutrons are detected from the assembly's "§fissile content," which is a weighted average of all fission events in the assembly. In passive neutron coincidence counting (PNCC) the concept of "$^{240}Pu_{eff}$" was introduced in a similar context. In Equation 1, we introduce an analogous term called "$^{239}Pu_{DN\text{-}eff}$" which stands for "^{239}Pu delayed neutron effective mass" and which provides a way to partition the signal between the various contributors:

$$^{239}Pu_{DN-eff} = C_1\,^{235}U + ^{239}Pu + C_2\,^{241}Pu \qquad (1)$$

Here, ^{235}U, ^{239}Pu, and ^{241}Pu are masses calculated via the CINDER[7,10] BU capability in MCNPX. The constants C_1 and C_2 weight the relative contribution of each isotope on a per gram basis. The method for quantifying these factors is described in the following section.

Delayed Neutron Count Rate as a Function of Fissile Content

In the MNCPX output tallies, we obtain the neutron fluxes that allow us to determine C_1 and C_2 from Equation 2. [7]

$$C_1 = \frac{A_{239}\beta_{235}\iiint_{tVE}\Phi(r,E,t)(\nu(E)\sigma_f(E))_{235}\,dEdVdt}{A_{235}\beta_{239}\iiint_{tVE}\Phi(r,E,t)(\nu(E)\sigma_f(E))_{239}\,dEdVdt}, C_2 =$$

$$\frac{A_{239}\beta_{241}\iiint_{tVE}\Phi(r,E,t)(\nu(E)\sigma_f(E))_{241}\,dEdVdt}{A_{241}\beta_{239}\iiint_{tVE}\Phi(r,E,t)(\nu(E)\sigma_f(E))_{239}\,dEdVdt}. \qquad (2)$$

The coefficients C_1 and C_2 can be determined starting from the total neutron fission yield for a generic isotope i. The neutron

Figure 6. Delayed neutron count rate from the 64 virtual assemblies as function of 239PuDN-effective, IE, BU, and CT

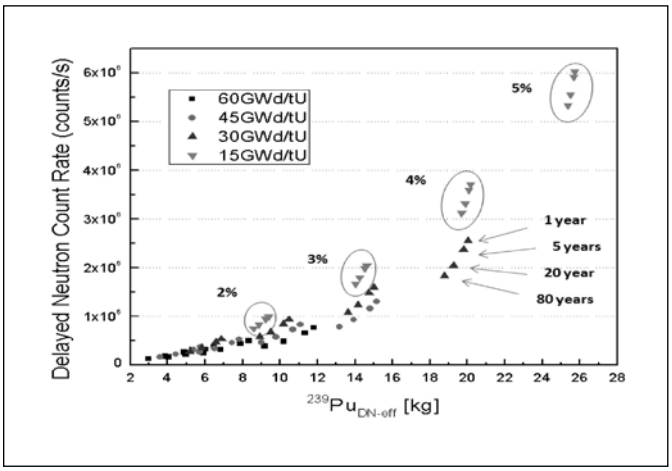

flux in the fuel is denoted by ϕ for neutrons of energy E at the position r and time t per unit energy. Both multiplication in the fuel and neutron absorption alter the interrogating flux. N_i is the nuclei number density of isotope i. The volume over which the measurement takes place is denoted by V (cm^3), the incident neutron energy is denoted by E (MeV), the number of prompt fission neutrons is denoted by ν, the microscopic fission cross-section is denoted by σf (barn), and the average number of DN emitted per fission over the whole energy range is denoted by β. All terms are from MCNPX calculations apart from β, for which the average value from Rinard et al.[9] is used.

In Figure 6, the delayed neutron count rate is graphed as a function of the "Fissile Content ^{239}PuDNeffective" for a set of 64 virtual spent fuel assemblies in water.[7] These 17x17 pressurized water assemblies spanned a broad range of values for IE (2, 3, 4, and 5 wt percent), BU (15, 30, 45, and 60 GWd/tU), and CT (one, five, twenty, and eighty years).[11] The DN count rate decreases as the BU increases since neutron absorber population increases and the fissile content decreases. The variation in the delayed neutron count rate as a function of BU confirms the dominance of ^{235}U over the fissile isotopes of Pu. The change in the delayed neutron count rate is more rapid at lower BU since ^{235}U is the dominant fissile isotope, and as such, it is being depleted at a faster rate. Later in time (when the BU is higher), the ^{239}Pu, ^{241}Pu and ^{235}U are being consumed to maintain the power output of the reactor.

This behavior is due to two primary factors: (1) the percentage of the count rate from ^{241}Pu is the greatest at high BU since ^{241}Pu has a fourteen-year half-life, and (2) its loss is easier to discern at elevated BU, where there is a greater impact from the neutron absorbers ^{155}Gd and ^{241}Am. It can be seen that all sixty-four data points do not fit on a smooth curve; instead, there is structure that is dependent on CT, BU and IE.

Figure 7 shows the DN change as a function of BU for ^{239}Pu and ^{235}U. The DN signal is a strong function of the ^{235}U fraction that is decreasing with BU.

Concept of DN and DDA Integration for Fissile Separation

The measurement of the DN yield in spent fuel is difficult because of the high neutron background, and the primary reason for investigating the technique is that the DN and DDA combination has the potential of determining both the ^{235}U and ^{239}Pu masses separately. Both the DN and DDA responses depend on multiplication, neutron absorption, and self-shielding in the assembly in a similar manner. Integrating both techniques offers the promise of canceling out systematic uncertainties common to both by using the DN/PN ratio. The DN signature provides important and unique information such as increased sensitivity to the ^{235}U content. The prompt-to-delayed ratio increases as a function of fissile content by a factor of about 3.2 for ^{239}Pu over ^{235}U. This "discrimination ratio" can be used for the potential separation of these two fissile isotopes. This separation will be evaluated in future work that combines DN and DDA.

Conclusion

The work presented here is part of an on-going study that we expect will lead to experimental testing of the concepts and practical aspects of an integrated DN-DDA instrument. We have shown the viability and promise of the approach. Experimental work will result in further refinements including optimization of parameters such as the timing structure to those most suitable for the signal and background measurements under realistic operational conditions and constraints. More work on the discrimination ratio and the analysis on an integration of both DN and PN signals in underway to determine the power of the method after merging both responses. The MCNPX modeling work enables response contributions and individual detector rates to be extracted which is a tremendous help to both instrument design and to understand the underlying physical dependences and device algorithms to make use of the signals. The integrated instrument described here provides passive neutron data conceptually similar to what has traditionally been used by safeguards agencies to verify spent fuel. The DDA signal provides multiplication rather directly and a fissile signal that emphasizes ^{239}Pu. On the other hand, the DN signal emphasizes ^{235}U. Combined signatures which are more robust and less dependent on operator declarations may be formed from which the fissile content can be derived.

Acknowledgements

The authors would like to acknowledge the support of the Next Generation Safeguards Initiative (NGSI), Office of Nonprolifera-

Figure 7. Delayed neutron count rate for ^{239}Pu (left) and ^{235}U (right) as a function of BU and CT. The CT decreased from the top curve (one year) to the bottom curve (eighty years)

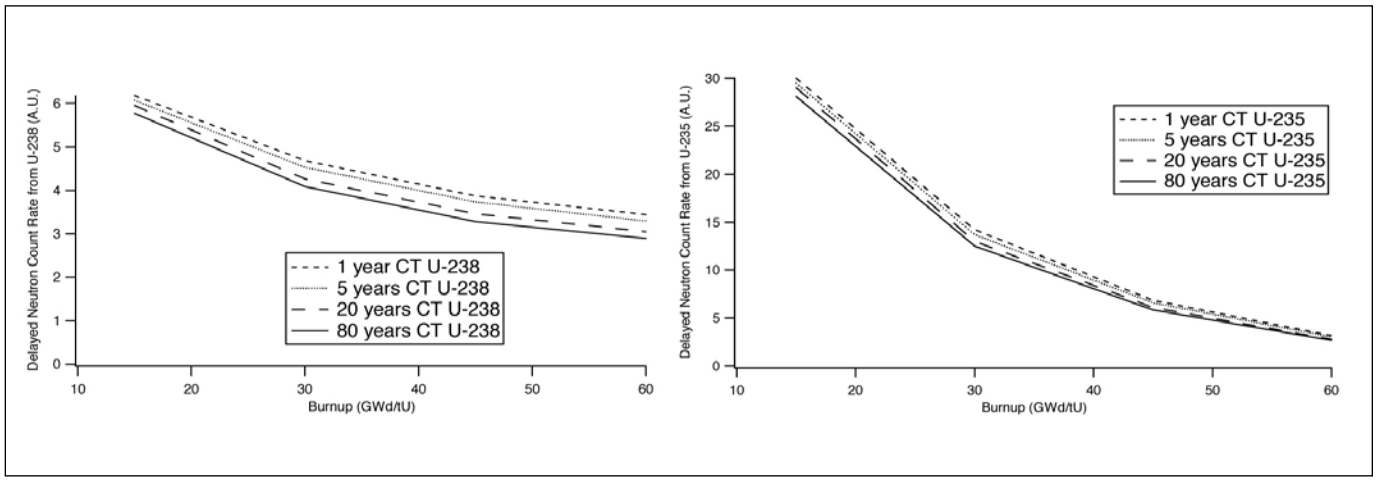

tion and International Security (NIS), National Nuclear Security Administration (NNSA).

References

1. Sandoval, N. P., S. J. Tobin, H. O. Menlove, M. T. Swinhoe, W. Koehler, M. L. Fensin, V. Mozin, M. Schear, J. Richard, and J. Hu. 2009. Determining the Pu Mass in LEU Spent Fuel Assemblies—Focus on Delayed Neutron Detection. Los Alamos National Laboratory Report: LA-UR-09-05317, Los Alamos, New Mexico USA.
2. Lee, T., H. O. Menlove, M. T. Swinhoe, and S. J. Tobin. 2010. Differential Die-Away Technique for Determination of the Fissile Contents in Spent Fuel Assembly, *Proceedings of the 51st Annual Meeting of the Institute of Nuclear Materials Management.*
3. Pelowitz, J. F. 2005. MCNPXTM USER' S MANUAL Version 2.5.0, Los Alamos National Laboratory report, LA-CP-05-0369 (2005); https://mcnpx.lanl.gov/ (last access Nov.21,2011).
4. Blanc, P., S. J. Tobin, T. Lee, J. Hu, J. Hendricks, and S. Croft. 2010. Delayed Neutron Detection with an Integrated Differential Die-Away and a Delayed Neutron Instrument, *Proceedings of the 51st Annual Meeting of the Institute of Nuclear Materials Management* and Los Alamos National Laboratory document LA-UR 10-04125.
5. Blanc, P., S. J. Tobin, S. Croft, H. O. Menlove, M. T. Swinhoe, and T. Lee. 2011. Optimization of the Combined Delayed Neutron and Differential Die-Away Prompt Neutron Signal Detection for Characterization of Spent Nuclear Fuel Assemblies, *Proceedings of Waste Management*, and Los Alamos National Laboratory document LA-UR 10 ¡V 08013.
6. Cobb, D. D., J. R. Philips, M. P. Baker, G. E. Bosler, G. W. Eccleston, J. K. Halbig, S. L. Klein, S. F. Klosterbuer, H. O. Menlove, C. A. Ostenak, and C. C. Thomas, Jr. 1982. Nondestructive Verification and Assay Systems for Spent Fuels, Los Alamos National Laboratory, LA-9041 Vol. 2, April 1982.
7. Blanc, P., S. J. Tobin, S. Croft, and H. O. Menlove, revised version by A. Favalli, H. Trellue, A. McKinney. 2011. Plutonium Mass Determination in Spent Fuel--Delayed Neutron Detection in an Integrated Delayed-Neutron and Differential Die-Away Instrument with ^{3}He Detectors and a DT Generator, Los Alamos National Laboratory report for the Next Generation Safeguards Initiative (NGSI) Effort, LA-UR 11-050626.
8. Fensin, M. L., J. S. Hendricks, and S. Anghaie. 2010. The Enhancements and Testing for the MCNPX 2.6.0 Depletion Capability, *Nuclear Technology,* 170, 1, p.68-79 (2010).
9. Rinard, P. M. 2001. Application Guide to Shufflers, Los Alamos National Laboratory report, LA-13819-MS.
10. Fensin, M. L., S. J. Tobin, N. P. Sandoval, M. T. Swinhoe, and S. J. Thompson. 2009. A Monte Carlo Linked Depletion Spent Fuel Library for Assessing Varied Nondestructive Assay Techniques for Nuclear Safeguards, *Proceedings of the Advances in Nuclear Fuel Management IV (ANFM),* and Los Alamos National Laboratory document LA-UR 09-01188.
11. Galloway, J. D., H. R. Trellue, M. L. Fensin, and B. L. Broadhead. 2012. Design and Description of the NGSI Spent Fuel Library with an Emphasis on Passive Gamma Signal, *Journal of Nuclear Materials Management*, Vol. 40, No. 3.

Delayed Gamma-Ray Spectroscopy for Spent Nuclear Fuel Assay

V. Mozin
Lawrence Livermore National Laboratory, Livermore, California USA

L. Campbell
Pacific Northwest National Laboratory, Richland, Washington USA

A. Hunt
Idaho Accelerator Center, Idaho State University, Pocatello, Idaho USA

B. Ludewigt
Lawrence Berkeley National Laboratory, Berkeley, California USA

Abstract

High-energy, beta-delayed gamma-ray spectroscopy is investigated as a nondestructive assay technique for the determination of plutonium mass in spent nuclear fuel. This approach exploits the unique isotope-specific signatures contained in the delayed gamma-ray emission spectra detected following active interrogation with an external neutron source. A high-fidelity modeling approach that couples radiation transport, analytical decay/depletion, and a newly developed gamma-ray emission source reconstruction code is described. Initial simulations and analysis were performed for "one-pass" delayed gamma-ray assay that focused on the long-lived signatures. Also presented are the results of an independent study that investigated "pulsed mode" measurements to capture the likely more isotope-specific, short-lived signatures. The initial modeling results outlined in this paper suggest that Pu-239 may be assayed in a typical 17x17 pressurized water reactor (PWR) assembly with a statistical uncertainty of a few percent using commercially available gamma-ray spectrometers and a neutron generator with a source strength on the order of 10^{11} n/s.

Introduction

Active nondestructive assay (NDA) techniques can potentially increase the accuracy of Pu content characterization in spent nuclear fuel assemblies as compared to existing methods applied in nuclear safeguards. The temporal and energy distributions of prompt and delayed responses following induced fissions can provide specific signatures for the direct measurement of fissionable material content. As part of the Next Generation Safeguard Initiative (NGSI)[1] effort to quantify plutonium mass in spent nuclear fuel assemblies, research is being performed on an integrated instrument for the detection of various signals (neutron and gamma rays) that are actively induced by an external deuterium-tritium (D-T) neutron generator. In this context, high-energy, beta-delayed gamma-ray spectroscopy offers the ability to directly and independently measure the Pu isotopic content. Response spectra of delayed gamma rays emitted from the fission products and their decay progeny extend into the high-energy region (above ~3.0 MeV), above interferences from the intense low-energy passive background, and provide signatures for the quantitative identification of fissile isotopes present in the fuel. Compared to conventionally detected prompt and delayed neutrons, delayed gamma rays are considerably more prolific, are emitted continuously during extended time periods after irradiation (seconds and hours), and are less vulnerable to the matrix effects and the media surrounding the assayed nuclear material.

The intensities of individual delayed gamma-ray peaks in measured spectra are governed by fission product mass distributions that are partially correlated with the mass of the initial heavy nucleus. Most of the fission products are initially neutron rich, undergo a series of beta decays to approach stability and, as a result, emit gamma rays with a complex time- and energy-dependent structure. Early emissions from short-lived fragments are likely to reveal potentially more sensitive signatures than responses acquired at later times. To exploit the temporal extent of the delayed gamma-ray emission, the assay can be performed in pulsed mode with irradiation and detection periods ranging from fractions of a second to several minutes.

Multiple applications of the delayed gamma-ray assay have been investigated in the past including determining the qualitative presence of fissile or fertile isotopes, waste packages characterization, transport containers screening, and uranium enrichment measurements.[2-6] More recent empirical studies involved nuclear forensics and the determination of the residual fission rates in irradiated nuclear fuel.[7-9] These works

demonstrated the potential of the delayed gamma-ray technique as an assay method, but fail to address the analysis principles necessary for spent nuclear fuel assay.

The specificity of the delayed gamma-ray responses to the Pu content can be limited by the small variability in fission product mass distributions for actinides with similar mass numbers. While U-235 and Pu-239 signatures can be separated with existing spectroscopic methods, distinguishing contributions from Pu-241 and U-238, which are inevitably present in the fuel can be increasingly complicated. Multiplication effects during active interrogation lead to a sustained population of fission-spectrum neutrons in the fuel regardless of the interrogating source energy. This results in a certain amount of fissions of fertile isotopes, especially U-238, that cannot be excluded from the response analysis. Another obstacle arises from the high spent fuel radioactivity that interferes with the delayed gamma-ray spectra acquisition. The passive background dominates the low energy response (below ~3.0 MeV) and must be mitigated in order to not exceed the count rate limit of the detector systems. In addition, geometry and self-shielding effects arising from the periodic configuration of the fuel assemblies, the presence of structural materials, and uneven fuel burnup profiles can considerably affect the sensitivity and statistical confidence when trying to determine the Pu inventory. Modeling tools developed for this project provide the capability to accurately account for these factors with a thorough investigation currently underway.

To become a practical method for routine measurement of Pu content in spent nuclear fuel assemblies, the delayed gamma-ray assay instrument must achieve significantly lower levels of uncertainty than the conventional methods and neutron techniques currently under investigation.[1] Additionally, measurements must be acquired within reasonably short assay times that are compatible with real-world fuel handling procedures.

This paper summarizes preliminary findings from two parallel studies of high-energy, beta-delayed gamma-ray spectroscopy for the assay of spent nuclear fuel assemblies. One study focused on the development of high-fidelity modeling approaches and the evaluation of a conventional "one-pass" interrogation, with earlier results presented in References 10 and 11. The other one investigated the merits and statistical uncertainties of a *pulsed* assay that takes advantage of the delayed gamma-ray signal at shorter decay times previously discussed in References 12-14.

One-pass Delayed Gamma-ray Assay

Delayed gamma-ray spectra obtained during the active interrogation of nuclear materials contain multiple features from which an inventory of fissionable isotopes can be derived. However, in the case of spent nuclear fuel assay, the interpretation of these signatures is complex and has to account for non-linear factors. The periodic geometry of the fuel assemblies, uneven burnup distributions among individual pins, and multiplication effects result in high variability of the interrogating neutron flux intensity and energy structure. Because of the energy-dependent fission product yields, detected responses cannot be normalized to the interrogating neutron source in a straightforward manner. Relatively small differences in fission product yield distributions lead to a considerable overlap of the delayed gamma-ray peaks from different fissionable isotopes present in the fuel. In addition, uneven interrogating source and detector efficiencies for different fuel pins in the assembly, along with a high variability of inventory profiles within and among assemblies, may preclude the absolute analysis of the assay signatures. Finally, the overall feasibility of acquiring delayed gamma-ray responses with low statistical uncertainties may be limited in the presence of a highly intense passive radioactive background.

Modeling Approach

In the absence of relevant experimental results, an understanding of multiple competing processes associated with the delayed gamma-ray assay of the spent nuclear fuel assemblies was achieved through an extensive theoretical study. A high-fidelity simulation of the assay conditions was developed in the form of a hybrid analytical and Monte Carlo calculation technique. The modeling approach externally couples radiation transport (MCNPX) with analytical decay/depletion (CINDER) codes, along with a newly developed gamma-ray emission source reconstruction code (DGSDEF).[15] This method offers the required spatial, energy, and time resolution to provide a detailed description of the assay system and fuel assembly effects. Passive and delayed gamma-ray spectra can be obtained for arbitrary assay geometries, interrogating source parameters, material compositions, and detector specifications. Calculations are performed using the full extent and accuracy of the most recent physical data libraries. The neutron flux resulting from the active interrogation is determined with a sixty-three-group energy structure. The corresponding multigroup neutron cross-sections, fission yield sets, decay constants, and branching ratios are obtained from a variety of sources, including international evaluated data libraries.[16-18] The temporal evolution of isotopic compositions is explicitly followed for all possible transmutation patterns described in the extensive dataset of 3,400 nuclides in ground and isomeric states with Z ranging from 1 to 103. Yield sets of 1,325 fission products are defined for sixty-seven fissionable nuclides, and divided by the incident neutron energy into three groups: *thermal*, *fast*, and *high* (14 MeV). The discrete gamma-ray emission source is reconstructed for a library of 979 isotopes with decay modes and radioactivity spectra as extracted from the ENDF/B-VI evaluation.

Experimental benchmarking of the delayed gamma-ray response modeling technique was performed at the LINAC facility of the Idaho Accelerator Center. Fissile and fertile material samples were irradiated with an accelerator-driven photo-neutron source for various interrogation time regimes. Delayed gamma-

Figure 1. An overlay of measured and simulation delayed gamma-ray spectra using typical HPGe resolution for the DU sample with calculated isotopic contributions to the total response. Total measured and simulated spectra overlap each-other and are offset by a factor of 10.

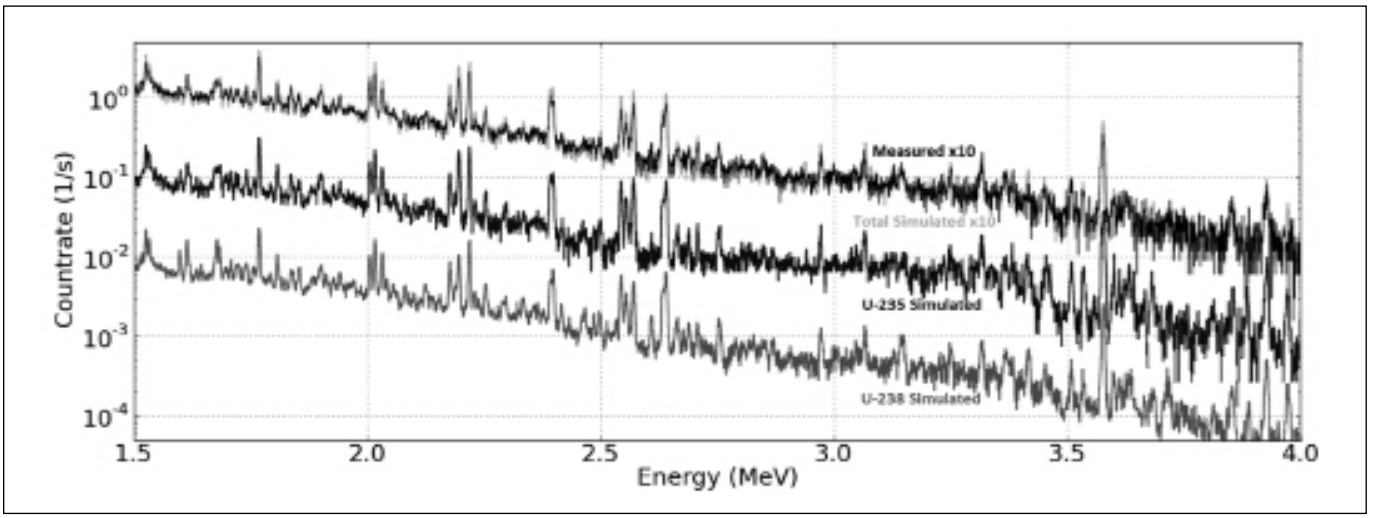

ray emissions from the long-lived fission products were collected in a "one pass" assay mode with relatively long irradiation and spectrum acquisition periods (thirty to sixty minutes) separated by a cool-down/transition time of less than two minutes. Investigation of faster responses (up to 10 seconds) was performed in the *pulsed* mode by detecting gamma-ray spectra between the neutron pulses. Figure 1 demonstrates an example of the results obtained for a thirty minutes irradiation, thirty seconds cool-down, fifty-five minutes acquisition interrogation time pattern of a 1.2 kg depleted uranium sample with 99.8 percent U-238 and 0.2 percent U-235. The interrogating source parameters (electron beam energy, photo-neutron converter material, and moderator thickness) were selected to induce fissions primarily in the thermal energy range and specifically to stimulate responses from U-235. A detailed peak-by-peak comparison of simulated and measured delayed gamma-ray spectra performed in Reference 19 for the series of "one pass" measurements with different samples confirms the good agreement qualitatively observed in Figure 1. More extensive experimental validation of the modeling technique is currently in progress. Analysis and benchmarking of the pulsed mode simulation capability is also subject to ongoing research focused on evaluating the quality of fission yield data libraries for fission products with very short half-lives.

Spent Nuclear Fuel Assay Instrument Design

Within the context of the NGSI project, the modeling technique was utilized to predict delayed gamma-ray assay responses from 17′17 PWR assemblies with extensive inventories obtained for various burnup, initial enrichment, and cooling time as provided in the NGSI Spent Fuel Library.[20] For detailed calculations of passive and active spectra, more than 2,000 isotopes were included in the fuel material definition of each pin. The spent fuel assay geometry is shown in Figure 2. The D-T source is coupled to the assembly through a layer of neutron spectrum tailoring material that is fully compatible with other neutron-generator-based instruments considered in the NGSI project. The parameters of the slot collimator and attenuating filters were analytically optimized to give an acceptable total detector count rate, selective attenuation of the low-energy passive background, and maximum efficiency to the high-energy delayed gamma rays. Response spectra were obtained for both a high-efficiency, high-purity germanium detector (HPGe) and a $LaBr_3$(Ce) scintillation detector. Modeling scenarios assumed the one pass assay mode with fifteen-minute interrogation, one-minute cool-down, and fifteen-minute live-time acquisition of the delayed gamma-ray spectrum.

An example of passive and delayed gamma-ray spectra with HPGe resolution, obtained for a 45 GWd/t burnup, 4 percent initial enrichment, five-year cooled PWR assembly, is depicted in Figure 3. These results indicate that the delayed gamma-ray spectrum is only slightly obstructed by the fuel radioactive background above 3 MeV, and is entirely driven by the interrogating source above 3.5 MeV. To improve the statistical quality of high-energy, delayed gamma-ray peaks in this simulation, the neutron source intensity was assumed to be 10^{12} n/sec, which may be higher than necessary for a realistic assay measurement. The maximum integrated detector count rate in the assumed assay configuration was determined to be just above 10^6 counts/sec., which is beyond the limit of conventional HPGe detectors and requires further setup optimization. Faster gamma spectrometers, such as $LaBr_3$(Ce) scintillation detectors, can potentially improve the rate of the delayed gamma-ray spectra acquisition, however their applicability may be limited by the coarser energy resolution.

Figure 2. Delayed gamma-ray spent fuel assay geometry used in the modeling study

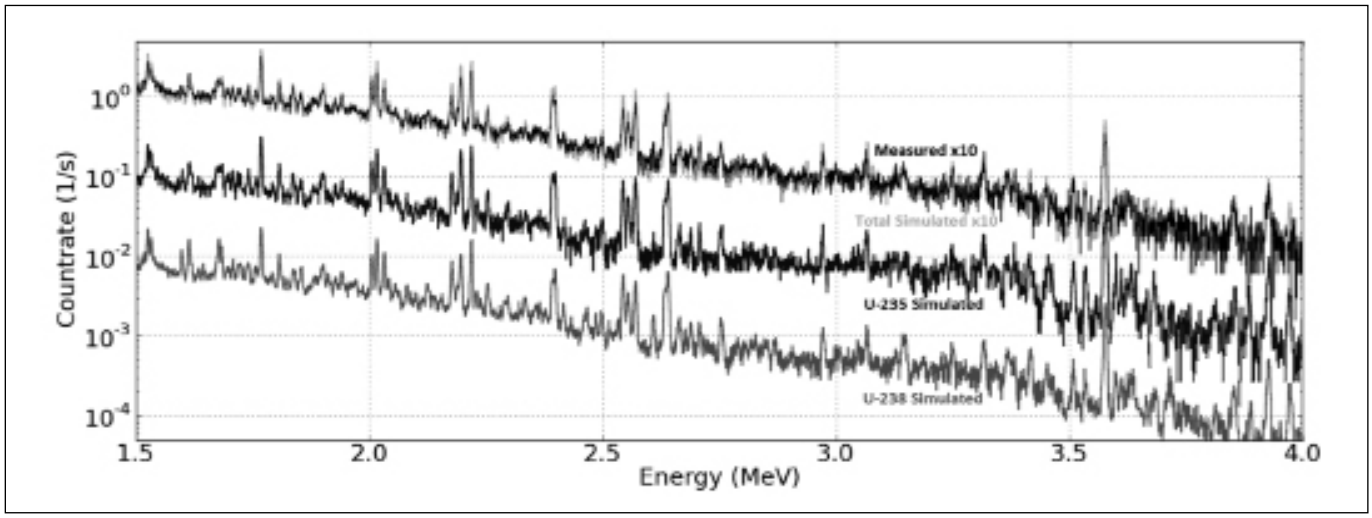

Figure 3. Passive and delayed gamma-ray spectra with HPGe resolution calculated for a 45 GWd/t 17′17 PWR spent fuel assembly

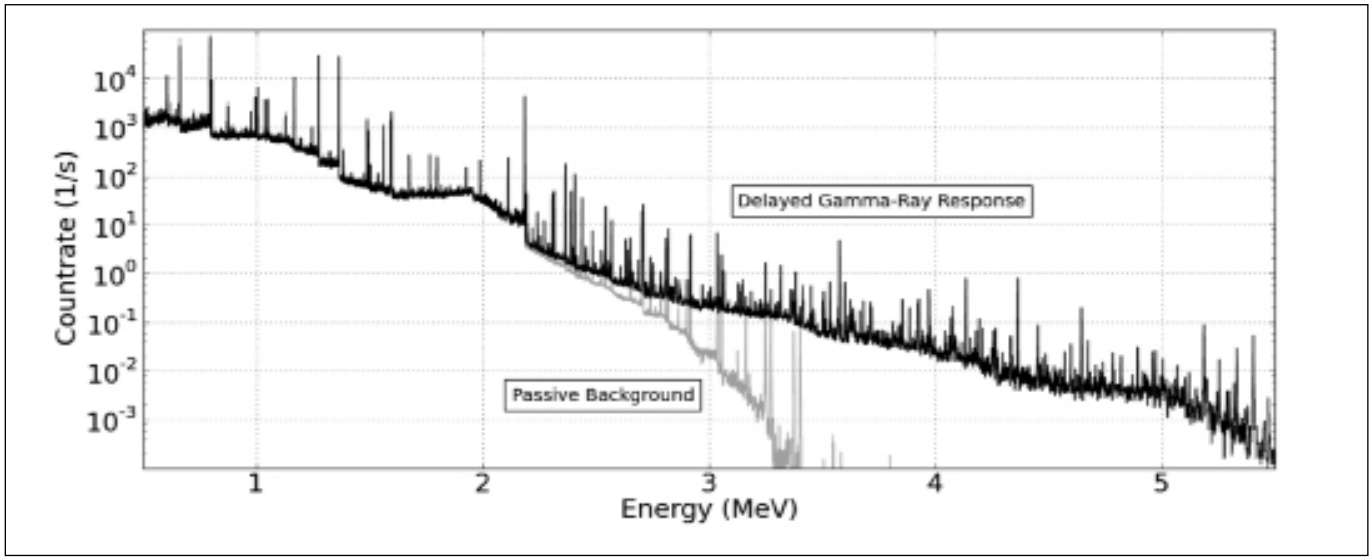

Assay Response Analysis

Assay modeling calculations performed for several spent fuel library assemblies with extensive fuel inventories indicate that the high-energy region of the delayed gamma-ray spectrum is almost entirely composed of contributions from four fissionable nuclides. While the majority of the integrated signal is generated by U-235 and Pu-239 isotopes, up to 20 percent of the counts can originate from the Pu-241 and U-238 present in the fuel. Relative contributions of these isotopes are dependent on assembly burnup and initial enrichment, and in the case of U-238, on the residual multiplication in the fuel assembly. Figure 4 demonstrates these individual components of the high-energy, delayed gamma-ray spectrum calculated for the same 45 GWd/t assembly, assuming 130 percent-efficiency HPGe and a similar size 3′4 inch $LaBr_3(Ce)$ detectors. The contributions of the individual isotopes to the total count rate are determined as the integrated area under each spectrum in the 3.5 to 5 MeV region, where passive background is assumed to be negligible. As in the prompt and delayed neutrons counting methods, this integrated high-energy delayed gamma-ray signal is proportional to the fission rate of the assayed material. If detector efficiency and assembly multiplication could be absolutely calibrated, this signature could be related to the total fissile content. Such measurements do not require high-resolution detectors and can be used for the detection of pin diversions and independent verification of the declared fuel parameters, such as burnup, initial enrichment, and cooling time.

Figure 4. Delayed gamma-ray spectrum with individual contributions from fissionable nuclides calculated assuming a 130 percent-efficiency HPGe detector (top), and a 3´4 in. $LaBr_3$(Ce) detector (bottom). The table lists values of isotope-specific integrated count rates as perce nt of the total over the 3.5 to 5 MeV region.

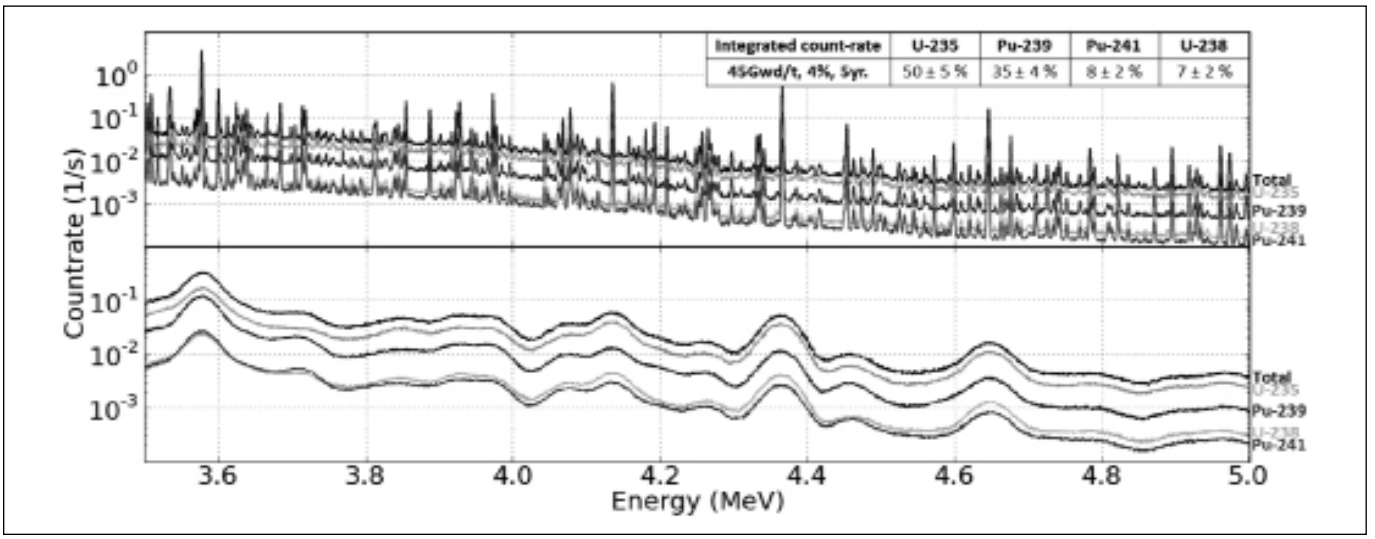

Although individual spectral features shown in Figure 4 appear similar for the four isotopes, a detailed relative intensity analysis[11] revealed that individual peak area ratios are specific to a particular fissionable nuclide. The variability of the composition-specific peak ratios was demonstrated for a set of PWR assemblies with a range of burnup and initial enrichment from the NGSI spent fuel library.

The delayed gamma-ray spectrum exhibits unique inventory-specific structures and peaks reflecting varying contributions from fissionable nuclides to each peak area. Therefore, the total response can be interpreted as a linear combination of four individual isotope-specific spectra that could be obtained during instrument calibration. Relative inventories of the four contributing nuclides can be determined from the regression fit of these components to the acquired spectrum. The sensitivity limits of this response analysis approach were investigated in a modeling study assuming a set of assemblies with simplified compositions. Each assembly assumed a 17x17 PWR configuration with the full inventory of fission products corresponding to 45 GWd/t burnup, and pre-defined compositions of fissionable isotopes as shown in Table 1. Delayed gamma-ray spectra were calculated between 3.5 and 5.0 MeV for HPGe and $LaBr_3$(Ce) detector resolutions in the same form as shown in Figure 4. The individual calibration spectra were obtained from a separate case, and fissile isotopic compositions were calculated using the Levenberg-Marquardt Orthogonal Distance Regression method.[21] For HPGe results, two additional scenarios were considered. In the first, fitting was performed using the areas and associated uncertainties of the ten most intense peaks (~1,000 counts) in this energy region. In the second, narrow spectral regions, about 25 keV wide, containing these peaks were used for the fit, while peak areas were not determined and no background subtraction was made. A subset of results shown in Table 1 indicates that the effectiveness of this analysis technique is dependent on the energy resolution of the fitted spectra. The algorithm performs better for the larger sets of data, with the highest accuracy achieved for the fitting of the full spectrum in this energy region.

Pulsed Delayed Gamma-ray Assay

A separate study, independent of the effort described above, was conducted for a high-energy, delayed gamma-ray spectroscopy instrument that utilizes a pulsed neutron source to capture the delayed gamma-ray signal at shorter decay time. A summary of this work is presented in this paper; a more detailed description of the methodology as applied to a single fuel pin is found in References 12 and 13, and earlier results for full fuel assemblies are described in Reference 14. (The goal of present research is to estimate the achievable measurement precision of a delayed gamma assay to assess if this method holds promise as a viable assay technique.)

Instrument Design

The conceptual design of the delayed gamma-ray instrument investigated and modeled is shown in Figure 5. A DT neutron source is surrounded by iron for spectrum tailoring. The 14 MeV neutrons scattering off iron nuclei have a relatively high cross-section of losing significant energy via inelastic processes. These less energetic neutrons enter the high density polyethylene (HDPE) where they are moderated to thermal energies. A lead reflector surrounds the moderator, with a window that allows gamma rays to escape and be observed by a HPGe detector. A significant thickness of lead is left in the window in order to selectively filter out the lower energy passive background radiation from the intensely radioactive fuel.

Table 1. Relative fissile isotopic compositions obtained with various parameters of calculated 3.5 to 5.0 MeV delayed gamma-ray spectra (assuming assemblies with simplified material inventories)

Assumed Fissionable Content Composition	5% U-235, 3% Pu-239, 2% Pu-241, 90% U-238	1% U-235, 3% Pu-239, 1% Pu-241, 95% U-238
Real Fissile Isotopes Ratio U-235 : Pu-239 : Pu-241	1 : 0.6 : 0.4	1 : 3 : 1
Full HPGe specturm	1 : 0.603 (±0.004) : 0.399(±0.003)	1 : 2.896 (±0.024) : 0.999(±0.012)
Full $LaBr_3$ specturm	1 : 0.687 (±0.017) : 0.350(±0.013)	1 : 2.721 (±0.078) : 0.067(±0.042)
10 HPGe peak areas	1 : 0.606 (±0.017) : 0.407(±0.013)	1 : 3.093 (±0.102) : 0.980(±0.046)
10 HPGe peak regions	1 : 0.606 (±0.016) : 0.405(±0.012)	1 : 3.115 (±0.103) : 0.983(±0.046)

Figure 5. Left: Cut-away view of the delayed gamma-ray instrument geometry for a PWR fuel assembly. Right: Top view of the instrument geometry as modeled in GEANT, including a cylindrical sleeve of high-density polyethylene (HDPE) moderator, lead shell for neutron reflection and gamma-ray shielding, DT neutron source (small circle) in a cylindrical iron plug and a coaxial 114 percent HPGe detector.

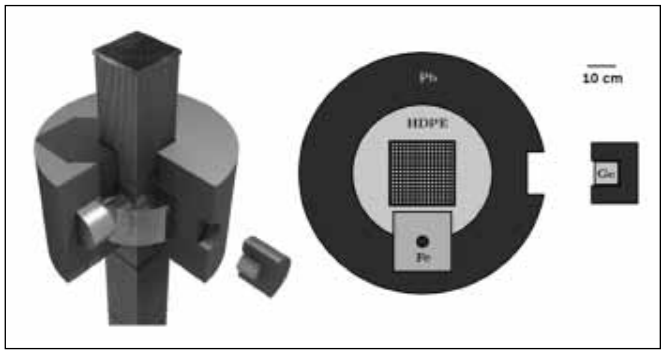

Simulations

The initial isotopic inventory of the fuel in the Pacific Northwest National Laboratory (PNNL) study was taken from simulations using the ORIGEN-2 code[22] for 3 percent enriched Westinghouse 17×17 PWR assemblies, with burnup values of 0, 5, 18, 33, 45, and 60 GWd/t and a ten-year cooling time. The passive spectrum was estimated by determining the isotopes responsible for 99 percent of the signal in windows bounded at 0, 0.663, 1.0, 1.5, 2.0, 2.5, 3.0, and 10.0 MeV. The emissions of these isotopes were propagated through the instrument and into the detector using the GEANT4 Monte Carlo radiation transport code[23] Spontaneous fission gamma rays were also simulated, using the fission C++ libraries from the Computational Nuclear Physics (CNP) group of Lawrence Livermore National Laboratory[24] for the gamma-ray distribution. Activation and (n,γ) reactions from spontaneous fission neutrons have not yet been simulated.

To simulate the actively induced signal, neutrons with energy of 14 MeV were emitted from the source and propagated through the instrument to the fuel using GEANT4. The number and distribution of fissions within the fuel was tracked. Because GEANT4 lacks high-precision neutron reaction cross sections for transuranic isotopes, these studies used models of fresh fuel of varying enrichments to estimate the fission efficiency and distribution for assemblies containing mixed uranium and plutonium isotopes by matching the fission inverse mean free paths of thermal neutrons. Using the ENDF-tabulated independent fission yields,[16] lifetimes, and branching ratios from the ENSDF library[25] and the National Nuclear Data Center,[26] the population of fission-induced transient isotopes was integrated over time assuming repeated cycles of ten seconds of neutron irradiation followed by ten seconds of measurement for total assay times ranging from ten to 100 minutes. Intermediate cool-down time periods were small in the experiment and were neglected in these calculations. We assumed that all fissions were induced by thermal neutrons, and considered the response from the fissions of the isotopes U-235, Pu-239, and Pu-241. Of the population of resulting fission product isotopes, eighty-two have sufficient gamma-ray intensities to produce a detectable signal in the detector. The radiation from these fission product isotopes was transported through the instrument using GEANT4 and the detector response was recorded. Subsequent preliminary simulations using MCNPX for this instrument geometry indicate non-thermal fissions make up about 5 percent to 10 percent of the total from the fissile isotopes, and fast fission of U-238 from fission multiplication neutrons are an additional approximate 5 percent effect while U-238 fast fission from direct DT source neutrons are about a 1 percent to 2 percent effect. In an actual measurement these effects would need to be taken into account, but they are not expected to make a significant difference for estimating the expected precision of the assay method.

Analysis

The delayed gamma-ray spectra from the pure fissile isotopes were simulated. The signal from an unknown sample was then compared to the isotopic signals. Linear least squares fitting to the fissile delayed gamma signals and a linear background was used to find the most likely quantities of fissile isotopes that could produce the observed signal, and the uncertainty on those quantities. For the results quoted here, the energy range of the fit was over a range of 2.5 to 4.8 MeV, where inclusion of the 2.5 to 3 MeV range necessitated two additional fitting vectors of the gamma spectra of Rh-106 and Tl-208, which are present as part of the passive component of the signal in spent fuel. From these fit parameters, the proportion of the fissile isotopes that make up the

Figure 6. Example pulse-height spectra of active-interrogation signal for pure U-235, Pu-239, and Pu-241 with a neutron generation rate of 10^{10} n/s, a measurement protocol of ten seconds irradiation, ten seconds measurement, and 10 minutes of total interrogation time. Pu is indicated by a strong Tc-106 signal. Pu-239 is differentiated based on a low Te-136 response. U-235 is relatively rich in the Rb isotope lines.

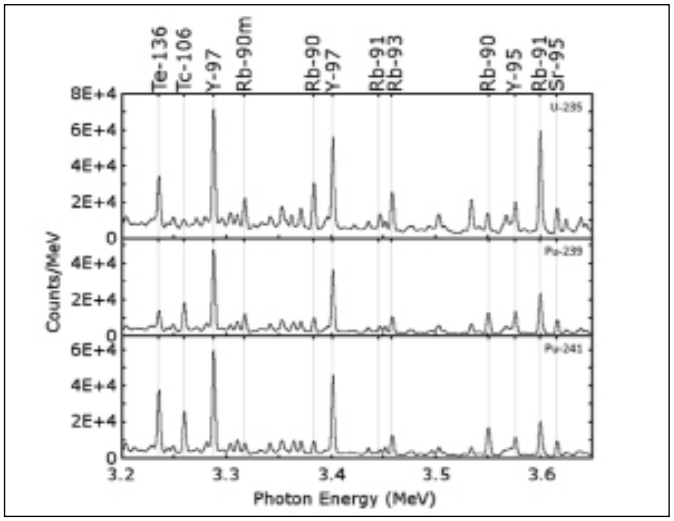

sample can be determined. The fissile fractions returned by this method are unaffected by issues of calibration or neutron transport. The height of the spectral peaks gives information about the absolute quantities. This requires the instrument to be calibrated to determine the spectral intensity at various compositions and can be affected by, for example, neutron absorbers which have built up within the spent fuel. This study used the simulations of neutron transport in fresh fuel for calibration; this should be sufficient to estimate achievable uncertainties with realistic designs, but should not be used for rigorous analysis.

Results

The passive spontaneous fission background proved to be negligible compared to radioactive decay at energies less than 3.0 MeV, and negligible compared to the expected active signal at higher energies. Above 3.0 MeV the decay radiation is also negligible compared to the expected active signal. The most significant effect of the background for measurements at energies higher than 3.0 MeV is in saturating the detector via gross count rate. In our studies, we assumed a detector that could operate at count rates of 100 kHz.

Figure 6 shows an example of high-energy delayed gamma-ray spectra for the pure isotopes within the 3.2 to 3.65 MeV energy range. This range allows the passive background to be neglected, while showing many strong peaks. Significant differences are evident between the spectra of the isotopes. The Tc-106 line at 3.2595 MeV, for example, is nearly absent in the U-235 spectrum while it shows significant contributions in both fissile Pu spectra. As shown in this simulation, the relative intensity of Te-136 line at 3.2361 MeV is visibly lower for Pu-239 compared to the other fissile isotopes. Several lines from rubidium isotopes—Rb-90m at 3.317 MeV, Rb-90 at 3.38324 MeV, Rb-93 at 3.45819 MeV, and Rb-91 at 3.59967 MeV – are more strongly emphasized in U-235 than the plutonium isotopes.

Table 2 lists the estimated fissile mass fractions and associated statistical uncertainties for 100 minutes of interrogation time using a neutron generator with an intensity of 3×10^{10} n/s and a single HPGe detector with 114 percent relative efficiency. The statistical uncertainty of the Pu-239 mass fraction is about 5 percent at the highest burnup of 60 GWd/MTU. Extrapolated from the 20 cm length within the interrogation instrument to the full assembly, this corresponds to approximately ¼ kg Pu mass uncertainty. To reduce the assay time to ten minutes, a source of approximately 5×10^{11} n/s would be required to obtain a similar uncertainty. The mass fractions could be converted into absolute masses with appropriate calibration procedures (a subject of ongoing research[1]). Systematic uncertainties have not yet been rigorously investigated, but preliminary analysis of the effects of uneven burnup within an assembly indicates a 1 percent to 2 percent effect. Research is also underway to optimize the instrument design and irradiation/measurement cycles to allow increased signal from a given neutron source.

If the spectrum is broadened to resolutions typical of $LaBr_3$(Ce) scintillation detectors, many of the individual peaks blur together. However, the fits are still possible, albeit with increased uncertainty as also seen in the one-pass study. An increase in signal by a factor of approximately 5 is necessary to achieve similar uncertainties in the fitted quantities. The faster response time of $LaBr_3$(Ce), however, allows it to handle much higher rates than HPGe, which could potentially overcome the difficulties associated with reduced resolution.

Benchmarking Studies

Benchmarking measurements were performed using the prompt gamma neutron activation analysis (PGNAA) facility at Oregon State University (OSU). The OSU PGNAA facility consists of an HPGe spectrometer (36.5 percent relative efficiency, 6.2 cm diameter, 5.46 cm length) with a 28.9 mm pinhole collimator that is 35.6 cm long. The HPGe spectrometer views a sample in the path of a collimated thermal neutron beam from the OSU TRIGA reactor. The sample used for the validation measurements was a pair of uranium foils with an enrichment of 93 percent and a total mass of 340 mg. Figure 7 shows the results of these measurements. Although the data is noisy, major peaks are represented and peak heights are approximately reproduced. A detailed comparison of measured and predicted data is found in Reference 14. Additional measurements of this type, using both uranium and plutonium foils and improved experimental apparatus, are currently in the planning stage at Oregon State University. These measurements will support efforts to identify deficiencies in the tabulated nuclear data and modeling methods needed to faithfully simulate delayed gamma-ray assay of spent fuel.

Table 2. Fitting results of simulated, high-energy, delayed gamma-ray spectra to estimate fissile mass fractions for a measurement protocol of ten seconds irradiation, ten seconds measurement, and 100 minutes of interrogation time with a neutron source strength of 3×10^{10} n/s. The listed errors are estimates of statistical uncertainties. Systematic uncertainties have not yet been rigorously investigated, but preliminary analysis of the effects of uneven burnup within an assembly indicates a 1 percent to 2 percent effect.

Burnup (GWd/MTU)	U-235 (mass fraction)		Pu-239 (mass fraction)		Pu-241 (mass fraction)	
	Calculated	True	Calculated	True	Calculated	True
0	1.001 ± 0.006	1	0.002 ± 0.025	0	-0.004 ± 0.009	0
5	0.904 ± 0.009	0.915	0.102 ± 0.024	0.084	-0.007 ± 0.011	0.001
18	0.742 ± 0.012	0.750	0.230 ± 0.026	0.230	0.027 ± 0.013	0.020
33	0.533 ± 0.018	0.546	0.402 ± 0.029	0.393	0.065 ± 0.018	0.061
45	0.365 ± 0.022	0.372	0.516 ± 0.031	0.525	0.118 ± 0.022	0.104
60	0.174 ± 0.028	0.191	0.679 ± 0.032	0.662	0.147 ± 0.027	0.147

Figure 7. Measured spectrum of 93 percent enriched uranium, alternating ten seconds of irradiation with ten seconds of measurement for 180 cycles, compared to theoretical predictions. Uniform scaling was applied to the simulation curve. The integrated signal in the Te-136 region is significantly over-predicted in the simulation, suggesting the ENDF-tabulated independent fission yields for this isotope may be incorrect.

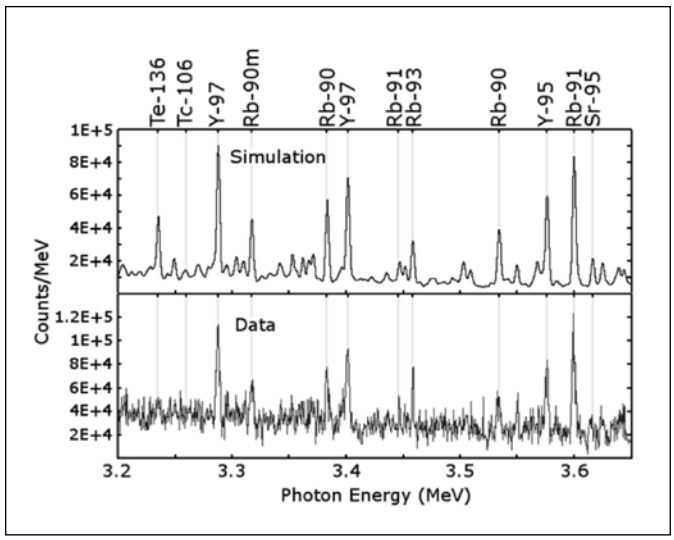

Conclusions and Outlook

The initial modeling and experimental benchmarking efforts outlined in this paper were performed to investigate delayed gamma-ray assay methods for the determination of plutonium mass in spent nuclear fuel. Analytical estimations and detailed assay simulations accomplished for a range of NGSI fuel assemblies with various burnup, initial enrichment and cooling time demonstrate that the response spectra can be obtained with a precision that is adequate for the subsequent inventory analysis. Individual signatures of fissionable isotopes contained in these responses can potentially be used to quantify the total fissile content and individual weight fractions of fissile and fertile nuclides present in spent fuel. The primary constraint for the delayed gamma-ray assay measurement is the count rate limitation of the high-resolution detector systems in the presence of intense spent fuel passive radioactivity. Collimation and attenuating materials used to mitigate the low-energy background also reduce the response in the high-energy region and thus increase interrogation time or neutron source intensity requirements. Present modeling results indicate that a neutron generator with a minimum intensity of a few times 10^{10} n/s is required for the spent fuel assembly assay, however it could be an order of magnitude higher if the response analysis demonstrates lower sensitivity or higher statistical quality of the results is desired. Commercial off-the-shelf DT neutron generators reach neutron yields of up to $1\text{x}10^{10}$ n/s. Higher output generators with yields of up to $5\text{x}10^{11}$ n/s are currently under development and could potentially serve this application as well as other neutron sources such as an electron accelerator-driven photo-neutron source.[27]

Determining the relative fissile isotopic inventory from the delayed gamma-ray assay spectra relies on complex algorithms capable of distinguishing the individual contributions of U-235, Pu-239, Pu-241, and U-238 from the detected cumulative response. Performing the interrogation in pulsed mode emphasizes the isotope-specific features of the spectrum, while a one-pass assay is possibly a more practical active interrogation technique. Long-lived responses can be collected in a simpler setup where the interrogating neutron source and response acquisition components can be separated in space and time. The comparative study of advantages and limitations of each approach is a subject of further investigation. Future work will also address systematic uncertainties arising in the assay of the spent fuel assemblies, as well as the development of more sophisticated response analysis methods.

The ability to perform an absolute quantification of Pu content in spent fuel with delayed gamma-ray assay is directly determined by the accuracy with which non-linear assay effects can be characterized. These factors are expected to vary considerably for different fuel types and interrogation environments. A

preliminary search for calibration procedures and self-normalizing response features can be performed by increasing the complexity of the delayed gamma-ray assay simulation scenarios. However, modeling studies are limited by the gaps in the physical data libraries as well as assumptions of the calculation techniques that may fail to account for the full complexity of spent fuel assembly interrogation. Experimental demonstrations replicating realistic assay conditions are ultimately required to establish the validity of the delayed gamma-ray assay for safeguards applications.

Acknowledgements

The authors would like to acknowledge the support of the Next Generation Safeguards Initiative (NGSI), Office of Nonproliferation and International Security (NIS), National Nuclear Security Administration (NNSA), as well as collaborators at Los Alamos National Laboratory. This work was performed under the auspices of the U.S. Department of Energy by Lawrence Livermore National Laboratory under Contract DE-AC52-07NA27344, by Pacific Northwest National Laboratory under Contract DE-AC05-76RL01830, and by Lawrence Berkeley National Laboratory under Contract DE-AC02-05CH11231.

Dr. Vladimir Mozin is a staff scientist at the Physics Division of the Lawrence Livermore National Laboratory. His present research interests revolve around developing computational and experimental methods to investigate non-destructive assay techniques for nuclear safeguards applications. He was previously employed as a radiochemical engineer at a spent nuclear fuel reprocessing facility. He received a Ph.D. in nuclear engineering at the University of California at Berkeley, and his M.S. in radioactive isotopes chemistry at the Moscow Institute of Physics and Engineering.

Dr. Luke Campbell is a staff scientist at the Radiation Detection and Nuclear Sciences division of the Pacific Northwest National Laboratory. His research includes novel radiation sources for active interrogation, delayed gamma assay methods for safeguards, and fundamental mechanisms of energy transport in radiation detector materials. He has a Ph.D. in physics from the University of Washington, and a B.S. in physics from the University of California, Davis

Dr. Alan W. Hunt is the deputy director of the Idaho Accelerator Center (IAC) at Idaho State University (ISU). In addition, he is an associate professor of physics within the department of physics. One of his primary research focuses is on active interrogation techniques for the detection, identification and quantification of fissile/fissionable materials. This includes extensive experimental work on the utilization of delayed gamma rays for fissile material accountancy applications.

Dr. Bernhard Ludewigt is a staff physicist at the Accelerator & Fusion Research Division of the Lawrence Berkeley National Laboratory. His research interests and scientific work include active interrogation methods for nuclear safeguards and homeland security applications, development of neutron and gamma sources, advanced radiation detectors, and medical applications of particle accelerators. He received a Ph.D. in nuclear physics at the University of Münster, Germany.

References

1. Humphrey, M. A., S. J. Tobin, and K. D. Veal. 2012. The Next Generation Safeguards Initiative's Spent Fuel Nondestructive Assay Project. *Journal of Nuclear Materials Management,* Vol. 40, No. 3.
2. Rennhofer H., 2010. Detection of SNM by delayed gamma rays from induced fission. *Nuclear Instruments and Methods A,* 317.
3. Saurel, N., and J. M. Capdevila. 2005. Experimental and simulated assay of actinides in a real waste package, *Nuclear Instruments and Methods in Physics Research A,* 550.
4. Gmar, M., and F. Jeanneau. 2005. Assessment of actinide mass embedded in large concrete waste packages by photon interrogation and photofission, *Applied Radiation and Isotopes*, 63.
5. Norman, E. B., Prussin, S. G., et al. 2004. Signatures of fissile materials: high-energy g-rays following fission, *Nuclear Instruments and Methods in Physics Research* A, 521.
6. Mantel, M., Gilat, J., and Amiel, S. 1969. Isotopic analysis of uranium by neutron activation and high resolution gamma ray spectrometry, *Journal of Radioanalytical and Nuclear Chemistry,* Vol. 2.
7. Beddingfeld, D. H., and F. E. Cecil. 1998. Identification of fissile materials from fission product gamma-ray spectra, *Nuclear Instruments and Methods in Physics Research A,* 417.
8. Marrs, R. E., Norman, E. B., et al. 2008. Fission-product gamma-ray line pairs sensitive to fissile material and neutron energy, *Nuclear Instruments and Methods in Physics Research A,* 592.
9. Krohnert, H. 2010. Freshly induced short-lived gamma-ray activity as a measure of fission rates in lightly re-irradiated spent fuel, *Nuclear Instruments and Methods in Physics Research A,* 624.
10. Mozin, V., S. J. Tobin, A. W. Hunt, J. Vujic. 2010. Delayed Gamma Technique for Fissile Material Assay, *Proceedings of the Institute of Nuclear Materials Management 51st Annual Meeting.*
11. Mozin, V., S. J. Tobin, B. Ludewigt, A. W. Hunt, J. Vujic. 2011. Delayed Gamma Assay for Spent Nuclear Fuel Safeguards, *Proceedings of the Institute of Nuclear Materials Management 52nd Annual Meeting.*
12. Campbell, L. W., L. E. Smith, and A. C. Misner. 2011. High-Energy Delayed Gamma Spectroscopy for Spent Nuclear Fuel Assay. *IEEE Transactions in Nuclear Science,* Vol. 58 231.

13. Campbell, L. W., L. E. Smith, A. C. Misner, and J. J. Ressler. 2009. High-Energy Delayed Gamma Spectroscopy for Spent Nuclear Fuel Assay, *Proceedings of the 50th Annual Meeting of the Institute of Nuclear Materials Management.*
14. Campbell, L. W., and L. E. Smith. 2010. Progress On High Energy Delayed Gamma Spectroscopy for Direct Assay of Pu in Spent Fuel, *Proceedings of the 51st Annual Meeting of the Institute of Nuclear Materials Management.*
15. Mozin, V., and S. J. Tobin. 2010. DGSDEF: Discrete gamma-ray source DEFinition code. *Los Alamos National Laboratory.* LA-CC-10-083.
16. Chadwick, M. B., P. Oblozinsky, and M. Herman. 2006. ENDF/B-VII.0: Next generation evaluated nuclear data library for nuclear science and technology. *Nuclear Data Sheets,* Vol. 107.
17. England, T. R., 1994. Fission Product Yield Evaluation for the U.S.A. Evaluated Nuclear Data Files. *Los Alamos National Laboratory Report,* LA-UR-94-3318.
18. Koning, A., R. Forrest, M. Kellett, R. Mills, R., H. Henriksson, and Y. Rugama. 2006. The JEFF-3.1 Nuclear Data Library. *JEFF Report 21*,OECD/NEA, France.
19. Mozin, V., and S. J. Tobin. 2010. Delayed Gamma-Ray Assay for Spent Nuclear Fuel Safeguards. *Los Alamos National Laboratory Report,* LA-UR 11-00261.
20. Galloway, J. D., H. R. Trellue, M. L. Fensin, and B. L. Broadhead. 2012. Design and Description of the NGSI Spent Fuel Library with an Emphasis on Passive Gamma Signal, *Journal of Nuclear Materials Management,* Vol. 40, No. 3.
21. Marquardt, D. 1963. An Algorithm for Least-Squares Estimation of Nonlinear Parameters. *SIAM Journal on Applied Mathematics* 11 (2). 431–441.
22. Oak Ridge National Laboratory. 2008. ORIGEN-2, Isotope Generation and Depletion Code, Oak Ridge, Tennessee.
23. Agostinelli, S., 2003. GEANT4 – A Simulation Toolkit, *Nuclear Instruments and Methods in Physics Research* A 506.
24. Lawrence Livermore National Laboratory. 2010. Physics Simulation Packages. Livermore, CA, http://nuclear.llnl.gov/simulation/main.html.
25. Brookhaven National Laboratory. 2010. Evaluated Nuclear Structure Data Files, maintained by National Nuclear Data Center, Upton, NY. http://www.nndc.bnl.gov/ensdf/.
26. Brookhaven National Laboratory. 2009. Nuclear wallet cards, maintained by National Nuclear Data Center. Upton, NY. http://www.nndc.bnl.gov/wallet/.
27. Ludewigt, B.A. 2010. Neutron Generators for Spent Fuel Assay. *Lawrence Berkeley National Laboratory Report,* LBNL-4426E.

Nuclear Safeguards ^{3}He Replacement Requirements

Louise G. Evans, Daniela Henzlova, Howard O. Menlove, Martyn T. Swinhoe, Stephen Croft, and Johnna B. Marlow
Los Alamos National Laboratory, Los Alamos, New Mexico USA

Robert D. McElroy
Oak Ridge National Laboratory, Oak Ridge, Tennessee USA

Abstract

One pressing research and development challenge currently facing the nuclear safeguards community is finding an alternative to ^{3}He gas for neutron detection. The high demand for ^{3}He gas for several scientific and global security applications has exceeded the gas supply.[1] This has resulted in the depletion of ^{3}He stockpiles and consequent shortfall in the availability of ^{3}He for conventional neutron detection. As part of finding a viable ^{3}He replacement neutron detection technology for safeguards use, performance requirements specific to safeguards applications must be defined. This article discusses the main detector performance parameters that form nuclear safeguards ^{3}He replacement requirements and provides recommended values for these parameters based on experience with traditional safeguards neutron coincidence counting applications. A ^{3}He replacement detector test program has been established at Los Alamos National Laboratory (LANL)[2] for the evaluation of ^{3}He alternative neutron detection technologies against safeguards-specific performance parameters. Here, the unique features of the LANL test program are also highlighted.

Introduction

Why are Safeguards-specific Alternatives to ^{3}He for Neutron Detection Being Pursued?

For more than four decades, neutron detection has played a fundamental role in the safeguarding and control of special nuclear materials (SNM) at nuclear fuel cycle facilities, which include: Defense production facilities, fuel fabrication plants, bulk plutonium handling facilities, and storage sites worldwide.[3] A move towards a nuclear renaissance and ongoing renewal of nuclear fuel cycle infrastructure, along with the consolidation of facilities in weapons programs, has resulted in the construction and planning of new nuclear material processing facilities. Each of these facilities requires implementation of a comprehensive safeguards program, in which neutron detection technologies are an essential element. From a technical standpoint, neutron measurements for safeguards applications have requirements that are unique to the quantitative assay of SNM. Neutron coincidence counting by shift register electronics is the passive neutron assay technique most widely used by the International Atomic Energy Agency (IAEA) inspectorate and thus will be the focus here. Neutron coincidence counting and the more demanding neutron multiplicity counting technique both measure correlated neutron distributions emitted from spontaneous and/or induced fission events.[4] The real coincidence (doubles) neutron counting rate requires the detection of a pair of neutrons correlated from a single fission event, whereas multiplicity counting requires the detection of three or more neutrons correlated from a single fission event. The doubles neutron counting rate is proportional to the square of the neutron detection efficiency and the triples neutron counting rate is proportional to the third power of the neutron detection efficiency. High efficiency systems are thus needed to attain useable counting precision in the correlated neutron counting rates. ^{3}He gas-filled proportional counters have therefore long been the cornerstone of safeguards neutron detection system designs due to the high neutron capture cross-section of ^{3}He (5,330 barns at thermal energy); permitting compact neutron counter design. Due to the current worldwide ^{3}He shortage, ^{3}He may no longer be the future workhorse detector material for nuclear safeguards. To continue to develop and deploy safeguards neutron detection systems, a viable, near-term, safeguards-specific alternative to ^{3}He-based measurement technology must be found. Any ^{3}He replacement technology must meet not only the requirement of high efficiency, but also other safeguards-specific requirements outlined here.

How are Safeguards Applications Distinct from Security Applications from a Neutron Detection Standpoint?

The current worldwide shortage of ^{3}He has resulted in a resurgence of research and development programs dedicated to finding an alternative neutron detection technology to ^{3}He. Several such programs have evaluated neutron detection systems targeted to specific application areas including, but not limited to,[5] Homeland security radiation portal monitoring (RPM).[6] However, the technology performance requirements for security neutron detection are distinct from performance requirements for safeguards correlated neutron detection. Neutron detection systems deployed for homeland and international security applications include: RPM, cargo monitors, body monitors, and handheld devices. These systems tend to provide relatively low neutron detection efficiencies due to their low effective neutron detection efficiency per unit volume of moderator (e.g., RPM) or small

Table 1. General and technical safeguards ^{3}He replacement requirements used to form technology evaluation criteria

Detector Performance Parameter Requirements	In-Plant Stability and Operational Requirements	Cost Requirements
• Neutron detection efficiency (ε) • Die-away time (τ) • Coincidence figure of merit (FOM) for doubles counting ($\varepsilon 2/\tau$) • Gamma-ray discrimination • Dead time (count rate capability)	• Stability (long-term and temperature) • Physical size of detector • Scalability • Sensitivity (RF and microphonics) • Safety • Reliability and maintenance • Component reproducibility • Infrastructure • Complexity of operation	• Affordability • Life cycle costs (cradle-to-grave)

physical size (e.g., handheld monitors). Safeguards neutron detection systems and portable applications require high neutron detection efficiency for coincidence counting and, at the same time, have a compact design for portability and to meet plant weight and size constraints. RPM neutron detection systems can have a larger volume since they do not need to meet the requirements of installation or portable operation within a nuclear plant. Security detection systems also require speedy detection. This requirement, combined with their low neutron detection efficiency, means that security detection systems typically must make decisions using total neutron counting rather than neutron coincidence counting. In security applications, all neutrons are considered indicative of nuclear material and temporal correlations are not recorded. Conversely, safeguards coincidence counting uses temporal correlations to distinguish fission neutrons from other sources and thus allow quantitative mass assays to be made. In addition to the requirement for high neutron efficiency, safeguards ^{3}He replacement requirements include other parameters specific to coincidence counting applications such as short neutron die-away time, which will be explained here. A ^{3}He replacement technology specific to the needs of safeguards applications is therefore required, distinct from security requirements. A review of the main safeguards ^{3}He replacement requirements is presented below.

General and Technical ^{3}He Replacement Requirements for Nuclear Safeguards Applications

The general and technical ^{3}He replacement requirements for nuclear safeguards applications can be grouped in to three broad categories: Detector performance parameter requirements, in-plant stability and operational requirements, and cost requirements. The evaluation of the parameters listed in Table 1 is essential for the acceptance of any potential safeguards ^{3}He replacement technology. A detector-level evaluation should address fundamental detector performance parameters and in-plant stability requirements. Operational and cost requirements form an integral part of any system-level evaluation. The latter two requirements are interlinked in the sense that the operational requirements such as maintenance and the detection system footprint also need to be factored in to the life cycle costs.

The selection of these parameters to form the key nuclear safeguards ^{3}He replacement requirements is explained below and can be justified by several safeguards motivations:

Neutron Detection Efficiency

The neutron detection efficiency is the fraction of neutrons detected of those emitted from an item that are incident on the detector face. High neutron detection efficiency is one of the two most important detector performance parameters for safeguards neutron measurements (along with short die-away time). Safeguards neutron measurements of SNM are based on the quantitative assay techniques of neutron coincidence counting (doubles) and neutron multiplicity (triples) counting.[4] These techniques can be applied using both passive and active modes; in other words, with and without a neutron interrogation source such as AmLi. As discussed, the real coincidence (doubles) neutron counting rate is proportional to the square of the neutron detection efficiency and the triples neutron counting rate is proportional to the third power of the neutron detection efficiency. High efficiency systems are thus needed to attain useable counting precision in the correlated neutron counting rates. One requirement of any ^{3}He replacement technology for safeguards applications is that the neutron detection efficiency is high and therefore similar to the ^{3}He neutron detection efficiency when configured in the expected measurement arrangement. The efficiency response of a safeguards replacement neutron detection system based on a ^{3}He replacement detector technology should also be spatially uniform and relatively insensitive to neutron energy. Energy sensitivity is a function of the detector system design and is dominated by the moderator configuration. The response of a safeguards replacement neutron detection system should be independent of the sample shape and container. In other words, scattered neutrons

should not change the counting rate response. A flat efficiency response better fits the applied theoretical Point Model[4] used to relate the detected neutron count rates to the assay mass. It also reduces the systematic uncertainty caused by the matrix material surrounding an assay item.

Potential detection technologies for ^{3}He replacement will likely differ in the amount and configuration of neutron moderator material (e.g., high density polyethylene, HDPE) used in both the detector vendor design and incorporated within the final detection system design. For testing of a technology at the detector module level, the evaluated detector type should be configured in a fashion that allows a reasonable extrapolation of the performance of a module to a full measurement system design; recognizing that the additional components of the full system (e.g., reflective end plugs) will impact the neutron detection efficiency. For traditional safeguards passive neutron detection in the thermal mode, an optimum moderator thickness should be determined for each evaluated detector for ^{240}Pu fission neutron spectra. However, ^{3}He replacement technologies based on fast neutron detection will not require this moderator optimization. Potential ^{3}He replacement technologies will likely also differ in the detector packaging and electronics configuration (i.e., internal or external electronics). When comparing the neutron detection efficiency between several potential ^{3}He replacement technologies as part of a test program, these differences in geometry need to be taken in to account to ensure a fair comparison between technologies. Two types of neutron detection efficiency therefore need to be defined—*intrinsic* neutron detection efficiency and *effective* neutron detection efficiency. The intrinsic neutron detection efficiency is defined per unit area of the front face of the detection system (active zone including detectors and any moderating materials). The effective neutron detection efficiency is defined per unit area of the total neutron detection system (including signal processing electronics and packaging). In addition, this is a useful metric for the direct comparison of the performance of a technology at the detector module level with an equivalent ^{3}He-based detector module, which will be described.

Die-Away Time

The neutron die-away time is the average time for a neutron to down-scatter to thermal energies and be captured in the detector, leak out from the detector, or be parasitically captured by the hydrogen in the moderator. The die-away time is therefore determined by the size, shape, composition, and efficiency of a safeguards neutron counting system.[7] For example, adding polyethylene to a neutron detection system to increase the neutron detection efficiency may also lengthen the die-away time. Conversely, the presence of thermal neutron absorbers such as cadmium (Cd) sleeves surrounding the individual neutron detectors may serve to shorten the die-away time, but in turn may be detrimental to neutron detection efficiency.[8] The interplay between these two parameters is factored in to the figure of merit discussed in the next section. The efficiency and die-away time can be optimized based on the requirements of a given application, e.g., whether short acquisition time or fast timing are an essential capability. Short die-away time is one of the two most important detector performance parameters for safeguards neutron measurements (along with high neutron detection efficiency). The technique of neutron coincidence counting employs shift register electronics to detect correlated pairs of neutrons (i.e., a trigger neutron is detected and opens a time window. A neutron correlated in time to the trigger is detected within the time window following the trigger, to form a correlated pair). The optimum coincidence gate width is set based on minimizing the uncertainty in the doubles counting rate. A short die-away time facilitates operation at short coincidence gate widths; minimizing the contribution of accidental doubles (chance or pileup coincidences) to the doubles rate uncertainty. This is due to the effect that the accidental coincidence rate increases in direct proportion to the coincidence gate width as shown in Equation 1.

$$A = S^2 \cdot G \qquad (1)$$

where, A is the accidental coincidence rate, S is the singles counting rate and G is the coincidence gate width governed by the temporal behavior of the neutron counting system and thus by the neutron die-away time. The optimum coincidence gate width is approximately 25 percent larger than the die-away time of a typical safeguards neutron counting system. A viable goal for any safeguards ^{3}He replacement technology is to achieve a die-away time of less than 100 μs, to be comparable with existing safeguards neutron counting systems. In turn, this would satisfy the above requirement of minimizing the contribution of accidental doubles to the doubles rate uncertainty. The exact required value is driven by the application since it also depends on the target precision and the available assay time. For example, neutron counting systems used for nuclear waste assay can operate with a longer coincidence gate width, and therefore tolerate a longer die-away time, because the neutron counting rates are lower than traditional safeguards counting and the contribution of accidental coincidences is minimal.

Coincidence Figure of Merit (FOM)

A key component to the evaluation of any ^{3}He replacement technology is defining a quantitative comparison metric or figure of merit. The coincidence figure of merit (FOM) for doubles counting is an important parameter for evaluating detector comparative performance for safeguards applications. The coincidence FOM was chosen as the comparison metric, as opposed to defining a multiplicity FOM, because coincidence counting is the passive neutron assay technique most widely used by the IAEA inspectorate.[2] However, the same FOM can also be applied to multiplicity counting for a system exhibiting single exponential die-away behavior. The basis of this FOM is the practical requirement to

Table 2. Measured neutron detection efficiency and calculated die-away time values for currently fielded ^{3}He-based safeguards neutron counting systems

System Description	Neutron Detection Efficiency (^{252}Cf neutron energy spectrum)	Die-Away Time (μs)	FOM
UNCL – Uranium Neutron Coincidence Collar (Boiling Water Reactor Fuel Measurements)	15.3percent	53	442
HLNCC – High Level Neutron Coincidence Counter	17 percent	43	672
AWCC – Active Well Coincidence Counter	33 percent	51	2135
ENMC – Epithermal Neutron Multiplicity Counter	65 percent	21.8	19381

minimize the statistical uncertainty in the doubles counting rate. The FOM is therefore derived from the relative uncertainty in the doubles counting rate, given by the Poisson approximation in Equation 2.

$$\frac{\sigma D}{D} = \frac{\sqrt{\left((D+A)+A\right)\cdot t}}{D\cdot t} \approx \frac{1}{D}\cdot\sqrt{\frac{2A}{t}} \qquad (2)$$

(For high counting rates, A >> D)

where, D is the doubles counting rate and A is the accidental coincidence rate, given by Equation 3.[7]

$$A = S^2\cdot G \approx S^2\cdot 1.257\tau \qquad (3)$$

where, S is the singles counting rate, G is the optimum coincidence gate width governed by the temporal behavior of the neutron counting system, and τ is the neutron die-away time.

$$\therefore \frac{\sigma D}{D} \approx \frac{1}{D}\sqrt{\frac{2\left(S^2\cdot 1.2\tau\right)}{t}} \approx S\frac{\sqrt{\tau}}{D} \approx \varepsilon\frac{\sqrt{\tau}}{\varepsilon^2} \approx \frac{\sqrt{\tau}}{\varepsilon} \qquad (4)$$

(Functional approximation only)

It is favorable to minimize the uncertainty in the doubles counting rate and therefore the inverse of this relationship should be maximized. Based on this figure of merit, given in Equation 5, optimal system performance requires high efficiency and a short die-away time.

$$FOM = \frac{\varepsilon^2}{\tau} \qquad (5)$$

Table 2 provides measured neutron detection efficiency and die-away time values, calculated from measured doubles rates,[7] of four LANL developed safeguards neutron counting systems[9,10] to provide an illustration of typical ^{3}He-based system performance.

Gamma-Ray Discrimination

Safeguards detection systems must routinely operate to withstand typical gamma-ray dose rate levels of up to 1 R/h on the detector face. This dose rate value is defined based on the need to assay bulk plutonium samples containing ^{241}Am.[11] For some safeguards applications, such as the assay of spent nuclear fuel, systems are expected to operate to withstand gamma-ray dose rate levels of up to 100 to 1,000 R/h, which translates to an operational level of 10 R/h with appropriate detector shielding for ^{3}He-based systems. Safeguards measurement scenarios are unlike RPM measurement scenarios where the typical gamma-ray exposure rate from the item of interest is near background and the maximum tolerable exposure rate is 10 mR/h based on standard medical isotope.[12] When performing safeguards neutron measurements, the gamma-ray counting rate should be negligible with respect to the neutron counting rate and thus should not impact the detection efficiency. A metric known as GARRn, the Gamma Absolute Rejection Ratio in the presence of neutrons can be used to quantify the gamma-ray contribution to the detected count rate in the presence of a neutron source. Originally, this metric was introduced to define the gamma sensitivity of neutron detectors fielded for Homeland security applications.[12] A precision of 1 percent in the singles neutron counting rate is a typical upper limit requirement in order to perform reliable safeguards neutron measurements. A target GARRn value for safeguards can therefore be defined based on this requirement. For routine system operation in the presence of gamma-ray interference, the contribution of gamma-rays to the detected counting rate should not exceed 0.3 percent. This corresponds to a GARRn value of 1.003.

Dead Time (Count Rate Capability)

Dead time is the time during which the detection system is unable to register detected pulses, which are consequently not counted and therefore do not contribute to the neutron counting rates. Dead time effects in ^{3}He-based safeguards neutron counting systems (combination of detector banks and electronics) are a complex interplay between the detector pulses and the action of the signal processing electronics.[13] The signal processing electronics contributes to the system dead time by modification of the pulse shape in the shaping amplifier and generation of the user end digital signal in the discriminator. In general, the system dead time is always determined by the dominant time constant of the whole system. The detector pulse shape and timing characteristics of the chosen signal processing electronics will affect the system dead time and dictate whether the system dead time is dominated by the detector pulse shape or timing of the shaping circuit. A safeguards neutron counting system with multiple proportional tubes should be able to attain neutron counting rates between 1-5 MHz with accurate dead time corrections based on traditional safeguards counting applications. However, higher neutron counting rates of up to 10 MHz may be encountered during the assay of spent nuclear fuel. This means that the pulse processing requirements of the ^{3}He replacement technology should include considerations for these high neutron counting rates if the neutron counting system is ultimately being applied to the measurement of spent nuclear fuel. Larger ^{3}He-based safeguards neutron detection systems are usually designed with groups of 10 to 100 ^{3}He tubes of adjustable diameter and length. This provides great flexibility in the design of the detector size and shape. Safeguards neutron coincidence counting systems typically use 1" diameter ^{3}He tubes to avoid the longer gas ionization collection times and resulting dead time from 2" diameter ^{3}He tubes. Note that the amplifier module (including pre-amplifier and pulse height discriminator) used in combination with the ^{3}He replacement technology can impact the system dead time and therefore the counting rate capability of the entire neutron detection system. The dead time impact is captured to an extent in the FOM because dead time reduces the detected neutron counting rates by reducing the neutron detection efficiency. A poor dead time correction will impact the system performance by yielding poor accuracy.

Stability (Long-term and Temperature)

A stable neutron detection system is required to obtain reliable counting rates from that system. The stable operation of a neutron detection system is essential when instruments must operate continuously in an unattended mode (i.e., unattended monitoring systems). Therefore a neutron detection system must be stable over long periods of time and be insensitive to fluctuations in environmental conditions, such as temperature and humidity, within the measurement area. ^{3}He systems have been demonstrated to have inherent long-term stability of $\pm$ 0.002percent in the singles neutron counting rate under constant environmental conditions over the lifetime of the system.[14] This excellent stability value can be partly attributed to characteristics of the high voltage (HV) response of ^{3}He. In other words, the singles neutron counting rate as a function of HV reaches a plateau region (~1-2 percent change/ 100 V) that continues over a long range of HV (several 100 V).[6] Selecting an operating HV in this plateau region allows stable operation of the neutron detection system. This means that slight drifts in amplifier gain or discriminator threshold level do not lead to a significant change in the neutron detection efficiency (neutron counting rate). Close attention must be paid to the response of the ^{3}He replacement technology to these environmental conditions. Care must be exercised for proportional tube based solutions, if the ^{3}He alternative does not exhibit true plateau behavior, then any instability (temperature related or otherwise) may be amplified. The required long-term stability of any ^{3}He replacement technology will be specific to the safeguards measurement application. Typical safeguards applications require measurement precision in the doubles neutron counting rate between 0.25 and 2 percent. Thus precision of the order of 0.125 to 1 percent in the singles neutron counting rate is typically required in order to perform reliable safeguards measurements. A long-term stability of less than 1 percent would therefore be a valid requirement for any ^{3}He replacement technology that will be used to perform routine safeguards measurements. Small sample measurements may require higher precision and thus better long-term stability. For the majority of safeguards applications, normalization measurements are performed as a function of time at regular time intervals using a calibrated reference source. However, recalibration can only be performed for small steady-state changes. In other words, irregular instabilities cannot be mitigated with this quality control activity.

The temperature stability of ^{3}He-based systems has been found to correspond to a range of $\pm$0.06 percent/ °C in the singles neutron counting rate, depending on the system design.[15] The temperature stability of a neutron counting system is a complex function of several effects; the dominant of which is the change in the neutron absorption cross-section of the detection medium. Heating of the neutron detection system causes the velocity of neutrons in the system to increase as they attain thermal equilibrium with the system. The neutron absorption cross-section of the detection medium is proportional to 1/v, where v is the neutron velocity. This increase in neutron velocity with temperature therefore leads to a decrease in the interaction probability of neutron absorption by approximately 0.15 percent/°C. ^{3}He-based measurement systems exhibit excellent temperature stability despite the cross-section effect, because the neutron cross-section effect is largely mitigated by other temperature dependent effects (e.g., amplifier gain). This may not be the case for detection medium alternatives to ^{3}He. It is therefore anticipated that temperature stability similar to the 0.06 percent/°C observed in ^{3}He is an important requirement for any ^{3}He replacement technology because this enables high

precision in the measured neutron counting rates. However, a range exceeding this target value could be tolerated in a controlled measurement environment and in the case where routine calibration measurements are performed in order to correct for temperature-dependent biases. The required uncertainty limit will be driven by the measurement application, which will in turn dictate a temperature stability limit that is tolerable. Other temperature dependent effects include: Electronics effects such as changes in amplifier gain and discriminator threshold level setting; expansion of the polyethylene moderator leading to a decrease in moderator density and change in the geometry of the detection system (minimized in a full well counter or close geometry); and accelerated release of any gas impurity content in to the detection gas volume. The magnitude of these effects and their impact on the response of a neutron counting system will be the subject of a future publication on the LANL test program findings.

Physical Size

The high efficiency for measuring neutrons from the sample normally has to be obtained in a relatively small foot print to accommodate cost and facility space requirements. The high efficiency per unit detector volume of the ^{3}He detector assembly permits compact safeguards neutron counter designs. ^{3}He replacement technologies should therefore also permit reasonably compact designs and satisfy facility space requirements. Ease of sample loading within the counter cavity also has to be taken in to account when considering the physical size of a ^{3}He replacement safeguards neutron counter design.

Scalability

Many safeguards neutron detection systems are designed in a well counter configuration, where the detectors completely surround the sample well and therefore surround the assay item contained within the well. This provides high efficiency and ensures a constant efficiency profile, independent of the sample shape and energy distribution where possible. Any ^{3}He replacement technology should therefore be scalable to a full size safeguards system build. The well or cavity volume will be determined by the measurement application and therefore by the assay sample container volume.

Sensitivity to Non-radiological Interferences

Any ^{3}He replacement technology must be insensitive to background sources of radio-frequency (RF) noise or micro-phonic vibrations of the type encountered in an operating nuclear facility (e.g., nearby motors and switches).

Safety

Uranium and plutonium processing facilities, in which safeguards neutron detection systems must operate, have unique criticality, fire, seismic qualification, and other safety requirements for installed systems. Any ^{3}He replacement technology must be able to meet these requirements. The detection alternatives of BF_3 and liquid scintillators are considered to be hazardous materials; the acceptance of which will be facility dependent. If liquid-based detection technology is employed for safeguards neutron detection systems, additional criticality concerns will need to be addressed via administrative and engineering controls. The ideal ^{3}He replacement detection technology will be based on low hazard materials. A safety analysis will not only need to take in to account the detection material, but also associated requirements for the measurement system, which include: the materials used for neutron moderation and shielding, together with the supporting framework and electronics.

Reliability and Maintenance

The installation of safeguards neutron counting systems within active processing facilities can result in limited access to the systems. Equipment operators or inspectors have only occasional access to the systems. Furthermore, neutron counting systems used in unattended and remote monitoring applications may have to operate without intervention on time frames of approximately six months to two years.[16] Therefore maintenance activities must occur infrequently, at time intervals greater than the typical inspection cycle. A system-level evaluation of any ^{3}He replacement technology must consider the mean time between failures (MTBF) of the component neutron detectors and associated electronics. Traditional ^{3}He based systems have a long history of deployment for safeguards applications and are therefore known to have a MTBF much longer than the expected operating lifetime of a typical nuclear facility. New ^{3}He replacement technologies are not yet established for in-plant use and therefore due consideration should be given to incorporation of state of health monitoring at the detector level. On a practical level, routine maintenance should not require complete disassembly of the neutron detection system to replace a simple component.

Component Reproducibility

Replacement of components for safeguards neutron counting systems in the field can become complicated and time consuming when the detector assemblies are not identical. If the installation of a spare component results in a change in neutron detection efficiency, recalibration of the entire counting system may be required. To avoid this costly recalibration activity, any ^{3}He replacement technology should be based on reproducible detector modules.

Infrastructure

Any ^{3}He replacement neutron detection technology should be applicable to a significant portion of the safeguards application area to minimize associated development, training (of operators and measurement experts) and maintenance costs. ^{3}He gas-filled proportional tubes have been applied successfully to a variety of neutron application areas. As a result, the wide range of neutron

detection systems and application areas could be supported with a limited infrastructure. That is, the same basic physics, electronics, application software, operational protocols, and maintenance procedures should be able to be used across a large installed base of neutron detection systems.

Complexity of Operation

A safeguards replacement neutron detection system based on a ^{3}He replacement detector technology should not have a high level of complexity of operation or the ability to produce results. The IAEA has rejected instruments in the past as being too *complicated*.

Affordability

The affordability of a safeguards assay system must be considered in light of alternate technologies and the cost of not performing the measurement at all. For the near term, limited quantities of ^{3}He are available for use in safeguards systems.

Life Cycle Costs (Cradle-to-Grave)

The cost of a full scale neutron well counter, based on a ^{3}He alternative neutron detection technology, cannot be priced solely on the cost of the individual neutron detectors. Other cost considerations include: the system level physics design using the replacement technologies; calibration; testing; required spare components; training; installation; procedures for operation; maintenance and recalibration; decommissioning; electronics; algorithm development; and software development.

Requirements Based Testing: The Los Alamos National Laboratory Test Program

As part of finding a viable ^{3}He alternative detection technology for nuclear safeguards applications, and to form the basis for comparison of the outlined requirements, an integrated detector test and evaluation program has been established at LANL.[2,17,18,19] The test program provides detailed procedures to perform experimental characterization of ^{3}He alternative neutron detectors. The program includes a Monte Carlo modeling component in order to compare the measured results with a ^{3}He-based reference system. The goals of this safeguards-specific test program are to:

- Evaluate neutron detectors for potential replacement of ^{3}He tubes;
- Emphasize detector performance parameters that are important to nuclear safeguards applications;
- Provide qualitative and quantitative guidelines for the required performance of ^{3}He alternative neutron detection technology based on experience with traditional safeguards neutron coincidence counting applications;
- Develop test program criteria based on performance guidelines;
- Develop detailed experimental procedures for the testing of ^{3}He alternative neutron detection technologies against test program criteria;
- Consider the detector properties that would allow commercial production for safeguards scale assay systems;
- Evaluate the comparative performance of ^{3}He alternative detection technologies and a Monte Carlo based ^{3}He reference system of a similar size; and
- Later perform an extended system-level evaluation as part of the future build of a full ^{3}He replacement safeguards neutron counter.

LANL Developed Comparison Method with an Equivalent ^{3}He System: How Does the Test Program Compare ^{3}He Alternatives with ^{3}He?

^{3}He alternative detection technologies that are being evaluated for safeguards ^{3}He replacement within the LANL test program have different shapes and dimensions that were determined by the individual detector vendors. A novel Monte Carlo normalization method has been developed to compare any geometry or type of ^{3}He alternative based neutron detection system with an equivalent or *reference* ^{3}He-based system in a valid way. This is a novel method for combining both empirical results and simulation results for a detector inter-comparison.

For the inter-comparison method, the Monte Carlo N-Particle Extended (MCNPX) radiation transport code[20] is used to model a *reference* ^{3}He-based system corresponding to the external dimensions of each of the evaluated ^{3}He alternative based detection systems in their safeguards detector module configuration (i.e., embedded in an optimum moderator thickness). The *reference* ^{3}He-based system model has design parameters determined by a typical safeguards neutron detector slab. That is, 4 atm, 1" diameter ^{3}He gas-filled proportional tubes with a 2" pitch embedded in a HDPE moderator block with front-back thickness of 4-5".[6] The distance of the ^{3}He tubes from the front face of the moderator should be optimized for a ^{240}Pu fission neutron spectrum using MCNPX. The modeled ^{3}He reference system is then used to calculate the corresponding intrinsic neutron detection efficiency, die-away time and coincidence FOM. The normalization ratio can then be calculated for these parameters to compare the measured response from each ^{3}He alternative technology based system with the Monte Carlo calculated response for its equivalent ^{3}He-based reference system. This enables a coincidence FOM for each ^{3}He alternative technology based system to be compared directly with the equivalent coincidence FOM for ^{3}He.

Reference calculations were validated by comparison with measurements performed using an existing *benchmark* ^{3}He-based neutron slab detector. The ^{3}He *benchmark* slab formed part of a fuel collar and consists of six 6 atm, 1" diameter ^{3}He gas-filled proportional tubes. Successful results of this validation were published by Henzlova, *et al.*[19]

Table 3. Summary of the nuclear safeguards ^{3}He replacement requirements used to form basis of the LANL test program measurements

Detector Performance or In-Plant Stability Parameter	Safeguards Requirement
Neutron detection efficiency (ε)	Spatially uniform Relatively insensitive to neutron energy when configured in a neutron detection system
Coincidence figure of merit (FOM) for doubles counting ($\varepsilon 2/\tau$)	$FOM_{replacement} \rightarrow$ FOM3He
Gamma-ray discrimination	Withstand gamma-ray dose rate of 1 R/h – 10 R/h on the detector face
Dead time (count rate capability)	1-5 MHz for traditional applications 10 MHz for spent nuclear fuel assay 0.2 MHz per amplifier
Long-term stability	+ 1 percent in the singles neutron counting rate
Temperature stability	0.15 percent/°C in the singles neutron counting rate
Humidity response	Pass – no change in singles neutron counting rate with a change in relative humidity
Scalability	Scalable to a full-size safeguards system build
Physical Size	Permit a compact system design with a small foot print Meet FOM requirements within size constraints
Sensitivity	Pass – no change in singles neutron counting rate in the presence of micro-phonic vibrations or an RF source

Summary and Conclusions

An essential first step in the assessment of the suitability of any ^{3}He replacement neutron detection technology for nuclear safeguards applications is the characterization of its fundamental properties and detector performance parameters. This article presents a review of the key nuclear safeguards ^{3}He replacement requirements, which are distinct from nuclear security requirements, and provides guidelines for the required performance of ^{3}He alternative neutron detection technology based on experience with safeguards neutron coincidence counting applications. Table 3 presents a summary of the safeguards-specific requirements that were used to form the basis of the LANL test program criteria for the evaluation of ^{3}He alternative neutron detection technologies. The LANL test program has also combined experimental results with simulation results to perform a novel direct comparison of the performance of ^{3}He alternative technologies with an equivalent ^{3}He neutron detection system. The result is a requirements based test program specific to neutron detection for nuclear safeguards applications, which is applicable to the evaluation of any proposed ^{3}He replacement technology

Acknowledgement

The authors would like to acknowledge support for this research provided by the U.S. Department of Energy National Nuclear Security Administration (DOE-NNSA), Office of Nonproliferation and International Security (NIS).

References

1. Kouzes, R. T. 2009. The ^{3}He Supply Problem, *PNNL-18388*.
2. Henzlova, D., L. G. Evans, H. O. Menlove, M. T. Swinhoe, and J. B. Marlow. 2011. Test Program to Compare Alternative Neutron Detectors for Potential ^{3}He Replacement for Nuclear Safeguards Applications, *LANL Technical Report*, LA-UR 11-00098.
3. Doyle, J. E. 2008. Nuclear Safeguards, Security, and Nonproliferation: Achieving Security with Technology and Policy, *Elsevier, Inc.*
4. Ensslin, N., W. C. Harker, M. S. Krick, D. G. Langner, M. M. Pickrell, and J. E. Stewart. 1998. Application Guide to Neutron Multiplicity Counting, *LANL Technical Manual*, LA-13422-M.
5. Zeitelhack, K. 2011. Status Report of the International Detector Initiative on Alternative Technologies to ^{3}He Detectors for Neutron Scattering Applications, *Proceedings of the ANIMMA 2nd International Conference.*
6. Van Ginhoven, R. M., R. T. Kouzes, and D. L. Stephens. 2009. Alternative Neutron Detector Technologies for Homeland Security, *PNNL-18471.*
7. Reilly, D., N. Ensslin, H. Smith, Jr., and S. Kreiner. 1991. Passive Nondestructive Assay of Nuclear Materials, NUREG/CR-5550, LA-UR-90-732.
8. Langner, D., M. S. Krick, N. Ensslin, G.E. Bosler, and N. Dytlewski. 1991. Neutron Multiplicity Counter Development, *Proceedings of the ESARDA 13th Annual Meeting.*
9. Croft, S., A. Favalli, M. T. Swinhoe, and C. D. Rael. 2011. State of the Art Monte Carlo Modeling of Active Collar Measurements and Comparison with Experiment, *Proceedings of the Institute of Nuclear Materials Management 52nd Annual Meeting.*

10. Stewart, J. E., H. O. Menlove, D. R. Mayo, W. H. Geist, L. A. Carrillo, and G. D. Herrera. 2000. The Epithermal Neutron Multiplicity Counter Design and Performance Manual: More Rapid Plutonium and Uranium Inventory Verifications by Factors of 5-20, *LANL Technical Manual*, LA-13743-M.
11. Menlove, H. O., R. J. Dickinson, I. Douglas, C. Orr, F. J. G. Rogers, G. Wells, R. Schenkel, G. Smith, A. Fattah, and A. Ramalho. 1987. Field Test and Calibration of Neutron Coincidence Counters for High-Mass Plutonium Samples, *LANL Technical Report*, LA-10815-MS.
12. Kouzes, R. T., J. R. Ely, A. T. Lintereur, and D. L. Stephens. 2009. Neutron Detector Gamma Insensitivity Criteria, *PNNL-18903*.
13. Iliev, M., K. Ianakiev, M. Newell, and D. Henzlova. 2011. Study of the Front End Electronics Contribution to the Dead Time in ^{3}He Proportional Counters, *Proceedings of the Institute of Nuclear Materials Management 52nd Annual Meeting*.
14. Henzlova, D., H. O. Menlove, M. T. Swinhoe, C. D. Rael, I. P. Martinez, and J. B. Marlow. 2010. Epithermal Neutron Multiplicity Counter (ENMC) Measurement Description and Results, LANL Technical Report, LA-UR 11-00094.
15. Menlove, H. O., D. Henzlova, and L. G. Evans. 2011. Temperature Stability Test Data for the AMPTEK A111 Amplifier Connected to GE-RS ^{3}He Tubes, *LANL Technical Report*, LA-UR 11-03853.
16. McElroy, R. D., B. M. Young, and S. Croft. 2011. Performance Considerations for Alternatives to ^{3}He-Based Neutron Counters for Safeguards Applications, *Proceedings of the Institute of Nuclear Materials Management 52nd Annual Meeting*.
17. Menlove, H. O., D. Henzlova, L. G. Evans, M. T. Swinhoe, and J. B. Marlow. 2011. ^{3}He Replacement for Nuclear Safeguards Applications – an Integrated Test Program to Compare Alternative Neutron Detectors, *Proceedings of the ESARDA 33rd Annual Meeting*.
18. Evans, L. G., D. Henzlova, H. O. Menlove, M. T. Swinhoe, C. D. Rael, I. P. Martinez, and J. B. Marlow. 2011. ^{3}He Replacement for Nuclear Safeguards Applications Part I: Test Program and Experimental Results, *Proceedings of the Institute of Nuclear Materials Management 52nd Annual Meeting*.
19. Henzlova, D., L. G. Evans, H. O. Menlove, M. T. Swinhoe, C. D. Rael, I. P. Martinez, and J. B. Marlow. 2011. ^{3}He Replacement for Nuclear Safeguards Applications Part II: Benchmarking and Simulation Results, *Proceedings of the Institute of Nuclear Materials Management 52nd Annual Meeting*.
20. Pelowitz, D. B. 2005. MCNPX User's Manual Version 2.5.0., *LANL Technical Manual*, LA-CP-05-0369.

Book Review

By Mark L. Maiello, Ph.D.

Fallout—The True Story of the CIA's Secret War on Nuclear Trafficking
Authors: *Catherine Collins and Douglas Frantz*
Free Press, New York, N.Y., 2011
ISBN 978-1-4391-8306-9

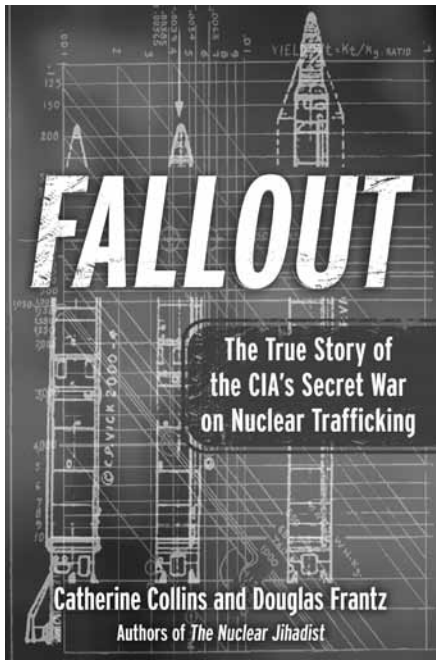

The story of the Abdul Qadeer Khan nuclear trafficking network still does not suffer from overexposure. Nor should it. For the scholar, student, and lay person, familiarity with the dangerous and frightening consequences of Khan's criminal activity is required to understand the current problems of nuclear proliferation. That the network was allowed to operate for many years due ultimately to the interests of governments, the missions and capabilities of intelligence and watchdog agencies, and the relations between a super power and an ally in the nonproliferation struggle is the scintillating story illuminated in *Fallout—The True Story of the CIA's Secret War on Nuclear Trafficking* by the wife and husband journalism team of Catherine Collins and Douglas Frantz. The latter was a member of *The New York Times* writing team that won the 2002 Pulitzer Prize for coverage of the aftermath of 9/11. The former holds credentials as a reporter and international correspondent with the *Chicago Tribune, Los Angeles Times* and *The New York Times.*

This is an intriguing account of a complicated story. One learns of the myriad and sometimes contradictory objectives that make surveillance and policing of nuclear trafficking the difficult task that it is. This is not the territory of the scientist or the policy maker. It is the land of intelligence gathering and the turf of politicians. The nonproliferation experts take a back seat to the police, spies and politicos when the stakes get this high.

The case against A. Q. Khan was painstakingly put together over the course of thirty years, a period the authors contend that was far too long for the network to be allowed to operate. In delaying the arrest of Khan, a web of proliferators spread weapons technology to states with motives unpalatable to the United States and put the world's most lethal technology on unprotected media for potential worldwide access. The delay is partly attributable to the Central Intelligence Agency and its desire to seek out and eventually destroy all aspects of the Khan network. But, political decisions by the U.S. government to monitor but not stop Khan's machinations in an effort to gain the cooperation of Pakistan against the U.S. enemies during the Carter, Regan, and the G. H. W. Bush administrations also contributed to the delay.

Other interesting themes abound in this book. Among the most useful for the non-proliferation expert is the discussion of the CIA's field operations. The CIA recruitment and subsequent protection of the Tinner family, Freiderich and his sons Urs and Marco, due to their association with Khan as purveyors of centrifuge technology among other restricted equipment, forms the basis for the subsequent shut down of Khan's activities, the US response to the parallel Swiss government investigation and later, to the International Atomic Energy Agency (IAEA) investigation. The CIA activities include illegal break-ins at Marco's Swiss home and office. Eventually, CIA operations including the protection of the Tinners as informers, culminates in an apparent subornation of Swiss sovereignty by the U.S. government. The break-ins revealed that sensitive centrifuge and even nuclear warhead designs were stored on unprotected computers. As the Khan network spread, the CIA enlisted experts at Los Alamos National Laboratory for the purpose of sabotaging vacuum pumps and centrifuges that were purchased by Iran and Libya through the Tinners for the sole purpose of slowing their weapons development. This plan, initially successful, ultimately failed in Iran as we all now know.

Of equal importance to the arms control professional are the interactions between the various governments involved including the Dutch who originally investigated Khan but were dissuaded by the U.S. from acting against him, the Pakistani government who harbored him, the Swiss who were concerned about the proliferation activities of their citizens, the Tinners, and the U.S., which pressured the Swiss into destroying the evidence against Kahn partly to fulfill the promise of protection made to Urs, Marco, and Freidrich. The description of the "strong-arming" employed to silence the Swiss government investigation of the Tinners involving Condoleezza Rice no less, is

fascinating. The authors also describe two encounters in which CIA Director George Tenet confronts then Pakistani President Perez Musharriff with the evidence against Kahn that results in the latter's house arrest and another between CIA deputy director Stephen Kappes and Moammar Kaddafi that finally convinces the Libyan dictator to renounce his nuclear ambitions.

Perhaps not as illuminating but just as relevant to nonproliferation specialists is the role of the IAEA in this affair. The revelations of Khan's activities, made clear to Mohammed ElBaradei and the IAEA through the U.S. government and Kaddafi's announcement, initially caught the agency unaware. Despite its later involvement, the affair reinforced what was already known: that sophisticated clandestine nuclear trafficking could evade IAEA scrutiny. No information was shared between the IAEA and U.S. or UK intelligence agencies further hamstringing the UN agency's ability.

As the story unfolds, the details concerning centrifuge manufacture, illegal container ship transport and communication between the proliferators is revealed. With apparently little difficulty from regulations or other local scrutiny, the manufacturing arm of Khan's network was initially set up in Dubai but moved to Malaysia where a more skilled work force could be found. "Inaccurate" labeling, invoicing, and middle men serve to transport by freighter five forty-foot long crates containing among other equipment centrifuges and associated electronics to Tripoli. Plans for a 1960s vintage Chinese nuclear warhead were later found that were also peddled to the Libyans by Khan.

In addition to Dubai, Malaysia, Libya and Iran there is an interesting connection with South Africa where a contracted operation by Tinner co-conspirators Gotthard Lerch and Gerhard Wisser was in operation to support the Libyan sale (both Lerch and Wisser were formerly involved in the defunct South African nuclear weapons program). Though Lerch was tipped off that the Americans were on to them, the group was unable to destroy all the incriminating equipment. Had they succeeded, they would have been able to resurface later untouched and resume operations—the great fear of the CIA and one important reason behind the prolonged life of Kahn's network. The evidence left behind raised new concerns about the timing of sales of a more advanced Pakistani centrifuge (the "P-2") to Iran and the speed with which Iran was developing its weapons capability.

Running parallel with the main story of tracking down and elucidating the mechanisms of the trafficking network are sub-stories with impact on the final cessation of Khan's activities. These included the fear at the CIA that the United States would appear to have assisted in the proliferation due to the long period of inaction before Khan was stopped, that Khan suspected a leak in his organization due the Libyan equipment seizure, that the data, blueprints and other information related to sensitive nuclear technology was unprotected for so long on computers owned by Khan, the Tinners and others, and that another national or sub-national buyer may have been sold nuclear technology and remains unidentified to this day (apparently, not all the Dubai equipment was found in Malaysia). In December 2010, the dogged pursuit of undestroyed evidence by independent Swiss lawyer Andreas Mueller facilitated the bringing of charges against the Tinners. If the case ever gets to trial, much of the information in this remarkable story including the CIA operations on foreign soil and the U.S. pressure put on the Swiss government to destroy evidence could be retold on a much more accessible stage.

This book is not sensationalistic nor is it written as a suspense thriller. And though some elements of suspense do make their way into the text, it is mainly due to the actual state of affairs the authors are describing. It is factually presented as befits the background of its newspaper-bred—not tabloid—investigative-reporter authors. A thirteen-page notes section useful for reference checks is also quite interesting to peruse. There is a ten-page index. The authors discuss just enough nuclear technology concerning centrifuges to make the actions of the conspirators clear. There is little hard science or engineering in the book.

This account is about the mechanics of nuclear subterfuge and espionage. If the reader is interested in the motivations of the conspirators, a search elsewhere is necessary. Little is mentioned of this issue in *Fallout*. Khan's motivation to develop an "Arab bomb" for Pakistan is mentioned as stemming ostensibly from his dislike of America's pro-Israeli stance. Other publications imply that the acquisition of money and fame were probably the overriding factors. The truth, for what it is worth, may never be fully known. The rationalization that money, albeit huge sums of it, is any compensation for proliferating the world's most lethal weapons—or at the least subverting the means to prevent their proliferation—is of course horribly wrong. But, the omission or discussion of this motive is somewhat unsatisfying. Ultimately, if no other sources are accessed, the reader of *Fallout* must conclude that a crime against human kind was committed because of politics. Presented more convincingly and more ominously is the conclusion that the consequences of this crime are yet to be fully realized.

Mark L. Maiello, Ph.D. is a health physicist with interests in radiological and nuclear security. His writing has appeared in these pages and other technical journals such as Health Physics and Health Physics News, where he is a contributing editor. He is co-editor of the book Radioactive Air Sampling Methods *(CRC Press, 2010) with Dr. Mark D. Hoover of NIOSH.*

Taking the Long View in a Time of Great Uncertainty

Looking Back at a Decade of Tumult—and Looking Forward to an Uncertain Future

By Jack Jekowski
Industry News Editor and Chair of the Strategic Planning Committee

A commonly accepted tenet among strategic planners is that you cannot do a good job of planning for the future if you don't have a good understanding of the past. In the second decade of the new millennium, it is important for us to look back over the first decade to understand the events that have created possible paths to the future. By discussing those possible paths in the context of INMM's mission we can gain a more comfortable sense of how INMM should prepare for dramatic changes.

INMM Mission

- The advancement of nuclear materials management in all its aspects,
- The promotion of research in the field of nuclear materials management,
- The establishment of standards, consistent with existing professional norms,
- The improvement of the qualifications of those engaged in nuclear materials management and safeguards through high standards of professional ethics, education, and attainments, and the recognition of those who meet such standards, and
- The increase and dissemination of information through meetings, professional contacts, reports, papers, discussions, and publications.

Capturing the Past in Timelines

The use of timelines to capture significant events and their place in history can help show how those events can be connected, leading to increased insight into how sequences of events may be harbingers of some future state. Two such timelines of direct interest to our membership include the International Atomic Energy Agency's (IAEA) *"50 Decisive Years: The IAEA in Time"* (http://www.iaea.org/Publications/Magazines/Bulletin/Bull482/pdfs/decades.pdf), and the National Nuclear Security Administration's (NNSA) Historical Timeline (http://nnsa.energy.gov/aboutus/ourhistory/timeline). The IAEA timeline captures significant turning points in the IAEA's fifty-year history through 2007; the NNSA interactive timeline captures milestones from 1939 to 2010.

Other timelines, such as the animated You Tube *"Nuclear Detonation Timeline 1945-1998"* (http://www.youtube.com/watch?v=I9lquok4Pdk), where 2,053 nuclear tests and explosions that took place between 1945 and 1998 are plotted visually and audibly on a world map, can create new perspectives and stir emotional reactions from viewers. The "doomsday clock" of the Bulletin of Atomic Scientists, (http://www.thebulletin.org/content/doomsday-clock/timeline), is yet another visual perspective created using the imagery of apocalypse (midnight) and the contemporary idiom of a nuclear explosion (countdown to zero), to convey threats to humanity and the planet. Perhaps one of the most comprehensive and detailed timelines of "things nuclear" can be found at http://www.nuclearfiles.org/menu/timeline/, which is a detailed *Timeline of the Nuclear Age,* from the 1930's through 2011.

Another timeline, in a different format, that provides a remarkable perspective of INMM is the *Journal of Nuclear Materials Management (JNMM)* archives that INMM members can access though the INMM Web site (http://www.inmm.org/source/JNMM_Archive_Search/index.cfm). This remarkable collection of historic technical articles and editorial perspectives provides a detailed look at the work the Institute and its membership have done over the past forty years.

By taking a closer look at critical national and international events of the past decade that directly relate to the mission of the INMM, some disturbing trends emerge that should prompt us all to help leaders better understand the technical, scientific, and policy issues that are critical to taking us down the right path. These disturbing trends seem to have built in intensity and impact as we head into 2012. A graphical synopsis of this timeline, "A Decade of Tumult," can be found at http://www.itpnm.com/whats-new-archives/adecadeoftumult-thenewmillennium.pdf.

A Decade of Significant Events

Historic events or discontinuities, whether moving the world closer to a desired state, or driving it father from it, will always have long-term consequences that contribute to a path to the future. One can either acquiesce to follow that path, making mitigation adjustments, or one can intervene proactively to dramatically change the path, creating a more favorable future. Some events below, taken from the "Decade of Tumult," paint a foreboding path to the future, while others provide a more optimistic glimmer of hope.

Foreboding Events
- 9/11
- Iranian nuclear program
- DPRK nuclear tests
- Ten years of war
- Fukushima Daiichi event
- Global economic crisis
- A.Q. Khan proliferation
- Middle East conflict
- Pakistan government instability

Glimmers of Hope Events
- Treaty of Moscow (SORT)
- Libya gives up its WMD
- Strengthened IAEA Safeguards
- Obama Prague Speech
- New START Treaty ratified
- The Arab Spring
- Saddam Hussein toppled
- Osama Bin Laden klled
- Gadhafi toppled

The fork in the road that is created by these two highly divergent sequence of events creates a complex cultural, political, social, and technical environment, often so intertwined that any one could tip the balance toward a particular path to the future. It is important to note that tracking smaller events may lead us to anticipate major discontinuities. This requires imagination, strategic discussions, knowledge of leading-edge technologies and an understanding of the past.

Note there are many localized events that occur within each (nuclear) state or society that influence the overall international picture. For example, some events directly impacting the Department of Energy, the NNSA, and the U.S. Nuclear Security Enterprise (NSE) over the previous decade include:
- Formation of NNSA (2002)
- Bidding of lab contracts (2005)
- NPR 2001 and 2010
- Overskei NWCITF Task Force
- Complex 2030
- Complex transformation
- Nuclear Security Enterprise
- Prague Agenda/New START
- Yucca Mountain license issues

Putting the Decade in an INMM Perspective

Once envisioned as a future full of hope and prosperity, the turn of the new millennium has brought with it a decade of war, economic hardships, and an uneasiness about the future, as the technologies and weapons of mass destruction seem to be within the reach of not only rogue nations, but also non-nation-state entities, including terrorist groups, whose stated goal is to bring down civilization as we know it.

It was many of these dramatic events during the first decade that contributed to the Executive Committee's decision in 2009 to establish an Organizational Strategic Planning Working Group to assess the ability of INMM to contribute to solutions. The recommendations of that working group established a new structure and strategic posture for the Institute to address the challenges of the new millennium. The continuing challenge to monitor these events and identify their future impact on the Institute now lies with the new Strategic Planning Committee and Institute membership.

Looking Forward to an Uncertain Future

In the first column of this series I posed eight questions for the membership to consider as we travel the path to the future. Intended to be thought-provoking and painted in caricature, these questions can be refined by discussions to provide more specific and manageable challenges for INMM. Two more questions have been added over the past year based on current events. Taken against a backdrop of historic events during the past decade, they take on even more importance now as we look at the uncertain path that lies ahead in the second decade:
- How will the world deal with the untenable situations in Iran and DPRK?
- What happens if other nation-states similarly pursue nuclear weapons?
- How are other nations responding to President Obama's global nuclear initiatives—what impact will those responses have on the INMM?
- What will be the worldwide response to the first terrorist nuclear event (either nuclear or dispersal)?
- Can nuclear forensics provide the deterrence needed to prevent terrorist attacks?
- Will unilateral reductions in the U.S. stockpile influence the decision of other nuclear weapons states to further reduce their own stockpiles?
- What is the evolving role of the United Nations and IAEA in the new "international order" proposed by President Barack Obama?
- What scientific, technological, and policy innovations can INMM promote to make the world a safer place?
- Should INMM have an interactive Web presence (social network)?
- How will the Fukushima Daiichi nuclear plant accident impact the future of the Nuclear Renaissance?

In addressing these questions there are a number of complex drivers that must be monitored in the coming years. These are the drivers for events that might be connected to cause our future path to change directions once again. As such, INMM members should be monitoring, discussing, and sharing information and ideas about them with respect to INMM's future direction:
- Continuing international tensions over the Iranian nuclear program
- Threats by Iran to close the Strait of Hormuz, and the possibility of escalation, including an Israeli attack on their nuclear facilities
- Concern over the security of the Pakistani nuclear stockpile and instability in their government
- Political upheavals across the Middle East (the "Arab Spring"), including the probable fall of the Syrian government in the near future, and unintended consequences from the withdrawal of troops from Afghanistan
- Occupy/99%ers movement
- Growing cyberthreats worldwide
- The growing worldwide economic crisis

- U.S. budget deficit and debt ceiling and its impact on the future of the NSE and DOE/NNSA
- Continuing international tensions over DPRK nuclear programs
- Rise of China and the relentless march to match the U.S. military strike capability
- The continuing impact of the Fukushima Daiichi nuclear incident on nuclear power programs worldwide
- The politicization of the spent fuel problem in the United States
- Continued international concern over the vulnerability of nuclear materials and the proliferation of nuclear technology
- 2012 U.S. presidential elections
- Global Zero initiatives

This is not a very comfortable view into the future, but by engaging strategic discussions on these and other related topics, we can better prepare ourselves and INMM for the challenges ahead. In that process we need to be able to share with others new to our discipline the historical lessons learned and knowledge that has created our nuclear world.

We encourage *JNMM* readers to actively participate in these strategic discussions, and to provide your thoughts and ideas to the Institute's leadership. With your feedback we hope to explore these and other issues in future columns, addressing the critical uncertainties that lie ahead for the world and the possible paths to the future based on those uncertainties.

Jack Jekowski can be contacted at jpjekowski@aol.com.

---

i 2012 has been the subject of a Hollywood movie, a Super Bowl commercial, many scary predictions, and some dire religious prognostications dealing with Eschatology – otherwise known as the "End of Times." An Internet search on "2012 End of the World" produced 139 million results.

Submit your articles to the peer-reviewed *Journal of Nuclear Materials Management.*

Put your work before your peers
Network with others
Make yourself more competitive

To submit your paper:

1. ***Read the Author Submission Guidelines below.***
2. ***Email your paper in a Word document to JNMM Managing Editor Patricia Sullivan at psullivan@inmm.org.***
3. ***Respond promptly to review comments.***
4. ***Remember: JNMM is published four times a year in English. All graphs and images are published in black-and-white. References should follow Chicago Manual of Style guidelines.***

Questions?
Contact JNMM Managing Editor Patricia Sullivan at psullivan@inmm.org.

The quarterly JNMM is the premier international journal for the nuclear materials management profession. JNMM readers are the leaders in the field. They work in government, industry and academia around the world.

REACH THIS IMPORTANT AUDIENCE.

Author Submission Guidelines

The *Journal of Nuclear Materials Management* is the official journal of the Institute of Nuclear Materials Management. It is a peer-reviewed, multidisciplinary journal that publishes articles on new developments, innovations, and trends in safeguards and management of nuclear materials. Specific areas of interest include facility operations, international safeguards, materials control and accountability, nonproliferation and arms control, packaging, transportation and disposition, and physical protection. *JNMM* also publishes book reviews, letters to the editor, and editorials.

Submission of Manuscripts: *JNMM* reviews papers for publication with the understanding that the work was not previously published and is not being reviewed for publication elsewhere. Papers may be of any length. All papers must include an abstract.

The *Journal of Nuclear Materials* Management is an English-language publication. We encourage all authors to have their papers reviewed by editors or professional translators for proper English usage prior to submission.

Papers should be submitted as Word or ASCII text files only. Graphic elements must be sent in TIFF, JPEG or GIF formats as separate electronic files and must be readable in black and white.

Submissions may be made via e-mail to Managing Editor Patricia Sullivan at psullivan@inmm.org. Submissions may also be made via by regular mail. Include one hardcopy and a CD with all files. These submissions should be directed to:

Patricia Sullivan
Managing Editor
Journal of Nuclear Materials Management
111 Deer Lake Road, Suite 100
Deerfield, IL 60015 USA

Papers are acknowledged upon receipt and are submitted promptly for review and evaluation. Generally, the author(s) is notified within ninety days of submission of the original paper whether the paper is accepted, rejected, or subject to revision.

Format: All papers must include:

- Author(s)' complete name, telephone number and e-mail address
- Name and address of the organization where the work was performed
- Abstract
- Camera-ready tables, figures, and photographs in TIFF, JPEG, or GIF formats. Black and white only.
- Numbered references in the following format:
  1. Jones, F. T. and L. K. Chang. 1980. Article Title. *Journal* 47(No. 2): 112–118. 2. Jones, F. T. 1976. *Title of Book*, New York: McMillan Publishing.
- Author(s) biography

JNMM is published in black and white. **Authors wishing to include color graphics must pay color charges of $700 per page.**

Peer Review: Each paper is reviewed by at least one associate editor and by two or more reviewers. Papers are evaluated according to their relevance and significance to nuclear materials safeguards, degree to which they advance knowledge, quality of presentation, soundness of methodology, and appropriateness of conclusions.

Author Review: Accepted manuscripts become the permanent property of INMM and may not be published elsewhere without permission from the managing editor. Authors are responsible for all statements made in their work.

Reprints: Reprints may be ordered at the request and expense of the author. Contact Patricia Sullivan at psullivan@inmm.org or +1-847-480-9573 to request a reprint.

Calendar

May 14–16, 2012
Applying the IAEA State-Level Concept Workshop
University of Virginia
Charlottesville, Virginia USA
Sponsor: INMM International Safeguards Technical Division and the Northeast Chapter
Contact: Institute of Nuclear Materials Management
+1-847-480-9573
E-mail: inmm@inmm.org
Web site: www.inmm.org

July 15–19, 2012
53rd INMM Annual Meeting
Renaissance Orlando
Resort at SeaWorld
Orlando, Florida USA
Sponsor: Institute of Nuclear Materials Management
Contact: INMM
+1-847-480-9573
Fax: +1-847-480-9282
E-mail: inmm@inmm.org
Web site: www.inmm.org

August 18–23, 2013
PATRAM 2013
Hilton San Francisco Union Square
San Francisco, California USA
Hosted by the U.S. Department of Energy, the U.S. Nuclear Regulatory Commission, and the U.S. Department of Transportation in cooperation with INMM
Web site: http://www.patram.org

September 23-28, 2012
The 9th International Conference on Facility Operations-Safeguards Interface
Hilton Savannah Desoto
Savannah, Georgia USA
Sponsors: American Nuclear Society and the Institute of Nuclear Materials Management
Web site: http://icfo-9.org/

Cut the Threat Posed by the World's Most Dangerous Weapons

For forty years, the **Arms Control Association** has provided decision-makers, scholars, media, and the general public with accurate and timely information on biological, chemical, and nuclear weapons and the best methods to halt their spread and prevent their use, such as the dismantling of U.S. and Russian nuclear missiles.

Information is influence. Help us set the course for effective arms control solutions by supporting our work. Membership includes:

- Original news reporting and analysis in our monthly journal, ***Arms Control Today.***
- In-depth interviews with top policymakers.
- And so much more!

Visit **www.armscontrol.org/discount** to save 20% on an ACA membership or *Arms Control Today* subscription.

Arms Control Association
ACA
Recipient of the 2010 MacArthur Award

Arms Control TODAY

Follow us on:

Decommissioning?

The new AURAS-3000 Box Counter from ORTEC will make short work of those bulky free release construction waste containers!

www.ortec-online.com/solutions/waste-assay.aspx

- Free Release Assay of large waste containers up to 3 m^3: B25 ISO Box, smaller boxes with demonstrated regulatory compliance.[1]
- Container Weights up to 6000 kg, with on-line weighing to 3000 kg and 1 kg resolution.
- Full Quantitative Assay of all detectable gamma emitters, with non-gamma emitter estimates by correlated scaling factors.
- FAST: High sensitivity, large area integrated HPGe detectors (85 mm diameter) achieve rapid release levels.
- Individual and averaged activity AND MDA reporting.
- Highly automated.
- Extensive Safety Protection.
- Tested to EMC, Electrical and Safety standards.

[1]http://www.ortec-online.com/download.asbx?AttributeFileId=0b1f5761-c46b-4901-91ac-e0b810655b6a

801 South Illinois Ave., Oak Ridge, TN 37831-0895 U.S.A. • (865) 482-4411 • Fax (865) 483-0396 • ortec.info@ametek.com
For International Office Locations, Visit Our Website
www.ortec-online.com

ORTEC®

AMETEK
ADVANCED MEASUREMENT TECHNOLOGY